THE ROLE OF HISTOPATHOLOGY IN CANCER DIAGNOSIS AND PROGNOSIS

EDITED BY: Luigi Tornillo and Renato Franco

PUBLISHED IN: Frontiers in Medicine

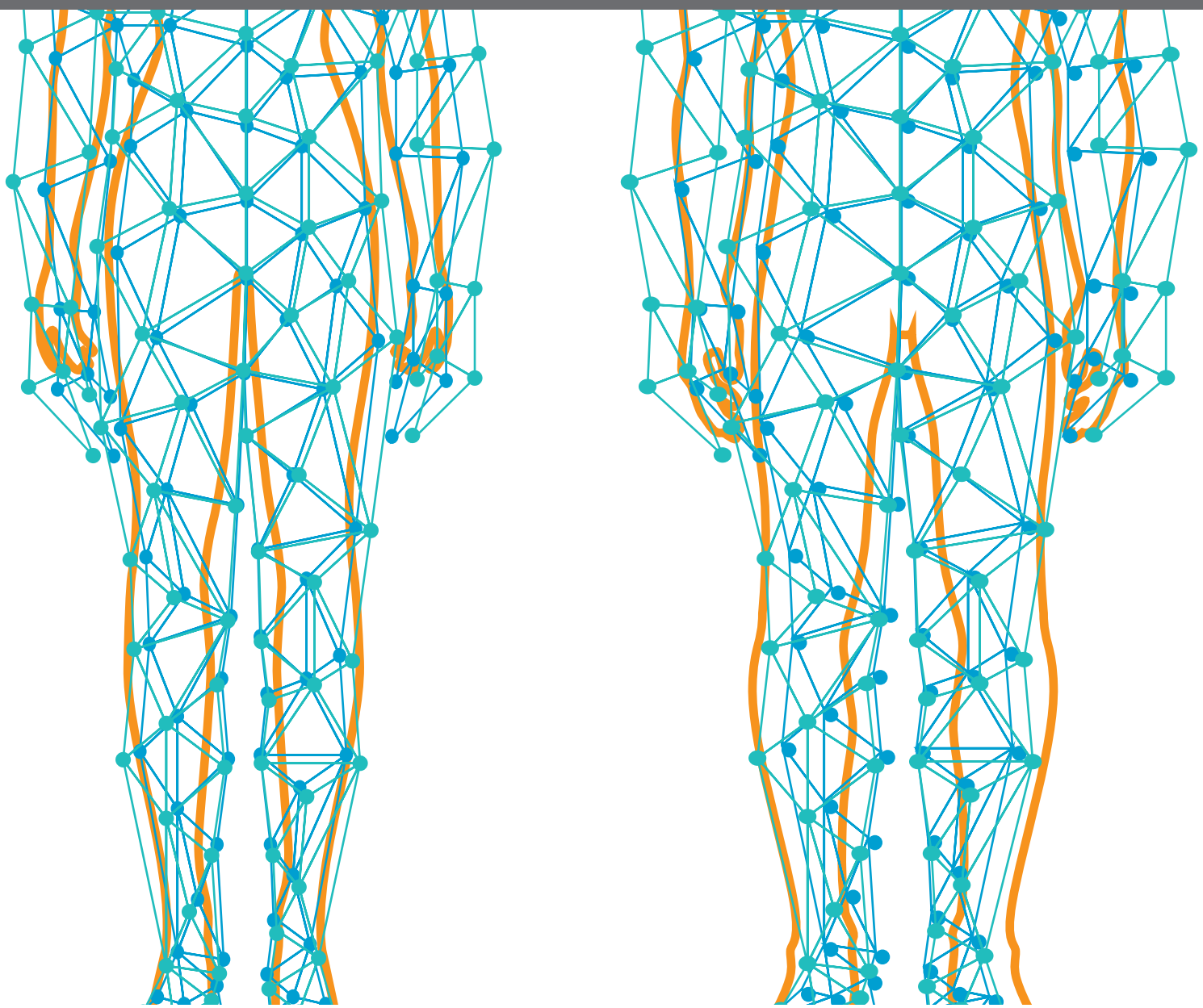

frontiers Research Topics

frontiers

ISSN 1664-8714
ISBN 978-2-83250-721-6
DOI 10.3389/978-2-83250-721-6

About Frontiers

Frontiers is more than just an open-access publisher of scholarly articles: it is a pioneering approach to the world of academia, radically improving the way scholarly research is managed. The grand vision of Frontiers is a world where all people have an equal opportunity to seek, share and generate knowledge. Frontiers provides immediate and permanent online open access to all its publications, but this alone is not enough to realize our grand goals.

Frontiers Journal Series

The Frontiers Journal Series is a multi-tier and interdisciplinary set of open-access, online journals, promising a paradigm shift from the current review, selection and dissemination processes in academic publishing. All Frontiers journals are driven by researchers for researchers; therefore, they constitute a service to the scholarly community. At the same time, the Frontiers Journal Series operates on a revolutionary invention, the tiered publishing system, initially addressing specific communities of scholars, and gradually climbing up to broader public understanding, thus serving the interests of the lay society, too.

Dedication to Quality

Each Frontiers article is a landmark of the highest quality, thanks to genuinely collaborative interactions between authors and review editors, who include some of the world's best academicians. Research must be certified by peers before entering a stream of knowledge that may eventually reach the public - and shape society; therefore, Frontiers only applies the most rigorous and unbiased reviews.
Frontiers revolutionizes research publishing by freely delivering the most outstanding research, evaluated with no bias from both the academic and social point of view. By applying the most advanced information technologies, Frontiers is catapulting scholarly publishing into a new generation.

What are Frontiers Research Topics?

Frontiers Research Topics are very popular trademarks of the Frontiers Journals Series: they are collections of at least ten articles, all centered on a particular subject. With their unique mix of varied contributions from Original Research to Review Articles, Frontiers Research Topics unify the most influential researchers, the latest key findings and historical advances in a hot research area! Find out more on how to host your own Frontiers Research Topic or contribute to one as an author by contacting the Frontiers Editorial Office: frontiersin.org/about/contact

THE ROLE OF HISTOPATHOLOGY IN CANCER DIAGNOSIS AND PROGNOSIS

Topic Editors:
Luigi Tornillo, University of Basel, Switzerland
Renato Franco, University of Campania Luigi Vanvitelli, Italy

Citation: Tornillo, L., Franco, R., eds. (2022). The Role of Histopathology in Cancer Diagnosis and Prognosis. Lausanne: Frontiers Media SA.
doi: 10.3389/978-2-83250-721-6

Table of Contents

frontiers in Medicine

ORIGINAL RESEARCH
published: 05 June 2020
doi: 10.3389/fmed.2020.00205

Mucinous Histology Might Be an Indicator for Enhanced Survival Benefit of Chemotherapy in Stage II Colon Cancer

Yong Huang[1†], Kuanxue Ge[2†], Guangshun Fu[1], Junfeng Chu[3] and Wei Wei[1]*

[1] Department of General Surgery, Jiangdu People's Hospital Affiliated to Medical College of Yangzhou University, Yangzhou, China, [2] Department of Gastroenterology, Jiangdu People's Hospital Affiliated to Medical College of Yangzhou University, Yangzhou, China, [3] Department of Radiotherapy, Jiangdu People's Hospital Affiliated to Medical College of Yangzhou University, Yangzhou, China

Background: It was a difficult question to identify candidates who would benefit most from adjuvant chemotherapy in stage II colon cancer because of the paucity of relevant conclusive clinical trial results. We aimed to assess if mucinous adenocarcinoma (MUA) could be an indicator for the efficacy of adjuvant chemotherapy in stage II colon cancer.

Methods: Using SEER*Stat software V.8.3.5, eligible patients were then recruited from the SEER database. A χ^2 test was applied to compare the distribution of different categorical variables between nonmucinous adenocarcinoma (NMUA) and MUA groups. We then used the Kaplan–Meier method to analyze overall survival (OS) of different histological types in stage II colon cancer, and the log-rank test was then used to assess the OS differences. The Cox proportional regression risk models were also built in our analyses to eliminate potential crossed bias from other prognostic factors.

Results: A total of 50,065 patients diagnosed with stage II colon cancer were recruited from the SEER database from 2004 to 2011; all the patients were divided into two groups, including NMUA (n = 44,785) and MUA (n = 5,280). The Cox analysis of the histological type indicated that the survival difference between MUA and NMUA failed to reach statistical significance in stage II colon cancer (P = 0.360). In NMUA, patients treated with adjuvant chemotherapy were independently associated with 37.2% decreased risk of overall mortality compared with those not [hazard ratio (HR) = 0.628, 95% confidence interval (CI) = 0.601-1.656, $P < 0.001$]; in MUA, the number increased to 41.5% (HR = 0.585, 95% CI = 0.515-0.665, $P < 0.001$).

Conclusions: Our study showed that the survival difference between MUA and NMUA failed to reach statistical significance in stage II colon cancer. More importantly, our study had provided the first evidence that chemotherapy would offer higher survival improvement in MUA compared with NMUA in stage II colon cancer; mucinous histology might be an indicator for enhanced survival benefit of chemotherapy in stage II colon cancer.

Keywords: mucinous histology, survival benefit, chemotherapy, stage II, colon cancer

OPEN ACCESS

Edited by:
Luigi Tornillo, University of Basel, Switzerland

Reviewed by:
Samir Abdullazade, University Medical Center Schleswig-Holstein, Germany
Andrea Ronchi, University of Campania Luigi Vanvitelli, Italy

***Correspondence:**
Wei Wei
jd.k.kenny@163.com

[†]These authors have contributed equally to this work

Specialty section:
This article was submitted to Pathology, a section of the journal Frontiers in Medicine

Received: *26 February 2020*
Accepted: *27 April 2020*
Published: *05 June 2020*

Citation:
Huang Y, Ge K, Fu G, Chu J and Wei W (2020) Mucinous Histology Might Be an Indicator for Enhanced Survival Benefit of Chemotherapy in Stage II Colon Cancer. Front. Med. 7:205. doi: 10.3389/fmed.2020.00205

INTRODUCTION

Colorectal cancer is the most prevalent malignancy of gastrointestinal cancer (1). Currently, surgical resection is the only curative treatment in patients with colorectal cancer. After the curative resection, however, patients with colorectal cancer would still have a high rate of recurrence, which was up to 30–40% (2). Stage II colon, defined as T3-T4 without lymph node or distant metastases according to the eighth edition of the American Joint Committee on Cancer (AJCC) Tumor Node Metastasis (TNM) staging system, was reported to make up ∼36% of all the colon cancer (3). However, it was reported that the recurrence rate of stage II disease was ∼25%, and there had been a continuous debate about the efficacy of adjuvant chemotherapy in stage II colon cancer (4).

The paucity of relevant conclusive clinical trial results made it a challenging problem to identify those who would benefit most from adjuvant chemotherapy in stage II colon cancer (5–8). Despite this, the European Society for Medical Oncology had clinical recommendations of adjuvant chemotherapy for high-risk stage II colon cancer (with risk factors such as lymph nodes sampling <12, poorly differentiated tumor, vascular or lymphatic or perineural invasion, tumor presentation with obstruction or tumor perforation and pT4 stage) (9). And some previous studies also had the similar recommendations (5, 10).

Mucinous adenocarcinoma (MUA), composed of more than 50% extracellular mucins, was a histologic subtype of colorectal cancer (11), and it accounted for approximately 10% of colorectal cancer (12, 13). Mucinous adenocarcinoma had distinct clinicopathological features compared with nonmucinous adenocarcinoma (NMUA) (14), and it remained debatable whether MUA was an adverse prognostic factor in patients with colon cancer (15–17). Few prior studies listed MUA as a high-risk factor for the treatment of chemotherapy. We therefore conducted this large population-based study to assess if MUA could be an indicator for the efficacy of adjuvant chemotherapy in stage II colon cancer.

PATIENT POPULATION AND SELECTION

Sponsored by the National Cancer Institute, the Surveillance, Epidemiology, and End Results (SEER) program is an authoritative population-based cancer surveillance program. It was established in 1973 and covered approximately 30% of the total US population in SEER-participating regions. The SEER program collected registry and patient information, including general demographics, disease stage, cancer incidence, surgical variables, pathological type, and survival data (1). The latest follow-up information of patients ended in 2016.

Using SEER*Stat software V.8.3.5, eligible patients were then recruited from the SEER database. The flow diagram of the data selection process is shown in **Figure 1**. First, patients diagnosed with colon cancer were selected from the SEER database between 2004 and 2011 ($n = 188,946$). We chose to select cases diagnosed before 2011 in order to obtain longer follow-up data. These patients were restaged according to the eighth edition of the AJCC TNM staging system, and node-negative patients with tumor deposit were redefined as N1. Then, 27,856 patients

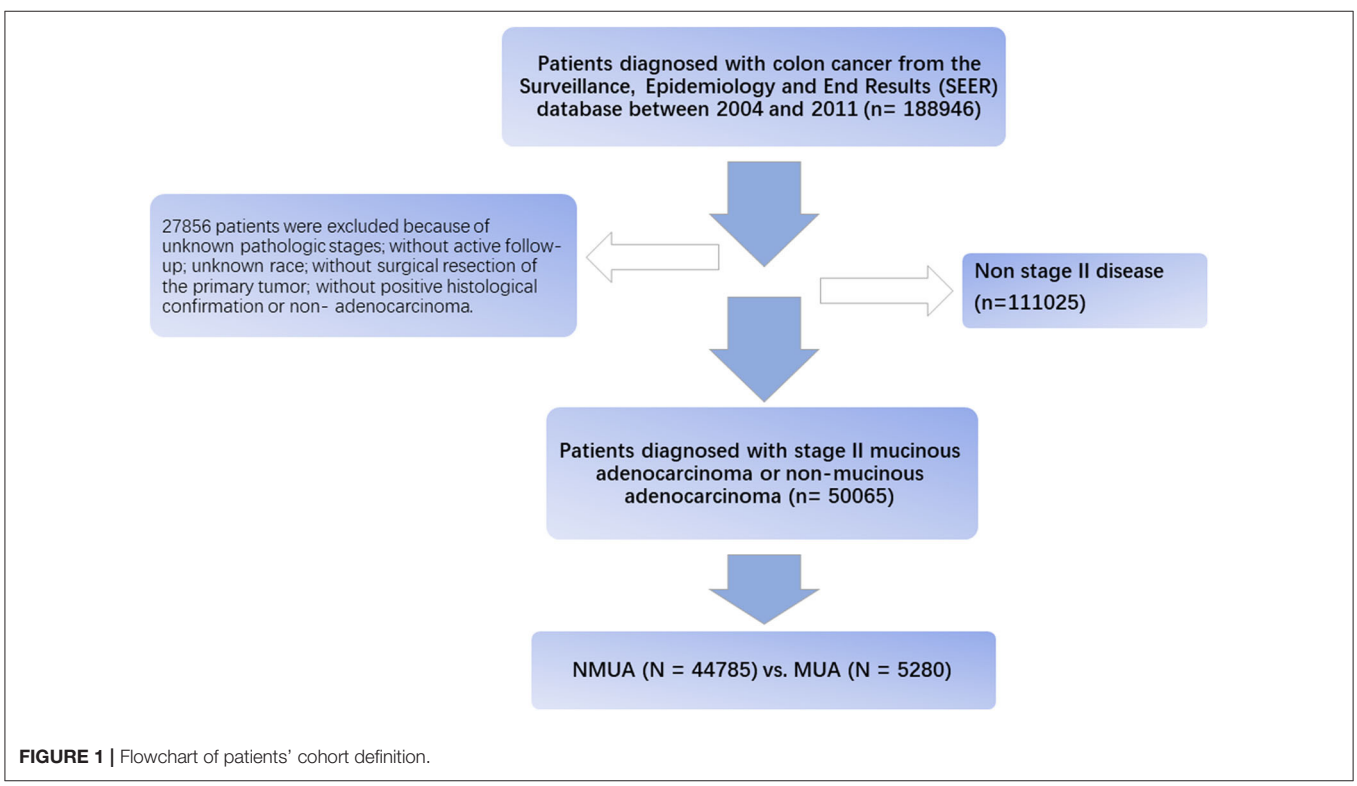

FIGURE 1 | Flowchart of patients' cohort definition.

were excluded because of unknown pathologic stages, without active follow-up, unknown race, without surgical resection of the primary tumor, without positive histological confirmation, or nonadenocarcinoma. We also excluded patients with distant metastases or lymph node positivity; only patients diagnosed with stage II colon cancer were included in our analyses.

The following demographic and clinical characteristics were extracted from the SEER database:

T stage (T3 and T4), age at diagnosis (years), race (white, black, or other), gender (male and female), tumor site (cecum, ascending colon, hepatic flexure, transverse colon, splenic flexure, descending colon, and sigmoid colon), tumor grade (grade I/II, grade III/IV, or unknown), the receipt of chemotherapy (no/unknown or yes), and the histological type (NMUA or MUA).

Statistical Analyses

All the eligible patients were divided into two groups, including NMUA and MUA groups. A χ^2 test was applied to compare the distribution of different categorical variables between NMUA and MUA groups. The outcome of interest used in the current study was overall survival (OS). We then used the Kaplan–Meier method to analyze the OS according to the histology of colon cancer and the log-rank test was then used to assess the OS differences. In order to eliminate potential crossed bias from other prognostic factors, the Cox proportional regression risk models were also built in our analyses. Only those factors with $P < 0.20$ in univariate analyses would be included in the multivariate analyses. All the hazard ratios (HRs) of patient characteristics are shown with 95% confidence intervals (CIs). $P < 0.05$ was considered statistically significant. All statistical analyses were conducted using IBM SPSS, version 23 (IBM Corp., Armonk, NY, USA).

TABLE 1 | Demographic and patient characteristics according to the histology in stage II colon cancer.

Characteristics	Number of patients (%)		*P*
	NMUA (*n* = 44,785)	MUA (*n* = 5,280)	
T stage			<0.001
T3	39,136 (87.4)	4,397 (83.3)	
T4	5,649 (12.6)	883 (16.7)	
Age (years)			0.009
≤65	14,297 (31.9)	1,592 (30.2)	
>65	30,488 (68.1)	3,688 (69.8)	
Race			<0.001
White	36,655 (81.1)	4,512 (85.5)	
Black	4,902 (10.9)	502 (9.5)	
Other	3,228 (7.2)	266 (5.0)	
Gender			0.003
Male	21,729 (48.5)	2,447 (46.3)	
Female	23,056 (51.5)	2,833 (53.7)	
Tumor location			<0.001
Cecum	10,260 (22.9)	1,559 (29.5)	
Ascending colon	9,995 (22.3)	1,439 (27.3)	
Hepatic flexure	2,818 (6.3)	371 (7.0)	
Transverse colon	5,281 (11.8)	693 (13.1)	
Splenic flexure	1,931 (4.3)	230 (4.4)	
Descending colon	2,987 (6.7)	284 (5.4)	
Sigmoid colon	11,513 (25.7)	704 (13.3)	
Grade			<0.001
Grade I/II	36,426 (81.3)	4,046 (77.2)	
Grade III/IV	7,746 (17.3)	879 (16.6)	
Unknown	613 (1.4)	325 (6.2)	
Chemotherapy			0.048
No/unknown	37,558 (83.9)	4,372 (82.8)	
Yes	7,227 (16.1)	908 (17.2)	

RESULTS

Baseline Cohort Characteristics

A total of 50,065 patients diagnosed with stage II colon cancer were recruited from the SEER database from 2004 to 2011. All the patients were divided into two groups, including NMUA ($n =$ 44,785) and MUA ($n = 5,280$). The median follow-up time of the whole cohort was up to 74 months, which was more than 5 years. Among the whole cohort, 24,173 patients (48.3%) were male and 25,889 patients (51.7%) were female. The median age was 73 years. And the pathological tumor stage showed that 43,533 patients (87.0%) were in the T3 stage, and 6,532 patients (13.0%) were in the T4 stage. Of all the patients, 16.2% ($n = 8,135$) of them had been treated with chemotherapy.

The descriptive patient characteristics of eligible patients were compared between NMUA and MUA (**Table 1**). It was found that MUA was more likely to be correlated with T4 stage ($P < 0.001$), older age ($P = 0.009$), white race ($P < 0.001$), female ($P < 0.003$), proximal colon ($P < 0.001$), and the receipt of chemotherapy with a borderline P value ($P = 0.048$).

Prognostic Value of MUA in Stage II Colon Cancer

As shown in **Figure 2**, stage II MUA had similar OS as compared with stage II NUMC ($P = 0.360$). The 5-year OS rates of MUA and NMUA were 64.9 and 65.4%, respectively. **Table 2** shows the results of univariate analyses of characteristics including T stage, age at diagnosis, race, gender, tumor site, tumor grade, the receipt of chemotherapy, and the histological type. Those clinicopathological factors with $P < 0.20$ in univariate analyses were included in multivariate analyses: T stage ($P < 0.001$), age at diagnosis ($P < 0.001$), race ($P < 0.001$), gender ($P = 0.001$), tumor site ($P < 0.001$), tumor grade ($P < 0.001$), and the receipt of chemotherapy ($P < 0.001$). However, univariate Cox analysis of the histological type indicated that the survival difference between MUA and NMUA failed to reach statistical significance in stage II colon cancer ($P = 0.360$). And we can also see that patients treated with adjuvant chemotherapy were independently associated with 37.8% decreased risk of overall mortality compared with patients without the receipt of adjuvant

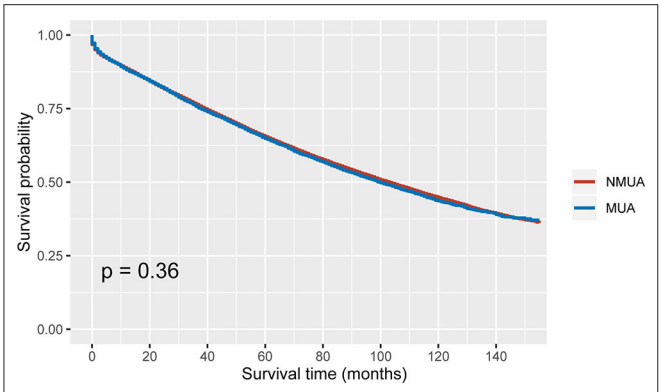

FIGURE 2 | Kaplan–Meier curves for overall survival in stage II colon cancer.

chemotherapy in stage II colon cancer (HR = 0.622, 95% CI = 0.597-0.648, $P < 0.001$).

Mucinous Histology Might Be an Indicator for Enhanced Survival Benefit of Chemotherapy in Stage II Colon Cancer

Using Kaplan–Meier method, it was found that the receipt of chemotherapy offered significantly improved OS in both MUA and NMUA groups. In NMUA, the 5-year OS rates of chemotherapy and nonchemotherapy groups were 78.8 and 62.9%, respectively ($P < 0.0001$, **Figure 3A**). In MUA, the 5-year OS rates of chemotherapy and nonchemotherapy groups were 79.6 and 61.8%, respectively ($P < 0.0001$, **Figure 3B**). The aforementioned results indicated that the receipt of chemotherapy had 15.9% increased 5-year OS rate compared with nonchemotherapy in NMUA, whereas the efficacy of chemotherapy seemed to be more obvious in MUA: the receipt of chemotherapy had 17.8% increased 5-year OS rate compared with nonchemotherapy in MUA. In addition, we also conducted the subgroup analyses in pT3 N0 M0 colon cancer. It was found that the receipt of chemotherapy also offered significantly improved OS in pT3 N0 M0 MUA, and the 5-year OS rates of chemotherapy and nonchemotherapy groups were 92.0 and 89.6%, respectively ($P < 0.0001$, **Figure 4A**); however, the receipt of chemotherapy did not offer OS difference between pT3 N0 M0 MUA and pT3 N0 M0 NMUA ($P = 0.19$, **Figure 4B**).

Cox proportional hazards models were then employed to verify the above findings. **Table 3** shows the results of univariate analyses of characteristics including T stage, age at diagnosis, race, gender, tumor site, tumor grade, the receipt of chemotherapy and the histological type in stage II NMUA, and those clinicopathological factors with $P < 0.20$ in univariate analyses were included in multivariate analyses: T stage ($P < 0.001$), age at diagnosis ($P < 0.001$), race ($P < 0.001$), gender ($P < 0.001$), tumor site ($P < 0P < 0.001$), tumor grade ($P < 0.001$), and the receipt of chemotherapy ($P < 0.001$). The results of multivariate analyses showed that patients treated with adjuvant chemotherapy were independently associated with 37.2% decreased risk of overall mortality compared with those not in stage II colon cancer (HR = 0.628, 95% CI = 0.601–1.656, $P < 0.001$).

Table 4 shows the results of univariate analyses of characteristics including T stage, age at diagnosis, race, gender, tumor site, tumor grade, the receipt of chemotherapy, and the histological type in stage II MUA, and those clinicopathological factors with $P < 0.20$ in univariate analyses were included in multivariate analyses: T stage ($P < 0.001$), age at diagnosis ($P < 0.001$), race ($P < 0.001$), tumor grade ($P = 0.056$), and the receipt of chemotherapy ($P < 0.001$). However, both gender ($P = 0.261$) and tumor site ($P = 0.892$) did not show enough prognostic value in univariate analyses. The results of multivariate analyses showed that patients treated with adjuvant chemotherapy were independently associated with 41.5% decreased risk of overall mortality compared with those not in stage II colon cancer (HR = 0.585, 95% CI = 0.515-0.665, $P < 0.001$).

TABLE 2 | Univariate and multivariate analyses of prognostic factors in stage II colon cancer.

Variable	Univariate analyses		Multivariate analyses	
	HR (95% CI)	*P*	HR (95% CI)	*P*
Histology		0.360		
NMUA				
MUA				
T stage		<0.001		<0.001
T3			1	
T4			1.692 (1.635-1.752)	
Age (years)		<0.001		<0.001
≤65			1	
>65			3.073 (2.968-3.182)	
Race		<0.001		<0.001
White			1	
Black			1.116 (1.071-1.162)	<0.001
Other			0.715 (0.676-0.756)	<0.001
Gender		0.001		<0.001
Male			1	
Female			0.874 (0.853-0.897)	
Tumor location		<0.001		<0.001
Cecum			1	
Ascending colon			0.984 (0.949-1.021)	0.392
Hepatic flexure			1.026 (0.972-1.084)	0.353
Transverse colon			1.100 (1.054-1.149)	<0.001
Splenic flexure			1.126 (1.057-1.201)	<0.001
Descending colon			1.067 (1.009-1.128)	0.023
Sigmoid colon			1.095 (1.056-1.135)	<0.001
Grade		<0.001		<0.001
Grade I/II			1	
Grade III/IV			1.124 (1.088-1.161)	<0.001
Unknown			1.185 (1.087-1.292)	<0.001
Chemotherapy		<0.001		<0.001
No/unknown			1	
Yes			0.622 (0.597-0.648)	

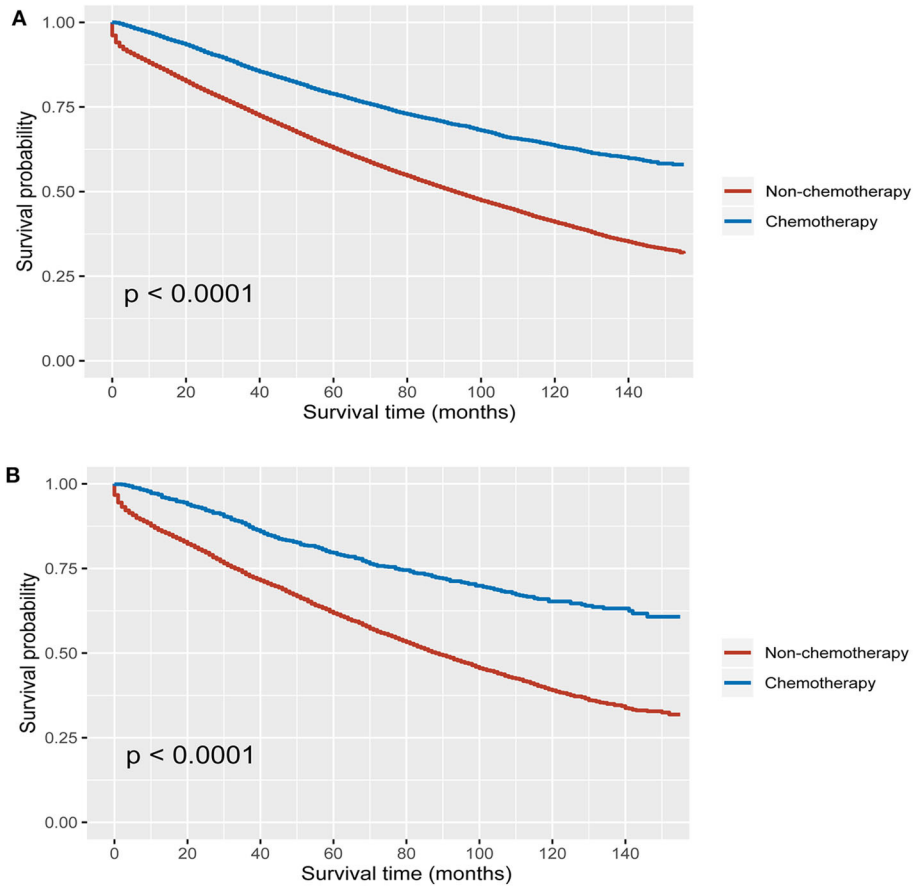

FIGURE 3 | Kaplan–Meier curves for overall survival in stage II colon cancer ith **(A)** MUA, **(B)** NMUA.

DISCUSSION

As a rare and special type of colorectal cancer, MUA was composed of more than 50% extracellular mucins and had distinct clinicopathological features compared with NMUA. It was reported that MUA was more likely to be associated with advanced stages in colorectal cancer and was less responsive to chemotherapy compared to NMUA (12, 18), but it remained debatable whether MUA was an adverse prognostic factor in patients with colon cancer (15–17). In stage II colon cancer, however, the finding that survival difference between MUA and NMUA was not statistically different was gradually becoming clear.

In 2011, a study involved 1,025 unselected patients from Italy showed that the OS of stage II colon cancer with MUA was not significantly different from those with NMUA (P = 0.206) (19). Later, in 2018, a study also found that the cancer-specific survival difference between MUA and NMUA was not statistically significant (P = 0.597) (20). Recently, Fields et al. (21) conducted a retrospective analysis and reported that the 5-year survival rates of patients with stage II NMUA and MUA were 65.1 and 63.5%, respectively, and the survival difference achieved statistical significance (P = 0.002). In adjusted analysis, however, they found there was no significant difference in survival between NMUA and MUA patients in stage II disease.

In our study, it was shown that MUA was more likely to be correlated with T4 stage (P < 0.001), which had been demonstrated in prior studies (12, 18). The Kaplan–Meier analyses showed that stage II MUA had similar OS as compared with stage II NMUA (P = 0.360), and the 5-year OS rates of MUA and NMUA were 64.9% and 65.4%, respectively. Moreover, the results of Cox analysis also indicated that the survival difference between MUA and NMUA failed to reach statistical significance in stage II colon cancer (P = 0.360). The 5-year OS rates of MUA and NMUA were similar to previous report (19). More importantly, we showed again no survival difference between MUA and NMUA in stage II colon cancer, even in pT3 N0 M0 colon cancer with receipt of chemotherapy

Despite clinical guidelines that had recommendations of adjuvant chemotherapy for high-risk colon cancer, the efficacy of adjuvant chemotherapy in high-risk disease had always been the subject of debate (22–24), indicating the necessity to identify candidates for adjuvant chemotherapy in stage II colon cancer. Few prior studies listed MUA as a high-risk factor. We therefore conducted this large population-based study to assess if MUA could be an indicator for the efficacy of adjuvant chemotherapy

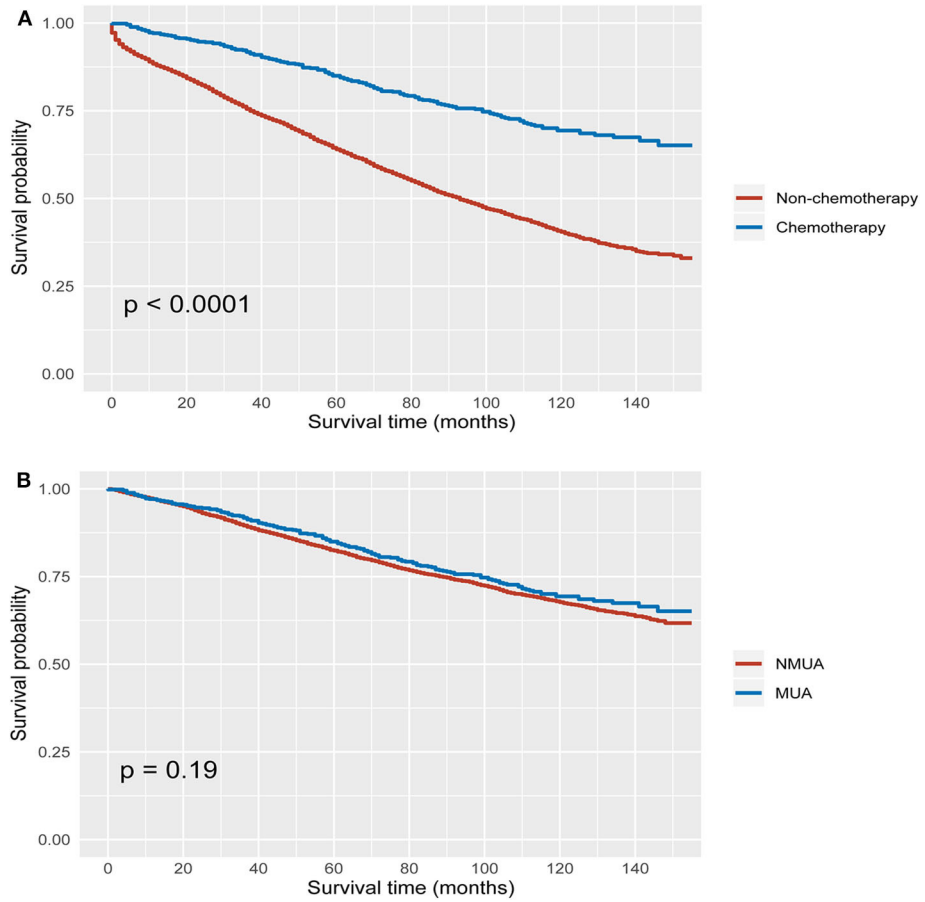

FIGURE 4 | Kaplan–Meier curves for overall survival in stage II colon cancer with **(A)** pT3 N0 M0 MUA, **(B)** pT3 N0 M0 colon cancer with the receipt of chemotherapy.

in stage II colon cancer. The results of our study indicated that the receipt of chemotherapy had 15.9% increased 5-year OS rate compared with nonchemotherapy in NMUA (the 5-year OS rates of chemotherapy and nonchemotherapy groups were 78.8 and 62.9%, respectively, $P < 0.0001$) However, the efficacy of chemotherapy seemed to be more obvious in MUA: the receipt of chemotherapy had 17.8% increased 5-year OS rate compared with nonchemotherapy in MUA (the 5-year OS rates of chemotherapy and nonchemotherapy groups were 79.6 and 61.8%, respectively, $P < 0.0001$). The results of multivariate Cox analyses showed that patients treated with adjuvant chemotherapy were independently associated with 37.2% decreased risk of overall mortality compared with patients without the receipt of chemotherapy in stage II NMUA. However, adjuvant chemotherapy had 41.5% independently decreased risk of overall mortality in stage II NMUA, showing that the therapeutic effect of chemotherapy had been enhanced in MUA.

To our knowledge, few previous studies focused on the response to chemotherapy in stage II MUA (20, 21). In a recent study, Fields et al. (21) performed a retrospective analysis to evaluate the survival benefit of chemotherapy in patients with stages II and III colon cancer with the histology of MUA. The researchers reported that there was a significant survival difference between patients undergoing chemotherapy and those not undergoing chemotherapy (HR = 0.79, 95% CI = 0.69–0.90, $P < 0.001$) in stage II MUA. Therefore, they concluded that adjuvant chemotherapy had significantly improved OS compared to those not undergoing chemotherapy in stage II colon cancer with the histology of MUA. In addition, Hu et al. (20) reported that the disease-free survival was identical in MUA and adenocarcinoma patients after neoadjuvant chemotherapy and believed the histology of MUA can be used as a high-risk factor in stage II colorectal cancer patients. The two researches supported the receipt of chemotherapy in stage II MUA; however, both of them did not have direct comparison of the chemosensitivity between stage II colon cancer with MUA and NMUA. And Hu et al. (20) had mixed colon cancer patients and rectal cancer patients together, which would impact the clinical application of study results in stage II colon cancer.

Recently, Rosati et al. (25) recruited 474 patients from 94 centers enrolled in the per-protocol population defined in the TOSCA trial. They found that the evaluation of MUA histology could be considered an indicator for longer chemotherapy treatment in stage II colon cancer, which was consistent with

TABLE 3 | Univariate and multivariate analyses of prognostic factors in stage II NMUA.

Variable	Univariate analyses		Multivariate analyses	
	HR (95% CI)	*P*	HR (95% CI)	*P*
T stage		<0.001		<0.001
T3			1	
T4			1.715 (1.652-1.779)	
Age (years)		<0.001		<0.001
≤65			1	
>65			3.027 (2.918-3.140)	
Race		<0.001		<0.001
White			1	
Black			1.125 (1.078-1.174)	<0.001
Other			0.714 (0.674-0.757)	<0.001
Gender		<0.001		<0.001
Male			1	
Female			0.870 (0.847-0.893)	
Tumor location		<0.001		<0.001
Cecum			1	
Ascending colon			0.976 (0.939-1.014)	0.210
Hepatic flexure			1.024 (0.965-1.085)	0.435
Transverse colon			1.095 (1.046-1.147)	<0.001
Splenic flexure			1.108 (1.035-1.185)	0.003
Descending colon			1.046 (0.986-1.109)	0.133
Sigmoid colon			1.084 (1.044-1.127)	<0.001
Grade		<0.001		<0.001
Grade I/II			1	
Grade III/IV			1.133 (1.095-1.173)	<0.001
Unknown			1.203 (1.081-1.339)	0.001
Chemotherapy		<0.001		<0.001
No/unknown			1	
Yes			0.628 (0.601-1.656)	

TABLE 4 | Univariate and multivariate analyses of prognostic factors in stage II MUA.

Variable	Univariate analyses		Multivariate analyses	
	HR (95% CI)	*P*	HR (95% CI)	*P*
T stage		<0.001		<0.001
T3			1	
T4			1.557 (1.410-1.718)	
Age (years)		<0.001		<0.001
≤65			1	
>65			3.415 (3.049-3.824)	
Race		<0.001		0.014
White			1	
Black			1.031 (0.899-1.183)	0.663
Other			0.738 (0.599-0.909)	0.004
Gender		0.261		
Male				
Female				
Tumor location		0.892		
Cecum				
Ascending colon				
Hepatic flexure				
Transverse colon				
Splenic flexure				
Descending colon				
Sigmoid colon				
Grade		0.056		0.222
Grade I/II			1	
Grade III/IV			1.030 (0.931-1.139)	0.572
Unknown			1.139 (0.980-1.324)	0.089
Chemotherapy		<0.001		<0.001
No/unknown			1	
Yes			0.585 (0.515-0.665)	

our study. The response of chemotherapy, however, was still debated in the histologic type of MUA. Some studies have shown that MUA had a poor response to chemotherapy, whereas others have shown a survival benefit of chemotherapy in MUA (26–29). In stage II colon cancer, therefore, our study had provided the first evidence that chemotherapy would offer higher survival improvement in MUA compared with NMUA in stage II colon cancer. Mucinous adenocarcinomas have higher chemotherapy sensitivity in stage II disease as compared with other tumor stages, and mucinous colon cancer treatment algorithms should take staging information into account.

Our study has two important limitations. First, though SEER database was a database with reliable information, inevitably, it has some inherent limitations with the lack of some features including the types and doses of chemotherapy and information on tumor relapse, and it did not pay enough attention to molecular biology of colon cancer. Second, our research was a retrospective one, which had inherent deficiencies that could lead to confusion or observer bias.

CONCLUSIONS

Our study showed that the survival difference between MUA and NMUA failed to achieve statistical significance in stage II colon cancer. More importantly, our study had provided the first evidence that chemotherapy would offer higher survival improvement in MUA compared with NMUA in stage II colon cancer, indicating MUA had higher chemotherapy sensitivity in stage II disease as compared with other tumor stages, and mucinous colon cancer treatment algorithms should take staging information into account. Mucinous histology might be an indicator for enhanced survival benefit of chemotherapy in stage II colon cancer.

DATA AVAILABILITY STATEMENT

Publicly available datasets were analyzed in this study. This data can be found here: https://seer.cancer.gov/.

AUTHOR CONTRIBUTIONS

WW conceived and designed the study. YH and KG collected and analyzed the data. YH, KG, and GF performed the statistical analysis. GF and JC wrote the first draft of the manuscript. YH, KG, and WW revised the final data and the manuscript. All the authors reviewed the final draft of the manuscript and approved the submitted version.

REFERENCES

1. Petkov VI, Miller DP, Howlader N, Glider N, Howe W, Schussler N, et al. Breast-cancer-specific mortality in patients treated based on the 21-gene assay: a SEER population-based study. *NPJ Breast Cancer.* (2016) 2:16017. doi: 10.1038/npjbcancer.2016.17
2. Chang GJ, Kaiser AM, Mills S, Rafferty JF, Buie WD. Practice parameters for the management of colon cancer. *Dis Colon Rectum.* (2012) 55:831–43. doi: 10.1097/DCR.0b013e3182567e13
3. O'Connell JB, Maggard MA, Ko CY. Colon cancer survival rates with the new American Joint Committee on Cancer sixth edition staging. *J Natl Cancer Insti.* (2004) 96:1420–5. doi: 10.1093/jnci/djh275
4. Carrato A. Adjuvant treatment of colorectal cancer. *Gastroint Cancer Res.* (2008) 2(4 Suppl 2):S42–6.
5. Benson BA. American society of clinical oncology recommendations on adjuvant chemotherapy for stage II colon cancer. *J Clin Oncol.* (2004) 22:3408–19. doi: 10.1200/JCO.2004.05.063
6. Johnston GP. Stage II colorectal cancer: to treat or not to treat. *Oncologist.* (2019) 10:332–4. doi: 10.1634/theoncologist.10-5-332
7. Mamounas E, Wieand S, Wolmark N, Bear HD, Atkins JN, Song K, et al. Comparative efficacy of adjuvant chemotherapy in patients with dukes' B versus dukes' C colon cancer: results from four national surgical adjuvant breast and bowel project adjuvant studies (C-01, C-02, C-03, and C-04). *J Clin Oncol.* (1999) 17:1349. doi: 10.1200/JCO.1999.17.5.1349
8. Wolmark N, Rockette H, Mamounas E, Jones J, Wieand S, Wickerham DL, et al. Clinical trial to assess the relative efficacy of fluorouracil and leucovorin, fluorouracil and levamisole, and fluorouracil, leucovorin, and levamisole in patients with dukes' B and C carcinoma of the colon: results from national surgical adjuvant breast. *J Clin Oncol.* (1999) 17:3553. doi: 10.1200/JCO.1999.17.11.3553
9. Labianca R, Nordlinger B, Beretta GD, Mosconi S, Mandala M, Cervantes A, et al. Early colon cancer: ESMO Clinical Practice Guidelines for diagnosis, treatment and follow-up. *Ann Oncol.* (2013) 24(Suppl 6):vi64–72. doi: 10.1093/annonc/mdt354
10. Liu Q, Huang Y, Luo D, Zhang S, Cai S, Li Q, et al. Evaluating the guiding role of elevated pretreatment serum carcinoembryonic antigen levels for adjuvant chemotherapy in stage IIA colon cancer: a large population-based and propensity score-matched study. *Front Oncol.* (2019) 9:37. doi: 10.3389/fonc.2019.00037
11. Fenoglio-Preiser C, Muñoz N, Carneiro F. Pathology and genetics of tumours of the digestive system. *Histopathology.* (2001) 38:585. doi: 10.1046/j.1365-2559.2001.01219.x
12. Green JB, Timmcke AE, Mitchell WT, Hicks TC, Gathright BJJ, Ray JE. Mucinous carcinoma-Just another colon cancer? *Dis Colon Rectum.* (1993) 36:301. doi: 10.1007/BF02050301
13. Consorti F, Lorenzotti A, Midiri G, Di Paola M. Prognostic significance of mucinous carcinoma of colon and rectum: A prospective case-control study. *J Surg Oncol.* (2000) 73:70–4. doi: 10.1002/(SICI)1096-9098(200002)73:2<70::AID-JSO3>3.0.CO;2-J
14. Lee DW, Han S-W, Lee HJ, Rhee Y-Y, Bae JM, Cho N-Y, et al. Prognostic implication of mucinous histology in colorectal cancer patients treated with adjuvant FOLFOX chemotherapy. *Br J Cancer.* (2013) 108:1978–84. doi: 10.1038/bjc.2013.232
15. Hyngstrom JR, Hu C-Y, Xing Y, You YN, Feig BW, Skibber JM, et al. Clinicopathology and outcomes for mucinous and signet ring colorectal adenocarcinoma: analysis from the national cancer data base. *Ann Surg Oncol.* (2012) 19:2814–21. doi: 10.1245/s10434-012-2321-7
16. Kanemitsu Y, Kato T, Hirai T, Yasui K, Morimoto T, Shimizu Y, et al. Survival after curative resection for mucinous adenocarcinoma of the colorectum. *Dis Colon Rect.* (2003) 46:160–7. doi: 10.1007/s10350-004-6518-0
17. Verhulst J, Ferdinande L, Demetter P, Ceelen W. Mucinous subtype as prognostic factor in colorectal cancer: a systematic review and meta-analysis. *J Clin Pathol.* (2011) 65:381–8. doi: 10.1136/jclinpath-2011-200340
18. Kim SH, Shin SJ, Lee KY, Kim H, Kim TI, Kang DR, et al. Prognostic value of mucinous histology depends on microsatellite instability status in patients with stage III colon cancer treated with adjuvant FOLFOX chemotherapy: a retrospective cohort study. *Annals of Surgical Oncology.* (2013) 20:3407–13. doi: 10.1245/s10434-013-3169-1
19. Catalano V, Loupakis F, Graziano F, Bisonni R, Torresi U, Vincenzi B, et al. Prognosis of mucinous histology for patients with radically resected stage II and III colon cancer. *Ann Oncol.* (2012) 23:135–41. doi: 10.1093/annonc/mdr062
20. Hu X, Li YQ, Li QG, Ma YL, Peng JJ, Cai S. Mucinous adenocarcinomas histotype can also be a high-risk factor for stage ii colorectal cancer patients. *Cell Physiol Biochem.* (2018) 47:630–40. doi: 10.1159/000490018
21. Fields AC, Lu P, Goldberg J, Irani J, Bleday R, Melnitchouk N. The role of adjuvant chemotherapy in stage II and III mucinous colon cancer. *J Surg Oncol.* (2019) 120:1190–200. doi: 10.1002/jso.25705
22. Min KK, Won DD, Sun MP, Kim T, Lee IK. Effect of adjuvant chemotherapy on stage II colon cancer: analysis of korean national data. *Cancer Res Treat.* (2017) 50:4. doi: 10.4143/crt.2017.194
23. Babcock BD, Aljehani MA, Jabo B, Choi AH, Morgan JW, Selleck MJ, et al. High-Risk stage II colon cancer: not all risks are created equal. *Ann Surg Oncol.* (2018) 25:1980–5. doi: 10.1245/s10434-018-6484-8
24. Babaei M, Balavarca Y, Jansen L, Lemmens V, van Erning FN, van Eycken L, et al. Administration of Adjuvant Chemotherapy for Stage II-III Colon Cancer Patients: A European Population-based Study. Int J Cancer. (2018) 142:1480–9. doi: 10.1002/ijc.31168
25. Rosati G, Galli F, Cantore M, Bergamo F, Banzi M, Zampino MG, et al. Predictive impact of mucinous tumors on the clinical outcome in patients with poorly differentiated, stage ii colon cancer: a TOSCA subgroup analysis. *Oncologist.* (2020) doi: 10.1634/theoncologist.2019-0736. [Epub ahead of print].
26. Yu D, Gao P, Song Y, Yang Y, Chen X, Sun Y, et al. The differences on efficacy of oxaliplatin in locally advanced colon cancer between mucinous and nonmucinous adenocarcinoma. Cancer Med. (2018) 7:600–15. doi: 10.1002/cam4.1333
27. Negri VF. Mucinous histology predicts for reduced fluorouracil responsiveness and survival in advanced colorectal cancer. *Ann Oncol.* (2005) 16:1305–10. doi: 10.1093/annonc/mdi244
28. Hugen N, Verhoeven RHA, Radema SA, de Hingh IHJT, Pruijt JFM, Nagtegaal ID, et al. Prognosis and value of adjuvant chemotherapy in stage III mucinous colorectal carcinoma. *Ann Oncol.* (2013) 24:2819–24. doi: 10.1093/annonc/mdt378
29. Catalano V, Loupakis F, Graziano F, Torresi U, Bisonni R, Mari D, et al. Mucinous histology predicts for poor response rate and overall survival of patients with colorectal cancer and treated with first-line oxaliplatin- and/or irinotecan-based chemotherapy. *Br J Cancer.* (2009) 100:881–7. doi: 10.1038/sj.bjc.6604955

Conflict of Interest: The authors declare that the research was conducted in the absence of any commercial or financial relationships that could be construed as a potential conflict of interest.

frontiers in Medicine

ORIGINAL RESEARCH
published: 11 November 2020
doi: 10.3389/fmed.2020.596226

Role of Retinoblastoma Protein Family (Rb/p105 and Rb2/p130) Expression in the Histopathological Classification of Borderline Ovarian Tumors

Valeria Masciullo[1†], Paola Valdivieso[1†‡], Giulia Amadio[1], Angela Santoro[2], Giuseppe Angelico[2], Alessandro Sgambato[3], Silvia Boffo[4], Antonio Giordano[4], Giovanni Scambia[1,5] and Gian Franco Zannoni[2,6]*

[1] Unità di Ginecologia Oncologica, Dipartimento Scienze della Salute della Donna, del Bambino e di Sanità Pubblica, Fondazione Policlinico Universitario A. Gemelli IRCCS, Roma, Italy, [2] Unità di Gineco-Patologia e Patologia Mammaria, Dipartimento Scienze della Salute della Donna, del Bambino e di Sanità Pubblica, Fondazione Policlinico Universitario A. Gemelli IRCCS, Roma, Italy, [3] Istituto di Patologia Generale, Università Cattolica del Sacro Cuore, Roma, Italy, [4] Department of Biology, College of Science and Technology, Sbarro Institute for Cancer Research and Molecular Medicine, Temple University, Philadelphia, PA, United States, [5] Istituto di Clinica Ostetrica e Ginecologica, Università Cattolica del Sacro Cuore, Roma, Italy, [6] Istituto di Anatomia Patologica, Università Cattolica del Sacro Cuore, Roma, Italy

Borderline ovarian tumors (BOT) are uncommon but not rare epithelial ovarian neoplasms, intermediate between benign and malignant categories. Emerging knowledge supports the notion that subtypes of borderline ovarian tumors comprise distinct biologic, pathogenetic, and molecular entities, precluding a single unifying concept for BOT. The identification of valuable markers for the diagnosis and classification of these tumors is in need. Among the molecular candidates, the Retinoblastoma (Rb) family members Rb/p105 and Rb2/p130 seem to play a pivotal role in ovarian cancer. In particular, Rb/p105, when in the unphosphorylated form, acts as a growth suppressor controlling cell cycle and tumor progression; whereas, the phosphorylated form activates gene transcription and cellular proliferation. While Rb/p105 is ubiquitously confined to the nuclei of cycling and quiescent cells, Rb2/p130 activity is also regulated by intracellular localization. According to this, Rb family members could represent a novel marker in diagnosis and classification risk for patients with BOT. In this study, we evaluated the expression and subcellular localization of proteins of the retinoblastoma (Rb) gene family in 65 ovarian borderline tumors. Statistically significant differences were found in nuclear and cytoplasmic expressions of Rb/p105 and Rb2/p130 according to different examined histotypes. In detail, the nuclear expression of Rb/p105 and Rb2/p130 was more frequently detected in serous (84.6%) than sero-mucinous (42.1%) and mucinous (50%) types. Conversely, the cytoplasmic expression of Rb2/p130 was not detected in serous tumors and frequently observed in mucinous subtypes (80%). Our findings suggest that Rb proteins do not play a key role in the tumor progression of serous borderline tumors since any cases showed cytoplasmic localization. By contrast, the observed higher cytoplasmic expression of Rb2/p130 in intestinal mucinous BOTs is indicative of Rb

OPEN ACCESS

Edited by:
Renato Franco, University of Campania Luigi Vanvitelli, Italy

Reviewed by:
Sabrina Battista, Consiglio Nazionale Delle Ricerche (CNR), Italy
Serenella Anzilotti, Institute of Research and Medical Care (IRCCS) SDN, Italy

***Correspondence:**
Antonio Giordano
giordano@temple.edu

[†] *These authors have contributed equally to this work*

[‡] ***Present address:***
Paola Valdivieso, Laboratory for Muscle Plasticity, Department of Orthopedics, Balgrist University Hospital, University of Zurich, Zurich, Switzerland

Specialty section:
This article was submitted to Pathology, a section of the journal Frontiers in Medicine

Received: *18 August 2020*
Accepted: *15 October 2020*
Published: *11 November 2020*

Citation:
Masciullo V, Valdivieso P, Amadio G, Santoro A, Angelico G, Sgambato A, Boffo S, Giordano A, Scambia G and Zannoni GF (2020) Role of Retinoblastoma Protein Family (Rb/p105 and Rb2/p130) Expression in the Histopathological Classification of Borderline Ovarian Tumors. Front. Med. 7:596226. doi: 10.3389/fmed.2020.596226

protein family involvement in the cancerogenesis pathway of mucinous ovarian tumors. Also, mucinous BOTs of intestinal-type, exhibiting low nuclear and high cytoplasmic levels of Rb2/p130 might potentially be considered a high-risk category of malignant evolution. Further studies on larger series are needed to clarify how BOTs could be stratified in different prognostic groups according to their Rb proteins immunohistochemical profile.

Keywords: pRb/p105, pRb2/p130, diagnosis, retinoblastoma protein family, borderline ovarian tumors

BACKGROUND

Borderline ovarian tumors (BOTs) represent one of the controversial topics in gynecologic pathology (1). They are a heterogeneous group of tumors that account for 10–20% of all ovarian epithelial neoplasms. The most common BOT histotypes are serous (50%) and mucinous (45%) with less common subtypes (5%) including sero-mucinous, endometrioid, clear cell, and borderline Brenner tumors (2, 3). The 97% of all stages of BOT have a good prognosis with a mean 10-years survival (4), although recurrences and malignant transformation can occur in a very small proportion of cases (5). In contrast to serous BOTs, that are rarely characterized by evolution in a low-grade serous carcinoma whereas are often associated with peritoneal implants and relapses (5), mucinous carcinoma frequently develops from benign and borderline mucinous tumors (6, 7). Similarly, sero-mucinous BOTs are often the land of endometrioid or clear cell carcinoma and usually represent a morphologic continuum in the middle of benign and malignant counterparts.

BOTs often occur in young women, however, the absence of stromal invasion warrants a better prognosis compared to ovarian carcinoma (8, 9). Nevertheless, since the standard treatment of BOTs is usually surgery, the fertility of these women may be affected (10). Identifying the genetic background for diagnosis and prognosis should avoid a radical resection and help in developing new targeted therapies, especially in younger women with a desire for childbearing. Thus, a better understanding of the clinical phenotype and pathogenesis of BOTs would contribute to their earlier detection and is essential for the development of more effective treatments.

Previous studies support the idea that the serous and mucinous BOT have distinct carcinogenic pathways. For example, the expression of p21 and MDM2 differs between mucinous and serous forms (11). In other studies, a higher rate of p53 mutation was observed in mucinous compared to serous BOTs and p21 and bcl-2 overexpression appeared specific to serous forms and different between serous benign, serous BOTs and serous carcinoma (12–14).

The retinoblastoma gene family consists of three members and their products are Rb/p105, Rb2/p130, and RbL1/p107, together known as "pocket proteins" family (15, 16). Their most important target is the E2F-family of transcription factors, which control the expression of genes that mediate G1-S transition (15, 16). The localization of these proteins into the nucleus or around the nuclear membrane has been shown at the molecular level during the different phases of the cell cycle (17, 18). In detail, during the cell progression through the S into the G2/M phases of the division cycle, pRB undergoes phosphorylation, while in the late M phase, pRB is rapidly dephosphorylated. When pRB is in the unphosphorylated form, it acts as a growth suppressor by repressing transcription of E2F. By contrast, the phosphorylated pRB status (p-pRB) leads to the activation of E2F-responsive genes and entry into the S phase. While Rb/p105 is ubiquitously confined to the nuclei of cycling and quiescent cells, Rb2/p130 activity is also regulated by intracellular localization. The phosphorylation status of Rb2/p130 itself, therefore, is important in the regulation of the cell cycle (19). The hyperphosphorylated form of pRb2/p130 is cytoplasmic and typical of cells progressing into the G1 phase (20). Alteration of Rb family members is frequently involved in gynecological cancers (21–23). We previously showed that the loss of Rb2/p130 or its cytoplasmic expression occurs in 40% of ovarian tumors and is inversely correlated with tumor grade (24). However, little is known about Rb proteins expression in borderline ovarian tumors.

In this study, we utilized immunohistochemistry to evaluate the expression pRb/p105 and pRb2/p130 family members in a large, single-institution, and series of mucinous, sero-mucinous and, serous BOTs.

MATERIALS AND METHODS

Data Collection

Sixty-five ovarian BOTs were retrospectively collected from patients who underwent salpingo-oophorectomy for ovarian cancer in the Division of Gynecologic Oncology of the Fondazione Policlinico Universitario A.Gemelli IRCCS, Rome, Italy between 2010 and 2016; all selected patients did not receive chemotherapy or radiotherapy before surgical enucleation. All the subjects gave written informed consent before enrollment. Twenty specimens were defined as mucinous BOTs, 19 were classified as sero-mucinous, whereas 26 cases were classified as serous BOTs. Histological classification of tumors was carried out according to the WHO system, and disease staging was established according to the International Federation of Gynecologists and Obstetricians (FIGO) criteria.

Immunohistochemistry

After surgical resection, tissues were immediately fixed in 10% formalin and then paraffin-embedded for immunohistochemical analysis. The immunostaining was performed using a

Abbreviations: BOT, Borderline Ovarian Tumor; RB, Retinoblastoma; pRb, Retinoblastoma protein product or hypo-phosphorylated form; p-pRb, hyper-phosphorylated form.

streptavidin-biotin complex immunoperoxidase method (DakoCytomation). Detection for the retinoblastoma gene family members was performed using purified mouse anti-human retinoblastoma protein (Rb) monoclonal antibody (BD Pharmigen) diluted 1:50 and mouse monoclonal antibody Rb2 p130 (clone 130-P215; Novus Biologicals, Inc.) diluted 1:25.

Paraffin blocks of each specimen were sectioned at 3 μm, mounted on a slide, and dried overnight at 37°C. All sections were dewaxed in xylene and dehydrated in descending graded alcohols to Phosphate-Buffered Saline (PBS; pH 7.4).

Antigen retrieval was performed by microwaves in a 10 mM citrate buffer (pH 6), at 750 W for 10 min (two cycles of 5 min each), followed by cooling at room temperature for at least 20 min before incubation with the antibodies. Sections were treated with 0.4% H_2O_2 methanol solution (15 min at room temperature to inhibit endogenous peroxidase activity), quickly rinsed in water, and then in PBS.

Sections were then placed in a humidified chamber and incubated with primary antibody at room temperature for 40 min. The sections were then washed in PBS (two times for 5 min each).

Antigen detection was carried out by exposure to a biotinylated universal secondary antibody for 10 min followed by a streptavidin-peroxidase complex working solution for 10 min.

After another PBS wash, the antigen-antibody complex was visualized by staining with the chromogen 3,3′-diaminobenzidine/ tetrachloride solution (DAB, Vector) for 5 min. The sections were rinsed in deionized water; cell nuclei were counterstained with hematoxylin and dehydrated in graded alcohols followed by xylene.

Specimens of human colon cancer, follicular cyst, and fallopian tube served as positive controls for pRb and pRb2, respectively. For negative control, slides were simultaneously incubated with PBS in the absence of the primary antibody. The results were independently reviewed by three experienced pathologists (GFZ, GA, and AS), who were blinded to the clinical outcome at the time of evaluation. Discrepancies in the evaluation (<10% of cases) were resolved by re-observation of the cases using a multi-headed microscope.

For each sample, at least 20 high-power fields were randomly chosen and ∼2,000 cells were counted. Quantitative scoring of protein expression was based on the percentage of positive cells as follows: negative (0%); lower positive (1–30%) or upper positive (>30%) cells). Cases showing a value more than the median (30%) of immunoreactive neoplastic cells were considered as evidence of upper positivity. In this way a cut-off of 30% was considered statistically significant and, therefore, functionally operative.

Statistical Analysis

The associations between Rb proteins staining and other clinic-pathological parameters were analyzed using contingency table methods and tested for significance using the Fisher's exact $\chi 2$ test. All calculations were performed using the Statistical Package for Social Science (SPSS 17.0 software, Chicago, IL) and the result was considered statistically significant when the *P*-value was ≤ 0.05.

RESULTS

Clinic-Pathological Features

The series included 20 mucinous, 19 sero-mucinous, and 26 serous BOTs. The mean and median age of the patients were 44.7 and 44 years (range 20–72), respectively. All mucinous and sero-mucinous selected tumors (39) were stage 1, without

TABLE 1 | Clinical data of the patients with BOTs.

	N° (% of Cases)
Histologic types	
Serous subtype*	26 (40.0)
Sero-Mucinous subtype	19 (29.2)
Mucinous subtype**	20 (30.8)
Stage	
1	59 (90.8)
2	1 (1.5)
3	5 (7.7)
Implants	
Not Implants	59 (90.8)
Implants without invasion	5 (7.7)
Implants with invasion	1 (1.5)
Recurrences	
No	61 (93.8)
Yes	4 (6.2)
Clinical outcome	
Dead	0
Alive	65 (100)

**5 serous BOTs showed micro-invasive foci.*

***1 mucinous BOT showed foci of intraepithelial carcinoma and an area of invasive mucinous carcinoma with expansive pattern of growth.*

TABLE 2 | Nuclear Distribution of Rb/p105-negative and Rb/p105-positive cases according to tumoral characteristics.

Rb/p105 Nuclear	Total	Rb/p105 negative (0%)	Rb/p105 positive (1–30%)	Rb/p105 positive (>30%)	*P*
	N°	N° (%)	N° (%)	N° (%)	
Histologic types	65	25 (38.4)	33 (50.8)	7 (10.8)	
Serous subtype	26	4 (15)	22 (84.6)	0 (15.4.)	<0.0001
Sero-Mucinous subtype	19	11 (57.9)	6 (31.6)	2 (10.5)	
Mucinous subtype	20	10 (50.0)	5 (25.0)	5 (25.0)	
Stage					0.04
1	59	25 (42.3)	27 (45.8)	7 (11.9)	
2+3	6	0	6 (100)	0	
Implants					NS
Absent	59	24 (41.4)	27 (46.5)	7 (12.1)	
Present	6	1 (14.3)	6 (85.7)	(0)	
Recurrences					NS
Absent	61	24 (39.4)	31 (50.8)	6 (9.8)	
Present	4	1 (25.0)	2 (50.0)	1 (25.0)	

Numbers in parentheses represent the percentage of specimens achieving that particular score. NS, not significant.

evidence of implants or recurrences, whereas serous tumors included stage 1 ($n = 20$), stage 2 ($n = 1$), and stage 3 ($n = 5$) cases and follow-up data were available for all 65 patients. Five serous BOTs were classified as BOTs with microinvasive foci. One mucinous BOT showed foci of intraepithelial carcinoma and an area of malignant invasive mucinous carcinoma with an expansive pattern of growth.

Fifty-nine cases were limited to the ovary, without peritoneal implants and six cases (all serous BOTs) were associated with peritoneal implants (only one of invasive type). Sixty-one cases did not relapse; the remaining four developed peritoneal recurrences. By the time this study was undertaken, no patients had died of the disease.

The clinic-pathologic characteristics of patients are summarized in **Table 1**. The expression levels of Rb/p105 and Rb2/p130 were determined by immunohistochemistry.

Correlation of Rb/p105 With Clinic-Pathological Parameters in BOTs

The expression of Rb/p105 according to clinic-pathological parameters is shown in **Table 2**.

Notably, the immune-reactivity for Rb/p105 was only nuclear in our series. Moreover, the nuclear Rb staining in intestinal-type mucinous BOTs tended to concentrate at the bases of the papillary projections (**Figure 1**).

The nuclear expression of Rb/p105 was observed in 40 (61.6%) out of the 65 patients, whereas it was not detectable in the remaining 25 cases (38.4%). The expression of nuclear Rb/p105 was more frequently detected in serous (22 cases; 84.6%) than in serous mucinous (8/19, 42.1%) and mucinous (10/20, 50%) types, and this difference was statistically significant ($P < 0.0001$). Positive staining was observed in 34 (57.6%) out of 59 stages 1 and in all 6 (100 %) stage 2/3 cases and this difference was slightly significant ($p = 0.04$). No statistically significant correlation was observed between the nuclear expression of Rb/p105, implants, and recurrences (**Table 2**).

Correlation of Rb2/p130 Expression With Clinic-Pathological Parameters in BOTs

Nuclear Rb2/p130 expression was detected in 33 (50.8%) of the 65 cases whereas it was absent in the remaining 32 cases (40.2%) (**Figure 2**). The expression of nuclear Rb2/p130 was more frequent in serous (21/26, 80.8%) than in sero-mucinous (10/19, 52.6%) and intestinal (2/20, 1.0%) types and these differences were statistically significant ($P < 0.0001$). Positive staining was observed in 27 (45.7%) out of the 59 stage 1 and in all 6 (100%) stage 2/3 cases and this difference was significant ($p = 0.03$). No statistically significant correlation was observed between the nuclear expression of Rb2/p30, implants, and recurrences (**Table 3A**).

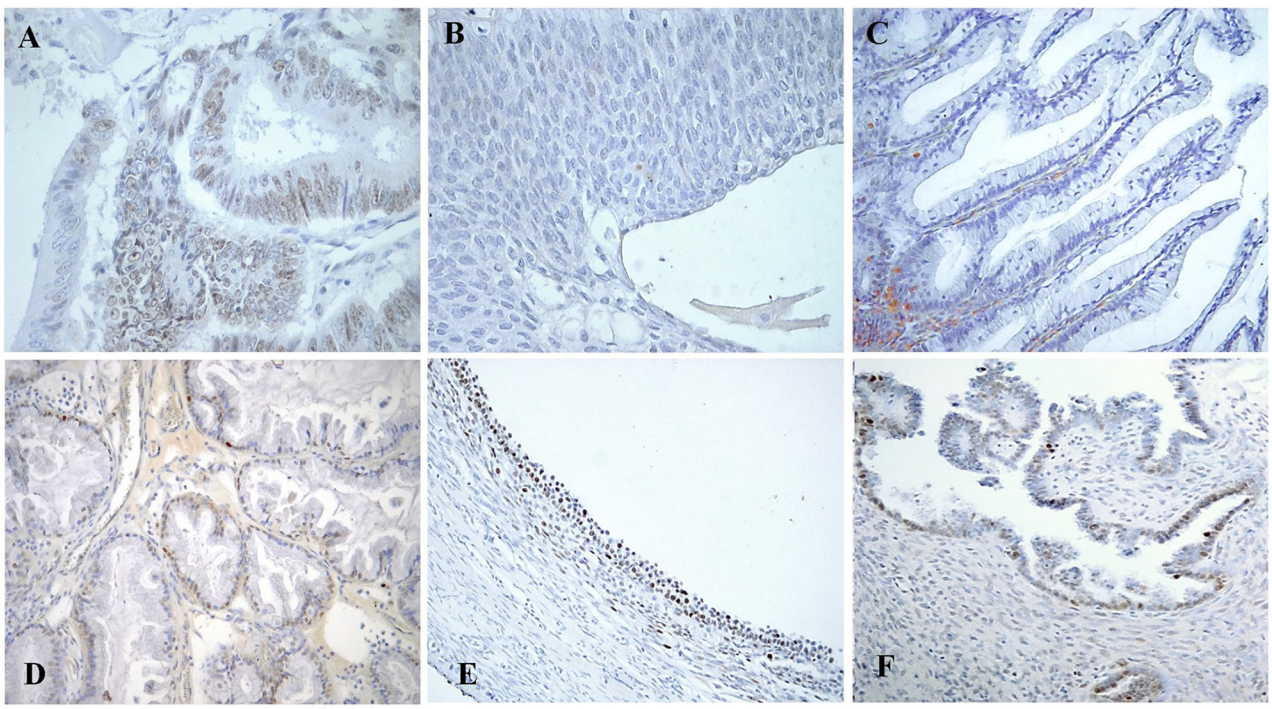

FIGURE 1 | Immunohistochemical staining of Rb/p105 expression in the cells nuclei. **(A)** Colon Carcinoma as positive control for pRb (X400). **(B)** Brenner BOT as negative control for pRb (X400). **(C)** Mucinous BOT of intestinal type showing a concentration of positive nuclei at the base of the papillary projection ("Arrow"; X200). **(D)** Sero-mucinous BOT with intermediate staining of positive nuclei (X200). **(E)** Follicular cyst as an example of internal positive control for pRb (X200). **(F)** Serous BOT with lower pRb staining (X200).

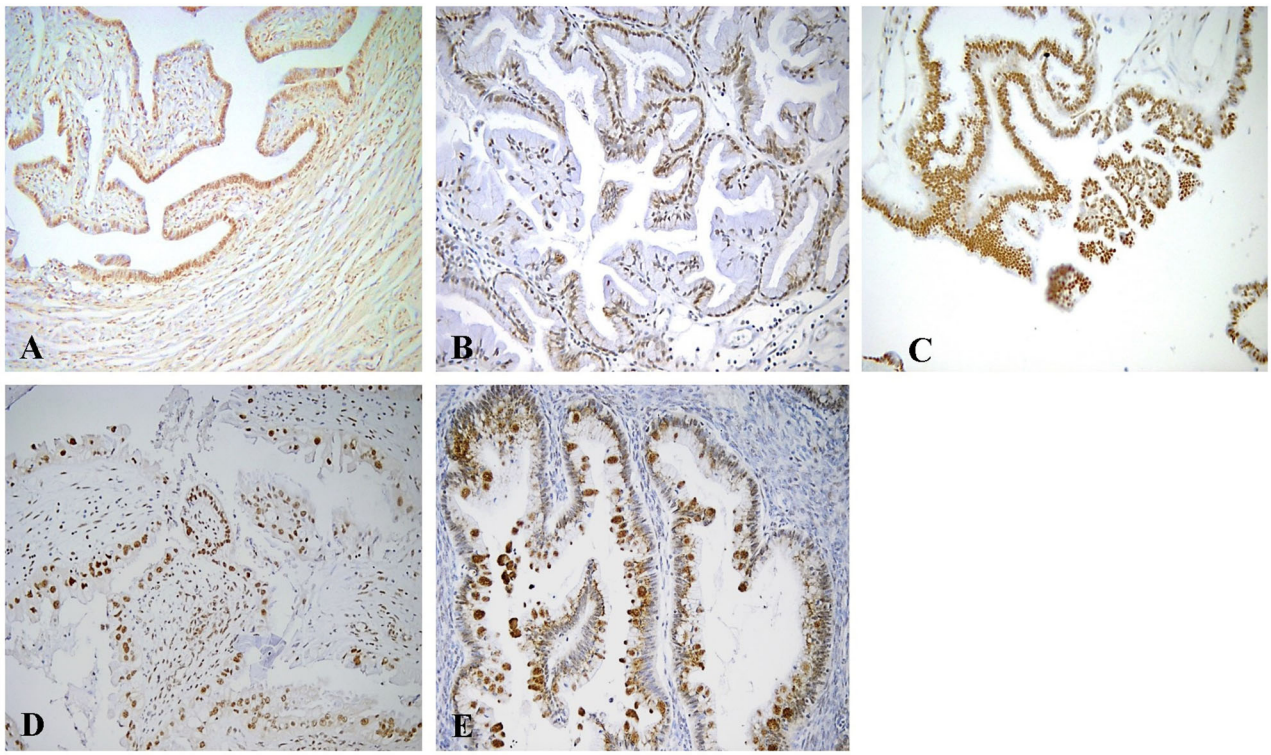

FIGURE 2 | Immunohistochemical staining of Rb2/p130 expression. **(A)** Tube as internal positive control for Rb2/p130 (X100)**. (B)** Mucinous benign tumor with positive nuclei for Rb2/p130 (X200). **(C)** Serous BOT with nuclear Rb2/p130 staining (X200). **(D)** Sero-mucinous BOT with intermediate staining of positive nuclei (X200). **(E)** Mucinous BOT showing cytoplasmic Rb2/p130 staining (X200).

The cytoplasmic expression of Rb2/p130 was detected in 18 (27.7%) cases whereas it was not evident in the remaining 47 cases (72.3%). Unlike nuclear Rb2/p130 expression, the cytoplasmic expression of Rb2/p130 was not detected in serous tumors, rarely detected in sero-mucinous (2/19, 10.6%) and frequently observed in mucinous subtypes (16/20, 80%) (**Figure 3**); this difference was statistically significant ($P < 0.0001$). The cytoplasmic expression of Rb2/p130 according to clinic-pathological parameters is shown in **Table 3B**. In **Figure 4** we have shown Rb/p130 immunohistochemistry in an intestinal-type mucinous ovarian tumor composed of benign, borderline, and malignant areas. Notably, the Rb2/p130 expression moves from nuclear expression in the benign counterpart to nuclear-cytoplasmic in the BOT counterpart and cytoplasmic in the malignant counterpart (**Figures 4A,B**).

DISCUSSION

Borderline ovarian tumors (BOTs) represent about 15% to 20% of all ovarian malignancies and differ from invasive ovarian cancers by many characters (1, 2). On the one hand, they are characterized by cellular proliferation and nuclear atypia but, on the other hand, they usually do not show an infiltrative growth pattern (2). Recent knowledge supports the notion that subtypes of borderline ovarian tumors comprise distinct biologic, pathogenetic, and molecular entities, precluding a single unifying concept for BOT (2). Serous borderline tumors (SBT) share molecular and genetic alterations with low-grade serous carcinomas and can present at higher stages with peritoneal implants and/or lymph node involvement, which validates their borderline malignant potential (5). All other (non-serous) subtypes of BOT commonly present at stage I are confined to the ovary(ies) and are associated with overall survival approaching that of the general population (6, 7).

The retinoblastoma (Rb) gene family includes Rb2/p130, RB/p105, and p107 genes, which encode nuclear proteins (pRB) acting as negative regulators of cell proliferation, when in their dephosphorylated status (15, 16). Alteration of Rb family members is frequently involved in gynecological cancers (21–23).

Dong et al., in a series of 168 specimens, demonstrated high pRb expression in 41% percent of the benign, 50% of the borderline, and 71% of the malignant tumors; in this study, protein accumulation increased progressively with poorer differentiation and there was a trend for high pRb expression to be associated with an advanced stage of disease (14). Additionally, Milde-Langosch et al. demonstrated a correlation between higher pRb expression and shorter survival suggesting thus that pRb expression could play a role in early tumorigenesis, while in later stages, the tumor is independent of pRb (25).

TABLE 3A | Nuclear distribution of Rb2/p130-negative and Rb2/p130-positive cases according to tumoral characteristics.

Rb2/p130 Nuclear	Total	Rb2/p130 negative (0%)	Rb2/p130 positive (1–30%)	Rb2/p130 positive (>30%)	*P*
	N°	N° (%)	N° (%)	N° (%)	
Histologic types					<0.0001
Serous subtype	26	5 (19.2)	7 (26.9)	14 (53.9)	
Sero-Mucinous subtype	19	9 (47.4)	5 (26.3)	5 (26.3)	
Mucinous subtype	20	18 (90.0)	2(10.0)	0	
Stage					0.03
1	59	32 (54.3)	12 (20.3)	15 (25.4)	
2+3	6	0	2 (33.3)	4 (66.7)	
Implants					NS
Absent	59	31 (53.4)	12 (20.7)	15 (25.9)	
Present	6	1 (14.3)	2 (28.6)	4 (57.1)	
Recurrences					NS
Absent	61	30 (49.2)	12 (19.7)	19 (31.1)	
Present	4	2 (50.0)	2 (50.0)	0	

Numbers in parentheses represent the percentage of specimens achieving that particular score. NS, not significant.

TABLE 3B | Cytoplasmic distribution of Rb2/p130-negative and Rb2/p130-positive cases according to histologic types.

Rb2/p130 Cytoplasmatic	Total	Rb2/p130 negative (0%)	Rb2/p130 positive (1–30%)	Rb2/p130 positive (>30%)	*P*
	N°	N° (%)	N° (%)	N° (%)	
Histologic types					<0.0001
Serous subtype	26	26 (100)	0	0	
Sero-Mucinous subtype	19	17 (89.4)	1 (5.3)	1 (5.3)	
Mucinous subtype	20	4 (20.0)	7 (35.0)	9 (45.0)	

Numbers in parentheses represent the percentage of specimens achieving that particular score.

Other authors reported significantly lower pRb levels in low malignant potential ovarian tumors (LMP) than in carcinomas and in this latter group, a reduction of pRb expression with increasing grade, advancing stage and bulk residual disease; in their study, a low pRb to Ki-67 ratio appeared as an indicator of poor survival in uni- and multivariate analysis, along with the histologic type and FIGO stage (26).

We were the first to demonstrate that loss of Rb2/p130 or its cytoplasmic expression occurs in 40% of ovarian tumors and are inversely correlated with tumor grade (24). This has been confirmed by Worley MJ et al. who evaluated the immunohistochemical Rb2/p130 expression in a series of benign, borderline (SBT), and malignant ovarian tumors (low-grade (LGSC) and high-grade (HGSC) serous carcinoma), demonstrating a significant decrease in Rb2/p130 expression during the progression from cystadenoma to SBT to LGSC. They reported no loss of expression in benign forms, whereas 10% of SBTs, 47% of LGSCs, and 16% of HGSCs had a loss of expression (27).

Differences in additional molecular markers support the idea that the serous BOTs are histologically and clinically distinct from the mucinous BOTs. For example, the expression of p21 and MDM2 differs between mucinous and serous LMP tumors (11). In other studies, a higher rate of p53 mutation was observed in mucinous relative to serous BOTs, and p21 and bcl-2 overexpression appeared specific to serous BOTs and differences among benign, borderline and malignant forms (12, 13).

In the present study, the observed differences in the expression of pRb/p105 and pRb2/p130 between serous, sero-mucinous, and mucinous BOTs supports the concept that these tumors follow different pathogenic pathways. In our series, the nuclear expression of Rb/p105 and pRb2/p130 was highly detected in serous (84.6%) compared to sero-mucinous (42.1%) and mucinous (50%) types. On the other hand, the cytoplasmic expression of Rb2/p130 was not detected in serous tumors but frequently observed in mucinous subtypes (80%). Our findings suggest that both pRb and pRb2/p130 do not play a key role in the tumor progression of serous borderline tumors since these proteins remain located in the nucleus and never showed cytoplasmic localization.

By contrast, the observed higher cytoplasmic expression of Rb2/p130 in mucinous BOTs, is suggestive of the involvement of Rb proteins in the carcinogenesis of mucinous ovarian tumors. To furtherly support our hypothesis, in **Figure 4** we have shown pRb2/p130 immunohistochemistry in an intestinal-type mucinous ovarian tumor composed of benign, borderline, and malignant areas. Notably, the Rb2/p130 expression moves from nuclear expression in the benign counterpart, to nuclear-cytoplasmic in the BOT counterpart and cytoplasmic in the malignant counterpart.

Despite no statistically significant relationships between pRb immunohistochemistry and prognosis have been observed, our results may suggest that mucinous BOTs, exhibiting low nuclear and high cytoplasmic levels of Rb2/p130, may potentially be considered the BOT histotype with a higher carcinogenic risk. In fact, loss of pRb2/p130 expression has been previously reported to inversely correlate with tumor grade and to be a poor prognostic indicator in several human cancers (14, 16, 18). Moreover, its cytoplasmic localization, which implicates a loss of function, has been observed in several tumor types, including lymphoma and gastric cancer (28).

On the other hand, the normal pRb2/p130 nuclear localization, as more frequently observed in our series for serous and sero-mucinous BOT histotypes, enables its oncosuppressive function through the interaction with the E2F4 and E2F5 transcription factors.

CONCLUSION

In conclusion, we have demonstrated a specific histology-related Rb proteins profile of serous, sero-mucinous, and mucinous borderline tumors.

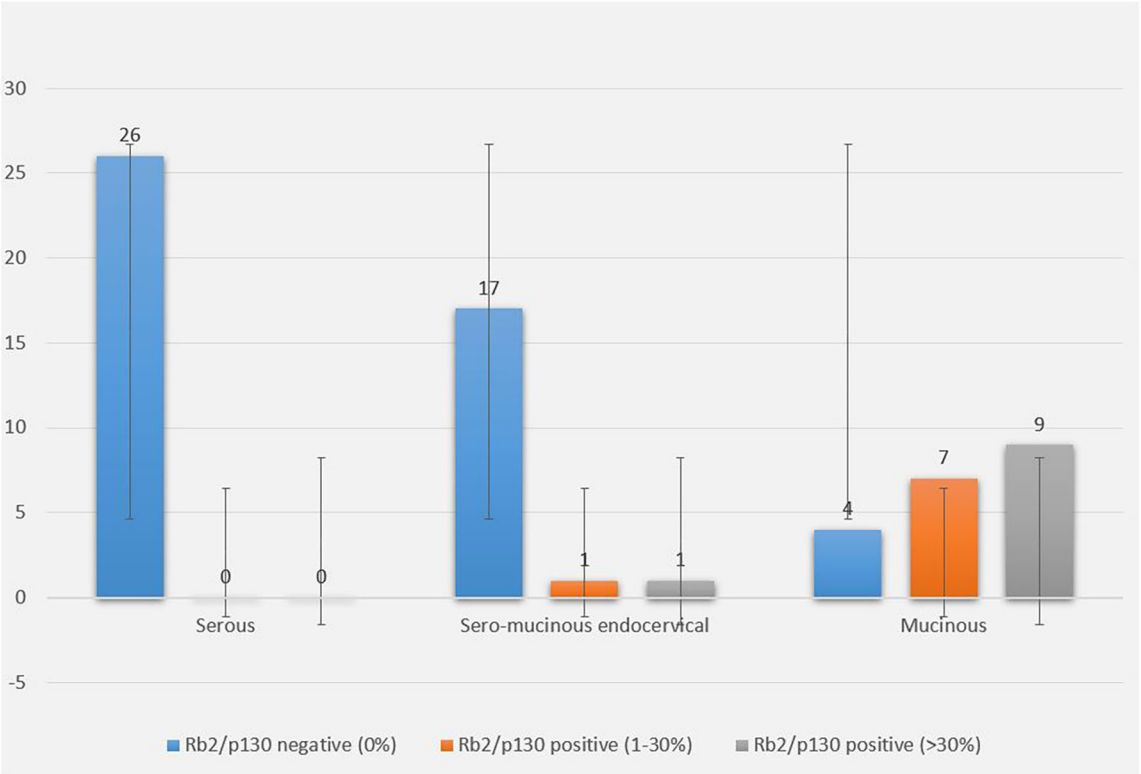

FIGURE 3 | Rb2/p130 cytoplasmic expression in BOTs. The graph shows cytoplasmic distribution of Rb2/p130 expression according to histologic types, with focus on the percentage of stained neoplastic cells.

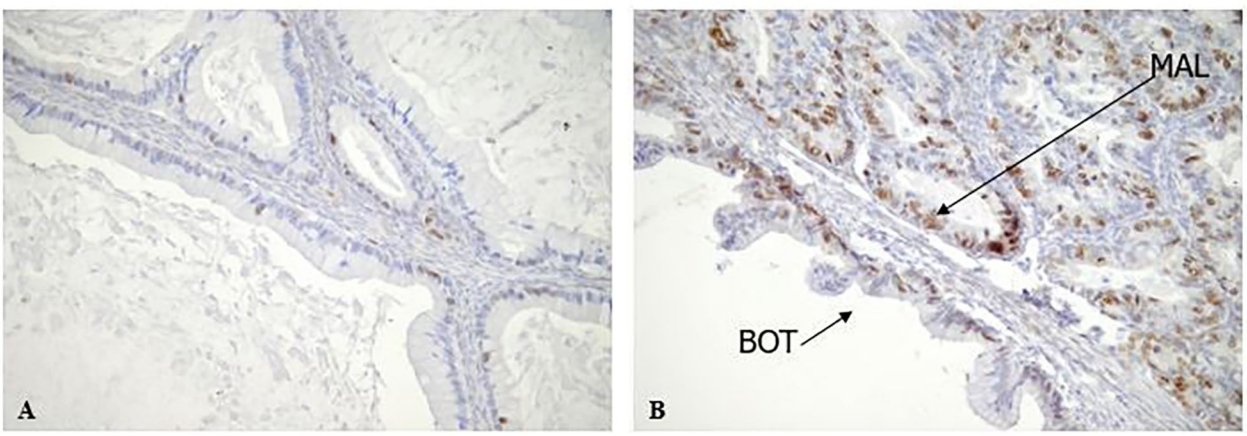

FIGURE 4 | Rb2/p130 expression in Mucinous BOTs. **(A,B)** Rb2/p130 expression shows a mix of patterns, in a mucinous BOT including combination of benign, borderline and invasive carcinoma. In particular Rb2/p130 expression is nuclear in benign area (A, X200) and nuclear-cytoplasmic in borderline component (B, X200); cytoplasmic positivity has been observed in invasive carcinoma (B, X200).

Our findings indicate a clear role of pRb2/p130 protein in the tumor progression of intestinal-type mucinous BOTs thus suggesting a possible role of Rb proteins as prognostic factors in ovarian cancer.

Further studies on larger series are needed in order to clarify how BOTs could be stratified in different prognostic groups according to their pRb immunohistochemical profile.

DATA AVAILABILITY STATEMENT

The original contributions presented in this study are included in the article/supplementary materials, further inquiries can be directed to the corresponding author/s.

ETHICS STATEMENT

The studies involving human participants were reviewed and approved by Fondazione Policlinico Universitario A. Gemelli IRCSS - Universita' Cattolica del Sacro Cuore, Roma, Italia. The patients/participants provided their written informed consent to participate in this study.

AUTHOR CONTRIBUTIONS

VM and GZ: study conceptualization and methodology design. GAn, ASa, GS, and PV: formal analysis and the original draft preparation. GAn, ASa, GAm, ASg, PV, SB, and AG: review and editing. All authors contributed to the article and approved the submitted version.

ACKNOWLEDGMENTS

This manuscript has been released as a pre-print at Research Square (29).

REFERENCES

1. Seidman JD, Kurman RJ. Ovarian serous borderline tumors: a critical review of the literature with emphasis on prognostic indicators. *Hum Pathol*. (2000) 31:539–57. doi: 10.1053/hp.2000.8048
2. Hauptmann S, Friedrich K, Redline R, Avril S. Ovarian borderline tumors in the 2014 WHO classification: evolving concepts and diagnostic criteria. *Virchows Arch*. (2017) 470:125–42. doi: 10.1007/s00428-016-2040-8
3. Siriaunkgul S, Robbins KM, McGowan L, Silverberg SG. Ovarian mucinous tumors of low malignant potential: a clinicopathologic study of 54 tumors of intestinal and mullerian type. *Int J Gynecol Pathol*. (1995) 14:198–208. doi: 10.1097/00004347-199507000-00002
4. Sherman ME, Mink PJ, Curtis R, Cote TR, Brooks S, Hartge P, et al. Survival among women with borderline ovarian tumors and ovarian carcinoma: a population-based analysis. *Cancer*. (2004) 100:1045–52. doi: 10.1002/cncr.20080
5. Kurman RJ, Trimble CL. The behavior of serous tumors of low malignant potential: are they ever malignant? *Int J Gynecol Pathol*. (1993) 12:120–7. doi: 10.1097/00004347-199304000-00006
6. Lee KR, Scully RE. Mucinous tumors of the ovary: a clinicopathologic study of 196 borderline tumors (of intestinal type) and carcinomas, including an evaluation of 11 cases with 'pseudomyxoma peritonei'. *Am J Surg Pathol*. (2000) 24:1447–64. doi: 10.1097/00000478-200011000-00001
7. Riopel MA, Ronnett BM, Kurman RJ. Evaluation of diagnostic criteria and behavior of ovarian intestinal-type mucinous tumors: atypical proliferative (borderline) tumors and intraepithelial, microinvasive, invasive, and metastatic carcinomas. *Am J Surg Pathol*. (1999) 23:617–35. doi: 10.1097/00000478-199906000-00001
8. Hart WR. Borderline epithelial tumors of the ovary. *Mod Pathol*. (2005) 18(Suppl. 2):S33–50. doi: 10.1038/modpathol.3800307
9. Prat J. Pathology of borderline and invasive cancers. *Best Pract Res Clin Obstet Gynaecol*. (2017) 41:15–30. doi: 10.1016/j.bpobgyn.2016.08.007
10. du Bois A, Trillsch F, Mahner S, Heitz F, Harter P. Management of borderline ovarian tumors. *Ann Oncol*. (2016) 27(Suppl. 1):i20–2. doi: 10.1093/annonc/mdw090
11. Palazzo JP, Monzon F, Burke M, Hyslop T, Dunton C, Barusevicius A, et al. Overexpression of p21WAF1/CIP1 and MDM2 characterizes serous borderline ovarian tumors. *Hum Pathol*. (2000) 31:698–704. doi: 10.1053/hupa.2000.7641
12. Lee JH, Kang YS, Park SY, Kim BG, Lee ED, Lee KH, et al. p53 mutation in epithelial ovarian carcinoma and borderline ovarian tumor. *Cancer Genet Cytogenet*. (1995) 85:43–50. doi: 10.1016/0165-4608(95)00116-6
13. Fauvet R, Dufournet C, Poncelet C, Uzan C, Hugol D, Darai E. Expression of pro-apoptotic (p53, p21, bax, bak and fas) and anti-apoptotic (bcl-2 and bcl-x) proteins in serous vs. mucinous borderline ovarian tumours. *J Surg Oncol*. (2005) 92:337–43. doi: 10.1002/jso.20424
14. Dong Y, Walsh MD, McGuckin MA, Cummings MC, Gabrielli BG, Wright GR, et al. Reduced expression of retinoblastoma gene product (pRB) and high expression of p53 are associated with poor prognosis in ovarian cancer. *Int J Cancer*. (1997) 74:407–15. doi: 10.1002/(sici)1097-0215(19970822)74:4<407::aid-ijc8>3.0.co;2-z
15. Claudio PP, Howard CM, Baldi A, De Luca A, Fu Y, Condorelli G, et al. p130/pRb2 has growth suppressive properties similar to yet distinctive from those of retinoblastoma family members pRb and p107. *Cancer Res*. (1994) 54:5556–60.
16. Paggi MG, Baldi A, Bonetto F, Giordano A. Retinoblastoma protein family in cell cycle and cancer: a review. *J Cell Biochem*. (1996) 62:418–30. doi: 10.1002/(SICI)1097-4644(199609)62:3%3C418::AID-JCB12%3E3.0.CO;2-E
17. Claudio PP, De Luca A, Howard CM, Baldi A, Firpo EJ, Koff A, et al. Functional analysis of pRb2/p130 interaction with cyclins. *Cancer Res*. (1996) 56:2003–8.
18. Mileo AM, Mattarocci S, Matarrese P, Anticoli S, Abbruzzese C, Catone S, et al. Hepatitis C virus core protein modulates pRb2/p130 expression in human hepatocellular carcinoma cell lines through promoter methylation. *J Exp Clin Cancer Res*. (2015) 34:140. doi: 10.1186/s13046-015-0255-1
19. Cicchillitti L, Fasanaro P, Biglioli P, Capogrossi MC, Martelli F. Oxidative stress induces protein phosphatase 2A-dependent dephosphorylation of the pocket proteins pRb, p107, and p130. *J Biol Chem*. (2003) 278:19509–17. doi: 10.1074/jbc.M300511200
20. Verona R, Moberg K, Estes S, Starz M, Vernon JP, Lees JA. E2F activity is regulated by cell cycle-dependent changes in subcellular localization. *Mol Cell Biol*. (1997) 17:7268–82. doi: 10.1128/MCB.17.12.7268
21. Sanseverino F, Torricelli M, Petraglia F, Giordano A. Role of the retinoblastoma family in gynecological cancer. *Cancer Biol Ther*. (2003) 2:636–41. doi: 10.4161/cbt.2.6.679
22. Susini T, Massi D, Paglierani M, Masciullo V, Scambia G, Giordano A, et al. Expression of the retinoblastoma-related gene Rb2/p130 is downregulated in atypical endometrial hyperplasia and adenocarcinoma. *Hum Pathol*. (2001) 32:360–7. doi: 10.1053/hupa.2001.23514
23. Zamparelli A, Masciullo V, Bovicelli A, Santini D, Ferrandina G, Minimo C et al. Expression of cell-cycle-associated proteins pRB2/p130 and p27kip in vulvar squamous cell carcinomas. *Hum Pathol*. (2001) 32:4–9. doi: 10.1053/hupa.2001.20371
24. D'Andrilli G, Masciullo V, Bagella L, Tonini T, Minimo C, Zannoni GF, et al. Frequent loss of pRb2/p130 in human ovarian carcinoma. *Clin Cancer Res*. (2004) 10:3098–103. doi: 10.1158/1078-0432.CCR-03-0524
25. Milde-Langosch K, Hagen M, Bamberger AM, Löning T. Expression and prognostic value of the cell-cycle regulatory proteins, Rb, p16MTS1, p21WAF1, p27KIP1, cyclin E, and cyclin D2, in ovarian cancer. *Int J Gynecol Pathol*. (2003) 22:168–74. doi: 10.1097/00004347-200304000-00009
26. Konstantinidou AE, Korkolopoulou P, Vassilopoulos I, Tsenga A, Thymara I, Agapitos E, et al. Reduced retinoblastoma gene protein to Ki-67 ratio is an adverse prognostic indicator for ovarian adenocarcinoma patients. *Gynecol Oncol*. (2003) 88:369–78. doi: 10.1016/S0090-8258(02)00092-6

27. Worley MJ Jr., Landen CN, Slomovitz BM, Malpica A, Palla SL, Ramirez PT. Expression of the retinoblastoma-related gene Rb2/p130 in the pathogenesis of serous carcinoma of the ovary. *Appl Immunohistochem Mol Morphol*. (2010) 18:509–11. doi: 10.1097/PAI.0b013e3181e78fe0
28. Cito L, Pentimalli F, Forte I, Mattioli E, Giordano A. Rb family proteins in gastric cancer (review). *Oncol Rep*. (2010) 24:1411–8. doi: 10.3892/or_00001000
29. Masciullo V, Valdivieso P, Amadio G, Santoro A, Angelico G, Sgambato S, et al. Role of retinoblastoma protein family (Rb/P105 And Rb2/P130) expression in the hystopathological classification of borderline ovarian tumors. Preprint. (2020). doi: 10.21203/rs.3.rs-48452/v1

Conflict of Interest: The authors declare that the research was conducted in the absence of any commercial or financial relationships that could be construed as a potential conflict of interest.

frontiers in Medicine

ORIGINAL RESEARCH
published: 03 December 2020
doi: 10.3389/fmed.2020.615080

Serous Effusions Diagnostic Accuracy for Hematopoietic Malignancies: A Cyto-Histological Correlation

Jinnan Li, Sha Zhao, Wenyan Zhang, Yong Jiang, Xianglan Zhu, Xueqin Den, Weiping Liu and Xueying Su**

Department of Pathology, West China Hospital of Sichuan University, Chengdu, China

OPEN ACCESS

Edited by:
Renato Franco, University of Campania Luigi Vanvitelli, Italy

Reviewed by:
Andrea Ronchi, University of Campania Luigi Vanvitelli, Italy
Fernando Schmitt, University of Porto, Portugal

****Correspondence:***
Xueying Su
xueying.su@icloud.com
Weiping Liu
liuweiping2001@vip.sina.com

Specialty section:
This article was submitted to Pathology, a section of the journal Frontiers in Medicine

Received: *08 October 2020*
Accepted: *09 November 2020*
Published: *03 December 2020*

Citation:
Li J, Zhao S, Zhang W, Jiang Y, Zhu X, Den X, Liu W and Su X (2020) Serous Effusions Diagnostic Accuracy for Hematopoietic Malignancies: A Cyto-Histological Correlation. Front. Med. 7:615080. doi: 10.3389/fmed.2020.615080

Background: The aim of this study was to establish the liability of cytological diagnostic and, along with ancillary techniques, to sub-classify hematopoietic malignancies in serous effusions.

Methods: We retrospectively reviewed the serous effusions of hematopoietic malignancies over an 11-year period, along with ancillary studies, clinical and histological data. We compared cytological along with histological diagnosis to evaluate the value of cytology itself. Furthermore, the discrepant cases were reviewed.

Results: In this study, a total of 242 cases were identified as hematopoietic malignancies. Ancillary technologies were performed: in 24 cases FCM, 242 cases ICC, 35 cases ISH, 81 cases PCR and 10 cases FISH. Cyto-histological correlation was available for 122 cases. The subtyping of hematopoietic malignancies was achieved using cytological material in 65/122 cases (53.3%). Of the 65 cases, T-Acute lymphoblastic leukemia/lymphoma (22.1%) was the leading subtype, followed by Burkitt lymphoma (5.7%), plasmacytoma (5.7%). Cyto-histological correlation showed a 100% concordant rate of diagnosis for hematopoietic malignancies and a high degree of agreement on sub-classification (51.6%). In this regard, T-acute lymphoblastic leukemia/lymphoma, plasmacytoma, extranodal NK/T-cell lymphoma, nasal type, anaplastic large cell lymphoma, myeloid sarcoma, and follicular lymphoma showed the highest degree of agreement (100%). The sub-classification on cytology was achieved in 53 out of the remaining 120 cases without histological diagnosis (44.2%). T-acute lymphoblastic leukemia/lymphoma (20.8%) was again the most frequently encountered subtype, followed by plasmacytoma (5.8%) and Burkitt lymphoma (4.2%).

Conclusions: This large series study provided evidence that combining cytology and ancillary studies enabled the accurate serous effusions cytological diagnoses and subsequent sub-classification for the described malignancies.

Keywords: hematopoietic malignancies, serous effusions, ancillary studies, cytology, cyto-histological correlation

INTRODUCTION

Hematopoietic malignancies (HM) are common causes of malignant serous effusions (SE), which suggest advanced stage of disease and poor prognosis (1, 2). In malignant SE caused by HM, cytology remains the first-line, cost effective and rapid diagnostic method. Some previous studies evaluated the diagnostic value of SE cytology for HM, and a few of them analyzed the sub-classification (3–6). However, no studies involved cyto-histological correlation with WHO classification criteria. The objective of the current study is to investigate the diagnostic value of SE cytology for HM, by doing a cyto-histological correlation. Furthermore, the reasons of discrepancy are analyzed. Our experience of SE cytological diagnosis of an HM is also summarized. The main finding of this study, includes a proposal of a further appropriate approach for accurate diagnosis of HM, in SE, and proves the value of cytology for the HM described, as well as their sub-classification.

MATERIALS AND METHODS

Study Cases

Archives of the pathology department of West China Hospital of Sichuan University, from 2008 to 2019, were researched for HM with SE. The diagnoses were in accordance with WHO classification of Tumors of Haematopoietic and Lymphoid Tissue (2008/2017) criteria (7, 8).

Flow Chart of Cytological Diagnosis

The conventional smears and SurePath, liquid-based preparation slides (BD, Franklin Lakes, NJ) or cell blocks, were prepared for all cases. Papanicolaou staining was performed on alcohol-fixed smears and liquid-based preparation slides. Diff-Quick staining was performed on air-dry slides in some cases. Haematoxylin and eosin stain (HE) staining was performed on cell block sections. Paraffin-embedded (FFPE) cell blocks or formalin-fixed liquid-based preparation slides were used for ancillary studies. The remaining fresh material was stored at 4°C. The flowchart was summarized in **Figure 1**. Cytomorphological assessment of all samples was performed within 24 h. An immediate flow cytometry (FCM) analysis was performed on SE submitted with either clinical or cytomorphological suspicion of HM. Abnormal cases indentified by FCM were submitted for further immunocytochemistry (ICC) and/or molecular assays.

Immunophenotyping

FCM was performed by six-color immunofluorescent staining. The initial evaluation of the samples was based on a screening panel of three tubes with the appropriate combination of the following commercially available fluorescence-labeled antibodies: CD2, CD3, CD4, CD5, CD7, CD8, CD10, CD19, CD20, CD30, CD38, CD45, CD56, kappa light chain, and lambda light chain. More specific markers were applied in cases with abnormal findings. Data acquisition and analysis were performed using CellQuest software (Becton Dickinson).

ICC was performed on either SurePath preparation slides or cell block sections using the Envision method. The panel of specific markers depended on cytomorphology and/or result of FCM. The following antibodies were used: CD3ε, CD5, CD20, CD45RO, CD10, CD56, CD30, CD79a, CD99, CD138, BCL2, BCL6, MUM1, MYC, SOX11, ALK, GZM-B, TIA-1, TdT, CCND1, MPO, PC, and Ki-67.

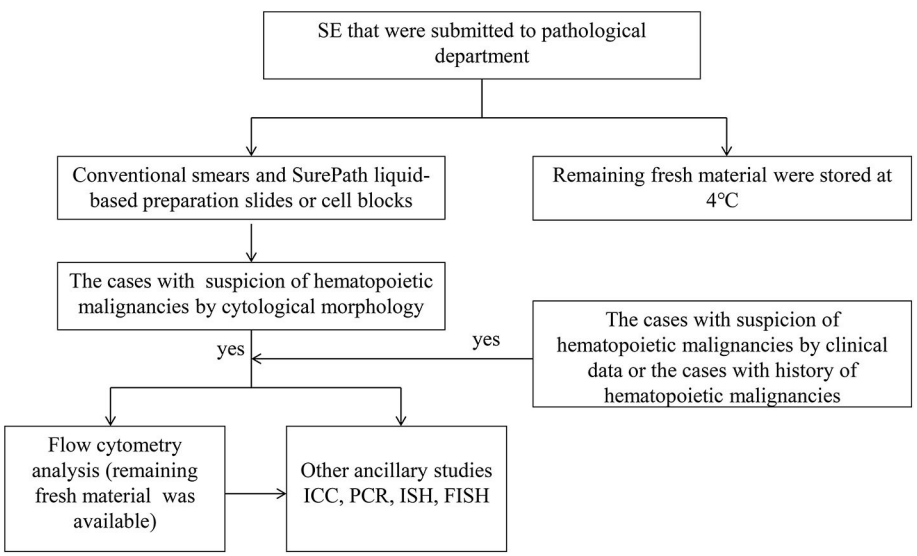

FIGURE 1 | Diagnostic approach of HM in SE recommended. SE indicates serous effusion; ICC, immunohistochemistry; PCR, polymerase chain reaction; ISH, *in situ* hybridization; FISH, fluorescence *in situ* hybridization.

TABLE 1 | Characteristics of patients and samples.

Patient characteristics	No. of patients (%)
Sex	
Male	157 (64.9%)
Female	85 (35.1%)
Age, year	2–91
Mean	47.2
Previous history of hematopoietic malignancies	
Yes	39 (16.1%)
No	53 (83.9%)
Location of effusions	
Pleural	188 (77.7%)
Peritoneal	49 (20.2%)
Pericardial	5 (2.1%)
Cell block or SurePath	
Cell block	211 (87.2%)
SurePath	31 (12.8%)

In situ Hybridization (ISH) for Epstein-Barr Virus (EBV) Encoded RNA

ISH was carried out with a fluorescein-labeled oligonucleotide probe complementary for 2 EBV-encoded small RNAs, EBER-1 and EBER-2 (EBER1/2) (Dako-Y520001). Rabbit anti-FITC antibody conjugated with alkaline phosphatase (AP) (Dako, Denmark) was used to combine with the probe, while NBT/BCIP was used as a substrate. The hybridizing signal located in the cell nucleus.

PCR Assays

Genomic DNA, from FFPE cell blocks, was extracted by phenol-chloroform procedures. PCR analysis of B-cell and T-cell clonality by following the previous reported protocol (9).

Fluorescence *In situ* Hybridization (FISH) Analysis

FISH analysis was carried out on the cell block sections, using probes specific for rearrangement detection. The following probes were used: Vysis LSI *BCL6* dual-color break-apart, Vysis LSI *BCL2* dual-color break-apart, Vysis LSI *MYC* dual-color break-apart, Vysis LSI *IGH/BCL2* dual-color and dual fusion probes. The hybridization protocol and the scoring criteria used for the assays have been published previously (10).

RESULTS

Clinical Manifestations

A total of 188 pleural fluids, 49 ascites and 5 pericardial fluids from 242 patients (157 males, 85 females) were diagnosed as HM. The clinicopathologic data was listed in **Table 1**. The mean patient age was 47.2 years-old (range 2–91 years). The SE samples represented the initial source of diagnosis in 167/242 patients (69.0%). The histological diagnoses were available for 122 cases (50.4%). For this group, the SE samples represented the initial source of diagnosis in 47/122 cases (38.5%). There were 36 cases (36/122, 29.5%) with concurrent histopathological biopsy. The remaining 39 patients (39/122, 32.0%) had previous histological diagnoses of HM.

Evaluation of Cytomorphology

There were cytomorphological features which provided clues for the diagnosis of HM: medium to large-sized atypical lymphocytes (**Figure 2A**), unexplainable immature lymphocytes (hand mirror-shaped blasts) (**Figure 2B**), irregular lymphocytes (**Figure 2G**), prominent mitotic figures and unexplainable apoptosis (**Figures 2C,G**), uniformed and diffused lymphocytes (**Figures 3A,B**).

ANCILLARY STUDIES

FCM and ICC

FCM was performed in 24 samples and identified 15 B-cell lymphomas, 7 T-cell lymphomas and 2 NK/T-cell lymphomas. ICC (**Figures 2D–F,H**) was achieved in all the cases and revealed 156 B-cell lymphomas (64.5%), 74 T-cell lymphomas (30.6%), 6 NK/T-cell lymphomas (2.5%), 3 myeloid neoplasm (1.2%) and 3 precursor lymphoid neoplasm (1.2%) (Cell lineage was unclassified).

ISH for EBV Encoded RNA

Thirty-five samples were submitted for EBER1/2 analysis (**Figure 2I**), and positive staining was demonstrated in 8/35 cases (22.9%).

PCR Assays

PCR analysis for B-cell and/or T-cell monoclonality was performed in 81 samples. A total of 72 positive cases, including 49 cases with B-cell monoclonality, 17 cases with T-cell monoclonality and 6 cases with both B and T-cell monoclonality, were identified. The remaining 9 negative cases, included: 2 without B-cell monoclonality, 5 without T-cell monoclonality and 2 without both B-cell and T-cell monoclonality.

FISH Analysis

FISH analysis was performed in 10 cases. There were 8 positive cases: 4 with both *IGH/MYC* and *MYC* rearrangements, 1 with isolated *MYC* rearrangement, 1 with isolated *IGH/MYC* rearrangement and 2 with both *MYC* and *BCL2* rearrangements (**Figures 3C–F**). For the 2 remaining cases no rearrangements were found.

CYTOLOGICAL DIAGNOSES

Group of Patients With Histological Correlation (122 Cases)

The cytological diagnoses of 78 B-cell lymphomas, 35 T-cell lymphomas, 6 NK/T-cell lymphomas, 2 myeloid neoplasms and 1 ALL/LBL, were established according to cytomorphology and ancillary studies. The specific subtyping of HM was achieved in 65/122 cases (53.3%). Of these 65 cases, T-acute lymphoblastic leukemia/lymphomas (T-ALL/LBL) was the

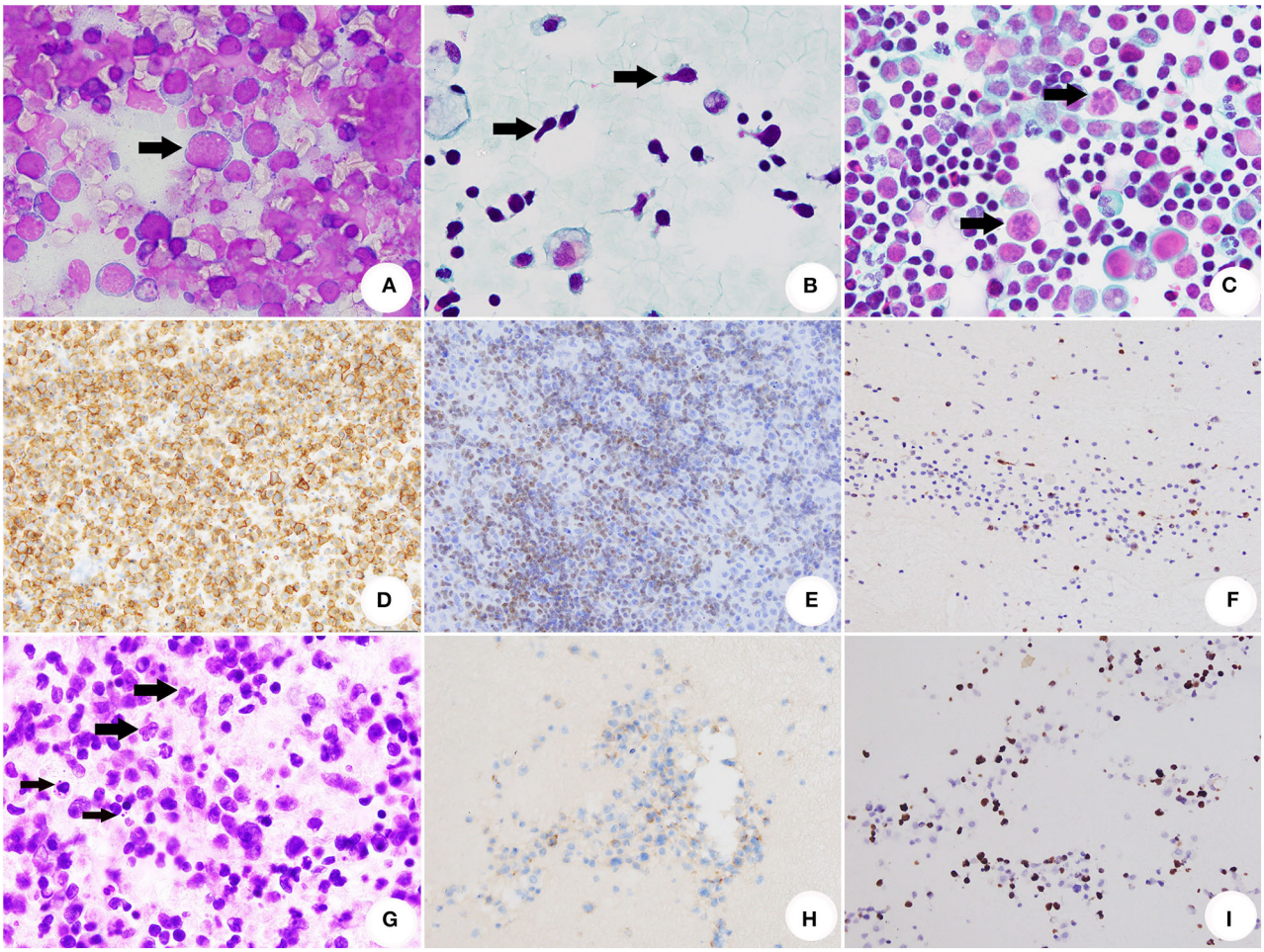

FIGURE 2 | Cytomorhpology, ICC and ISH of SE caused by HM. **(A)** The conventional smear of BL showed non-cohesive atypical lymphocytes with cytoplasmic/nuclear (DiffQuik® stain, original magnification × 1,000). **(B)** The conventional smear of T-ALL/LBL. The arrows indicated several lymphoblasts with hand mirror-shaped morphology (Papanicolaou stain, original magnification × 1,000). **(C)** The conventional smear of AITL. The arrows indicated abnormal mitosis (Papanicolaou stain, original magnification × 1,000). **(D)** The neoplastic cells of BL were positive for CD20 (ICC stain, original magnification × 400). **(E)** T-ALL/LBL was positive for TDT (ICC stain, original magnification × 400). **(F)** AITL was illustrated by positivity of CXCL13 (ICC stain, original magnification × 400). **(G)** Section of cell block for ENKTCL. The thick arrows indicated medium-sized and large-sized atypical presented irregularly folded nuclei with the granular chromatin. Nucleoli were generally inconspicuous or small. The thin arrows indicated apoptosis (HE, original magnification × 1,000). **(H)** Neoplastic cells of ENKTCL were positive for CD56 (immunocytochemistry stain, original magnification × 400). **(I)** EBV infection of ENKTCL was demonstrated by ISH for EBER (Epstein-Barr virus-ISH, original magnification × 400).

leading subtype (27 cases), followed by 7 Burkitt lymphomas (BL), 7 plasmacytomas, 6 extranodal NK/T-cell lymphomas, nasal type (ENKTCL), 3 mantle cell lymphomas (MCL) and 3 anaplastic large cell lymphomas (ALCL). The cyto-histological correlation showed a 100% overall concordance rate of diagnosis of HM and a high agreement rate of sub-classification (51.6%). In this regard, T-ALL/LBL, plasmacytoma, ENKTCL, ALCL, myeloid sarcoma (MS) and follicular lymphoma (FL) showed the highest degree of agreement (100%). According to the cyto-histological correlation, the agreement rate of BL, B-ALL/LBL, angioimmunoblastic T cell lymphoma (AITL), MCL, Indolent B-cell lymphoma and ALL/LBL was 77.8, 66.6, 66.6, 60.0, 50.0, and 33.3%, respectively. Limitation of cytology, inadequate ancillary studies and false negative of ICC were the main reasons for discrepancy. Due to limitation of cytology and/or inadequate ancillary studies, the sub-classification of cytological diagnoses was failed in splenic marginal zone lymphoma (SMZL), chronic lymphocytic leukemia/small lymphocytic lymphoma (CLL/SLL), diffuse large B-cell lymphoma (DLBCL), lymphoplasmacytic lymphoma (LPL), mucosa-associated lymphatic tissue lymphoma (MALT lymphoma), Primary cutaneous gamma delta T-cell lymphoma (PCGD-TCL), primary mediastinal large B-cell lymphoma (PMLBL) and High-grade B-cell lymphoma (HGBL), NOS. From the point of histological diagnoses, the most common type was DLBCL (38 cases, 31.4%), followed by T-ALL/LBL (25 cases, 20.5%), BL (8 cases, 6.6%), plasmacytoma (7 cases, 5.7%), ENKTCL (6 cases, 4.9%) and MCL (5 cases, 4.1%). However, most

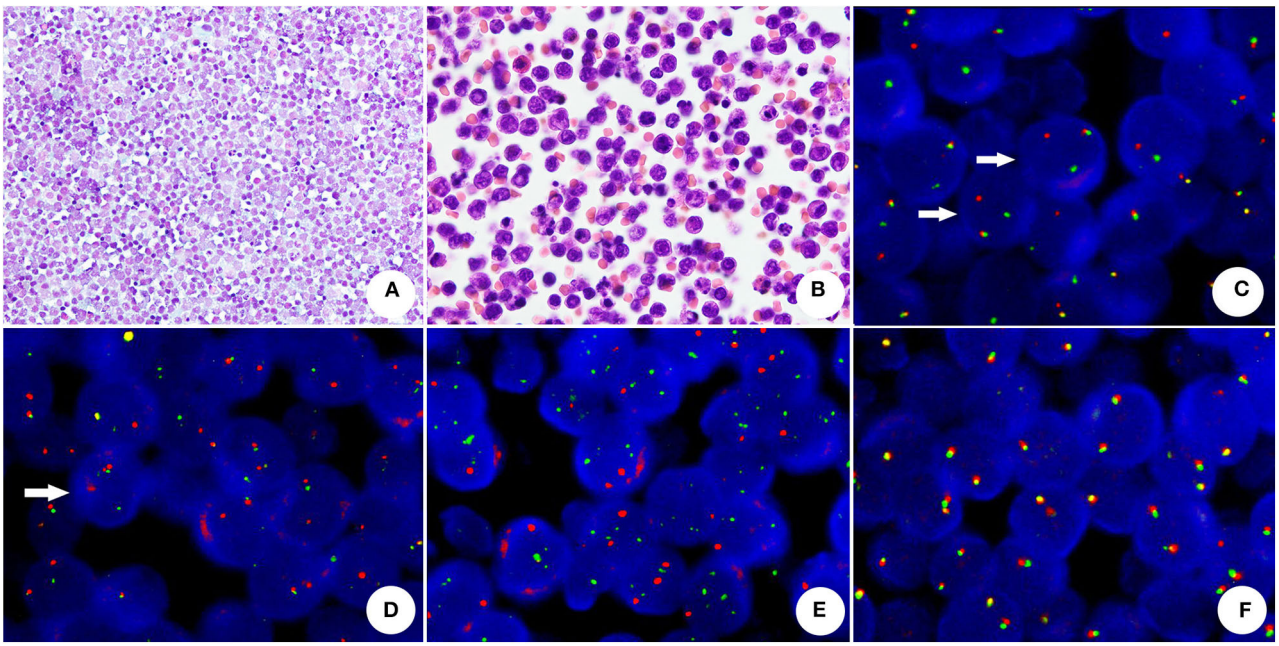

FIGURE 3 | The cytomorphology and FISH assay of HGBL with *MYC* and *BCL2* rearrangements **(A)** The conventional smear presented uniformed and non-cohesive atypical lymphocytes with numerous cytoplasmic/nuclear vacuoles (Papanicolaou stain, original magnification × 400). **(B)** The cell block section showed medium atypical lymphocytes with round or oval nuclei, chromatin and micronucleoli (HE, original magnification × 1,000). **(C)** *BCL2* rearrangement-positive tumor cells, showing one split red and green signals (arrow) and one yellow fusion signal (dual-color, break-apart probe). **(D)** *MYC* rearrangement was demonstrated by split red-green signals (arrow) and a normal fusion signal in a neoplastic cell (dual-color, break-apart probe). **(E)** Absence of *MYC/IGH* rearrangement (dual-color, dual-fusion probe), neoplastic cells did not reveal abnormal fusion signals. **(F)** The neoplastic cells without *BCL6* rearrangement showed normal fusion signals (dual-color, break-apart probe).

of DLBCL were diagnosed as large B-cell lymphomas (LBCL) by cytology. The cytological and histological diagnoses, as well as diagnostic coincidence rates and reasons for discrepancy were summarized in **Table 2**.

Group of Patients Without Histological Correlation (120 Cases)

The diagnostic of 78 B-cell lymphomas, 39 T-cell lymphomas, 1 myeloid neoplasm and 2 ALL/LBLs, was established according to cytomorphology and ancillary studies. The specific subtyping of HM was achieved in 53/120 (44.2%) cases. Of these 53 cases, T-ALL/LBL was also the leading subtype (25 cases), followed by plasmacytomas (7 cases), BL (5 cases), B-ALL/LBL (5 cases) and ALCL (5 cases). These cytological diagnoses were summarized in **Table 3**.

DISCUSSION

The use of cytological evaluation of SE for diagnostic purposes of HM has been taken with controversy, particularly in the setting of initial diagnostic and sub-classification. The current study assessed cytology combined with ancillary studies as the first line diagnostic tool for SE, in the context of HM, by having a cyto-histological correlation. Nowadays, this report demonstrated the largest study of cytological diagnosis of HM in SE.

In our practices, ancillary studies including FCM, ICC, ISH, PCR and FISH, as adjunct to cytomorphologic evaluation contributed to subtyping of the HM in 118/242 cases (48.8%). The subtyping rate was 33.0% in a report from Canada (3). The different diagnostic process and the differences in the distribution of HM between Asian and Western populations were likely the main reasons for the discrepancies. Previous studies suggested that distribution of HM subtypes, using SE, differed strikingly by geographic variations (3, 5, 6). T-ALL/LBL was the most common type and account for 21.5% of HM in our study. A similar result was reported in an Indian study, T-ALL/LBL was also the most common subtype (36.9%) (6). However, the ratio of T-ALL/LBL in an European report was only 3.1% (3). In our study, the 3 most frequent subtypes, either with or without histological diagnosis were similar. T-ALL/LBL was the most common subtype, followed by plasmacytoma and BL. ENKTCL accounted for 4.1% in the group of patients with histological diagnosis, and it was not to be diagnosed in the group of patients without histological correlation. There were three possible reasons for this: in the first place, ENKTCL rarely present SE as initial symptom; secondly, inadequate ancillary studies leaded to the failure of sub-classification; finally, limitation of physician diagnostic experience also contributed to sub-classification failure. In another previous study from ours, 3/5 cases of ENKTCL were initially diagnosed by cytological examination (11). Considering

TABLE 2 | The cyto-histological correlation of patients with histological correlation.

Histological diagnosis	No. of cases	Cytological diagnosis	Coincidence rate	Reason for discrepancy
BL	9	7 BL 2 B-cell NHL	77.8%	Inadequate ancillary studies
B-ALL/LBL	3	2 B-ALL/LBL 1 ALL/LBL	66.6%	False negative of ICC
MZL	5	3 MZL 2 Indolent B-cell lymphoma	60.0%	Inadequate ancillary studies
SMZL	1	1 B-cell NHL	0	Limitation of cytology
CLL/SLL	2	2 Indolent B-cell lymphoma	0	Inadequate ancillary studies
DLBCL	38	30 LBCL 8 B-cell NHL	0	Limitation of cytology
Plasmacytoma	7	7 Plasmacytoma	100%	/
MCL	5	3 MCL 2 B-cell NHL	60.0%	Inadequate ancillary studies
FL	1	1 FL	100%	/
LPL	1	1 B-cell NHL	0	Limitation of cytology
MALT lymphoma	1	1 B-cell NHL	0	Inadequate ancillary studies
HGBL with *MYC* and *BCL2* rearrangement	1	1 HGBL with MYC and BCL2 rearrangement	100%	/
HGBL, NOS	1	1 B-cell NHL	0	Inadequate ancillary studies
Indolent B-cell lymphoma	2	1 Indolent B-cell lymphoma 1 B-cell NHL	50%	Inadequate ancillary studies
ENKTCL	6	6 ENKTCL	100%	/
T-ALL/LBL	25	25 T-ALL/LBL	100%	/
ALCL	3	3 ALCL	100%	/
AITL	3	2 AITL 1 TCL	66.6%	Inadequate ancillary studies
PCGD-TCL	1	1 TCL	0	Limitation of cytology
PTCL, NOS	1	1 PTCL, NOS	100%	/
PMLBL	1	1 LBCL	0	Limitation of cytology
Myeloid sarcoma	2	2 Myeloid sarcoma	100%	/
ALL/LBL	3	2 T-ALL/LBL 1 ALL/LBL	33.3%	/

BL, Burkitt lymphoma; ALL/LBL, lymphoblastic leukemia/lymphoma; MZL, marginal zone B-cell lymphoma; SMZL, splenic marginal zone lymphoma; CLL/SLL, chronic lymphocytic leukemia/small lymphocytic lymphoma; DLBCL, Diffuse large B-cell lymphoma; MCL, Mantle cell lymphoma; FL, Follicular lymphoma; LPL, Lymphoplasmacytic lymphoma; MALT lymphoma, mucosa-associated lymphatic tissue lymphoma; HGBL, High-grade B-cell lymphoma with MYC and BCL2 rearrangement; ENKTCL, Extranodal NK/T-cell lymphoma, nasal type; ALCL, Anaplastic large cell lymphoma; AITL, Angioimmunoblastic T cell lymphoma; PCGD-TCL, Primary cutaneous gamma delta T-cell lymphoma; PTCL, NOS, Peripheral T-cell lymphoma, not otherwise specified; PMLBL, primary mediastinal large B-cell lymphoma.

all these aspects, the latter two reasons were likely to contribute to the differences. According to histological diagnosis in the group of patients with histological correlation, DLBCL (38/122, 31.1%) was the most common type. Even though there was no cytological diagnosis without histological correlation, LBCL was the most frequent entity found. Limitations of cytology itself may contribute for this discrepancy.

In addition, T-ALL/LBL, BL, plasmacytoma, and ENKTCL also accounted in the top five subtypes of histological diagnoses, which were similar to cytological diagnoses. Fifty-nine cases had discrepancies of sub-classification between cytological and histological diagnoses. Upon review of these discordant cases, inadequate ancillary studies, false negative results, limitation of physician diagnostic experience and limitations of cytological diagnosis were likely the main reasons for these discrepancies. In this group, cell blocks were available in 91/122 cases (74.6%), and in the remaining 31 cases, SurePath liquid-based preparation was performed, after making traditional smears. Limited ancillary studies in these 31 cases leaded to the difficulty of sub-classification. In addition, false negative results, especially for immunophenotype, contributed to challenge of cytological diagnoses (9, 10, 12). Cytology, coupled with FMC, highlighted it with an important role in the diagnosis and sub-classification of HM (12–19). In our practice, cytology combined with FCM also could contribute to sub-classification of HM in SE samples. In our opinion, the value of FCM had more importance for mature T-cell lymphoma diagnosis. Most mature T-cell lymphomas mixing with various reactive cells including B lymphocytes, eosinophils, histocytes, and mesothelial cells leaded to the challenge in sub-classification on cytology. FCM had a high sensitivity to lead to the detection of complex lesion. Two cases of AITL and 2 cases of peripheral T-cell lymphoma, not otherwise

TABLE 3 | The cytological diagnoses of patients without histological correlation.

Cytological diagnosis	No. of cases (%)
B-cell lymphoma	78 (65.0%)
B- cell NHL	28 (23.3%)
LBL	26 (21.7%)
Indolent B-cell lymphoma	3 (2.5%)
Plasmacytoma	7 (5.8%)
BL	5 (4.2%)
B-ALL/LBL	5 (4.2%)
PEL	2 (1.7%)
MCL	1 (0.8%)
HGBL with *MYC* and *BCL2* rearrangement	1 (0.8%)
T-cell lymphoma	39 (32.5%)
Mature T-cell lymphoma	8 (6.7%)
T-ALL/LBL	25 (20.8%)
ALCL	5 (4.2%)
PTCL, NOS	1 (0.8%)
Myeloid sarcoma	1 (0.8%)
ALL/LBL	2 (1.7%)

NHL, Non-Hodgkin's lymphoma; LBL, Large B-cell lymphoma; BL, Burkitt lymphoma; B-ALL/LBL, Lymphoblastic leukemia/lymphoma; PEL, Primary effusion lymphoma; MCL, Mantle cell lymphoma; HGBL, High-grade B-cell lymphoma; ALL/LBL, Lymphoblastic leukemia/lymphoma; ALCL, Anaplastic large cell lymphoma; PTCL, NOS, Peripheral T-cell lymphoma, not otherwise specified.

specified (PTCL, NOS), were successfully diagnosed by using cytology along with FCM, ICC and PCR.

Some types of HM which have specific cytomorphologic features, immunophenotyping or molecular genetic changes can be diagnosed by cytology. In the first approach to the patient, cytomorphological features are important diagnostic clues for most of lymphomas. From our observations, there are some characteristics that might point out a specific diagnosis. For example: nuclear cleft and "hand mirror-shaped like" cells are features of ALL/LBL; cytoplasmic and/or nuclear vacuoles are most frequently present in BL; ALCL reveals classic hallmark cells. It is required, subsequently, a panel of immune markers for sub-classification, like: TdT, CD34, Cd117, and CD99 for ALL/LBL (9); CD5, SOX11, and CCND1 for MCL (20); CD3, CD56, TIA-1, GZM-B, and EBER-ISH for ENKTCL (11). Thirdly, some lymphomas reveal hallmark cytogenetic abnormalities, such as: *t*(8, 14) (q24;q32), or its variants, was demonstrated in most cases of BL (8, 21); *MYC* rearrangement accompanied with *BCL2* or *BCL6* gene rearrangement was detected in "double hit" lymphomas (DHL). Finally, clinical manifestations and laboratory parameters also play a great role in the cytological diagnosis. Some specific subtypes of HM with special clinical manifestations, such as breast implant-associated anaplastic large cell lymphoma (BI-ALCL) occurring on peri-implant breast seroma and primary effusion lymphoma (PEL), were diagnosed better with cytology then with histology (22, 23).

In conclusion, our study is the largest series review of SE cyto-histological correlation for HM diagnosis. Our data supported the finding that SE cytology could be a reliable and accurate diagnostic tool for the diagnosis and sub-classification of HM. The clinical information, cytomorphology and appropriate ancillary studies equally contributed to an accurate diagnosis and sub-classification.

DATA AVAILABILITY STATEMENT

The original contributions presented in the study are included in the article/supplementary material, further inquiries can be directed to the corresponding author/s.

ETHICS STATEMENT

The studies involving human participants were reviewed and approved by Ethics Committee On Biomedical Research, West China Hospital Of Sichuan University. The ethics committee waived the requirement of written informed consent for participation. Written informed consent was not obtained from the individual(s) for the publication of any potentially identifiable images or data included in this article.

AUTHOR CONTRIBUTIONS

JL conceived the idea, designed the study, and wrote the paper. SZ, WZ, and WL performed histological correlation. SZ, YJ, XZ, and XD performed ancillary studies. XS and WL supervised the research. All authors contributed to the article and approved the submitted version.

FUNDING

This work was supported by a funding: Department of Science and Technology of Sichuan Province. Award Number: 2018SZ0193.

REFERENCES

1. Das DK. Serous effusions in malignant lymphomas a review. *Diagn Cytopathol.* (2006) 34:335–47. doi: 10.1002/dc.20432
2. Chen YP, Huang HY, Lin KP, Medeiros LJ, Chen TY, Chang KC. Malignant effusions correlate with poorer prognosis in patients with diffuse large B-cell lymphoma. *Am J Clin Pathol.* (2015) 143:707–15. doi: 10.1309/AJCP6LXA2LKFZAMC
3. Tong LC, Ko HM, Saieg MA, Boerner S, Geddie WR, da Cunha Santos G. Subclassification of lymphoproliferative disorders in serous effusions: a 10-year experience. *Cancer Cytopathol.* (2013) 121:261–70. doi: 10.1002/cncy.21257
4. Das DK, Al-Juwaiser A, Francis IM, Sathar SS, Sheikh ZA, Shaheen A, et al. Cytomorphological and immunocytochemical study of non-Hodgkin's lymphoma in pleural effusion and ascitic fluid. *Cytopathology.* (2007) 18:157–67. doi: 10.1111/j.1365-2303.2007.00448.x
5. Savvidou K, Dimitrakopoulou A, Kafasi N, Konstantopoulos K, Vassilakopoulos T, Angelopoulou M, et al. Diagnostic role of cytology in serous effusions of patients with hematologic malignancies. *Diagn Cytopathol.* (2019) 47:404–11. doi: 10.1002/dc.24110

6. Patel T, Patel P, Mehta S, Shah M, Jetly D, Khanna N. The value of cytology in diagnosis of serous effusions in malignant lymphomas: an experience of a tertiary care center. *Diagn Cytopathol.* (2019) 47:776–82. doi: 10.1002/dc.24197
7. Swerdlow SH, Campo E, Harris NL, Jaffe ES, Pileri SA, Stein H, et al. *WHO Classification of Tumours of Haematopoietic and Lymphoid Tissues*. Lyon: IARC (2008).
8. Swerdlow SH, Campo E, Harris NL, Jaffe ES, Pileri SA, Stein H, et al. *WHO Classification of Tumours of Haematopoietic and Lymphoid Tissues*. Lyon: IARC (2017).
9. Li J, Zhang W, Wang W, Jiang Y, Zhao S, Liu W, et al. Forty-nine cases of acute lymphoblastic leukaemia/lymphoma in pleural and pericardial effusions: a cyto-histological correlation. *Cytopathology.* (2018) 29:172–78. doi: 10.1111/cyt.12515
10. Li J, Zhang W, Zhao S, Jiang Y, Liu W, Zhu X, et al. The accuracy of diagnosing Burkitt lymphoma in serous effusion specimen: a cyto-histological correlation with ancillary studies. *Cytopathology.* (2019) 30:378–378 doi: 10.1111/cyt.12707
11. Su XY, Huang J, Jiang Y, Tang Y, Li GD, Liu WP. Serous effusion cytology of extranodal natural killer/T-cell lymphoma. *Cytopathology.* (2012) 23:96–102. doi: 10.1111/j.1365-2303.2011.00937.x
12. Bhaker P, Das A, Rajwanshi A, Gautam U, Trehan A, Bansal D, et al. Precursor T-lymphoblastic lymphoma: Speedy diagnosis in FNA and effusion cytology by morphology, immunochemistry, and flow cytometry. *Cancer Cytopathol.* (2015) 123:557–65. doi: 10.1002/cncy.21584
13. Meda BA, Buss DH, Woodruff RD, Cappellari JO, Rainer RO, Powell BL, et al. Diagnosis and subclassification of primary and recurrent lymphoma. The usefulness and limitations of combined fine-needle aspiration cytomorphology and flow cytometry. *Am J Clin Pathol.* (2000) 113:688–99. doi: 10.1309/0Q7F-QTGM-6DPD-TLGY
14. Liu K, Stern RC, Rogers RT, Dodd LG, Mann KP. Diagnosis of hematopoietic processes by fine-needle aspiration in conjunction with flow cytometry: a review of 127 cases. *Diagn Cytopathol.* (2001) 24:1–10. doi: 10.1002/1097-0339(200101)24:1<1::AID-DC1000>3.0.CO;2-J
15. Bangerter M, Brudler O, Heinrich B, Griesshamnuer M. Fine needle aspiration cytology and flow cytometry in the diagnosis and subclassification of non-Hodgkin's lymphoma based on the World Health Organization classification. *Acta Cytol.* (2007) 51:390–98. doi: 10.1159/000325753
16. Zeppa P, Vigliar E, Cozzolino I, Troncone G, Picardi M, De Renzo A, et al. Fine needle aspiration cytology and flow cytometry immunophenotyping of non-Hodgkin lymphoma: can we do better? *Cytopathology.* (2010) 21:300–10. doi: 10.1111/j.1365-2303.2009.00725.x
17. Cozzolino I, Rocco M, Villani G, Picardi M. Lymph node fine-needle cytology of non-hodgkin lymphoma: diagnosis and classification by flow cytometry. *Acta Cytol.* (2016) 60:302–14. doi: 10.1159/000448389
18. Dong HY, Harris NL, Preffer FI, Pitman MB. Fine-needle aspiration biopsy in the diagnosis and classification of primary and recurrent lymphoma: a retrospective analysis of the utility of cytomorphology and flow cytometry. *Mod Pathol.* (2001) 14:472–81. doi: 10.1038/modpathol.3880336
19. Barrena S, Almeida J, Del Carmen García-Macias M, López A, Rasillo A, Sayagués JM, et al. Flow cytometry immunophenotyping of fine-needle aspiration specimens: utility in the diagnosis and classification of non-Hodgkin lymphomas. *Histopathology.* (2011) 58:906–18. doi: 10.1111/j.1365-2559.2011.03804.x
20. Zhang YH, Liu J, Dawlett M, Guo M, Sun X, Gong Y. The role of SOX11 immunostaining in confirming the diagnosis of mantle cell lymphoma on fine-needle aspiration samples. *Cancer Cytopathol.* (2014) 122:892–97. doi: 10.1002/cncy.21465
21. Hecht J L, Aster J C. Molecular biology of Burkitt's lymphoma. *J Clin Oncol.* (2000) 18:3707–21. doi: 10.1200/JCO.2000.18.21.3707
22. Ronchi A, Montella M, Argenzio V, Lucia A, De Renzo A, Alfano R, et al. Diagnosis of anaplastic large cell lymphoma on late peri-implant breast seroma: management of cytological sample by an integrated approach. *Cytopathology.* (2018) 29:294–99. doi: 10.1111/cyt.12541
23. Shimada K, Hayakawa F, Kiyoi H. Biology and management of primary effusion lymphoma. *Blood.* (2018) 132:1879–88. doi: 10.1182/blood-2018-03-791426

Conflict of Interest: The authors declare that the research was conducted in the absence of any commercial or financial relationships that could be construed as a potential conflict of interest.

frontiers in Medicine

ORIGINAL RESEARCH
published: 15 December 2021
doi: 10.3389/fmed.2021.799163

α-Fetoprotein-Producing Endometrial Carcinoma Is Associated With Fetal Gut-Like and/or Hepatoid Morphology, Lymphovascular Infiltration, *TP53* Abnormalities, and Poor Prognosis: Five Cases and Literature Review

Tomoyuki Otani[1,2], Kosuke Murakami[3], Naoki Shiraishi[4], Man Hagiyama[1], Takao Satou[2], Mitsuru Matsuki[5], Noriomi Matsumura[3] and Akihiko Ito[1]*

[1] Department of Pathology, Kindai University Faculty of Medicine, Osaka-Sayama, Japan, [2] Division of Hospital Pathology, Kindai University Hospital, Osaka-Sayama, Japan, [3] Department of Obstetrics and Gynecology, Kindai University Faculty of Medicine, Osaka-Sayama, Japan, [4] Genome Medical Center, Kindai University Hospital, Osaka-Sayama, Japan, [5] Department of Radiology, Kindai University Faculty of Medicine, Osaka-Sayama, Japan

OPEN ACCESS

Edited by:
Luigi Tornillo, University of Basel, Switzerland

Reviewed by:
Steven Christopher Smith, Virginia Commonwealth University Health System, United States
José Manuel Lopes, Universidade do Porto, Portugal

***Correspondence:**
Tomoyuki Otani
tomoyu@gmail.com

Specialty section:
This article was submitted to Pathology, a section of the journal Frontiers in Medicine

Received: *21 October 2021*
Accepted: *16 November 2021*
Published: *15 December 2021*

Citation:
Otani T, Murakami K, Shiraishi N, Hagiyama M, Satou T, Matsuki M, Matsumura N and Ito A (2021) α-Fetoprotein-Producing Endometrial Carcinoma Is Associated With Fetal Gut-Like and/or Hepatoid Morphology, Lymphovascular Infiltration, TP53 Abnormalities, and Poor Prognosis: Five Cases and Literature Review. Front. Med. 8:799163. doi: 10.3389/fmed.2021.799163

The clinicopathological, immunohistochemical, and molecular characteristics of α-fetoprotein (AFP)-producing endometrial carcinoma (AFP+ EC) are poorly understood. From 284 cases of endometrial carcinoma in our pathology archive, we identified five cases (1.8%) of AFP+ EC with fetal gut–like (4/5) and/or hepatoid (2/5) morphology. All cases exhibited lymphovascular infiltration. In addition, 24 cases of endometrial carcinoma with elevated serum AFP levels were retrieved from the literature. The patient age ranged from 44 to 86 years (median: 63). Of 26 cases whose FIGO (International Federation of Gynecology and Obstetrics) stage and follow-up information was available (mean follow-up 24 months), 15 were stage I or II and 11 were stage III or IV. Even in stage I or II disease, death or relapse occurred in more than half of the patients (8/15). Detailed analysis of our five cases revealed that, on immunohistochemistry, AFP+ EC was positive for SALL4 (4/5), AFP (3/5), and HNF1β (4/5) in >50% of neoplastic cells and negative for estrogen and progesterone receptors (5/5), PAX8 (4/5), and napsin A (5/5). Four cases exhibited aberrant p53 immunohistochemistry and were confirmed to harbor *TP53* mutations by direct sequencing. No mutation was found in *POLE*, *CTNNB1*, or *KRAS*. In conclusion, AFP+ EC merits recognition as a distinct subtype of endometrial carcinoma, which occurs in 1.8% of endometrial carcinoma cases, are associated with *TP53* abnormalities, exhibit lymphovascular infiltration, and can show distant metastasis even when treated in early stage.

Keywords: endometrial cancer, uterine corpus, alpha-fetoprotein (AFP), fetal gut-like, enteroblastic, hepatoid

INTRODUCTION

Alpha-fetoprotein (AFP), an oncofetal protein that is physiologically produced by the liver, yolk sac, and gut during the prenatal period (1), is known to be produced in specific types of tumors. Hepatocellular carcinoma in adults and yolk sac tumor, a subtype of germ cell tumor, in children and young adults are the two most famous examples. Curiously, a small subset of carcinomas of the stomach (2, 3) and lung (4, 5) is also associated with elevated serum AFP levels and these relatively rare carcinomas exhibit histomorphological resemblance to hepatocellular carcinoma or immature endoderm-derived structures, such as the fetal gut or fetal lung. In the endometrium, AFP-producing neoplasms are rare. These include hepatoid carcinoma, unspecified adenocarcinoma with AFP production, and yolk sac tumor. AFP-producing endometrial carcinoma (AFP+ EC) (6–28), which can be defined to include endometrial hepatoid carcinoma (10–16, 19–21, 24–28) and adenocarcinoma with AFP production (6–9, 17, 18, 22, 23), are known only in scattered case reports. Some of them are reported to coexist with conventional (i.e., Müllerian) endometrial carcinoma or carcinosarcoma (11–16, 19–21, 24–26). A few reports have characterized their cases of AFP-producing adenocarcinoma as endometrioid carcinoma (18, 22), though relevant immunohistochemistry (IHC) is rarely reported.

Endometrial yolk sac tumor is somewhat better characterized and reported in a few case series, often together with ovarian examples and/or other germ cell tumors (29–33). Especially in postmenopausal women, endometrial yolk sac tumors also often coexist with Müllerian carcinoma or carcinosarcoma. The yolk sac tumor component in these mixed tumors is interpreted as "retrodifferentiation" (34) of Müllerian carcinoma and sometimes designated as "somatically derived yolk sac tumor" (29, 30). Approximately half of yolk sac tumors of the endometrium in older patients do not show characteristic features of the tumors of the same name in young patients, such as microcystic and reticular architecture, loose myxoid stroma, or Schiller-Duval bodies, and instead exhibit predominantly glandular and papillary architecture. Therefore, at least some of these "glandular yolk sac tumors" (32) can be regarded as the same tumors that are reported under the name of AFP+ EC.

In this study, we reviewed cases of AFP+ EC reported in the literature and performed detailed pathological, immunohistochemical, and molecular analyses of five cases from our pathology archive.

MATERIALS AND METHODS

Case Selection

Two cases of AFP+ ECs were diagnosed during the routine diagnostic practice at Kindai University Hospital, Osaka-Sayama, Japan. To search for additional cases, all cases of endometrial neoplasms that underwent hysterectomy at Kindai University Hospital between 2015 and 2020 were identified and pathology slides were retrieved from the pathology archive. All available slides were reviewed. In this part of the study, AFP+ EC was defined as an endometrial neoplasm bearing a sufficient morphological and immunohistochemical resemblance to AFP-producing carcinomas of the stomach and lung, at least in some part of the tumor. AFP-producing carcinomas of the stomach and lung with characteristic histomorphology include gastric carcinoma with enteroblastic differentiation, fetal adenocarcinoma of the lung, and hepatoid adenocarcinoma of both organs. Morphologically suggestive cases were stained for AFP, SALL4, PAX8, and CK7 to aid in the diagnosis. To be included as AFP+ EC in this part of the study, AFP and, given the high sensitivity of this marker for AFP-producing carcinomas of the stomach and lung, SALL4 were required to be positive in $\geq$1% of tumor cells. PAX8 and CK7 were used as Müllerian markers. Serum AFP levels were not available at the time of histological examination. Two pathologists (TO and AI) reviewed the candidate cases and identified three additional cases of AFP+ EC. We also searched for endometrial yolk sac tumors with typical morphology as seen in young patients. In total, five cases of AFP+ ECs were included in the study. Clinical data were obtained from medical records. This study was approved by the Institutional Review Board of Kindai University Faculty of Medicine (R02-311).

Additional cases were searched in the PubMed database (**Figure 1**). The query terms were "(alpha-fetoprotein OR AFP) AND (carcinoma OR adenocarcinoma OR carcinosarcoma OR müllerian) AND (endometrium OR endometrial OR uterus OR uterine)" and "hepatoid AND (endometrium OR endometrial OR uterus OR uterine)." The search with these terms retrieved 159 and 38 articles written in English, respectively, which amounted to 165 articles after excluding the duplicate results. Based on the title and abstract, 23 articles were considered for inclusion. Since a detailed histological review was impossible with these reported cases, all cases of endometrial tumors with elevated serum AFP levels histologically described as carcinoma or carcinosarcoma (but not yolk sac tumor) were included. Hepatoid carcinoma was considered as carcinoma and not a variant of yolk sac tumor for the purpose of this study. Our intention was to include all cases of endometrial hepatoid carcinoma regardless of serum AFP levels, but all reported cases of endometrial hepatoid carcinoma were associated with elevated serum AFP levels. Eventually, 24 cases of endometrial carcinoma and carcinosarcoma with AFP production from 23 articles were selected as AFP+ EC for our case review.

Immunohistochemistry

IHC was performed on 4-μm-thick formalin-fixed paraffin-embedded (FFPE) tissue sections. Antibodies and their clones, sources, and dilutions are presented in **Supplementary Table 1**. D2-40 and CD31 IHC were used to aid in the identification of vascular invasion. Immunostaining for p53 (35) and mismatch repair proteins (MLH1, PMS2, MSH2, and MSH6) (36) were interpreted according to previous reports. HER2

Abbreviations: AFP, α-fetoprotein; AFP+ EC, α-fetoprotein-producing endometrial carcinoma; FFPE, formalin-fixed paraffin-embedded; FIGO, International Federation of Gynecology and Obstetrics; IHC, immunohistochemistry.

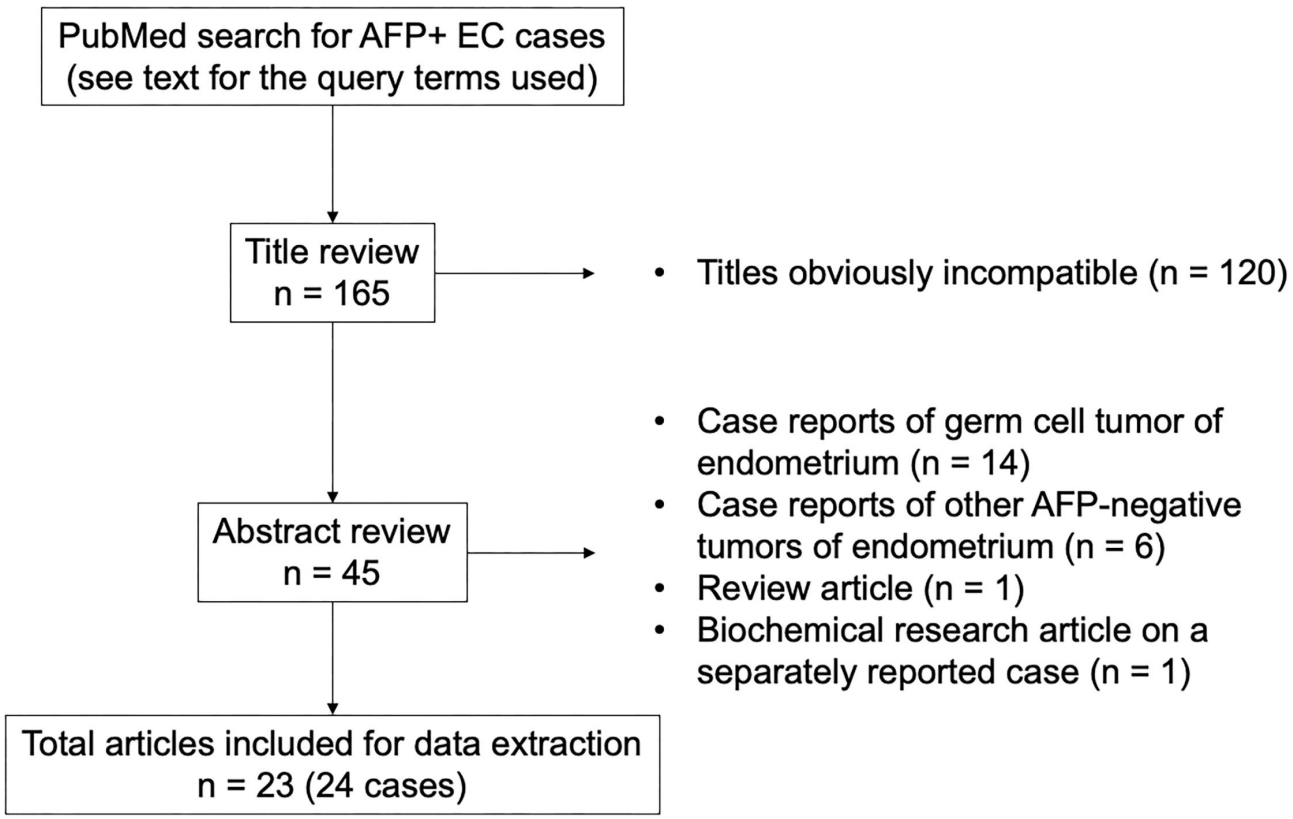

FIGURE 1 | Selection of reported cases.

immunostaining was scored according to a previous study (NCT01367002) (37). Staining results were interpreted by two pathologists (TO and AI) independently, and in case of discrepancy, a consensus was achieved using a multiheaded microscope.

Molecular Analysis for *TP53*, *POLE*, *CTNNB1*, *KRAS*, and *PIK3CA*

Tumor tissue was macrodissected from 10-μm-thick FFPE tissue sections to increase tumor purity. Genomic DNA was extracted using the QIAamp DNA FFPE Tissue Kit (Qiagen, Hilden, Germany) according to the manufacturer's instructions. PCR was performed with KOD FX Neo (TOYOBO, Osaka, Japan) (38) and the products were subjected to 2% agarose gel electrophoresis and sequenced using a 3500xL Genetic Analyzer (Applied Biosystems, Foster City, CA). For *TP53*, *POLE*, and *CTNNB1*, primers were designed using primer-BLAST (NCBI). Primers for *TP53* and *POLE* were designed to amplify exons 4-8 and exons 9, 13, and 14, respectively. Primers for *CTNNB1* were designed to amplify the region containing the mutation hotspots in exon 3. Primer sequences have been previously reported for *KRAS* exon 2 (39) and *PIK3CA* exons 10 and 21 (40). The primer sequences used in this study are listed in **Supplementary Table 2**.

Since it was difficult to histologically determine whether the metastatic lesions originated from an endometrial neoplasm or breast carcinoma in case 1, the genetic mutation detected in endometrial neoplasm was searched for in the tissue of the bone metastasis using the method described above.

RESULTS

Clinical Characteristics

From 284 cases of endometrial carcinoma that had undergone hysterectomy at Kindai University Hospital between January 2015 and December 2020, five cases of AFP+ ECs were identified. No case was diagnosed as endometrial yolk sac tumor during this period. The clinical characteristics of these five cases are shown in **Table 1**. Additional 24 cases were identified in the English literature via a PubMed search and are summarized in **Table 2**. Overall, 29 cases of AFP+ EC were available for our analysis. The patient age ranged from 44 to 86 years (median, 63). Of the 26 cases whose FIGO (International Federation of Gynecology and Obstetrics) stage was available, 12 were stage I, 3 were stage II, and 11 were stage III or IV. The serum AFP levels were elevated in all the cases retrieved from the literature. Among the five cases from our institution, the serum AFP levels were elevated in two cases measured in patients with disease (cases 3 and 5), were within normal limits in two cases measured in a disease-free state (cases

TABLE 1 | Clinicopathological characteristics of AFP-producing endometrial carcinoma.

Case	Age	Gravidity/Sx parity		Serum AFP (ref <10 ng/mL)	FIGO stage	Metastasis	Surgery	Postoperative therapy	Follow-up	Gross findings	AFP+ component	Other component	Myometrial invasion	LVI[c]
1	63	3/3	AVB	N/A	IA	Liver, lungs, bone (post surgery)	THBSO, LND	TC	DOD 11 Mo	28-mm nodular lesion associated with endometrial polyp	Fetal gut-like	CS[b]	Little	Present
2	73	2/2	AVB	WNL in disease-free state	IA	None	THBSO, LND	TC; RTx for Rec	Rec 17 Mo NED 32 Mo	27-mm lobulated polypoid mass with myometrial invasion	Hepatoid, fetal gut-like	CS[b]	<1/2	Present
3	76	3/3	AVB	96 ng/mL at Rec	IB	Lungs (post surgery)	THBSO, LND	TC	Rec 24 Mo AWD 24 Mo	52-mm polypoid mass with myometrial invasion	Hepatoid, non-clear glandular	–	>1/2	Extensive
4	48	0/0	AVB	WNL in disease-free state	IVB	LN	THBSO[a], LND	TC	NED 43 Mo	11-cm uterus containing necrotic material, adhering to large and small intestines	Fetal gut-like, non-clear glandular	–	Extensive	Present
5	78	2/2	AVB	1,335 ng/mL 5 Mo post surgery	IVB	LN, bone	THBSO	TC	AWD 12 Mo	8-cm uterus containing necrotic material	Fetal gut-like, non-clear glandular	–	Extensive	Extensive

AFP, α-fetoprotein; AVB, abnormal vaginal bleeding; AWD, alive with disease; CS, carcinosarcoma; FIGO, International Federation of Gynecology and Obstetrics; LN, lymph nodes; LND, pelvic and para-aortic lymphadenectomy; LVI, lymphovascular invasion; Mo, months; N/A, not available; NED, no evidence of disease; Rec, recurrence; RTx, radiation therapy; SO, salpingo-oophorectomy; Sx, presenting symptom; TC, paclitaxel and carboplatin; THBSO, total hysterectomy and bilateral salpingo-oophorectomy; WNL, within normal limits.

[a] *Sections of large and small intestines attached to the uterus were also resected.*

[b] *Associated with endometrial polyp.*

[c] *Investigated with D2-40 and CD31 immunohistochemistry.*

TABLE 2 | Reported cases of AFP-producing endometrial carcinoma.

References	Age	Sx	Serum AFP (ng/mL)[b]	Histology as reported	AFP IHC	p53 IHC	Myometrial invasion	LVI	FIGO stage[c]	Metastasis	Follow-up
Kawagoe (6)	65	AVB	1,476	CS	+	NR	2/3	NR	III	LN	NED 3 Mo
Matsukuma and Tsukamoto (7)	63	NR	670	Adeno	+	NR	slight	NR	I	LN, lung[e]	DOD 12 Mo
Kubo et al. (8)	55	AVB	676	Papillary adeno	+	NR	>1/2	NR	III	Vagina, Douglas pouch; LN, liver, lung, bone[f]	DOD 3 Mo
Phillips et al. (9)	68[a]	NR	21,000[a]	CS	+	NR	NR	NR	I	NR	DOD 7 y[f]
Yamamoto et al. (10)	62	AVB	280.3	Hep, tubular adeno	+	NR	present	present	IV	Lung	DOD 3 Mo
Hoshida et al. (11)	66	AVB	16,170	Hep, EEC	+	NR	>1/2	present	III	Uterine cervix, LN	DOD 32 Mo
Toyoda et al. (12)	60	AVB	31,950	Hep, EEC	+	NR	< 1/2	present	III	LN; lung[f]	DOD 12 Mo
Adams et al. (13)	66	AVB	351 on POD4	Hep, EEC	+	NR	1/2	NR	I	None[g]	NED 8 y
Takahashi and Inoue (14)	68	AVB	2,800	Hep, CS	+	NR	The tumor invaded the parametrium	present	NR	NR	NR
Takano et al. (15)	63	AVB	5,060	Hep, CS	+	NR	little or none	NR	I	None[g]	NED 12 Mo
Takeuchi et al. (16)	61	epigastric discomfort	453	Hep, EEC	+	NR	1/2	NR	IV	Omentum	NED 12 Mo
Tran et al. (17)	44	AVB	1,493 IU/mL	SC	+	+	NR	extensive	IV	Ov, sigmoid colon, diaphragm	NED 15 Mo
Kodama et al. (18)	59	abd swelling	1,292.8	EEC	+	NR	>1/2	present	II	None	NED 60 Mo
Ishibashi et al. (19)	86	AVB	7,824	Hep, EEC	+	NR	slight	absent	I	LN[f]	Rec 11 Mo AWD 36 Mo
Hwang et al. (20)	75	AVB	90,508	Hep, EEC	+	NR	>1/2	NR	I	None	NED 3 Mo
Kawaguchi et al. (21)	63	AVB	10,131	Hep, CS	+	NR	NR	NR	II	None	NED 2 y
Kawaguchi et al. (21)	82	AVB	401	Hep, CS	+	NR	>1/2	NR	I	Lung[f]	DOD 1y
Akhavan et al. (22)	57	AVB	465.3	EEC	NR	NR	>1/2	NR	II	Lung, skin, brain[f]	DOD <1 y
Chen et al. (23)	65	AVB	244.8	CS	NR	NR	>1/2	NR	NR	NR	NR
Wu et al. (24)	61	AVB	253.3	Hep, EEC	+	+	>1/2	NR	III	LN; lung[f]	DOD 10 Mo
Kuroda et al. (25)	63	AVB	151	Hep, SC	+	+ in SC NR in Hep	<1/2	NR	I	None	NED 2 Mo
Li et al. (26)	67	AVB	31,896	Hep, CS	+	NR	>1/2	extensive	III	Ov; liver, peritoneum[f]	Rec 2 Mo DOD 11 Mo
Yin et al. (27)	64	AVB	3,931	Hep	+	NR	NR	NR	NR	NR	NR
Liu et al. (28)	48	AVB	1,210	Hep	+	–[d]	superficial	absent	I	None	NED 63 Mo

abd, abdominal; adeno, adenocarcinoma; AFP, α-fetoprotein; AVB, abnormal vaginal bleeding; AWD, alive with disease; CS, carcinosarcoma; DOD, died of disease; EEC, endometrial endometrioid carcinoma; FIGO, International Federation of Gynecology and Obstetrics; Hep, hepatoid carcinoma; IHC, immunohistochemistry; LN, lymph nodes; LVI, lymphovascular invasion; NED, no evidence of disease; Mo, months; NR, not reported; Ov, ovaries; POD, postoperative day; Rec, recurrence; SC, serous carcinoma; Sx, presenting symptom; y, years.

[a] *At recurrence.*

[b] *Pre-operative if not otherwise indicated.*

[c] *According to FIGO 2008.*

[d] *Not reported whether wildtype or null.*

[e] *At autopsy.*

[f] *Post surgery.*

[g] *Intraoperative peritoneal washing cytology was positive.*

2 and 4), and could not be evaluated in one case (case 1, archival case). Pre- or perioperative values were not available in these cases. Of note, case 3 had a normal serum AFP level measured in the disease-free state after surgery, but it increased during the observation period, and lung metastasis was eventually discovered.

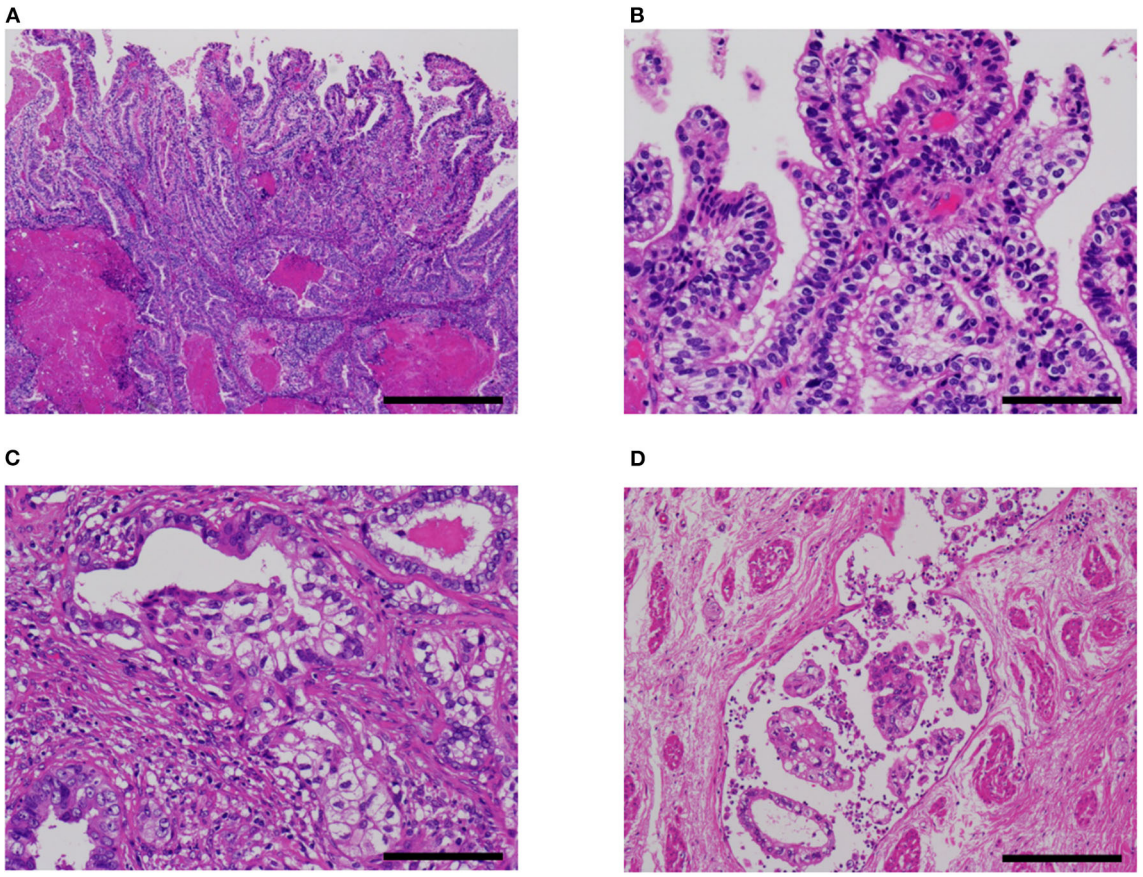

FIGURE 2 | Fetal gut-like pattern of α-fetoprotein-producing endometrial carcinoma (case 5). **(A,B)** Fetal gut-like pattern was composed of tall columnar neoplastic cells with clear cytoplasms and large nuclei in papillary and glandular architecture. **(C)** Variable degrees of intraglandular piling-up of neoplastic cells could be seen and imparted clear cell carcinoma-like appearance. **(D)** In case 5, lymphovascular invasion was extensive. Hematoxylin-eosin; original magnification ×40 **(A)**, ×200 **(B,C)**, and ×100 **(D)**; 500 **(A)**, 100 **(B,C)**, and 200 μm **(D)**.

Follow-up information was available from 26 cases, with a mean follow-up period of 24 months. Of the 11 patients with FIGO stage III or IV disease (mean follow-up, 14 months), 6 died of disease and 1 was alive with disease. Of the 15 patients with FIGO stage I or II disease (mean follow-up, 34 months), five died of disease and additional three suffered from recurrence; 4 of 7 patients with recurrence-free survival had a follow-up period of no more than 1 year.

Histopathological Analysis

Pathological characteristics of our five cases are shown in **Table 1**. Four of the five cases had a fetal gut-like component (**Figure 2**). This component was composed of tall columnar cells with large nuclei and clear cytoplasms forming glandular and papillary structures, resembling carcinoma with enteroblastic differentiation of the stomach and fetal adenocarcinoma of the lung. When its apical border was smooth, this component had a superficial resemblance to the secretory variant of endometrioid carcinoma, with tall cells and optically clear cytoplasms (**Figures 2A,B**). In other parts, intraglandular piling-up of neoplastic cells in invasive glands gave them a near-solid, nest-like appearance and this was reminiscent of clear cell carcinoma (**Figure 2C**).

Hepatoid carcinoma, seen in two cases, was composed of tightly arranged trabecular neoplastic epithelium with intervening sinusoid-like capillaries (**Figure 3**). Between tumor cells, canaliculi-like structures could often be observed. The tumor cells had a moderate amount of eosinophilic or clear cytoplasms. Tumor cell nuclei had coarse chromatin and nuclear atypia was moderate to severe. In case 2, a gradual transition between the hepatoid carcinoma and fetal gut-like component was observed. Hepatoid carcinoma showed exophytic polypoid growth into the uterine cavity in both cases and also showed myoinvasion in one case (case 3, **Figure 3C**).

A non-clear glandular component was observed in three cases (**Figure 4**). In two cases (cases 3 and 5), this component invaded the myometrium as discrete glandular structures. In case 4, the neoplastic epithelium formed confluent, anastomosing glands, which some observers might call reticular. The non-clear

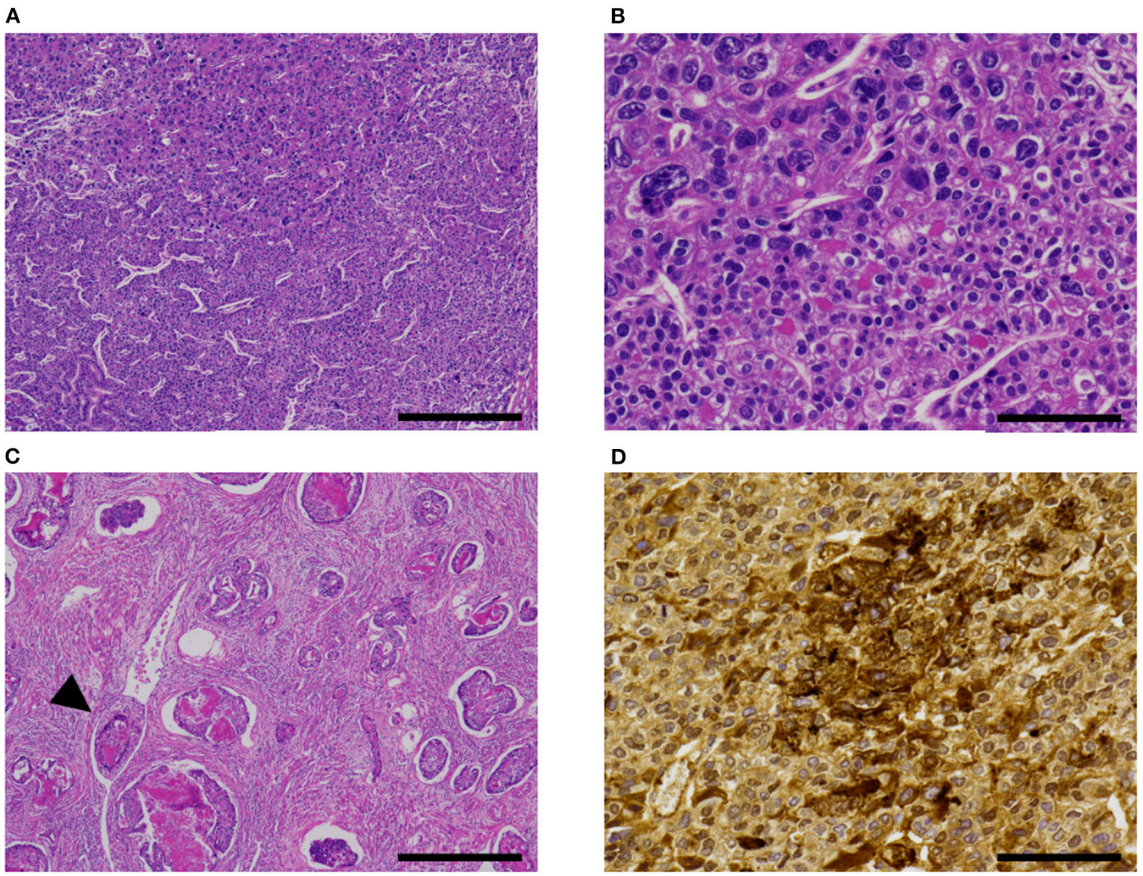

FIGURE 3 | Hepatoid carcinoma (case 3). **(A)** This pattern was composed of tightly arranged trabecular neoplastic epithelium with intervening sinusoid-like capillaries. **(B)** Canaliculi-like small lumina were also observed. Tumor cell nuclei had coarse chromatin and showed moderate to severe nuclear atypia. **(C)** In case 3, this carcinoma exhibited extensive myoinvasion and vascular invasion (arrowhead; retraction clefts are also pictured). **(D)** Neoplastic cells were positive for AFP **(D)**. Hematoxylin-eosin **(A–C)**; original magnification ×40 **(A,C)** and ×200 **(B,D)**; scale bars = 500 μm **(A,C)** and 200 μm **(B,D)**. AFP, α-fetoprotein.

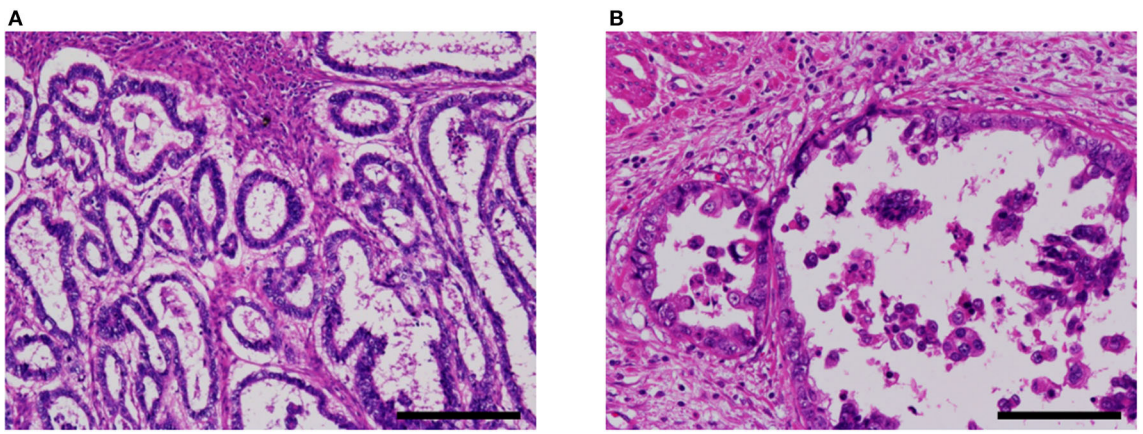

FIGURE 4 | Non-clear glandular pattern of α-fetoprotein-producing endometrial carcinoma (case 5). **(A,B)** This pattern was associated with smooth **(A)** or ragged **(B)** luminal border, which imparted low-grade endometrioid-like or clear cell carcinoma-like appearance, respectively. Hematoxylin-eosin; original magnification ×100 **(A)** and ×200 **(B)**; scale bars = 200 μm **(A)** and 100 μm **(B)**.

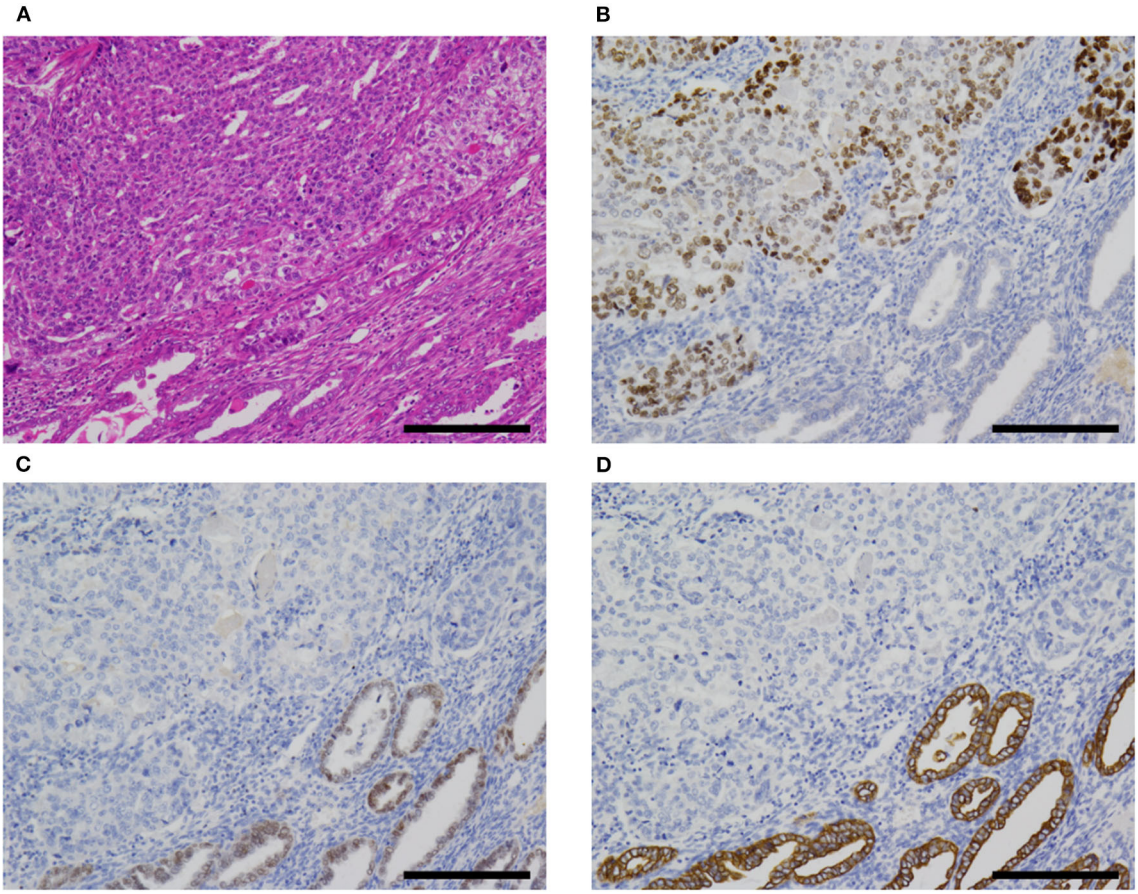

FIGURE 5 | AFP+ EC associated with Müllerian component (case 2). **(A)** In cases 1 (not shown) and 2, AFP+ EC was associated with Müllerian carcinosarcoma (sarcomatous component not shown). **(B–D)** The former (upper left) was SALL4+ **(B)**, PAX8- **(C)**, and CK7- **(D)**, while the latter (lower right) was SALL4-, PAX8+, and CK7+. Hematoxylin-eosin **(A)**; original magnification ×100; scale bars = 200 μm. AFP+ EC, α-fetoprotein-producing endometrial carcinoma.

glandular pattern was low-grade endometrioid-like when the apical border was smooth (**Figure 4A**) and clear cell carcinoma-like when associated with hobnail-like nuclear protrusion (**Figure 4B**).

Two cases were associated with carcinosarcoma (cases 1 and 2; **Figure 5**). These two cases were also associated with an endometrial polyp. In both cases, the epithelial component was most consistent with serous carcinoma, at least in part, but some areas were difficult to classify and might represent a transition between AFP+ and Müllerian components.

All cases exhibited lymphovascular infiltration (**Figures 2D**, **3C**).

Immunohistochemistry and Molecular Analysis

The immunohistochemistry and molecular analysis results are shown in **Table 3** and **Figures 3D**, **5**, **6**. The AFP-positive component of all the five cases was at least focally positive for AFP (**Figure 3D**) and SALL4 (**Figure 5B**). PAX8 (**Figure 5C**) and CK7 (**Figure 5D**) were never diffusely positive, although the epithelial component of coexisting carcinosarcoma in two cases stained diffusely with PAX8 and CK7 (**Figures 5C,D**). Estrogen and progesterone receptors were always negative in AFP-positive component. HNF1β was diffusely positive in the AFP-positive component at least weakly, whereas napsin A was always negative. p53 IHC was abnormal in four of the five cases (**Figure 6A**) and wild-type in the remaining case (**Figure 6B**). Two cases showed strong positive staining of >80% of neoplastic cells (**Figure 6A**), while the other two cases with abnormal staining showed heterogeneous expression.

All the four cases with abnormal p53 IHC were found to harbor mutations in *TP53* gene. Two cases harbored mutations in exon 21 of *PIK3CA*. No mutations were found in *POLE* exons 9, 13, and 14, *CTNNB1* exon 3, *KRAS* exon2, or *PIK3CA* exon 10. In case 1, *TP53* c.742C>T mutation was detected in both endometrial and bone lesions.

DISCUSSION

AFP+ EC is a rare neoplasm. The 2020 WHO Classification of Female Geniatal Tumors (41) does not mention AFP+ EC or hepatoid carcinoma. Yolk sac tumor is described under the

heading of "germ cell tumors of the uterine corpus." Previous cases reported as AFP+ EC, excluding cases reported as yolk sac tumor, are summarized in **Table 2**.

Hepatoid carcinoma (**Figure 3**) has been recognized as a type of AFP+ EC since 1996 (10, 11). This histological type of endometrial carcinoma is often reported to exhibit exophytic growth into the uterine cavity grossly and vascular infiltration microscopically (**Table 2**) (10–16, 19–21, 24–28).

Fetal gut-like carcinoma (**Figure 2**) has not been recognized as such in endometrial carcinoma, as far as we are aware. In the previous literature, this pattern in endometrium has been reported as yolk sac tumor by some authors: Ravishankar et al. (30) reported 11 cases and Fadare et al. (32) reported 9 plus 3 cases of endometrial yolk sac tumors, mostly in postmenopausal patients. According to their reports, the histology of some examples was indistinguishable from yolk sac tumors in younger patients, while others showed exclusively glandular and papillary architecture. The latter histological pattern is consistent with what we termed the fetal gut-like pattern in this article. Fetal gut-like morphology is not uncommonly seen in AFP-producing carcinoma of the stomach and the lung: carcinomas with this pattern are called enteroblastic carcinoma in the stomach (2, 3) and fetal adenocarcinoma in the lung (4). In the gynecological tract, AFP-producing carcinomas of the ovary (42–44) and uterine cervix (45, 46) have been described to exhibit this morphology.

Three of our cases also contained a non-clear glandular component (**Figure 4**) showing the immunophenotype of AFP+ EC: namely, AFP+, SALL4+ and PAX8-. This component might simply be a fetal gut-like component with decreased cytoplasmic glycogen. Although difficult to distinguish from much more common Müllerian carcinoma by histomorphology alone (**Figure 4**), this immunohistochemical pattern is inconsistent with Müllerian carcinoma and we consider this non-clear glandular component to be an integral part of AFP+ EC. In theory, it is entirely conceivable that AFP+ EC composed exclusively of non-clear glandular component exists. Indeed, some of the previously reported AFP-producing "endometrioid" carcinomas (18, 22) might fit this description.

AFP+ EC is an aggressive neoplasm. About half of the cases in our series and the literature were diagnosed at FIGO stage III or IV. Although other cases were diagnosed earlier, these patients hardly fared better: 5 out of 15 patients with stage I or II disease succumbed to the disease and additional 3 experienced recurrence, while 6 out of 10 patients with stage III or IV disease died of disease. This aggressive behavior even in patients with early-stage disease is most likely related to the often extensive vascular infiltration of this neoplasm. In keeping with this hypothesis, disproportionately many cases of relapse in stage I or II patients manifested as distant metastasis (five out of seven cases with available information). As for cases reported as endometrial yolk sac tumor, which should contain at least some AFP+ ECs, the outcomes are somewhat mixed: Ravishankar et al. (30) reported poor outcomes comparable to our series, while cases reported by Fadare et al. (32) seem to have fared better.

The similarity between AFP-producing neoplasms of the endometrium and stomach is striking: they arise in older patients

TABLE 3 | Immunohistochemical and molecular analysis of AFP-producing endometrial carcinoma.

Case		Immunohistochemistry								Molecular analysis				
		AFP	SALL4	PAX8	CK7	ER/PR	HNF1β	Napsin A	p53 IHC	MMR[e]	HER2	*TP53*	*POLE*	*CTNNB1*	*KRAS*	*PIK3CA*
1	AFP+	1+	2+	-	3+[a]	-	4+	-	Aberrant[b]	Normal	2+	c.742C>T (R248W)	wt	wt	wt	wt
	AFP-	-	-	4+	4+	1+	-	-	Aberrant[c]	Normal	2+					
2	AFP+	3+	4+	-	-	-	4+	-	Aberrant[d]	Subclonal loss of MLH1[f]	1+	c.675_695delinsC (V225fs)	wt	wt	wt	c.3062A>G (Y1021C)
	AFP-	1+	1+	4+	4+	1+	2+	-	Aberrant[c]	Subclonal loss of MLH1[f]	2+					
3		3+	3+	-	1+[a]	-	2+	-	Aberrant[b]	Normal	1+	c.763A>T (I255F)	wt	wt	wt	wt
4		3+	3+	-	-	-	3+	-	wt	Normal	0	wt	wt	wt	wt	wt
5		1+	4+	1+	3+[a]	-	3+	-	Aberrant[b]	Normal	3+	c.376-3_376-1delinsT (splice acceptor site)	wt	wt	wt	c.1658_1659delinsC (S553fs)

-, positive in <1% of tumor cells; +, positive in 1–25% of tumor cells; 2+, positive in 26–50% of tumor cells; 3+, positive in 51–75% of tumor cells; 4+, positive in 76–100% of tumor cells; AFP, α-fetoprotein; AFP+, AFP-positive (fetal gut-like or hepatoid) component; AFP-, AFP-negative (Müllerian) epithelial component; CK, cytokeratin; ER, estrogen receptor; IHC, immunohistochemistry; PR, progesterone receptor; wt, wild-type.

[a]*Mosaic-like.*

[b]*Diffuse (>80% tumor cells).*

[c]*Heterogeneous.*

[d]*Null (no tumor cells).*

[e]*Mismatch repair proteins (i.e., MLH1, PMS2, MSH2, and MSH6).*

[f]*Only some tumor cells express MLH1 and PMS2; all tumor cells retain MSH2 and MSH6 expression.*

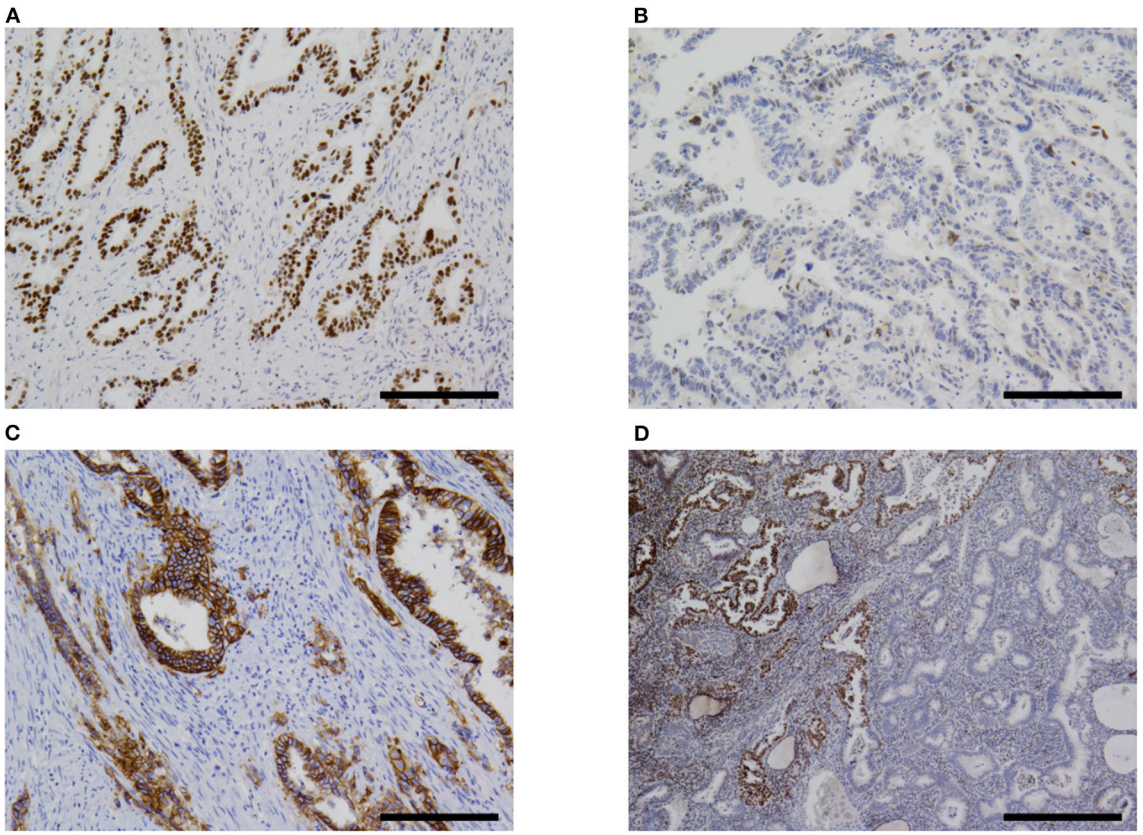

FIGURE 6 | Immunohistochemistry. **(A)** Most cases of α-fetoprotein-producing endometrial carcinoma were p53-aberrant on immunohistochemistry (case 5 shown). **(B)** Only one case in our series was p53-wildtype (case 4). **(C)** Some overexpressed HER2 (case 5). **(D)** One case (case 2) in our series showed subclonal loss of expression of MLH1 and PMS2 (not shown). Original magnification ×100 **(A–C)** and ×40 **(D)**, scale bars = 200 μm **(A–C)** and 500 μm **(D)**.

and can be associated with conventional adenocarcinoma; although typical yolk sac tumor morphology with reticular and microcystic pattern can occur, fetal gut-like pattern (carcinoma with enteroblastic differentiation in stomach and fetal gut-like carcinoma/glandular yolk sac tumor in endometrium) seems to be more frequent (47); fetal gut-like neoplasm and hepatoid carcinoma often coexist; hepatoid carcinoma grows exophytically into the lumen; they are associated with *TP53* mutation, vascular infiltration, and hematogenous metastasis (2, 3). Indeed, hepatoid carcinoma of the endometrium was at first described as an endometrial carcinoma analogous to hepatoid carcinoma of the stomach (24, 27). Some authors propose to call all these AFP-producing neoplasms associated with conventional carcinoma in various organs with the name of "somatically derived yolk sac tumor" (29).

HER2 is reported to be positive in 30% of endometrial serous carcinomas (37). The use of anti-HER2 therapy in these cases was recently described in the National Comprehensive Cancer Network guidelines (48). HER2 is overexpressed in many AFP-producing gastric carcinomas (49) and a case of fetal gut-like adenocarcinoma of the uterine cervix with amplified and overexpressed HER2 has been reported (46). We hypothesized that AFP+ EC might also be associated with HER2 overexpression, but the frequency of HER2 positivity by immunohistochemistry was not significantly different from that reported for serous carcinoma (50). However, our number of cases is small and the possibility remains that further accumulation of cases might reveal an association between AFP+ EC and HER2 overexpression and/or amplification.

In addition to prognostication and possible therapeutic impact, another important reason to recognize AFP+ EC is the post-operative surveillance: serum AFP can be a useful tumor marker for patients with this disease. Our case 3 is a case in point. Although serum AFP levels were not available from pre- or perioperative period, this patient was followed up with serum AFP after postsurgical pathological examination demonstrated that the tumor cells were immunohistochemically positive for AFP. Serum AFP levels were within normal limits for some time after surgery, but began to show an increase, while serum carcinoembryonic antigen, CA19-9, and CA-125 levels stayed normal from preoperative period. Pulmonary recurrence was diagnosed eventually. The elevated serum AFP level was the first indication of disease recurrence in this patient.

For further accrual of cases, we proposed the diagnostic criteria for AFP+ EC in **Table 4**. The relationship between histomorphology, immunohistochemistry, and serum AFP levels is not straight-forward in gastric and pulmonary cancers and they do not always concur. In WHO Classifications of respective

TABLE 4 | Proposed essential and desirable diagnostic criteria for AFP-producing endometrial carcinomas.

	Essential	Desirable
AFP-producing endometrial carcinoma	- Histomorphology consistent with carcinoma. Hepatoid morphology is allowed. - Positive IHC for AFP in ≥1% of tumor cells. - Absence of morphological patterns characteristic of yolk sac tumor but inconsistent with carcinoma. These include a reticular/microcystic pattern, Schiller-Duval bodies, and loose myxoid stroma.	- Positive IHC for SALL4. - Negative or non-diffuse IHC for ER, PR, PAX8 and CK7.
Hepatoid carcinoma of the endometrium	- Carcinoma resembling hepatocellular carcinoma.	- Positive IHC for AFP and/or SALL4. - Negative or non-diffuse IHC for ER, PR, PAX8 and CK7.
Fetal gut-like carcinoma of the endometrium	- Carcinoma resembling fetal gut epithelium (columnar epithelium with clear cytoplasm). - Exclusion of clear cell carcinoma and secretory variant of endometrioid carcinoma	- Positive IHC for AFP and/or SALL4. - Negative or non-diffuse IHC for ER, PR, PAX8 and CK7.
Non-clear glandular AFP-producing endometrial carcinoma	- Gland-forming adenocarcinoma without clear cells. - Positive IHC for AFP and/or SALL4.	- Negative or non-diffuse IHC for ER, PR, PAX8 and CK7.

AFP, α-fetoprotein; CK, cytokeratin; ER, estrogen receptor; IHC, immunohistochemistry; PR, progesterone receptor.

TABLE 5 | Immunohistochemical characteristics of AFP-producing endometrial carcinoma and other endometrial neoplasms in differential diagnosis.

Tumor type	AFP	SALL4	PAX8	CK7	ER/PR	HNF1β	Napsin A	p53	Others
AFP-producing endometrial carcinoma	+	+	-	-/+	-	+	-	Aberrant/wt	
Endometrioid carcinoma	-	-	+	+	+	-	-	wt	
Clear cell carcinoma	-	-	+	+	-	+	+	wt/aberrant	
Serous carcinoma	-	-	+	+	-/+	-	-	Aberrant	
Yolk sac tumor[a]	+	+	-	-	-	+	-	Variable (32)	
Gastric-type adenocarcinoma of uterine cervix	-	-	+	+	-	+	-	Aberrant/wt	HIK1083+, MUC6+
AFP-producing adenocarcinoma of uterine cervix (45,46)	+	+	-	NK	-	NK	NK	Aberrant in 2 reported cases	
Metastatic adenocarcinoma	-	-	Variable	Variable	Variable	Variable	Variable	Variable	

AFP, α-fetoprotein; CK, cytokeratin; ER, estrogen receptor; NK, not known; PR, progesterone receptor; wt, wild-type.
[a] *There is a conceptual overlap between AFP-producing endometrial carcinoma and yolk sac tumor.*

fields, histological classification is always given priority. Fetal adenocarcinoma of the lung is defined by histomorphology and only a few immunohistochemistry to differentiate between low-grade and high-grade subtypes (β-catenin) and to exclude endometriosis (TTF1 positivity for low-grade fetal adenocarcinoma) (51). Hepatoid adenocarcinoma of the lung is mentioned, but not formally defined (51). AFP-producing carcinoma, hepatoid adenocarcinoma, and adenocarcinoma with enteroblastic differentiation of the stomach are also not formally defined, but hepatoid and enteroblastic adenocarcinomas seem to be histomorphological categories, while AFP-producing carcinoma seems to denote a loose collection of carcinomas with immunohistochemical or serological evidence of AFP production (52). Definition employing IHC has been used in some studies: Kinjo et al. defined AFP-producing gastric cancer as gastric tumors with immunohistochemical positivity for AFP or glypican 3 in ≥1% of tumor cells (47); Akazawa et al. defined gastric adenocarcinoma with enteroblastic differentiation as a morphologically appropriate tumor that stains positive for AFP, glypican 3, or SALL4 in >10% of the tumor (3); Fujimoto et al. used somewhat different thresholds for the latter tumor and required that >5% of the tumor be positive for glypican 3 or SALL4 or that >1% of the tumor be positive for AFP (49). Our proposed diagnostic criteria are largely in line with these definitions and prioritize histomorphology with discreet use of immunohistochemistry. Elevation of serum AFP levels are treated as important, but nonessential characteristics. To date, no cases of endometrial fetal gut-like or hepatoid carcinoma without elevated serum AFP levels have been reported, but this may be due to publication bias. Since we did not make elevated serum AFP levels a prerequisite for diagnosis, cases with appropriate morphology and immunophenotype but normal serum AFP levels can be diagnosed as AFP+ EC with these criteria. This decision would also allow for the diagnosis of cases for which serum AFP values are not available (our cases 1, 2, and 4).

Differential diagnoses of AFP+ EC include endometrioid, clear cell, serous, and gastric-type uterine carcinoma, and metastatic carcinoma. Some reports in the previous literature have emphasized the similarity between AFP+ EC and secretory variant of endometrioid carcinoma, both being composed of tall columnar cells with clear cytoplasms (**Figures 2A,B**) (32, 53). Since AFP+ EC can grow in solid, papillary, and glandular patterns with variable amounts of optically clear cells and hobnail-like cells and is positive for HNF1β on IHC at least weakly, clear cell carcinoma also looms as a serious diagnostic consideration (30). Incidentally, HNF1β, which is widely known as a positive marker of clear cell carcinoma of the gynecological tract, also stains positive in yolk sac tumor (54). In this context,

immunostaining with napsin A would be helpful, as it would be positive in clear cell carcinoma and negative in AFP+ EC (30, 32). Non-clear glandular AFP+ EC (**Figure 4A**) and hepatoid carcinoma (**Figure 3**) might resemble low-grade and high-grade endometrioid carcinoma, respectively. High-grade cytology and abnormal p53 IHC can lead to the consideration of serous carcinoma. If AFP+ EC extends to the uterine cervix, clear cytoplasms might cause confusion with gastric-type adenocarcinoma. Although not explored in our study, glandular yolk sac tumor is reported to be positive for CDX2, reflecting its endodermal differentiation (34); this can be a cause of misdiagnosis as metastatic gastrointestinal adenocarcinoma, especially in patients with a history of these malignancies (55). In all cases, a low threshold to perform relevant immunostaining and evaluation of serum AFP levels can be a key to correct diagnoses. Immunohistochemical characteristics of AFP+ EC and its differential diagnoses are summarized in **Table 5**. Regarding cervical carcinomas, it should be noted that AFP-producing cervical carcinoma with fetal gut-like morphology has been reported (45, 46).

Some observations are warranted regarding the pathogenesis of AFP+ EC. This subset of endometrial carcinoma is unusual in that it is immunohistochemically negative for PAX8 and thus cannot be said to show Müllerian differentiation. However, many cases are associated with Müllerian carcinoma or carcinosarcoma. Although not directly comparable to AFP+ EC, Acosta et al. (33) showed that in malignant tumors of the uterus and ovaries with Müllerian and germ cell components, both components are clonally related. We believe it reasonable to suppose that AFP+ EC is of Müllerian origin and exhibits divergent line of differentiation. Another example of endometrial carcinoma of Müllerian origin with divergent differentiation is endometrial mesonephric-like adenocarcinoma (56).

Whether AFP+ EC and "AFP-producing carcinomas" of other organs such as stomach and lung should be classified as "carcinomas" or "yolk sac tumors" is an unresolved nosological problem. Several arguments can be put forward for the case of separation of AFP+ EC from yolk sac tumor. One important consideration would be the problem of case recognition. It is quite understandable that some pathologists would be reluctant to diagnose such cases as are reported here as a yolk sac tumor. For others, a diagnosis of yolk sac tumor might not be on the differential list at all. Once the existence of endometrial carcinoma with AFP production is widely recognized, this highly malignant tumor will be more frequently diagnosed appropriately. Second, there is the issue of continuity with previous literature: before allowing the concept of somatically derived yolk sac tumor to encompass all AFP-producing neoplasms of older patients aside from liver cancer, how to position cases reported in the past as AFP-producing carcinomas should be considered. Third, recognizing the category of AFP+ EC would make the classification of AFP-producing endometrial neoplasms more consistent with classifications of tumors in other organs, such as stomach and lung. Whether this separation is justified or not should be examined with the accumulation of further cases. From the existing data, the frequency of *TP53* abnormalities seems to be higher in AFP+ EC than in cases reported as somatically derived yolk sac tumors of the endometrium (32).

Our study has several limitations. First, because AFP+ EC is a rare tumor, we could only study a limited number of cases in detail. To compensate for this, we included cases from the previous literature in some parts of the analysis, which may have resulted in a heterogeneous set of cases. Second, we could not identify any endometrial yolk sac tumors morphologically comparable to yolk sac tumors in younger patients in our predesignated time period: comparing them with AFP+ ECs should have enabled us to study whether AFP+ EC is better considered a "carcinoma," "germ cell tumor," or something intermediate. These points should be addressed in future studies and shed some light on these aggressive neoplasms.

In conclusion, we revealed that AFP+ EC is a clinicopathologically distinct subtype of endometrial carcinoma, occurring in 1.8% of endometrial carcinoma cases. They occur mainly in postmenopausal women and are associated with *TP53* abnormalities and vascular infiltration, which can be extensive. These carcinomas can show aggressive behavior even in FIGO stage I cases and merit further studies to elucidate their characteristics and optimal treatment.

DATA AVAILABILITY STATEMENT

The original contributions presented in the study are included in the article/**Supplementary Materials**, further inquiries can be directed to the corresponding author.

ETHICS STATEMENT

The studies involving human participants were reviewed and approved by Institutional Review Board of Kindai University Faculty of Medicine. The patients/participants provided their written informed consent to participate in this study.

AUTHOR CONTRIBUTIONS

TO drafted the manuscript. TO and AI conceived the study, performed histopathological analysis, and analyzed data. KM participated in the study design. TO and NS performed molecular analysis. MH provided technical assistance. KM, MM, TS, and NM provided care for the patients and collected clinical data and specimens. All authors revised the manuscript.

ACKNOWLEDGMENTS

The authors thank Life Science Research Institute, Kindai University for technical assistance.

SUPPLEMENTARY MATERIAL

The Supplementary Material for this article can be found online at: https://www.frontiersin.org/articles/10.3389/fmed.2021.799163/full#supplementary-material

REFERENCES

1. Gitlin D, Perricelli A, Gitlin GM. Synthesis of α-fetoprotein by liver, yolk sac, and gastrointestinal tract of the human conceptus. *Cancer Res.* (1972) 32:979–82.
2. Yamazawa S, Ushiku T, Shinozaki-Ushiku A, Hayashi A, Iwasaki A, Abe H, et al. Gastric cancer with primitive enterocyte phenotype: an aggressive subgroup of intestinal-type adenocarcinoma. *Am J Surg Pathol.* (2017) 41:989–97. doi: 10.1097/PAS.0000000000000869
3. Akazawa Y, Saito T, Hayashi T, Yanai Y, Tsuyama S, Akaike K, et al. Next-generation sequencing analysis for gastric adenocarcinoma with enteroblastic differentiation: emphasis on the relationship with hepatoid adenocarcinoma. *Hum Pathol.* (2018) 78:79–88. doi: 10.1016/j.humpath.2018.04.022
4. Morita S, Yoshida A, Goto A, Ota S, Tsuta K, Yokozawa K, et al. High-grade lung adenocarcinoma with fetal lung–like morphology. *Am J Surg Pathol.* (2013) 37:924–32. doi: 10.1097/PAS.0b013e31827e1e83
5. Suzuki M, Kasajima R, Yokose T, Ito H, Shimizu E, Hatakeyama S, et al. Comprehensive molecular analysis of genomic profiles and PD-L1 expression in lung adenocarcinoma with a high-grade fetal adenocarcinoma component. *Transl Lung Cancer Res.* (2021) 10:1292–304. doi: 10.21037/tlcr-20-1158
6. Kawagoe K. A case of mixed mesodermal tumor of the uterus with alpha-fetoprotein production. *Jpn J Clin Oncol.* (1985) 15:577–83.
7. Matsukuma K, Tsukamoto N. Alpha-fetoprotein producing endometrial adenocarcinoma: report of a case. *Gynecol Oncol.* (1988) 29:370–7. doi: 10.1016/0090-8258(88)90238-7
8. Kubo K, Lee GH, Yamauchi K, Kitagawa T. Alpha-fetoprotein-producing papillary adenocarcinoma originating from a uterine body. A case report. *Acta Pathol Jpn.* (1991) 41:399–403. doi: 10.1111/j.1440-1827.1991.tb01665.x
9. Phillips KA, Scurry JP, Toner G. Alpha-fetoprotein production by a malignant mixed müllerian tumour of the uterus. *J Clin Pathol.* (1996) 49:349–51. doi: 10.1136/jcp.49.4.349
10. Yamamoto R, Ishikura H, Azuma M, Hareyama H, Makinoda S, Koyama Y, et al. Alpha-fetoprotein production by a hepatoid adenocarcinoma of the uterus. *J Clin Pathol.* (1996) 49:420–2. doi: 10.1136/jcp.49.5.420
11. Hoshida Y, Nagakawa T, Mano S, Taguchi K, Aozasa K. Hepatoid adenocarcinoma of the endometrium associated with alpha-fetoprotein production. *Int J Gynecol Pathol.* (1996) 15:266–9. doi: 10.1097/00004347-199607000-00012
12. Toyoda H, Hirai T, Ishii E. Alpha-fetoprotein producing uterine corpus carcinoma: a hepatoid adenocarcinoma of the endometrium. *Pathol Int.* (2000) 50:847–52. doi: 10.1046/j.1440-1827.2000.01124.x
13. Adams SF, Yamada SD, Montag A, Rotmensch JR. An α-fetoprotein-producing hepatoid adenocarcinoma of the endometrium. *Gynecol Oncol.* (2001) 83:418–21. doi: 10.1006/gyno.2001.6383
14. Takahashi Y, Inoue T. Hepatoid carcinoma of the uterus that collided with carcinosarcoma. *Pathol Int.* (2003) 53:323–6. doi: 10.1046/j.1440-1827.2003.01467.x
15. Takano M, Shibasaki T, Sato K, Aida S, Kikuchi Y. Malignant mixed mullerian tumor of the uterine corpus with alpha-fetoprotein-producing hepatoid adenocarcinoma component. *Gynecol Oncol.* (2003) 91:444–8. doi: 10.1016/S0090-8258(03)00512-2
16. Takeuchi K, Kitazawa S, Hamanishi S, Inagaki M, Murata K. A case of alpha-fetoprotein-producing adenocarcinoma of the endometrium with a hepatoid component as a potential source for alpha-fetoprotein in a postmenopausal woman. *Int J Gynecol Cancer.* (2006) 16:1442–5. doi: 10.1136/ijgc-00009577-200605000-00076
17. Tran TAN, Ortiz HB, Holloway RW, Bigsby GE, Finkler NJ. Alpha-fetoprotein-producing serous carcinoma of the uterus metastasizing to the ovaries, mimicking primary ovarian yolk sac tumor: a case report and review of the literature. *Int J Gynecol Pathol.* (2007) 26:66–70. doi: 10.1097/01.pgp.0000225843.21503.30
18. Kodama J, Seki N, Yanai H, Kusumoto T, Nakamura K, Hongo A, et al. α-fetoprotein-producing endometrial adenocarcinoma without an obvious hepatoid component. *Oncol Lett.* (2010) 1:243–5. doi: 10.3892/ol_00000043
19. Ishibashi K, Kishimoto T, Yonemori Y, Hirashiki K, Hiroshima K, Nakatani Y. Primary hepatoid adenocarcinoma of the uterine corpus: a case report with immunohistochemical study for expression of liver-enriched nuclear factors. *Pathol Res Pract.* (2011) 207:332–6. doi: 10.1016/j.prp.2011.02.010
20. Hwang JH, Song SH, Kim YH, Shin BK, Lee JK, Lee NW, et al. Primary hepatoid adenocarcinoma of the endometrium with a high alphafetoprotein level. *Scott Med J.* (2011) 56:120. doi: 10.1258/smj.2011.011100
21. Kawaguchi R, Furukawa N, Yamada Y, Ooi H, Kobayashi H. Carcinosarcoma of the uterine corpus with alpha-fetoprotein-producing hepatoid adenocarcinoma: a report of two cases. *Case Rep Oncol.* (2011) 4:358–62. doi: 10.1159/000330239
22. Akhavan A, Karimi Zarchi M, Akhavan Tafti M, Navabii H. α-fetoprotein produced by endometrioid adenocarcinoma of uterus. *BMJ Case Rep.* (2012) 2012:bcr0220125830. doi: 10.1136/bcr.02.2012.5830
23. Chen F, Yu C, You X, Mi B, Wan W. Carcinosarcoma of the uterine corpus on 18F-FDG PET/CT in a postmenopausal woman with elevated AFP. *Clin Nucl Med.* (2014) 39:803–5. doi: 10.1097/RLU.0b013e3182a77b90
24. Wu QY, Wan XY, Xie X, Lu BJ. Endometrial hepatoid adenocarcinoma: a rare cause of elevated serum α-fetoprotein. *J Obstet Gynaecol Res.* (2014) 40:873–7. doi: 10.1111/jog.12237
25. Kuroda N, Moritani S, Ichihara S. Combined hepatoid and serous carcinoma of the uterine corpus: an undescribed phenomenon. *Histopathology.* (2015) 67:135–7. doi: 10.1111/his.12614
26. Li JJX, Lee JHS, Chan VTC, Yu M-Y. Uterine carcinosarcoma with alpha-fetoprotein-producing hepatoid component: a case report and literature review. *Case Rep Pathol.* (2018) 2018:3972353. doi: 10.1155/2018/3972353
27. Yin H, Hu Y, Xiu Y, Luo R, Shi H. A rare case of primary endometrial hepatoid adenocarcinoma on 18F-FDG PET/CT. *Clin Nucl Med.* (2019) 44:E425–7. doi: 10.1097/RLU.0000000000002538
28. Liu Y, Zhou R, Wang S, Zhang G. Extra-hepatic hepatoid carcinomas in female reproductive system: three case-reports with a literature review. *Cancer Manag Res.* (2021) 13:1625–36. doi: 10.2147/CMAR.S288913
29. McNamee T, Damato S, McCluggage WG. Yolk sac tumours of the female genital tract in older adults derive commonly from somatic epithelial neoplasms: somatically derived yolk sac tumours. *Histopathology.* (2016) 69:739–51. doi: 10.1111/his.13021
30. Ravishankar S, Malpica A, Ramalingam P, Euscher ED. Yolk sac tumor in extragonadal pelvic sites: still a diagnostic challenge. *Am J Surg Pathol.* (2017) 41:1–11. doi: 10.1097/PAS.0000000000000722
31. Nogales FF, Prat J, Schuldt M, Cruz-Viruel N, Kaur B, D′Angelo E, et al. Germ cell tumour growth patterns originating from clear cell carcinomas of the ovary and endometrium: a comparative immunohistochemical study favouring their origin from somatic stem cells. *Histopathology.* (2018) 72:634–47. doi: 10.1111/his.13426
32. Fadare O, Shaker N, Alghamdi A, Ganesan R, Hanley KZ, Hoang LN, et al. Endometrial tumors with yolk sac tumor-like morphologic patterns or immunophenotypes: an expanded appraisal. *Mod Pathol.* (2019) 32:1847–60. doi: 10.1038/s41379-019-0341-6
33. Acosta AM, Sholl LM, Cin PD, Howitt BE, Otis CN, Nucci MR. Malignant tumours of the uterus and ovaries with mullerian and germ cell or trophoblastic components have a somatic origin and are characterised by genomic instability. *Histopathology.* (2020) 77:788–97. doi: 10.1111/his.14188
34. Nogales FF, Preda O, Nicolae A. Yolk sac tumours revisited. A review of their many faces and names. *Histopathology.* (2012) 60:1023–33. doi: 10.1111/j.1365-2559.2011.03889.x
35. Köbel M, Ronnett BM, Singh N, Soslow RA, Gilks CB, McCluggage WG. Interpretation of P53 immunohistochemistry in endometrial carcinomas: toward increased reproducibility. *Int J Gynecol Pathol.* (2019) 38:S123–31. doi: 10.1097/PGP.0000000000000488
36. Casey L, Singh N. POLE, MMR, and MSI testing in endometrial cancer: proceedings of the ISGyP companion society session at the USCAP 2020 annual meeting. *Int J Gynecol Pathol.* (2021) 40:5–16. doi: 10.1097/PGP.0000000000000710
37. Fader AN, Roque DM, Siegel E, Buza N, Hui P, Abdelghany O, et al. Randomized phase II trial of carboplatin-paclitaxel versus carboplatin-paclitaxel-trastuzumab in uterine serous carcinomas that overexpress human epidermal growth factor receptor 2/neu. *J Clin Oncol.* (2018) 36:2044–51. doi: 10.1200/JCO.2017.76.5966
38. Kato T, Hagiyama M, Takashima Y, Yoneshige A, Ito A. Cell adhesion molecule-1 shedding induces apoptosis of renal epithelial cells and exacerbates human nephropathies. *Am J Physiol Renal Physiol.* (2018) 314:F388–98. doi: 10.1152/ajprenal.00385.2017

39. Pao W, Wang TY, Riely GJ, Miller VA, Pan Q, Ladanyi M, et al. KRAS mutations and primary resistance of lung adenocarcinomas to gefitinib or erlotinib. *PLoS Med.* (2005) 2:e17. doi: 10.1371/journal.pmed.0020017
40. Dunlap J, Le C, Shukla A, Patterson J, Presnell A, Heinrich MC, et al. Phosphatidylinositol-3-kinase and AKT1 mutations occur early in breast carcinoma. *Breast Cancer Res Treat.* (2010) 120:409–18. doi: 10.1007/s10549-009-0406-1
41. Kim K-R, Lax S, Lazar A, Longacre T, Malpica A, Matias-Guiu X, et al. Tumours of the uterine corpus. In: WHO Classification of Tumours Editorial Board, editor. *Female Genital Tumours (WHO Classification of Tumours Series, 5th ed; vol 4)*. Lyon: International Agency of Research on Cancer (2020). p. 245–308.
42. Meguro S, Yasuda M. α-Fetoprotein-producing ovarian tumor in a postmenopausal woman with germ cell differentiation. *Ann Diagn Pathol.* (2013) 17:140–4. doi: 10.1016/j.anndiagpath.2011.07.010
43. Morimoto A, Sudo T, Sakuma T, Yasuda M, Fujiwara K. Alpha-fetoprotein-producing ovarian clear cell adenocarcinoma simulating fetal gut in a postmenopausal woman. *Gynecol Oncol Rep.* (2014) 8:24–6. doi: 10.1016/j.gynor.2014.03.001
44. Chao WT, Liu CH, Lai CR, Chen YJ, Chuang CM, Wang PH. Alpha-fetoprotein-producing ovarian clear cell adenocarcinoma with fetal gut differentiation: a rare case report and literature review. *J Ovarian Res.* (2018) 11:1–7. doi: 10.1186/s13048-018-0426-8
45. Toyoda S, Uchiyama T, Morita K, Ishida E, Sugiura A, Kita T, et al. Cytological diagnosis of a rare case of α-fetoprotein producing gastric-type adenocarcinoma of the uterine cervix. *Cytopathology.* (2019) 30:440–3. doi: 10.1111/cyt.12688
46. Fujimoto M, Minamiguchi S, Ishida A, Sumiyoshi S, Horikawa N, Chigusa Y, et al. HER2 -amplified cervical gastric-type mucinous carcinoma with a primitive enterocyte phenotype. *Histopathology.* (2020) 77:511–3. doi: 10.1111/his.14119
47. Kinjo T, Taniguchi H, Kushima R, Sekine S, Oda I, Saka M, et al. Histologic and immunohistochemical analyses of α-fetoprotein-producing cancer of the stomach. *Am J Surg Pathol.* (2012) 36:56–65. doi: 10.1097/PAS.0b013e31823aafec
48. National Comprehensive Cancer Network. *Uterine Neoplasms (Version 4.2021)*. Available online at: https://www.nccn.org/professionals/physician_gls/pdf/uterine.pdf (accessed October 12, 2021).
49. Fujimoto M, Matsuzaki I, Nishino M, Iwahashi Y, Warigaya K, Kojima F, et al. HER2 is frequently overexpressed in hepatoid adenocarcinoma and gastric carcinoma with enteroblastic differentiation: a comparison of 35 cases to 334 gastric carcinomas of other histological types. *J Clin Pathol.* (2018) 71:600–7. doi: 10.1136/jclinpath-2017-204928
50. Buza N. HER2 testing in endometrial serous carcinoma: time for standardized pathology practice to meet the clinical demand. *Arch Pathol Lab Med.* (2021) 145:687–91. doi: 10.5858/arpa.2020-0207-RA
51. Jain D, Asamura H, Cardona AF, MacMahon H, Nakatani Y. Fetal adenocarcinoma of the lung. In: WHO Classification of Tumours Editorial Board, editor. *Thoracic Tumours (WHO Classification of Tumours Series, 5th ed; vol 5)*. Lyon: International Agency of Research on Cancer (2021). p. 81–2.
52. Carneiro F, Fukayama M, Grabsch HI, Yasui W. Gastric adenocarcinoma. In: WHO Classification of Tumours Editorial Board, editor. *Digestive System Tumours (WHO Classification of Tumours Series, 5th ed; vol 1)*. Lyon: International Agency of Research on Cancer (2019). p. 85–95.
53. Oliva E, Wilbur DC, Sebire NJ, Soslow RA. Miscellaneous and metastatic malignancies. In: *Tumors of the Uterine Corpus and Trophoblastic Diseases (AFIP Atlas of Tumor Pathology, Fourth Series, Fascicle 30)*. Arlington, VA: American Registry of Pathology (2020). p. 421–43.
54. Fadare O, Zhao C, Khabele D, Parkash V, Quick CM, Gwin K, et al. Comparative analysis of napsin a, alpha-methylacyl-coenzyme a racemase (AMACR, P504S), and hepatocyte nuclear factor 1 beta as diagnostic markers of ovarian clear cell carcinoma: an immunohistochemical study of 279 ovarian tumours. *Pathology.* (2015) 47:105–11. doi: 10.1097/PAT.0000000000000223
55. Damato S, Haldar K, McCluggage WG. Primary endometrial yolk sac tumor with endodermal-Intestinal differentiation masquerading as metastatic colorectal adenocarcinoma. *Int J Gynecol Pathol.* (2016) 35:316–20. doi: 10.1097/PGP.0000000000000236
56. Mirkovic J, McFarland M, Garcia E, Sholl LM, Lindeman N, MacConaill L, et al. Targeted genomic profiling reveals recurrent KRAS mutations in mesonephric-like adenocarcinomas of the female genital tract. *Am J Surg Pathol.* (2018) 42:227–33. doi: 10.1097/PAS.0000000000000958

Conflict of Interest: The authors declare that the research was conducted in the absence of any commercial or financial relationships that could be construed as a potential conflict of interest.

frontiers in Medicine

CASE REPORT
published: 10 January 2022
doi: 10.3389/fmed.2021.819141

Case Report: Uterine Adenosarcoma With Sarcomatous Overgrowth and Malignant Heterologous Elements

Yunuén I. García-Mendoza[1], Mario Murguia-Perez[2], Aldo I. Galván-Linares[1], Saulo Mendoza-Ramírez[3], Norma L. García-Salinas[1], Julio G. Moctezuma-Ramírez[1], Blanca O. Murillo-Ortiz[4], Luis Jonathan Bueno-Rosario[5], Marco A. Olvera-Olvera[6] and Guillermo E. Corredor-Alonso[7]*

[1] Department of Surgical Pathology, Speciality Hospital N° 1 National Medical Center Bajio, Social Security Mexican Institute, University of Guanajuato, Leon, Mexico, [2] Head of Department of Surgical Pathology, Speciality Hospital N° 1 National Medical Center Bajio, Social Security Mexican Institute, University of Guanajuato, León, Mexico, [3] Pathology Unit, General Hospital of Mexico "Dr. Eduardo Liceaga", National Autonomous University of Mexico, México, Mexico, [4] Research Unit of Clinic Epidemiology, Speciality Hospital N° 1 National Medical Center Bajio, Social Security Mexican Institute, Leon, Mexico, [5] Head of Oncology Unit, Speciality Hospital N° 1 National Medical Center Bajio, Social Security Mexican Institute, Leon, Mexico, [6] Department of Radiology, Speciality Hospital N° 1 National Medical Center Bajio, Social Security Mexican Institute, University of Guanajuato, Leon, Mexico, [7] Department of Pathology, General Hospital 92, Social Security Mexican Institute, Acuña, Mexico

OPEN ACCESS

Edited by:
Luigi Tornillo, University of Basel, Switzerland

Reviewed by:
Antonio De Leo, University of Bologna, Italy
José Manuel Lopes, Universidade do Porto, Portugal

***Correspondence:**
Mario Murguia-Perez
drmariopatologia@gmail.com
orcid.org/0000-0003-4260-389X

Specialty section:
This article was submitted to Pathology, a section of the journal Frontiers in Medicine

Received: *20 November 2021*
Accepted: *14 December 2021*
Published: *10 January 2022*

Citation:
García-Mendoza YI, Murguia-Perez M, Galván-Linares AI, Mendoza-Ramírez S, García-Salinas NL, Moctezuma-Ramírez JG, Murillo-Ortiz BO, Bueno-Rosario LJ, Olvera-Olvera MA and Corredor-Alonso GE (2022) Case Report: Uterine Adenosarcoma With Sarcomatous Overgrowth and Malignant Heterologous Elements. Front. Med. 8:819141. doi: 10.3389/fmed.2021.819141

A 46- year-old woman presented a uterine adenosarcoma originating in the lower uterine segment. The diagnosis was made in an endometrial biopsy and confirmed in the pathological examination of the complete surgical specimen, both identifying heterologous malignant elements. In addition, complementary immunohistochemical studies were performed. We reviewed the literature, illustrating the clinical and morphological characteristics and the differential diagnoses to be evaluated.

Keywords: uterine adenosarcoma, heterologous elements, immunohistochemistry, uterine sarcoma classification, malignant neoplasm

INTRODUCTION

Endometrial cancer corresponds to the vast majority of malignant tumors of the uterine corpus (80% in Europe and more than 90% in the United States). It is the sixth most diagnosed cancer in women and the second most exclusively diagnosed female genital tract cancer (1). Uterine adenosarcoma (UA) is a mixed tumor of the uterus consisting of a benign glandular epithelium and a malignant mesenchymal component, which was reported as müllerian adenosarcoma by Clement and Scully in 1974 (2, 3). It is a rare tumor that corresponds to 8% of all uterine sarcomas and <0.5% of uterine malignant tumors (4, 5). The morphological characteristics of these neoplasms are distinguished from other biphasic tumors (epithelial and mesenchymal), both benign and malignant. UA are generally neoplasms of low malignant potential, except when accompanied by sarcomatous overgrowth and myometrial invasion (1, 4); these tumors can recur locally, and rarely metastasize (6).

About 15% of UA can have heterologous elements, such as skeletal muscle, cartilage, fat, and other components. Such heterologous elements are less common than the homologous variant (7). We present a case of uterine adenosarcoma with sarcomatous overgrowth (UASO) with heterologous elements in a middle-aged woman, and we review its clinical-pathological characteristics and management.

CASE DESCRIPTION

A 48-year-old woman with a gynecological-obstetric history of 2 pregnancies, obtained by cesarean section. Her condition began 6 months before admission, with intermittent metrorrhagia, dyspepsia, pain; increased abdominal volume and metrorragia were added. A Colposcopy and biopsy was performed, which reported a high-grade endometrial stromal sarcoma vs. carcinosarcoma. Subsequent symptoms were presented; abundant transvaginal bleeding and evidence of hypovolemic shock, requiring a transfusion of 3 blood packs and a hemostatic radiotherapy dose of 6 Gy. A revision of previous pathological material was requested to establish therapeutic conduct.

DIAGNOSTIC ASSESSMENT

The slide review revealed a mixed malignant neoplasm consisting mostly of spindle-shaped and ovoid stromal cells arranged in a tapered pattern, with pale eosinophilic cytoplasm, nuclei with dense chromatin, evident nucleoli, and atypical mitoses; They coexisted with glands with an endometrial, tubular, and semitortuous appearance, lined by columnar epithelium with a proliferative appearance, with pseudostratified, discrete atypia, almost absent, without mitosis and luminal secretion. Around these glands, we observed packing of the spindle cells, arranged in a string of pearls pattern, and toward the periphery, there were paucicellular areas. The formation of "leaf-shaped" structures was also identified, with a low columnar epithelial lining, without atypia, and below it, the elongated cells described above. Extensive areas of highly cellular cartilage were identified, with moderate pleomorphism, hyperchromasia, and evident nucleoli. No areas of necrosis were identified. It was reported as UASO with heterologous elements of grade 2 chondrosarcoma (**Figure 1**).

A computed tomography scan was performed that showed a neoformative process at the cervical level (**Figures 2A,B**). An abdominal ultrasound reported a uterine morphological alteration, at the level of the isthmus with an oval nodule with poorly defined margins, with internal vascularity, the endometrium with homogeneous echogenicity, and without alterations in the ovaries. With these findings, she was scheduled for a total abdominal hysterectomy with bilateral salpingo-oophorectomy and appendectomy.

We received in our pathological anatomy department a surgical specimen that included cervical, endocervical, and lower uterine segment deformity, identifying an irregular tumor located toward the left inferolateral portion. We observed a heterogeneous tumor originating in the lower uterine segment, 9 cm in diameter, friable, grayish-brown, with hemorrhagic areas and areas of cartilaginous appearance, protruding through the endocervical canal, with expansion to the exocervix, without ulceration of the epithelium. No involvement of the endometrium and myometrium of the fundus and uterine walls were identified; however, there is 100% invasion of the left muscular wall of the lower uterine segment (Myometrium of the lower uterine segment thickness: 1.7 cm. Tumor size: 9 cm) (**Figure 3**). The rest of the organs sent did not present macroscopic alterations. The histological sections showed what was previously observed, direct involvement of the left parametrium of endometrial stromal sarcoma and chondrosarcoma component, without vascular invasion. Surgical margins were negative. Immunohistochemistry was positive for CD10, estrogen and progesterone receptors, p53, cyclin D1, WT1, PMS2, b-catenin an S100, it last found chondrosarcoma component (**Figure 4**). The final diagnosis was UASO with heterologous elements of grade 2 chondrosarcoma, with extension toward the endocervix and protrusion of the endocervical canal (pT1C, FIGO IB).

The patient was discharged and was kept under active surveillance by the oncology service, and without receiving adjuvant therapy. However, three months after the surgery, the patient presented intermittent abdominal pain. Abdominopelvic computed tomography was performed identifying a tumor adhered to the pelvic and abdominal cavity with dimensions of 30 × 25 cm (**Figure 1C**), with multiples peritoneal implants, for which she was operated on again. The patient underwent optimal debulking plus packaging, presented bleeding of 5,000 ml, 4 globular units and expander fluids were administered. We received in the Pathology department, a multifragmented tumor with a soft necrohemorrhagic appearance, and in the histological study with the characteristics already mentioned above. During her hospitalization, she developed pulmonary embolism. A pulmonary embolism computed tomography was performed,

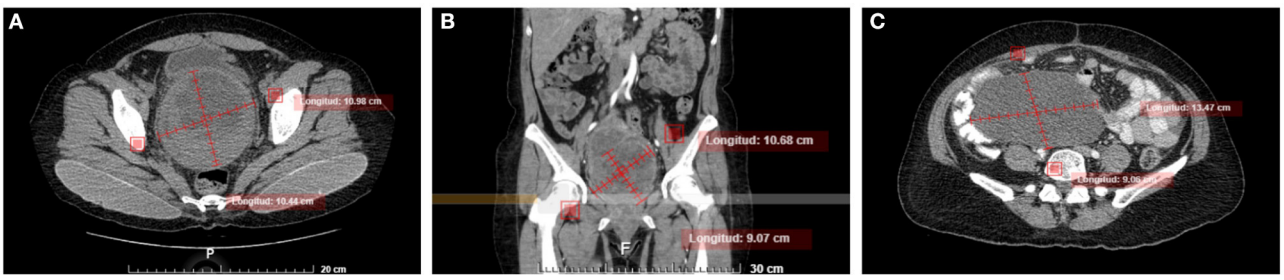

FIGURE 1 | Abdominal axial **(A)** and coronal **(B)** non-enhanced CT images show a large well-defined rounded tumor, with a heterogeneous appearance in the cervix and demonstrating mass effect in adjacent structures and preserving interface with the bladder wall and rectum. **(C)** Axial non-enhanced CT, three months after surgery shows a heterogeneous abdominal tumor that compresses and displaces adjacent structures.

where a thrombus was evidenced in the right pulmonary artery, which led to a pulmonary infarction of the right lower lobe. Acenocoumarin was administered, despite this, she developed right lower extremity thrombosis. It was assessed by the Departments of Clinical Oncology and Radiotherapy, concluding that it was out of clinical treatment based on the added underlying pathologies. He is currently in palliative treatment, with acenocoumarin and morphine for pain management.

DISCUSSION

Mixed uterine tumors with an epithelial and mesenchymal component comprise a heterogeneous group of neoplasms that are categorized as carcinosarcoma, adenosarcoma, adenofibroma, adenomyoma, and atypical polypoid adenomyoma, included in the 2020 World Health Organization (WHO) classification (1, 8). The WHO defines a uterine adenosarcoma (UA) as a mixed epithelial and mesenchymal tumor where the epithelial component is benign or atypical, and the stromal component has a low malignant potential (1). They are rare neoplasms and constitute the third most common subtype of uterine sarcoma, after leiomyosarcoma (LMS) and low-grade endometrial stromal sarcoma (LG-ESS). Of the uterine malignant tumors, it corresponds to <0.5% of the cases (4, 5), and 8% of the uterine sarcomas. Most occur in postmenopausal women, but about 30% of premenopausal women, including adolescents. The average age of presentation is 58 years (range 50–59 years) (1, 9). Symptoms are non-specific, although the most common is abnormal uterine bleeding (4). Other symptoms that may occur are an enlarged uterus, protrusion through the cervical canal, and pelvic pain, among others. The most characteristic symptom is a recurrent polypoid lesion, which is biopsied on several occasions, in which a definitive diagnosis cannot be reached; A misdiagnosis can even occur, of which the most frequent is a cervical polyp (10). These tumors can occasionally occur outside the uterus (ovary and fallopian tube) (11).

The pathogenesis of UA is uncertain. However, the association between exogenous hormone therapy and the development of malignant tumors in endometriosis is well-known, and many studies have suggested the possibility of neoplastic transformation at endometriotic sites (10). Macroscopically, they are polypoid or multipolypoid lesions that can potentially occupy the entire uterine cavity and protrude through the endocervical orifice. They generally begin in the lateral walls of the uterine fundus, but they can also originate in the lower uterine segment; depending on its growth, it can affect neighboring structures (1, 8). Microscopically, it is a mixed lesion, with a "benign" glandular component immersed in a low-grade sarcomatous stroma (1, 8, 10). The glandular component appears inactive, and may occasionally present hyperplastic features with or without atypia, or, as in our case, a proliferative in appearance. Occasionally other types of the epithelium (mucinous, squamous, secretory, or clear cells) may be found. Glands are often seen in the myometrial invasion areas of uterine adenocarcinoma, suggesting that, despite its inactive glandular appearance, this component is an active part of the neoplasm (1, 2, 4). The stromal component is the most striking feature of these tumors, in which a low-grade sarcoma with variable cytological atypia (generally low to moderate) is seen. One of the diagnostic keys of this entity is the densification of the stromal component around the glands, surrounding them like a collar (it is sometimes called in some texts "cambium layer"), identifying mitoses, which are not >4 per field at 40X. The stromal component also presents a paucicellular component below the superficial epithelium, giving a "leaf appearance." The anchoring of the uterine wall is usually well-defined; however, myometrial invasion is occasionally seen, which is related to a worse prognosis. Areas of heterologous differentiation (1, 8, 10) (skeletal muscle, lipoblasts, cartilage, etc.), or of stromal overgrowth (which is defined as a sarcomatous component that occupies 25% or more of the total tumor volume) (2, 10). Heterologous components can be observed in the last cases, especially rhabdomyosarcoma, and this represents a more aggressive clinical course. In one of the longest series published (7 cases), none of the cases with sarcomatous overgrowth presented heterologous areas (11). Our case presented a heterologous component of grade 2 chondrosarcoma, which is exceptional and has not been previously reported in the literature. UA that are considered high-grade have a high mitotic index (more than 4 mitoses per field at 40X) and are aneuploid with a fraction in the synthesis phase >10% (12, 13). In these cases, DICER1 gene mutations have also been observed, and less frequently, somatic alterations such as aberrations in the RAS or PI3K/PTEN signaling pathways, CDK4/MDM2 amplification, and TP53 and ARID1A mutations (14).

Due to its rarity, information on immunohistochemical markers that may be useful for the diagnosis of the entity is limited. Similar to endometrial stromal sarcoma, they are positive tumors for CD10, WT1, estrogen receptors, and progesterone. In cases with sarcomatous overgrowth, the expression of these markers is lower, which reflects the differentiation of the

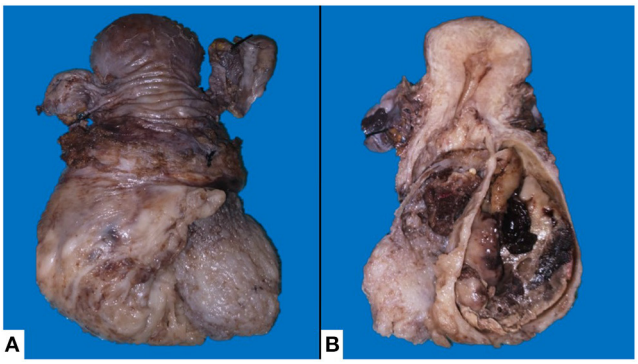

FIGURE 2 | Macroscopic surgical specimen. **(A)** External surface of the posterior aspect of the uterus, a lesion that completely distorts the architecture of the cervix can be seen, the lesion has a pseudo-encapsulated fleshy appearance with some areas of irregular myxoid appearance. **(B)** Uterus, cut surface, with tumor originating in the lower uterine segment, with protrusion through the endocervical canal and expansion of the exocervix, showing the involvement of the endocervical wall.

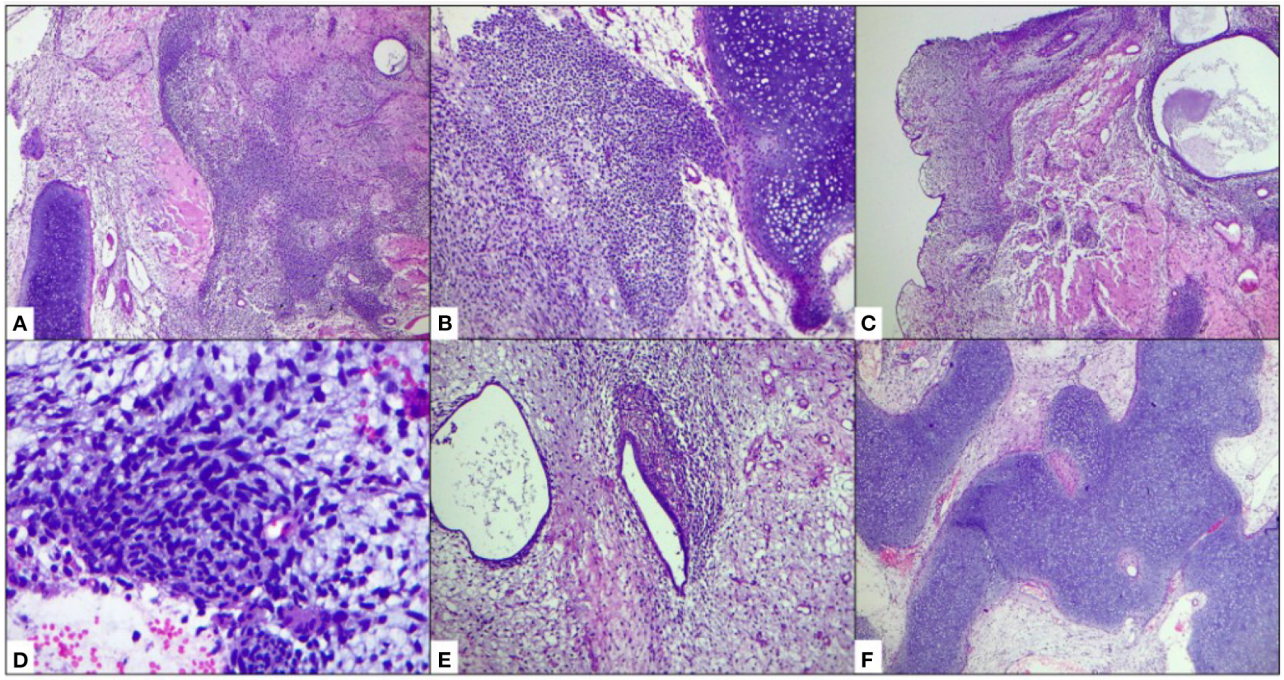

FIGURE 3 | Histology of the tumor. **(A,B)** A mixed malignant neoplasm made up of cartilaginous areas that alternate with areas of paucicellular spindle malignant cells is observed, within which tubular and ectatic glandular structures can be seen. **(C)** Formation of "leaf-shaped" structures. **(D)** Malignant high-grade spindle cell component. **(E)** Glands with a "benign" endometrial appearance, surrounded by packed malignant stromal cells (cambium layer). **(F)** Extensive areas with malignant chondroid differentiation.

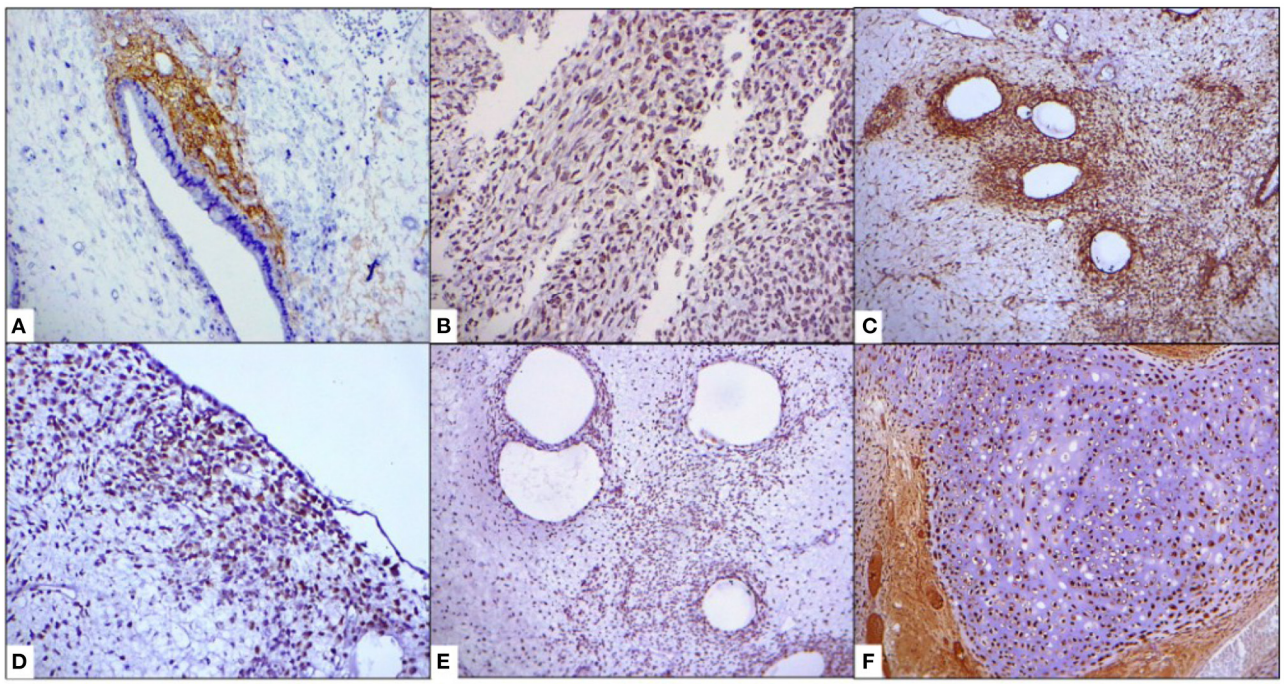

FIGURE 4 | Immunohistochemistry. **(A)** CD10. **(B)** p53. **(C)** Beta-catenina. **(D)** hTERT. **(E)** PMS2. **(F)** S-100.

mesenchymal component (10, 15). In a paper presented at the USCAP 2018 conference, Stout et al. found immunoexpression of PTEN (70%), TERT (90%), PMS2 (100%), and Beta-catenin (60%); compared with low-grade endometrial stromal sarcoma, the latter also expresses the aforementioned antibodies in variable percentages, but is distinguished by finding rearrangement of the JAZF1 gene by fluorescent *in situ* hybridization (FISH), not being found in any case in UA; in our case, in addition to the traditional markers, we found expression of PMS2, Beta-catenin, and h-TERT. Alterations in the TP53 signaling pathway have been reported to be related to nuclear atypia and marked pleomorphism identified at lower magnification; Furthermore, the expression of the p53 protein by immunohistochemistry correlates mostly with the mutation of the gene (16). We clarify that the case was not studied molecularly, firstly because we do not have access to molecular techniques to study the tumor, and secondly because it does not provide greater benefit to choose medical therapy.

The differential diagnosis is broad and consists mainly of tumors that present a biphasic pattern, and vary depending on the type of adenosarcoma to be considered. In low-grade UA, endometrial polyps with unusual characteristics, adenofibromas, adenomyoma, and atypical polypoid adenomyoma are considered. In the spectrum of UASO, it is mainly with carcinosarcoma, although undifferentiated uterine sarcoma, endometrial stromal sarcoma, and leiomyosarcoma must also be considered (1, 10, 12).

The treatment of choice is surgical, performing total abdominal hysterectomy or by laparoscopic approach, with or without bilateral salpingo-oophorectomy; in women of reproductive age, a myomectomy and polypectomy may be chosen. There is no standardized chemotherapy, hormonal therapy, or radiation therapy in UA, due to the small number of patients with this neoplasia; however, standardized chemotherapy for uterine sarcomas, such as doxorubicin, ifosfamide, or gemcitabine/docetaxel, and newer drugs, such as trabectedin, appear to have some efficacy in UASO (16, 17).

The prognosis of UA depends on the stage and the presence of sarcomatous overgrowth. It has been observed that a 2-year survival and progression-free rates for patients with low-grade UA were 100%, compared to 20% found in those with UASO. Survival rates range from 60% for tumors with myoinvasion, and <50% present metastasis. The pelvis or abdominal cavity is the first site of recurrence, and sarcomatosis is a frequent complication; distant metastases are less common, with the liver and lung being the most frequent sites, followed by bone, kidney, spleen, and rarely, brain (1, 10, 16).

Due to the low incidence and histological diversity of uterine adenosarcoma, only a few case reports and series provide data on prognostic factors and survival prediction (18). With the rapid development of artificial intelligence, a new choice is provided for adenosarcoma researchers. The deep learning method has the ability to analyze the non-linear correlations that are more common in the real world. It has been proven to be greatly effective for various clinical tasks, including image identification, pathological diagnoses, genomic analysis, metabolomics, and immunology studies. Qu et al. developed and validated a personalized survival prediction model for UA, combining the SEER database with a neural network model called "neural multitask logistic regression model" (N-MTLR), comparing it with the traditional model (CPH model), demonstrating survival time predictions that are much more accurate than the other model (19). It is possible that the extension of this model in an online program, in case of obtaining data from cases around the world, could offer more information about this rare tumor.

DATA AVAILABILITY STATEMENT

The original contributions presented in the study are included in the article/supplementary materials, further inquiries can be directed to the corresponding author/s.

AUTHOR CONTRIBUTIONS

MM-P: conceptualization, supervision, writing original draft, and project administration. YG-M: investigation, writing original draft, and software. AG-L: resources and data curation. SM-R: resources and methodology. NG-S, JM-R, BM-O, MO-O, and GC-A: resources. LB-R: visualization. All authors contributed to the article and approved the submitted version.

ACKNOWLEDGMENTS

Special thanks to pathology residents for prompt and neat surgical specimen work and case follow-up. Special mention to the team of histotechnologists of the Department of Pathology of the UMAE N° 1.

REFERENCES

1. WHO Classification of Tumours Editorial Board. *Female Genital Tumours*. Lyon: International Agency for Research on Cancer (2020).
2. Wang B, Yang HD, Shi XH, Li H. Advanced uterine adenosarcoma with sarcomatous overgrowth in a young woman: a case report. *Medicine.* (2019) 98:47. doi: 10.1097/MD.0000000000018119
3. Clement PB, Scully RE. Müllerian adenosarcoma of the uterus. A clinicopathologic analysis of ten cases of a distinctive type of müllerian mixed tumor. *Cancer.* (1974) 34:1138–49. doi: 10.1002/1097-0142(197410)34:4<1138::AID-CNCR2820340425>3.0.CO;2-9
4. Nathenson MJ, Ravi V, Fleming N, Wang WL, Conley A. Uterine adenosarcoma: a review. *Curr Oncol Rep.* (2016) 18:68. doi: 10.1007/s11912-016-0552-7
5. Omi M, Tonnoka A, Chiba T, Tanaka Y, Fusegi A, Aoki Y, et al. Immunohistochemical markers and the clinical course of adenosarcoma: a series of seven cases. *Diagn Pathol.* (2020) 15:119. doi: 10.1186/s13000-020-01036-5
6. Lee S-J, Park JY. A rare case of intramural müllerian adenosarcoma arising from adenomyosis of the uterus. *J Pathol Transl Med.* (2017) 51:443–40. doi: 10.4132/jptm.2017.06.11

7. Xie Y-P, Yao H-X, Shen Y-M. Müllerian adenosarcoma of the uterus with heterologous elements: two case reports and literature review. *Arch Gynecol Obstet.* (2012) 286:537–40. doi: 10.1007/s00404-012-2258-x
8. McCluggage WG. A practical approach to the diagnosis of mixed epithelial and mesenchymal tumours of the uterus. *Mod Pathol.* (2016) 29:S78–91. doi: 10.1038/modpathol.2015.137
9. Ghartimagar D, Shrestha B, Ghosh A, Shrestha MK, Shrestha J, et al. Adenosarcoma of uterus – rare biphasic malignant tumor: a case report. *J Nepal Med Assoc.* (2021) 59:200–3. doi: 10.31729/jnma.5373
10. Pinto A, Howitt B. Uterine adenosarcoma. *Arch Pathol Lab Med.* (2016) 140:286–90. doi: 10.5858/arpa.2014-0523-RS
11. Nannini M, Dondi G, Santini D, De Leo A, Dei Tos AP, et al. A single-centre experience on the management of adenosarcoma: a successful report of an integrated medical and surgical approach. *Clin Med Insights Oncol.* (2018) 12:1179554918782477. doi: 10.1177/1179554918782477
12. Gallardo A, Prat J. Müllerian adenosarcoma: a clinicopathologic and inmunohistochemical study of 55 cases challenging the existence of adenofibroma. *Am J Surg Pathol.* (2009) 33:278–88. doi: 10.1097/PAS.0b013e318181a80dol
13. Blom R, Guerrieri C. Adenosarcoma of the uterus: a clinicopathologic, DNA flow cytometric, p53 and mdm-2 analysis of 11 cases. *Int J Gynecol Cancer.* (1999) 9:37–43. doi: 10.1046/j.1525-1438.1999.09885.x
14. Bean GR, Anderson J, Sangoi AR, Krings G, Garg K. *DICER1* mutations are frequent in müllerian adenosarcomas and are independent of rhabdomyosarcomatous differentiation. *Mod Pathol.* (2019) 32:280–9. doi: 10.1038/s41379-018-0132-5
15. Stout I, Ghatak S, Wipf H, Dolan M, Khalifa M, Murugan P. Uterine adenosarcoma and low grade endometrial stromal sarcoma: a comparative study using novel immunohistochemical markers. *Mod Pathol.* (2019) 32(Suppl. 2):111–2. doi: 10.1177/1066896909337600
16. Schroeder BA, Pollack SM, Jones RL. Systemic therapy in advanced uterine adenosarcoma with sarcomatous overgrowth. *Ginecol Oncol.* (2014) 132:513. doi: 10.1016/j.ygyno.2013.09.035
17. Dondi G, Porcu E, De Palma A, Damiano G, De Crescenzo E, et al. Uterine preservation treatments in sarcomas: oncological problems and reproductive results: a systematic review. *Cancers.* (2021) 13:5808. doi: 10.3390/cancers13225808
18. Seagle BLL, Kanis MJ, Strohl AE, Shahabi S. Survival of women with mullerian adenosarcoma: a national cancer data base study. *Gynecol Oncol.* (2016) 143:636–41. doi: 10.1016/j.ygyno.2016.10.013
19. Qu W, Liu Q, Jiao X, Zhang T, Wang B, Li N, et al. Development and validation of a personalized survival prediction model for uterine adenosarcoma: a population-based deep learning study. *Front Oncol.* (2021) 10:623818. doi: 10.3389/fonc.2020.623818

Conflict of Interest: The authors declare that the research was conducted in the absence of any commercial or financial relationships that could be construed as a potential conflict of interest.

Publisher's Note: All claims expressed in this article are solely those of the authors and do not necessarily represent those of their affiliated organizations, or those of the publisher, the editors and the reviewers. Any product that may be evaluated in this article, or claim that may be made by its manufacturer, is not guaranteed or endorsed by the publisher.

frontiers in Medicine

CASE REPORT
published: 07 February 2022
doi: 10.3389/fmed.2022.835599

Case Report: Unclassified Renal Cell Carcinoma With Medullary Phenotype and *SMARCB1/INI1* Deficiency, Broadening the Spectrum of Medullary Carcinoma

Marina Valeri[1,2], *Miriam Cieri*[2], *Grazia Maria Elefante*[2], *Camilla De Carlo*[1,2], *Noemi Rudini*[2], *Giovanni Lughezzani*[1,3], *Nicolò Maria Buffi*[1,3], *Luigi Maria Terracciano*[1,2] *and Piergiuseppe Colombo*[1,2*]

[1] *Department of Biomedical Sciences, Humanitas University, Pieve Emanuele, Italy,* [2] *Department of Pathology, Istituto di Ricovero e Cura a Carattere Scientifico (IRCCS) Humanitas Clinical and Research Hospital, Rozzano, Italy,* [3] *Department of Urology, Istituto di Ricovero e Cura a Carattere Scientifico (IRCCS) Humanitas Clinical and Research Hospital, Rozzano, Italy*

OPEN ACCESS

Edited by:
Luigi Tornillo,
University of Basel, Switzerland

Reviewed by:
Rahul Mannan,
University of Michigan, United States
Deepika Sirohi,
The University of Utah, United States

***Correspondence:**
Piergiuseppe Colombo
piergiuseppe.colombo@hunimed.eu

Specialty section:
This article was submitted to Pathology, a section of the journal Frontiers in Medicine

Received: *14 December 2021*
Accepted: *10 January 2022*
Published: *07 February 2022*

Citation:
Valeri M, Cieri M, Elefante GM, De Carlo C, Rudini N, Lughezzani G, Buffi NM, Terracciano LM and Colombo P (2022) Case Report: Unclassified Renal Cell Carcinoma With Medullary Phenotype and SMARCB1/INI1 Deficiency, Broadening the Spectrum of Medullary Carcinoma. Front. Med. 9:835599. doi: 10.3389/fmed.2022.835599

Renal medullary carcinoma (RMC) is a rare entity with poor prognosis bearing inactivating genomic alterations in *SMARCB1/INI1* resulting in the loss of expression of INI1 and occurring in young patients with sickle cell trait or sickle cell disease. Recently, rare examples with histological characteristics of RMC have been described in older patients without hemoglobinopathies and provisionally termed "Renal cell carcinoma unclassified with medullary phenotype" (RCCU-MP). Fluorescence *in situ* Hybridization (FISH) can detect alterations in *SMARCB1/INI1* consisting mostly in inactivating translocation of one allele and deletion of the second. To date, only seven further cases of RCCU-MP have been described in the literature. Here we report the second Italian case of RCCU-MP, a 62-year-old man presenting with persistent dull back pain and incidentally discovering a 13 cm mass in the right kidney. The nomenclature of this entity is still debated and might be updated as a variant of medullary carcinoma in the upcoming WHO classification. In the meantime, we encourage awareness of these extraordinarily rare neoplasms with poor outcomes.

Keywords: renal medullary carcinoma, renal cell carcinoma unclassified with medullary phenotype, *SMARCB1/INI1*, sickle cell trait, kidney, case report

INTRODUCTION

Renal medullary carcinoma (RMC) is an aggressive neoplasm accounting for <0.5% of renal cell carcinomas (RCC) (1, 2). This rare entity occurs mainly in the third decade of life and almost all (> 95%) patients have sickle cell trait, sickle cell disease, or associated hemoglobinopathies (2). RMC is characterized by inactivating genomic alterations in *SMARCB1/INI1*, a tumor suppressor gene (3), resulting in the loss of immunohistochemical expression of INI1 in all cases (4–6). Recently, exceedingly rare tumors sharing morpho-phenotypic features with RMC, but occurring in older

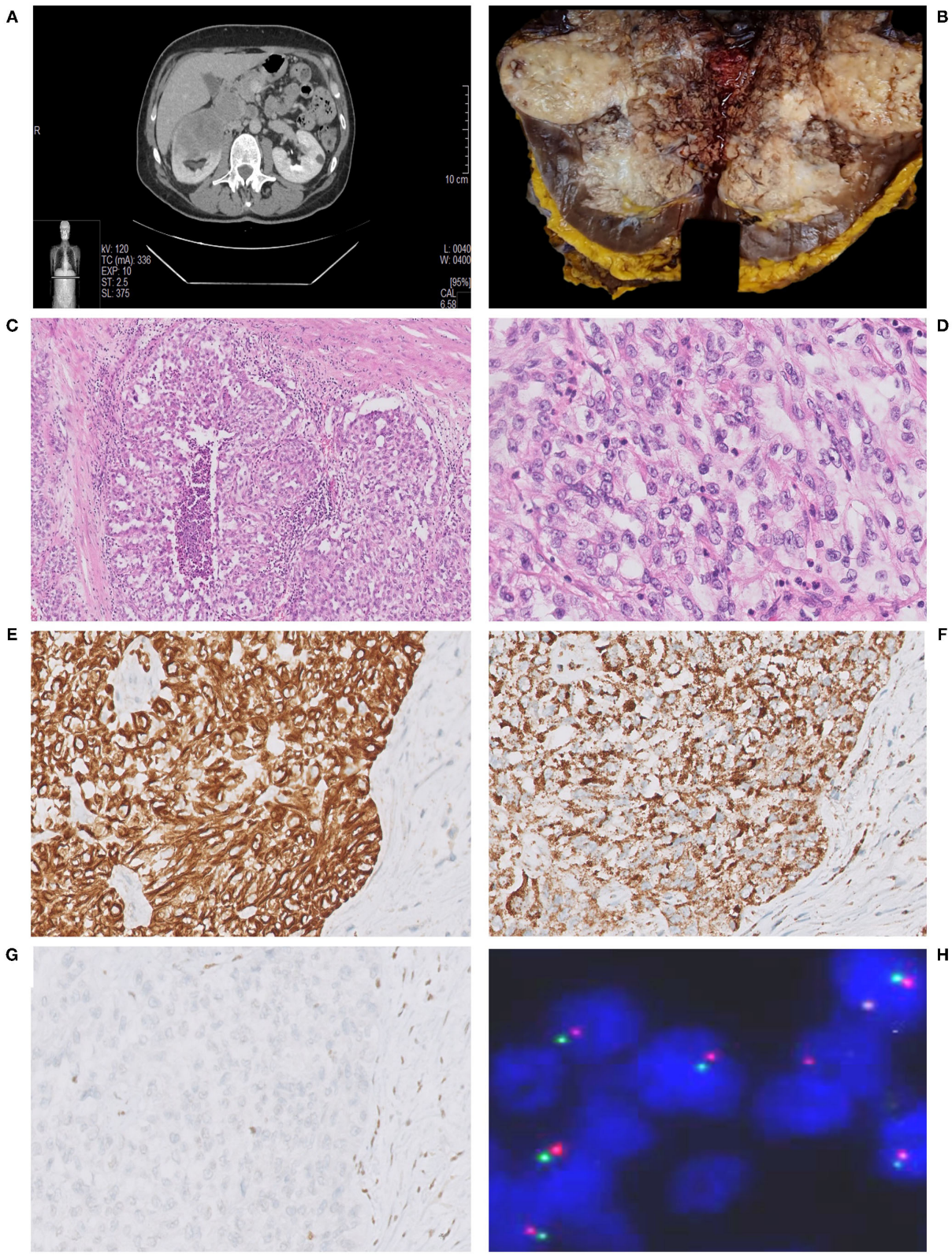

FIGURE 1 | Abdominal CT scan showing a bulky renal mass in the upper pole of the right kidney **(A)**. Grossly, renal parenchyma was partially replaced by a whitish, solid, and necrotic mass **(B)**. Histological view showing a solid proliferation of eosinophilic, highly pleomorphic, epithelioid cells, with nested growth pattern and focal pseudo-glandular differentiation, associated with desmoplastic stromal response. Multiple foci of necrosis were present (30% of tumor). Notably, many cells had a high

(Continued)

FIGURE 1 | nuclear-cytoplasmic ratio with vesicular nuclei and prominent nucleoli **(C,D)**. Immunohistochemically, the tumor was CK7+ in almost all cells **(E)** and fumarate hydratase (FH) expression was retained **(F)**; neoplastic cells showed the characteristic loss of INI1 **(G)**. Fluorescence *in situ* hybridization (FISH) with SPEC *SMARCB1/22q12* Dual Color Probe detected, in a representative tumoral area, a loss of one *SMARCB1* allele (single green and orange signal per cell) in almost half of the cells **(H)**.

patients without hemoglobinopathy have been reported in a few case reports and our recent small case series (7–9) and provisionally termed "RCC unclassified with medullary phenotype" (RCCU-MP) (7, 10). Alterations in *SMARCB1/INI1* can be detected by Fluorescence *in situ* Hybridization (FISH). Almost 85% of patients with RMC show a genetic loss, most commonly due to inactivating translocation of one *SMARCB1* allele and deletion of the second allele. Less frequently, deletion of both *SMARCB1* alleles, deletion of one *SMARCB1* allele and inDel of the second *SMARCB1* allele, or deletion of one *SMARCB1* allele and truncating non-sense mutation of the second *SMARCB1* allele might occur (11). Here we report the second Italian case of RCCU-MP, a fascinating entity whose definition might be further clarified by the new upcoming WHO classification.

CASE DESCRIPTION

A 62-year-old Italian man presented with persistent dull back pain. The patient was on anticoagulant therapy for recent pulmonary thromboembolism, had no previous history of malignancy or surgery, and presented no comorbidities. Ultrasound abdominal examination detected a renal mass, confirmed by a CT scan that documented a 13 × 10.8 × 5 cm solid tumor in the upper pole of the right kidney (**Figure 1A**), renal vein, and inferior vena cava thrombosis.

Right radical nephrectomy with cavotomy, thrombectomy, and regional lymphadenectomy was performed.

At gross examination, the tumor presented as a whitish, extensively necrotic mass of 13.1 cm in greatest dimension, infiltrating into the perinephric and renal sinus adipose tissue; neoplastic thrombosis was confirmed (**Figure 1B**). Incidentally, a metastatic nodule was documented in the ipsilateral adrenal gland.

Histologically, the tumor consisted of a proliferation of epithelioid cells, with enlarged and pleomorphic nuclei and eosinophilic cytoplasm, showing predominant solid and nested growth pattern, focally glandular, infiltrative borders, and extensive replacement of renal medulla (**Figures 1C,D**). The neoplasm was associated with desmoplastic stromal response, inflammatory lymphocytic infiltrate, and multiple foci of necrosis (∼30% of the tumor). One metastatic hilar lymph node was observed. Non-neoplastic kidney showed chronic interstitial nephritis and mild glomerulosclerosis. Histological features, together with medullary involvement, prompted us to the hypothesis of medullary carcinoma.

The tumor cells showed an immunophenotype specific of the proximal renal tubule, with immunopositivity for cytokeratin 7, PAX8, and FH (retained), and absence of GATA3 and OCT3/4. Focal immunoreactivity for CA IX and Racemase was found. Expression of INI1 was lost, as expected in the suspicion of RMC (**Figures 1E–G**). Blood tests did not show evidence of sickle cell trait, sickle cell disease, or any other hemoglobinopathy, therefore the diagnosis of RCCU-MP was made. To detect *SMARCB1/INI1* alterations, FISH was performed on paraffin sections of both tumoral areas and adjacent normal tissue using a commercial SPEC *SMARCB1/22q12* Dual Color Probe (Zyto*Light*®, according to the manufacturer's protocol). Loss of one *SMARCB1* allele was found in 42% of cells in the tumoral area (hemizygous deletion) (**Figure 1H**). Six months later, the patient experienced mediastinal nodal, hepatic, and bone metastases. Therefore, systemic therapy (Pembrolizumab + Axitinib and Radiotherapy on bone lesions) was administered. After 8 months of follow-up, the patient was alive with the disease.

DISCUSSION

In this study, we described the eighth case reported so far of RCCU-MP (7–9). The provisional diagnostic terminology of "RCCU-MP" has been recently proposed by international genitourinary pathologists for extraordinarily rare tumors with morphological and phenotypical characteristics of RMC but without sickle cell trait nor sickle cell disease (10, 12). However, the definite designation of these neoplasms is still debated (2).

In the past, this entity has been mislabeled as other RCC subtypes, such as unclassified RCC or Collecting duct carcinoma (CDC). Therefore, it has been possibly under-reported in the literature. Indeed, RCCU-MP is often a challenging diagnosis. In the absence of hemoglobinopathies, the differential diagnosis of RCCU-MP comprises CDC (HMWK+, OCT3/4-, INI1+), upper tract urothelial carcinoma (UTUC) (GATA3+, p63+, OCT3/4-, INI1+), Fumarate-Hydratase deficient RCC (FH-d RCC) (FH-, OCT3/4-, INI1+), ALK-rearranged RCC (ALK+, INI1+), and metastatic carcinoma (2). Rarely, some rhabdoid features might raise the differential diagnosis with rhabdoid tumors of the kidney (9).

Genes related to hypoxia have been advocated in the pathogenesis of *SMARCB1* abnormalities in RMC, triggered by red blood cell sickling and subsequent ischemia. *SMARCB1* has been suggested to be located in a hotspot region for *de novo* mutations susceptible to hypoxic stress mediated by peculiar medullary microvascular physiology (13). Given the overlapping features between RMC and RCCU-MP, Sirohi et al. recently suggested that a genetic predisposition unrelated to hemoglobinopathies might lead to *SMARCB1* abnormalities mediated by the same vascular mechanisms (14). Although interesting, this hypothesis needs further validation.

To the best of our knowledge, only seven further cases of RCCU-MP have been systematically collected and reported in the literature (7–9), whose clinical features

TABLE 1 | Clinical and pathologic data for RCCU-MP cases.

	References	Age (y)	Sex	Race /Country	Size (cm)	Side	pTNM	Sickle trait	Nodal status	Metastasis	Progression	Status	FU (mo)	Therapy	*SMARCB1/INI1*
Case 1	Sirohi et al. (7)	39	M	C/US	19	R	pT3cN1M1	HBE (-), HbS screen (-)	Aortocaval, supraclavicular	Adrenal, lung, bone, liver, mediast.	Presentation, 5mo	DOD	27	RN, CT, RT	IHC (lost)
Case 2	Sirohi et al. (7)	71	M	C/Italy	6.5	L	pT3aN1M1	HBE (-)	Hilar	Pelvic bone (5 cm)	Presentation	DOD	3	RN, CT	IHC (lost)
Case 3	Sirohi et al. (7)	58	M	C/US	3.4	L	pT3aN1Mx	No history, no anemia >9 y	Periaortic, paracaval	Peritoneum and bone	2 mo	DOD	3	RN	IHC (lost)
Case 4	Sirohi et al. (7)	24	F	C/US	5.5	L	pT3aN0Mx	HBE (-)	No	None	None	NED	12	RN	IHC (lost)
Case 5	Sirohi et al. (7)	30	M	A/US	4.5	R	Biopsy only	HBE (-)	Retroperitoneum	Lung, bone, and liver	3 mo	DOD	9	CT	IHC (lost)
Case 6	Lai et al. (8)	76	M	C/US	6.3	R	pT3aNxM1	No history	No	Lung	3 mo	AWD	3	RN, CT	IHC (lost)
Case 7	Tsuzuki et al. (9)	63	M	A/Japan	4.3	L	pT3aN0	HbS solubility testing (-)	No	None	7 mo	NED	4	RN, CT	IHC (lost); FISH (retained); seq. (wild-type)
Case 8	Current	62	M	C/Italy	13.1	R	pT3bN1M1	Hbs screen (-)	Hilar, subcarenal	Adrenal, liver, bone	6 mo	AWD	8	RN, CT, RT	IHC (lost); FISH (lost)

M, male; F, female; R, right; L, left; C, Caucasian; A, asian; LN, lymph node; HBE, hemoglobin electrophoresis; HbS, hemoglobin sickle; FU, follow-up; DOD, dead of disease; AWD, alive with disease; NED, no evidence of disease; RN, radical nephrectomy; CT, chemotherapy; RT, radiotherapy; IHC, immunohistochemistry; FISH, fluorescence in situ hybridization.

TABLE 2 | Morphologic features.

	References	Capsule	Margins	Location	Necrosis	Renal Vein Invasion	ISUP Grade	Main pattern	Other Patterns	Specific morphology	Dysplasia/ Ca *in situ*	Desmoplasia	Inflammation	HLRCC-like Nuclei
Case 1	Sirohi et al. (7)	No	Infiltrative	Cortex medulla	Yes	Yes	4	Solid, nested, cord-like	Tubular/ tubulopapillary	Rhabdoid	Yes	Fibroblastic	Acute	Focal
Case 2	Sirohi et al. (7)	No	Infiltrative	Cortex medulla	Yes	No	4	Solid	Infiltrative glandular pattern, focal cribriform	Sarcomatoid, focal giant cell	No	Fibroblastic	Acute and lymphoplasmacytic	No
Case 3	Sirohi et al. (7)	Focally	Polycyclic	Medulla	Yes	No	4	Solid, nested, cord-like	Tubular/ tubulopapillary	Rhabdoid	No	Fibroblastic	Lymphocytic	Focal
Case 4	Sirohi et al. (7)	No	Infiltrative	Medulla	No	No	3	Solid, nested, cord-like	Tubular/ tubulopapillary, reticular, cribriform	Rhabdoid	No	Sclerosis	Lymphocytic	No
Case 5	Sirohi et al. (7)	Biopsy	Biopsy	Biopsy	No	Biopsy	3	Infiltrative glandular	Reticular, non-glandular	NA	Yes	Fibromyxoid	Lymphocytic	No
Case 6	Lai et al. (8)	NA	Infiltrative	Cortex medulla	NA	No	3	Nested	Single glands and cribriform with cystic changes	NA	NA	Yes, nos	Acute	NA
Case 7	Tsuzuki et al. (9)	No	Infiltrative	Cortex medulla	Yes	No	3	Nested	Tubular, cord-like	Rhabdoid	NA	NA	Lymphocytic	NA
Case 8	Current	No	Infiltrative	Cortex medulla	Yes	Yes	4	Solid and nested	Glandular	No	No	Fibroblastic	Lymphocytic	No

NA, not assessed; ISUP, international society of urological pathology; HLRCC, hereditary leiomyomatosis and renal cell cancer; nos, not otherwise specified.

are summarized in **Table 1**. The patients were mostly Caucasian and men, with a mean age of 52 years, and almost all cases were locally advanced (pT3) with distant metastases. Interestingly, in only one case genetic alterations were investigated, with a negative result (9). All cases were centered in the renal medulla; the main morphological pattern was solid, either nested or cord-like, often with necrosis and diffuse polymorphism. Four cases showed rhabdoid features while desmoplasia and inflammation were documented in almost all patients. Morphological features are summarized in **Table 2**. All cases were INI1-(lost), PAX8+ and FH+(retained), 4/5 cases were CK7+, and 5/7 cases were OCT3/4+.

This is the eighth case of RCCU-MP reported so far. The current classification of this rare entity is still debated: RCCU-MP and RMC share both morphological and phenotypical features so they might be regarded as variants of the same disease in the next future.

Waiting for the new WHO classification, awareness of the diagnosis of these rare entities should be encouraged since they identify patients with poor prognoses and might reveal unacknowledged hemoglobinopathies.

DATA AVAILABILITY STATEMENT

The original contributions presented in the study are included in the article, further inquiries can be directed to the corresponding author/s.

ETHICS STATEMENT

Written consent was acquired from the patient.

AUTHOR CONTRIBUTIONS

PC and MV conceived, designed the study, wrote, and revised the final manuscript. LT, MC, GE, and CD reviewed the histological slides and revised the final manuscript. NR performed the FISH analysis. GL and NB performed surgery and provided clinical data. All authors contributed to the article and approved the submitted version.

REFERENCES

1. Swartz MA, Karth J, Schneider DT, Rodriguez R, Beckwith JB, Perlman EJ. Renal medullary carcinoma: clinical, pathologic, immunohistochemical, and genetic analysis with pathogenetic implications. *Urology.* (2002) 60:1083–9. doi: 10.1016/S0090-4295(02)02154-4
2. Baniak N, Tsai H, Hirsch MS. The differential diagnosis of medullary-based renal masses. *Arch Pathol Lab Med.* (2021) 145:1148–70. doi: 10.5858/arpa.2020-0464-RA
3. Hollmann TJ, Hornick JL. INI1-deficient tumors: diagnostic features and molecular genetics. *Am J Surg Pathol.* (2011) 35:47–63. doi: 10.1097/PAS.0b013e31822b325b
4. Ohe C, Smith SC, Sirohi D, Divatia M, De Peralta-Venturina M, Paner GP, et al. Reappraisal of morphologic differences between renal medullary carcinoma, collecting duct carcinoma, and fumarate hydratase-deficient renal cell carcinoma. *Am J Surg Pathol.* (2018) 42:279–92. doi: 10.1097/PAS.0000000000001000
5. Liu Q, Galli S, Srinivasan R, Marston W, Tsokos M, Merino MJ. Renal medullary carcinoma: molecular, immunohistochemistry, and morphologic correlation. *Am J Surg Pathol.* (2020) 37:368–74. doi: 10.1097/PAS.0b013e3182770406
6. Calderaro J, Moroch J, Pierron G, Pedeutour F, Grison C, Maillé P, et al. SMARCB1/INI1 inactivation in renal medullary carcinoma. *Histopathology.* (2012) 61:428–35. doi: 10.1111/j.1365-2559.2012.04228.x
7. Sirohi D, Smith SC, Ohe C, Colombo P, Divatia M, Dragoescu E, et al. Renal cell carcinoma, unclassified with medullary phenotype: poorly differentiated adenocarcinomas overlapping with renal medullary carcinoma. *Hum Pathol.* (2017) 67:134–45. doi: 10.1016/j.humpath.2017.07.006
8. Lai JZ, Lai HH, Cao D. Renal cell carcinoma, unclassified with medullary phenotype and synchronous renal clear cell carcinoma present in a patient with no sickle cell trait/disease: diagnostic and therapeutic challenges. *Anticancer Res.* (2018) 38:3757–61. doi: 10.21873/anticanres.12657
9. Tsuzuki S, Kataoka TR, Ito H, Ueshima C, Asai S, Yokoo H, et al. A case of renal cell carcinoma unclassified with medullary phenotype without detectable gene deletion. *Pathol Int.* (2019) 69:710–4. doi: 10.1111/pin.12858
10. Amin MB, Smith SC, Agaimy A, Argani P, Compérat EM, Delahunt B, et al. Collecting duct carcinoma versus renal medullary carcinoma: an appeal for nosologic and biological clarity. *Am J Surg Pathol.* (2014) 38:871–4. doi: 10.1097/PAS.0000000000000222
11. Msaouel P, Malouf GG, Su X, Yao H, Tripathi DN, Soeung M, et al. Comprehensive molecular characterization identifies distinct genomic and immune hallmarks of renal medullary carcinoma. *Cancer Cell.* (2021) 37:720–34. doi: 10.1016/j.ccell.2020.04.002
12. Colombo P, Smith SC, Massa S, Renne SL, Brambilla S, Peschechera R, et al. Unclassified renal cell carcinoma with medullary phenotype versus renal medullary carcinoma: lessons from diagnosis in an Italian man found to harbor sickle cell trait. *Urol Case Rep.* (2015) 3:215–8. doi: 10.1016/j.eucr.2015.07.011
13. Msaouel P, Tannir NM, Walker CL. A model linking sickle cell hemoglobinopathies and SMARCB1 loss in renal medullary carcinoma. *Clin Cancer Res.* (2018) 24:2044–9. doi: 10.1158/1078-0432.CCR-17-3296
14. Sirohi D, Ohe C, Smith SC, Amin MB. SWI/SNF-deficient neoplasms of the genitourinary tract. *Semin Diagn Pathol.* (2021) 38:212–21. doi: 10.1053/j.semdp.2021.03.007

Conflict of Interest: The authors declare that the research was conducted in the absence of any commercial or financial relationships that could be construed as a potential conflict of interest.

frontiers in Medicine

CASE REPORT
published: 24 February 2022
doi: 10.3389/fmed.2022.826705

Case Report: Early Distant Metastatic Inflammatory Myofibroblastic Tumor Harboring *EML4-ALK* Fusion Gene: Study of Two Typical Cases and Review of Literature

Qianqian Han[1†], *Xin He*[1†], *Lijuan Cui*[2], *Yan Qiu*[1], *Yuli Li*[1], *Huijiao Chen*[1] *and Hongying Zhang*[1*]

[1] Department of Pathology, West China Hospital, Sichuan University, Chengdu, China, [2] Department of Pathology, Suining Central Hospital, Suining, China

OPEN ACCESS

Edited by:
Renato Franco,
University of Campania Luigi Vanvitelli, Italy

Reviewed by:
Hyo Sup Shim,
Yonsei University College of Medicine, South Korea
José Manuel Lopes,
Universidade do Porto, Portugal

***Correspondence:**
Hongying Zhang
hy_zhang@scu. edu.cn

[†] These authors have contributed equally to this work

Specialty section:
This article was submitted to Pathology, a section of the journal Frontiers in Medicine

Received: 01 December 2021
Accepted: 24 January 2022
Published: 24 February 2022

Citation:
Han Q, He X, Cui L, Qiu Y, Li Y, Chen H and Zhang H (2022) Case Report: Early Distant Metastatic Inflammatory Myofibroblastic Tumor Harboring EML4-ALK Fusion Gene: Study of Two Typical Cases and Review of Literature. Front. Med. 9:826705. doi: 10.3389/fmed.2022.826705

Inflammatory myofibroblastic tumor (IMT) is a distinctive neoplasm that frequently arises in the lung and accounts for ∼1% of lung tumors. Distant metastatic IMT is extremely rare and has been poorly investigated. This analysis was specifically performed to explore the clinicopathological and genetic features of early distant metastatic IMT. Two typical patients with distant metastatic IMTs were selected, which accounted for 1.13% of all diagnosed IMTs in the last 5 years. One patient was a 55 year-old male, and the other patient was a 56 year-old female. Both primary tumors arose from the lung, and the initial clinical symptoms of the two patients involved coughing. Both of the imaging examinations showed low-density nodular shadows in the lungs with enhancement around the mass. Microscopically, dense arranged tumor cells, prominent cellular atypia, and high mitotic activity with atypical form were more prominent in the metastatic lesions than in the primary lesions. All of the primary and metastatic tumors in both cases showed positive anaplastic lymphoma kinase (*ALK*) immunostaining and *ALK* rearrangement *via* fluorescence *in situ* hybridization. The *EML4* (exon 6)-*ALK* (exon 20) fusion variant (v3a/b) was identified by using next-generation sequencing (NGS) and was verified by using reverse transcription polymerase chain reaction (RT-PCR). Furthermore, intronic variants of *NOTCH1* and synonymous variants of *ARAF* were also detected *via* NGS in one IMT for the first time and were verified in all of the primary and metastatic lesions *via* PCR. Distant metastasis occurred during a short period of time (1 and 2 months) after the first surgery. One patient presented with multiple metastases to the subcutaneous tissue and bone that responded to *ALK* inhibitor alectinib therapy, and the tumor was observed to regress 10 months after the initial *ALK* inhibitor therapy. In contrast, the other patient presented with subcutaneous neck metastasis without *ALK* inhibitor treatment and succumbed to the disease within 3 months after the surgery. This study demonstrated the possible role of *EML4-ALK*v3a/b in the malignant progression of IMT and proposed certain therapeutic effects of *ALK* inhibitors on multiple metastatic IMTs.

Keywords: inflammatory myofibroblastic tumor, early distant metastasis, *EML4-ALK* fusion variant 3a/b, NOTCH1, ARAF, ALK inhibitor

INTRODUCTION

Inflammatory myofibroblastic tumor (IMT) is a distinctive neoplasm composed of myofibroblastic and fibroblastic spindle cells accompanied by chronic inflammatory infiltration (1). IMTs frequently affect the lung, mesentery, omentum, and retroperitoneum, and most commonly occur in children and young adults (2, 3). However, among lung tumors, these entities are extremely rare and account for ∼1% of adult lung tumors (4). Approximately 50–60% of IMTs harbor anaplastic lymphoma kinase (*ALK*) gene rearrangement, which can fuse with multiple partner genes, including *ATIC, CLTC, EML4, NPM, TFG, TPM3/4*, and other genes (5, 6). In *ALK*-negative IMTs, *ROS1*, and *NTRK3* gene rearrangements are the most frequent mutations and exist in 5–10% of all IMTs, whereas *RET* and *PDGFRB* rearrangements are found in a few IMTs (7, 8). IMT is a borderline tumor with an appropriate prognosis; the metastatic rate is extremely low (<5%) (1). The clinicopathological and molecular characteristics of distant metastatic IMTs are largely unknown.

To the best of our knowledge, approximately 50 metastatic IMTs have been reported in the English literature (9–16), and most metastatic sites involve the lung, liver, and brain. Thirty-seven patients underwent ALK immunostaining, and 19 patients demonstrated positive results. Gene detection was only performed in 10 patients, and 8 patients had ALK rearrangements, including 3 patients with *EML4-ALK* fusions (8, 14–21). Although several studies have demonstrated *EML4-ALK* fusions in up to 20% of *ALK*-rearranged IMTs (8), the association between different *EML4-ALK* fusion variants and IMT disease progression has been insufficiently investigated. Until now, pathological indicators for predicting the biological behavior and prognosis of IMT have been deficient. Herein, we present two cases of metastatic IMTs, harboring *EML4-ALK* fusion, and review the literature to summarize the clinicopathological and genetic features that may help to predict the tendency of metastasis in IMT.

CASE PRESENTATION

Clinical Characteristics

Case 1 was a 55 year-old male, and case 2 was a 56 year-old female. Both of the patients had been coughing for 2 and 6 months before surgical resection. The imaging features are shown in **Figure 1**. Computed tomography (CT) scans found 4-cm low-density nodular shadows with slight enhancement around the mass in the right inferior lobe (**Figure 1a**) and a 3.3-cm lung nodule in the right upper lobe. In case 1, the metastatic lesion of the left neck was found and grew rapidly to 3 cm 1 month after the initial surgery, and it was also resected (**Figure 1b**). Case 2 had undergone lung lesion resection in December 2019. Nevertheless, subcutaneous painless lesions in the right thigh and the iliac region were found 2 months after the operation and were resected in March 2020. The resection margins were negative for all five tumor lesions. Detailed clinical features are summarized in **Supplementary Table 1**.

Pathological Features

All primary and metastatic lesions (5 specimens) were presented as gray and white nodular masses with solid and medium quality. Hematoxylin and eosin staining (H&E) was performed on all of the primary and metastatic lesions (**Figure 2**). Microscopically, tumors were arranged in fascicles and composed of spindle-shaped cells with lymphoplasmacyte and/or eosinophil infiltration. The nucleus was round or oval with a prominent nucleolus, and tumors of metastatic focus were homologous to those of the primary focus. Compared with primary tumors, metastatic tumors exhibited more densely arranged tumor cells, more obvious cellular atypia, more vacuolated nuclei, more prominent nucleoli, and higher mitotic figures with atypical forms (3–4/2 mm^2 in the lung and 10–15/2 mm^2 in the neck of Case 1; 8–9/2 mm^2 in the lung, 30–40/2 mm^2 in the thigh, and 20–30/2 mm^2 in the ilium of Case 2. Many new thin-walled capillaries were arranged in the tumors with diffuse lymphoplasmacyte infiltration. Some cellulose-like necrosis was observed in Case 1.

Immunohistochemistry Profile

All of the specimens showed a similar expression of immunostaining. Specifically, ALK-IHC showed diffuse cytoplasmic reactivity in all 5 specimens (**Figure 2g**), and the density in the metastatic lesions was higher than that in the primary lesions. Focal staining for smooth muscle actin was observed in Case 2 (**Figure 2h**) but was negative in Case 1. No tumor cells demonstrated positive staining with anti-S-100 protein, CD34, cytokeratin, or desmin.

Molecular Analysis

All five specimens were detected by using next-generation DNA sequencing (NGS) and were verified by using reverse transcription polymerase chain reaction (RT–PCR) or PCR. *ALK* rearrangement was confirmed *via* fluorescence *in situ* hybridization (FISH) in the pulmonary lesion of Case 1 (**Figure 3A**) and in all three lesions of Case 2. Subsequent NGS broad molecular profiling of the tumor tissue was performed, and the fusion break-point involved exon 6 of *EML4* and exon 20 of *ALK* in all of the primary and metastatic tumors of these cases with identical fusion sequences. Confirmatory RT-PCR and subsequent Sanger sequencing confirmed the fusion of *EML4-ALK* in all of the tumors (**Figures 3**, **4**). Otherwise, intronic variants of *NOTCH1* in exons 2 and 24 and synonymous variants of *ARAF* in exon 4 were also detected by using NGS in the above three primary and metastatic lesions of Case 2. PCR was performed, and *NOTCH1* and *ARAF* variants were demonstrated *via* Sanger sequencing (**Supplementary Figure 1**).

Treatment and Follow-Up

Patient one succumbed to disease only 3 months after initial presentation. In May 2020, whole-body CT examinations showed many soft tissue density lesions in the left axillary subcutaneous area, right upper abdominal subcutaneous area, left thigh medial subcutaneous area, and right iliac fossa area. Hence, the patient was orally administered alectinib (600 mg, two times daily). Whole-body CT in March 2021 indicated that all of the

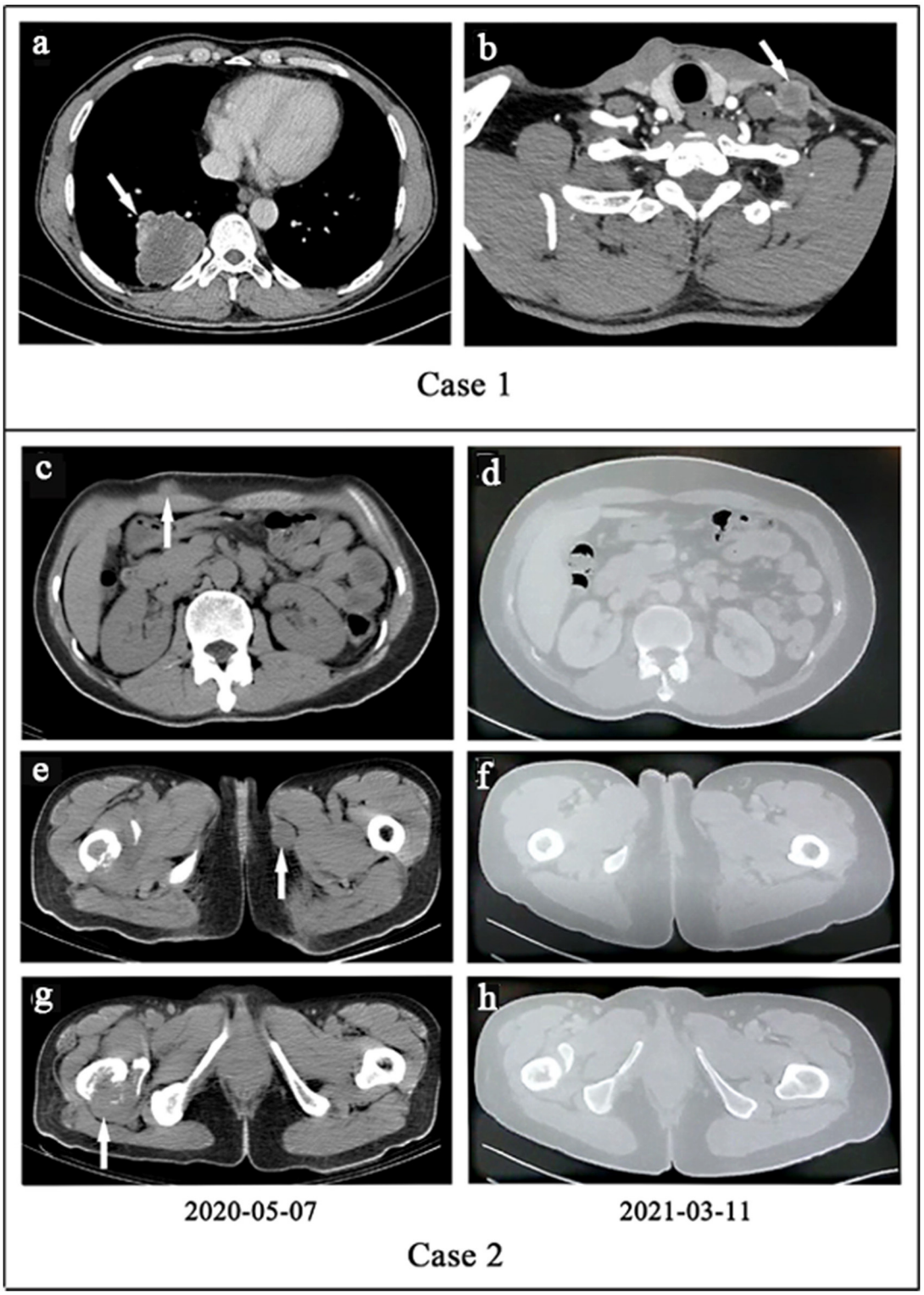

FIGURE 1 | (a,b) Case 1. **(a)** The computed tomography (CT) of primary lesion revealed a large, irregular mass with a non-uniform density shadow attached to the lower lobe of the right lung. **(b)** The CT of metastatic lesion showed an uneven density lesion within subcutaneous of the left neck with an unclear border. **(c–h).** Case 2. Treatment efficacy with Alectinib in Case 2 based on CT scans. **(c,e,g)** Before Alectinib treatment. Multiple low-density nodules were observed in subcutaneous of the right upper abdomen, the inner side of the left thigh, and the right femur. **(d,f,h)** Ten months after Alectinib treatment, multiple soft tissue density nodules decreased or disappeared.

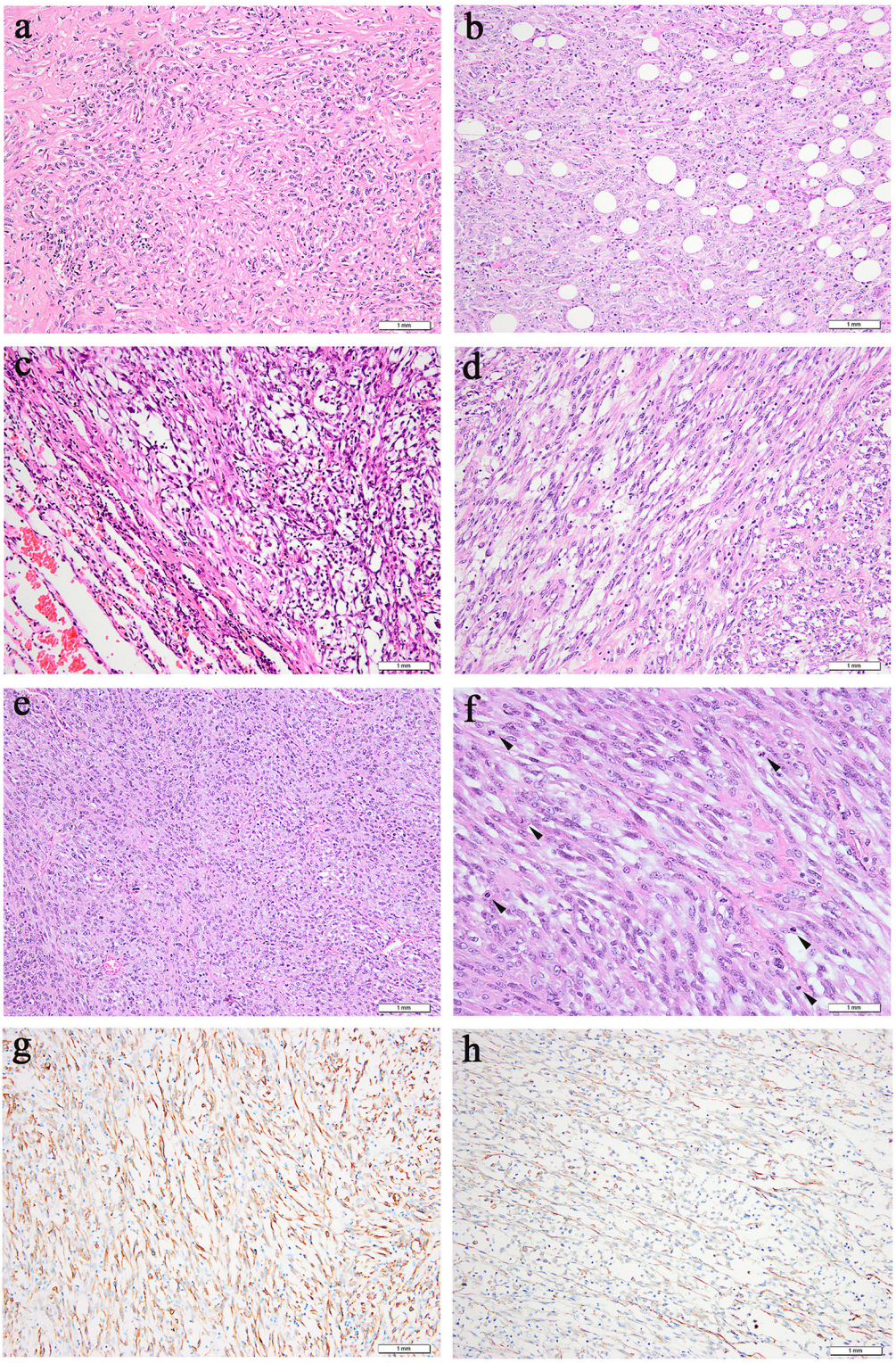

FIGURE 2 | Microscopic features (hematoxylin and eosin). **(a,b)** Case 1, **(c–f)** Case 2. **(a)** Prominent collagenous background was observed in the primary lung lesion. (**b)** Metastatic neck lesion showed adipose infiltration. **(c)** A clear boundary between tumors and normal lung tissue in some areas could be observed in primary lung lesion. **(d)** Spindle tumor cells of thigh lesion arranged in fascicular. **(e)** Metastatic lesion of ilium exhibited densely arranged tumor cells. **(f)** More dense tumor cells arrangement, more obvious atypia, more vacuolated and prominent nucleoli, higher mitotic activity (an arrowhead is shown) were observed in metastatic lesion of ilium. **(g)** Positive cytoplasmic ALK staining was observed in all 5 specimens. (**h)** Focally positive staining for smooth muscle actin was shown in Case 2.

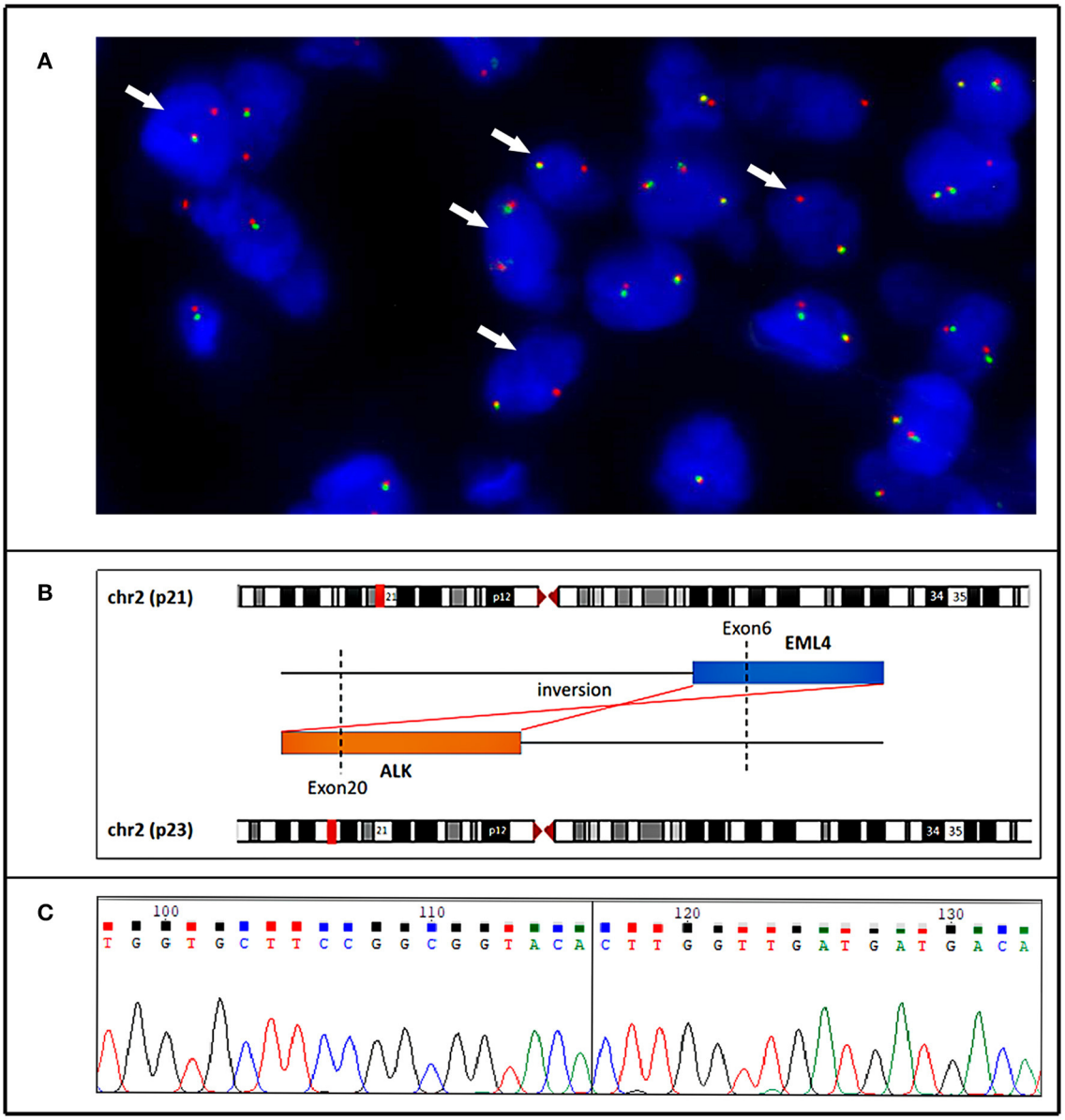

FIGURE 3 | Case 1. **(A)** Fluorescence *in situ* hybridization demonstrating an unbalanced rearrangement of the *ALK* locus in the neoplastic cells (loss of a green signal with an extra red signal). **(B)** Next generation sequencing (NGS-) based technology showing detection of *ALK* (exon 20) and *EML4* (exon 6) fusion and breakpoint information between the two genes. **(C)** A partial nucleotide sequence of the *EML4-ALK* fusion transcript, and the fusion site (arrow) involved exon 20 of the *ALK* gene and exon 6 of the *EML4* gene.

tumors had significantly responded (**Figures 1c–h**). Currently, the patient is still in good clinical condition without adverse events 16 months after the initiation of alectinib treatment.

DISCUSSION

The incidence of distant metastatic IMT was very low, accounting for 1.13% of the 177 identified patients with IMT for investigation in our institution from January 2016 to July 2021. A search of the English literature indicated that approximately 50 metastatic IMTs from some isolated cases or portions of other series studies had been described thus far (**Supplementary Table 2**) (9–16). Furthermore, epithelioid IMT with malignant potential was not included in this study. Metastatic lesions involved the lung, brain, lymphonodus, bone, abdomen, and pelvis. Additionally, the patient ages ranged from 5 to 81 years (mean: 36.2 years; median: 35.5 years), with a male-to-female ratio of 1.1:1. The distribution of age throughout all of the age groups was consistent with non-metastatic IMT without a significant difference (7). However, there was a slight male predominance in the gender

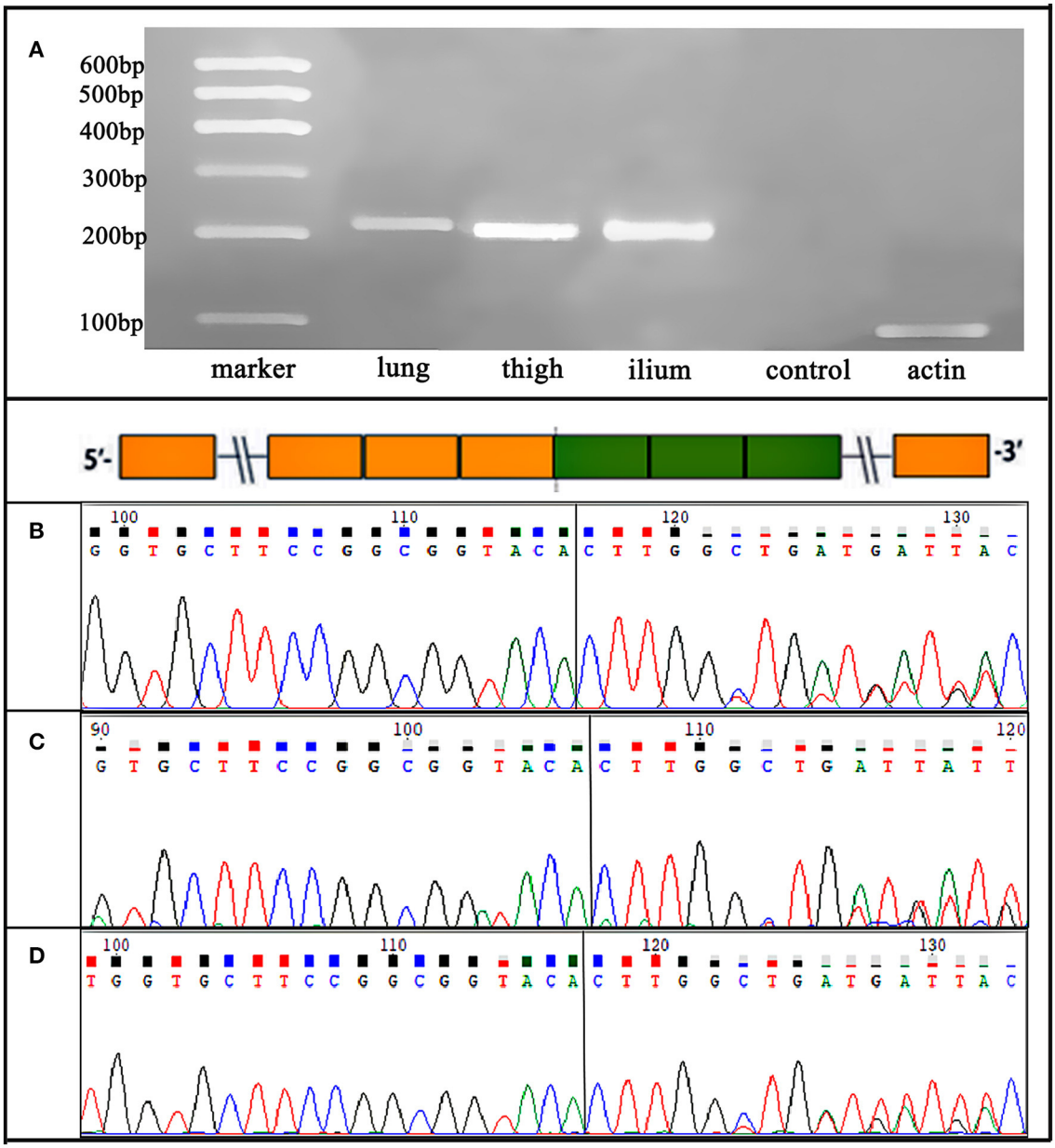

FIGURE 4 | Case 2. **(A)** RT-PCR for lung, right thigh, and ilium lesions confirmed an *EML4-ALK* fusion variants, which were detected by NGS. **(B-D)** Sanger sequencing verified the sequence of the *EML4* (exon 6)-*ALK* (exon 20) fusion transcript in the three primary and metastatic lesions.

distribution. Primary and metastatic lesions were simultaneously found in nearly half of the IMTs (16/35, 45.7%), and other metastatic intervals ranged from 1 month to 9 years. In this study, two lung IMTs with early distant metastasis were included: one IMT metastasized to the subcutaneous neck, and one IMT had multiple systemic metastases, with intervals of 1 and 2 months.

The correlation between morphology and biological behavior in IMT is still ambiguous. The histological characteristics of 50 metastatic IMTs were analyzed, and the primary tumor size was 1.3–22 cm (median: 6.8 cm; mean: 7.2 cm). Varying degrees of cellular or nuclear atypia in primary lesions were described in 25 patients, whereas a few patients harbored high mitotic figures (most of which were 30/2 mm^2). Among 16 previously reported metastatic IMTs of primary lung locations with detailed pathological descriptions, 10 IMTs had atypical features with large atypical nuclei, distinct nucleoli, high mitotic activity, or nuclear pleomorphism. Similar to earlier cases, some atypical morphological features were also shown in our cases, such as hypercellularity and prominent mitotic figures. Traditionally, larger tumor size, hypercellularity, the presence of tumor cell necrosis, high mitotic activity, and the presence of ganglion-like cells were considered to be associated with poor survival in

IMTs (8, 9). This series further illustrated that hypercellularity, atypical spindled cells, and high mitotic activity may predict malignant potential, and pathologists should be aware of these morphological changes. Of course, a further analysis of large samples is needed.

Previously, *ALK*-negative IMTs were considered to have higher metastatic potential (1). One study stated that *ALK* reactivity may be a favorable prognostic indicator in IMT because none of their 6 metastatic IMTs were reactive for *ALK* (9). However, among the 37 previously reported metastatic IMTs with *ALK* immunostaining information, more than half of the patients (51.4%, 19/37) harbored positive results, thus suggesting that ALK immunoreactivity does not appear to correlate with metastasis (**Supplementary Table 2**). Among the 4 patients with detectable specific *ALK* fusion partners, 3 harbored *EML4-ALK* fusions, and the other harbored *CARS-ALK* fusions. *EML4-ALK* may affect tumorigenesis and be used to identify IMT that develops malignant transformation or recurrence (15). In our series, the ALK staining density in most areas of the metastatic lesions was higher than that of the primary lesions, thus indicating a possible role of ALK in IMT metastasis. The prognostic significance of *EML4* as a fusion partner in IMTs remains unclear, but a potential link between *EML4-ALK* fusion and a malignant clinical course should be explored in further studies with a larger series.

In this study, both primary and metastatic lesions of the two IMTs were positive for ALK and harbored *EML4* (exon 6)-*ALK* (exon 20) fusion. To date, eighteen *EML4-ALK* fusion IMTs have been reported (including the present two IMTs) (8, 13–20) (**Supplementary Table 3**), eleven of which are located in the lung (11/18, 61.1%). The other cases included two IMTs in the abdominopelvic cavity, two IMTs in the limbs, one IMT in the head, one IMT in the trachea, and one IMT in the hypopharynx. Seven of eighteen *EML4-ALK*-rearranged IMTs had different degrees of cellular atypia and/or mitosis. Some studies have reported that *EML4-ALK* rearrangement is often combined with epithelioid cell morphology and distant metastasis or local infiltration tendency (8, 14, 17). Among the 6 cases (6/18, 33.3%) investigated with DNA sequencing, exon 6 of *EML4* fused with exon 20 of *ALK* in 4 cases, including the two IMTs that we investigated; additionally, exon 4 of *EML4* fused with exon 20 of *ALK* in one case, and the other case involved exon 2 of *EML4* and exon 20 of *ALK*. Some clinical studies have demonstrated that the *EML4* (exon 6)-*ALK* (exon 20) fusion variant (3a/b) is a high-risk feature, conferring accelerated metastatic spread, ALK inhibitor resistance, and worsened prognosis in ALK-positive non-small-cell lung cancer (NSCLC) (22–24). The 3a/b variants of the *EML4-ALK* fusion gene were identified by using FISH and Sanger sequencing in a malignant hypopharynx IMT, and strong ALK immunoreactivity was also observed in neoplastic cells (8), which was best illustrated by our cases. Early distant metastasis occurred in our two cases, which was also combined with the fusion of *EML4-ALK* fusion variant 3a/b, thus indicating that this specific fusion variant may also play a considerable role in the malignant progression of IMT. The presence of *EML4-ALK* fusion variant 3a/b in different malignant neoplasm types demonstrated the hypothesis that identical *ALK* fusions may drive inappropriate activation of the same kinase signaling pathway and could be oncogenic in disparate cellular lineages. The determination of *ALK* fusion status should be considered as part of the initial workup for this phenomenon to select patients for more aggressive disease surveillance.

Otherwise, synonymous variants of *ARAF* and intronic variants of *NOTCH1* were detected in one case (Case 2). A few examples have indicated that synonymous mutations in diseases may act as driver mutations (25). *NOTCH* signaling was shown to physically regulate interactions between adjacent cells as an evolutionarily conserved intercellular signaling pathway. *NOTCH1* encodes a member of the *NOTCH* family of proteins and drives an oncogenic transcriptional program that promotes cell growth proliferation and survival (26). Importantly, the oncogenic effects of *NOTCH1* are closely linked to the activation of the *MYC* oncogene and can regulate overlapping transcriptional programs in a feed-forwards loop transcriptional circuitry that amplifies the oncogenic effects of *NOTCH1* (25, 27). *ARAF* belongs to the RAF subfamily of the serine/threonine kinase family and may be involved in cell growth and development. They interact with the *RAS-MAPK* pathway and act as binary molecular switches, controlling intracellular signaling pathways and participating in basic cellular processes, such as cell proliferation, differentiation, adhesion, migration, and apoptosis (28, 29). *NOTCH1* or *ARAF* mutations have not been previously reported in IMTs. In this case, the disease progressed very rapidly, multiple subcutaneous metastases occurred in the whole body within a few months, and the malignancy of the metastatic lesion was higher than that of the primary lesions. Whether *NOTCH1* and *ARAF* act together with *ALK* mutations in the progression of IMTs needs further exploration.

From a morphological perspective, the main differential diagnostic consideration is spindle cell neoplasms, especially with inflammatory infiltration. First, the occurrence of distant metastasis and moderate-to-severe atypia excludes inflammatory pseudotumors and myofibroblast proliferation. Second, sarcomatoid carcinoma usually exhibits high-grade spindle cell morphology, but negative cytokeratin expression refuted this diagnosis. Third, epithelioid inflammatory myofibroblastic sarcoma is composed of plump epithelioid or histiocytoid tumor cells with vesicular chromatin and accompanied by a unique pattern of nuclear membrane or perinuclear *ALK* immunoreactivity (30). Moreover, the molecular detection of *EML4-ALK* fusion excludes leiomyosarcoma and other spindle mesenchymal tumors.

For prognosis, the follow-up time was 3 weeks to 36 months (median: 9 months; mean: 11.2 months) in 30 metastatic patients with follow-up information. However, not all of the patients undergoing *ALK* inhibitor therapy had a favorable prognosis. The patients without *ALK* inhibitor therapy were followed up for 3 weeks to 24 months (median: 8.5 months; mean: 9.4 months), and the disease-free survival rate was only 40.9% (9/22). The follow-up time for the patients treated with *ALK* inhibitors was 4–36 months (median: 13.5 months; mean: 16.4 months), and the disease-free survival rate was 75% (6/8), thus proving that the usage of *ALK* inhibitors is crucial to improve the survival

of the patients. Although *EML4-ALK* variant 3a/b-fused tumors may harbor a high risk of *ALK* inhibitor resistance, one of our cases responded effectively to the administration of the second-generation *ALK* inhibitor alectinib and encompassed an appropriate prognosis. Likewise, to the best of our knowledge, only one previous IMT with *EML4-ALK* fusion confirmed by FISH that responded to alectinib treatment was initially reported (15). The carcinogenic pathway is mainly mediated by *ALK*, and the fusion partner gene activates the *ALK* tyrosine kinase domain through a driver/oligomerization mechanism as a promoter (15). *EML4-ALK* fusion variant 3a/b-driven cancers were characterized by oncogene dependence, and ALK inhibitors may be more effective for this tumor subgroup (17, 18).

Of the *ALK* inhibitor treatments, crizotinib and two other ATP-competitive *ALK* inhibitors (ceritinib and alectinib) are approved for use as first-line therapies, whereas ceritinib and alectinib are two second-generation *ALK* inhibitors with acceptable safety profiles that have been proved to be effective against many of the prominent forms of crizotinib-resistant *ALK*-positive NSCLC (31). In the USA, oral alectinib monotherapy is indicated for the treatment of patients with ALK-positive metastatic NSCLC, as detected by a Food and Drug Administration-approved test (32). Alectinib was observed to inhibit autophosphorylation of *ALK* and to suppress phosphorylation of STAT3 and *ALK* (but not ERK1/2) in NSCLC cells expressing *EML4-ALK*, as well as inhibiting the growth of multiple cell lines bearing *ALK* fusions, amplifications, or activating mutations (31, 33). Two of sixteen *EML4-ALK*-rearranged IMTs (14, 16) were negative for *ALK via* IHC, which underlies the risk of negating systemic therapy with kinase inhibitors. Moreover, many *ALK* fusion variants show a diffuse cytoplasmic pattern, and the fusion partners cannot be identified *via* IHC, although a few fusions are related to the nuclear membrane (*RANBP2-ALK*), perinuclear (*RRBP1-ALK*) or a cytoplasmic granular pattern (*CLTC-ALK*) of *ALK* immunohistochemistry (1, 30). Thus, FISH or NGS detection at the DNA level should be suggested in IMTs with typical morphological features, regardless of the IHC results, especially in those patients with malignant potential.

In summary, this study presented two extremely rare early distant metastatic IMTs, both harboring *EML4-ALK* fusion variants 3a/b. We summarized the reported distant metastatic IMTs and found that tumor cell atypia and high mitotic activity may often indicate metastatic possibility. A systematic metastatic IMT was emphasized. In addition to *EML4-ALK* fusion variant 3a/b, synonymous variants of *ARAF* and intronic variants of *NOTCH1* were also detected *via* NGS, and this patient responded effectively to treatment with the second-generation *ALK* inhibitor alectinib. *EML4-ALK* fusion variants 3a/b could be oncogenic in disparate cellular lineages, thus causing the malignant progression of IMT, and *ALK* inhibitor administration could improve the prognosis. Of course, more studies are needed to clarify the relationship between *EML4-ALK* fusion variants and IMT progression, prognosis, and treatment effectiveness. Further studies using additional cases are needed to explore the prognostic factors of IMT to facilitate timely treatments.

DATA AVAILABILITY STATEMENT

All datasets generated for this study are included in the article/**Supplementary Material**.

ETHICS STATEMENT

The studies involving human participants were reviewed and approved by the Ethics Committee of West China Hospital of Sichuan University. The patients/participants provided their written informed consent to participate in this study.

AUTHOR CONTRIBUTIONS

QH: data analysis, test performance, writing, and review of the manuscript. XH: review of the manuscript and histopathology. LC: data curation. YQ: collection of information and software. YL: molecular experiments. HC: review of histopathology. HZ: project administration, study design, and the manuscript revision. All authors contributed to the article and approved the submitted version.

FUNDING

This work was supported by the National Natural Science Foundation of China (Grant No. 81972520), the 135 Project for Disciplines of Excellence-Clinical Research Incubation Project, West China Hospital, Sichuan University (Grant No. 2018HXFH011), Medical Science and Technology Project of Sichuan Provincial Health Commission (Grant No. 21PJ002), and Post-Doctor Research Project, West China Hospital, Sichuan University (Grant No. 2021HXBH004).

SUPPLEMENTARY MATERIAL

The Supplementary Material for this article can be found online at: https://www.frontiersin.org/articles/10.3389/fmed.2022.826705/full#supplementary-material

REFERENCES

1. Yamamoto H. Inflammatory myofibroblastic tumour. In: *Soft Tissue and Bone Tumours. WHO Classification of Tumours. 5th edn.* Lyon: International Agency For Research on Cancer (2020). p. 109–11.
2. Palaskar S, Koshti S, Maralingannavar M, Bartake A. Inflammatory myofibroblastic tumor. *Contemp Clin Dent.* (2011) 2:274–7. doi: 10.4103/0976-237X.91787
3. Koyuncuer A. Inflammatory myofibroblastic tumor of the small-bowel mesentery: a case report of nonspecific clinical presentation and a review of the literature. *Int J Surg Case Rep.* (2014) 5:1214–7. doi: 10.1016/j.ijscr.2014.11.054
4. Sagar AES, Jimenez CA, Shannon VR. Clinical and histopathologic correlates and management strategies for inflammatory myofibroblastic tumor of the lung. A case series and review of the literature. *Med Oncol.* (2018) 35:102. doi: 10.1007/s12032-018-1161-0

5. Cools J, Wlodarska I, Somers R, Mentens N, Pedeutour F, Maes B, et al. Identification of novel fusion partners of ALK, the anaplastic lymphoma kinase, in anaplastic large-cell lymphoma and inflammatory myofibroblastic tumor. *Genes Chromosomes Cancer.* (2002) 34:354–62. doi: 10.1002/gcc.10033
6. Lovly CM, Gupta A, Lipson D, Otto G, Brennan T, Chung CT, et al. Inflammatory myofibroblastic tumors harbor multiple potentially actionable kinase fusions. *Cancer Discov.* (2014) 4:889–95. doi: 10.1158/2159-8290.CD-14-0377
7. Yamamoto H, Yoshida A, Taguchi K, Kohashi K, Hatanaka Y, Yamashita A, et al. ALK, ROS1 and NTRK3 gene rearrangements in inflammatory myofibroblastic tumours. *Histopathology.* (2016) 69:72–83. doi: 10.1111/his.12910
8. Antonescu CR, Suurmeijer AJ, Zhang L, Sung YS, Jungbluth AA, Travis WD, et al. Molecular characterization of inflammatory myofibroblastic tumors with frequent ALK and ROS1 gene fusions and rare novel RET rearrangement. *Am J Surg Pathol.* (2015) 39:957–67. doi: 10.1097/PAS.0000000000000404
9. Coffin CM, Hornick JL, Fletcher CD. Inflammatory myofibroblastic tumor: comparison of clinicopathologic, histologic, and immunohistochemical features including ALK expression in atypical and aggressive cases. *Am J Surg Pathol.* (2007) 31:509–20. doi: 10.1097/01.pas.0000213393.57322.c7
10. Debelenko LV, Arthur DC, Pack SD, Helman LJ, Schrump DS, Tsokos M. Identification of CARS-ALK fusion in primary and metastatic lesions of an inflammatory myofibroblastic tumor. *Lab Invest.* (2003) 83:1255–65. doi: 10.1097/01.LAB.0000088856.49388.EA
11. Gaudichon J, Jeanne-Pasquier C, Deparis M, Veyssière A, Heyndrickx M, Minckes O, et al. Complete and repeated response of a metastatic ALK-rearranged inflammatory myofibroblastic tumor to crizotinib in a teenage girl. *J Pediatr Hematol Oncol.* (2016) 38:308–11. doi: 10.1097/MPH.0000000000000498
12. Telugu RB, Prabhu AJ, Kalappurayil NB, Mathai J, Gnanamuthu BR, Manipadam MT. Clinicopathological study of 18 cases of inflammatory myofibroblastic tumors with reference to ALK-1 expression: 5-year experience in a tertiary care center. *J Pathol Transl Med.* (2017) 51:255–63. doi: 10.4132/jptm.2017.01.12
13. Jiang YH, Cheng B, Ge MH, Cheng Y, Zhang G. Comparison of the clinical and immunohistochemical features, including anaplastic lymphoma kinase (ALK) and p53, in inflammatory myofibroblastic tumours. *J Int Med Res.* (2009) 37:867–77. doi: 10.1177/147323000903700332
14. Borak S, Siegal GP, Reddy V, Jhala N, Jhala D. Metastatic inflammatory myofibroblastic tumor identified by EUS-FNA in mediastinal lymph nodes with ancillary FISH studies for ALK rearrangement. *Diagn Cytopathol.* (2012) 40 (Suppl. 2):E118–25. doi: 10.1002/dc.21663
15. Sokai A, Enaka M, Sokai R, Mori S, Mori S, Gunji M, et al. Pulmonary inflammatory myofibroblastic tumor harboring EML4-ALK fusion gene. *Jpn J Clin Oncol.* (2014) 44:93–6. doi: 10.1093/jjco/hyt173
16. Saiki M, Ohyanagi F, Ariyasu R, Koyama J, Sonoda T, Nishikawa S, et al. Dramatic response to alectinib in inflammatory myofibroblastic tumor with anaplastic lymphoma kinase fusion gene. *Jpn J Clin Oncol.* (2017) 47:1189–92. doi: 10.1093/jjco/hyx133
17. Muscarella LA, Rossi G, Trombetta D, La Torre A, Di Candia L, Mengoli MC, et al. A malignant inflammatory myofibroblastic tumor of the hypopharynx harboring the 3a/b variants of the EML4-ALK fusion gene. *Oncol Lett.* (2017) 13:593–8. doi: 10.3892/ol.2016.5504
18. Jiang Q, Tong HX, Hou YY, Zhang Y, Li JL, Zhou YH, et al. Identification of EML4-ALK as an alternative fusion gene in epithelioid inflammatory myofibroblastic sarcoma. *Orphanet J Rare Dis.* (2017) 12:97. doi: 10.1186/s13023-017-0647-8
19. Vargas-Madueno F, Gould E, Valor R, Ngo N, Zhang L, Villalona-Calero MA. EML4-ALK rearrangement and its therapeutic implications in inflammatory myofibroblastic tumors. *Oncologist.* (2018) 23:1127–32. doi: 10.1634/theoncologist.2018-0014
20. Chang JC, Zhang L, Drilon AE, Chi P, Alaggio R, Borsu L, et al. Expanding the molecular characterization of thoracic inflammatory myofibroblastic tumors beyond ALK gene rearrangements. *J Thorac Oncol.* (2019) 14:825–34. doi: 10.1016/j.jtho.2018.12.003
21. Lopez-Nunez O, John I, Panasiti RN, Ranganathan S, Santoro L, Grélaud D, et al. Infantile inflammatory myofibroblastic tumors: clinicopathological and molecular characterization of 12 cases. *Mod Pathol.* (2020) 33:576–90. doi: 10.1038/s41379-019-0406-6
22. Tao H, Shi L, Zhou A, Li H, Gai F, Huang Z, et al. Distribution of EML4-ALK fusion variants and clinical outcomes in patients with resected non-small cell lung cancer. *Lung Cancer.* (2020) 149:154–61. doi: 10.1016/j.lungcan.2020.09.012
23. Christopoulos P, Endris V, Bozorgmehr F, Elsayed M, Kirchner M, Ristau J, et al. EML4-ALK fusion variant V3 is a high-risk feature conferring accelerated metastatic spread, early treatment failure and worse overall survival in ALK(+) non-small cell lung cancer. *Int J Cancer.* (2018) 142:2589–98. doi: 10.1002/ijc.31275
24. Woo CG, Seo S, Kim SW, Jang SJ, Park KS, Song JY, et al. Differential protein stability and clinical responses of EML4-ALK fusion variants to various ALK inhibitors in advanced ALK-rearranged non-small cell lung cancer. *Ann Oncol.* (2017) 28:791–7. doi: 10.1093/annonc/mdw693
25. Supek F, Miñana B, Valcárcel J, Gabaldón T, Lehner B. Synonymous mutations frequently act as driver mutations in human cancers. *Cell.* (2014) 156:1324–35. doi: 10.1016/j.cell.2014.01.051
26. Herranz D, Ambesi-Impiombato A, Palomero T, Schnell SA, Belver L, Wendorff AA, et al. A NOTCH1-driven MYC enhancer promotes T cell development, transformation and acute lymphoblastic leukemia. *Nat Med.* (2014) 20:1130–7. doi: 10.1038/nm.3665
27. Liu Y, Easton J, Shao Y, Maciaszek J, Wang Z, Wilkinson MR, et al. The genomic landscape of pediatric and young adult T-lineage acute lymphoblastic leukemia. *Nat Genet.* (2017) 49:1211–8. doi: 10.1038/ng.3909
28. Matallanas D, Birtwistle M, Romano D, Zebisch A, Rauch J, von Kriegsheim A, et al. Raf family kinases: old dogs have learned new tricks. *Genes Cancer.* (2011) 2:232–60. doi: 10.1177/1947601911407323
29. Freeman AK, Ritt DA, Morrison DK. The importance of Raf dimerization in cell signaling. *Small GTPases.* (2013) 4:180–5. doi: 10.4161/sgtp.26117
30. Lee JC, Li CF, Huang HY, Zhu MJ, Mariño-Enríquez A, Lee CT, et al. ALK oncoproteins in atypical inflammatory myofibroblastic tumours: novel RRBP1-ALK fusions in epithelioid inflammatory myofibroblastic sarcoma. *J Pathol.* (2017) 241:316–23. doi: 10.1002/path.4836
31. Golding B, Luu A, Jones R, Viloria-Petit AM. The function and therapeutic targeting of anaplastic lymphoma kinase (ALK) in non-small cell lung cancer (NSCLC). *Mol Cancer.* (2018) 17:52. doi: 10.1186/s12943-018-0810-4
32. Paik J, Dhillon S. Alectinib: a review in advanced, ALK-positive NSCLC. *Drugs.* (2018) 78:1247–57. doi: 10.1007/s40265-018-0952-0
33. Sakamoto H, Tsukaguchi T, Hiroshima S, Kodama T, Kobayashi T, Fukami TA, et al. CH5424802, a selective ALK inhibitor capable of blocking the resistant gatekeeper mutant. *Cancer Cell.* (2011) 19:679–90. doi: 10.1016/j.ccr.2011.04.004

Conflict of Interest: The authors declare that the research was conducted in the absence of any commercial or financial relationships that could be construed as a potential conflict of interest.

frontiers in Medicine

ORIGINAL RESEARCH
published: 03 March 2022
doi: 10.3389/fmed.2022.831952

Inflammatory Myofibroblastic Tumor of the Urinary Bladder: An 11-Year Retrospective Study From a Single Center

Can Chen[1†], Mengjun Huang[1†], Haiqing He[1†], Shuiqing Wu[1], Mingke Liu[1], Jun He[1], Hongjing Zang[2] and Ran Xu[1]*

[1] Department of Urology, The Second Xiangya Hospital of Central South University, Changsha, China, [2] Department of Pathology, The Second Xiangya Hospital of Central South University, Changsha, China

OPEN ACCESS

Edited by:
Renato Franco,
University of Campania Luigi Vanvitelli, Italy

Reviewed by:
Steven Christopher Smith,
Virginia Commonwealth University Health System, United States
Pei Dong,
Sun Yat-sen University Cancer Center (SYSUCC), China

***Correspondence:**
Ran Xu
xuran@csu.edu.cn

[†] These authors have contributed equally to this work

Specialty section:
This article was submitted to Pathology, a section of the journal Frontiers in Medicine

Received: 09 December 2021
Accepted: 07 February 2022
Published: 03 March 2022

Citation:
Chen C, Huang M, He H, Wu S, Liu M, He J, Zang H and Xu R (2022) Inflammatory Myofibroblastic Tumor of the Urinary Bladder: An 11-Year Retrospective Study From a Single Center. Front. Med. 9:831952. doi: 10.3389/fmed.2022.831952

Purpose: To share our experience in the diagnosis and treatment of an inflammatory myofibroblastic tumor of the urinary bladder (IMTUB).

Materials and Methods: A database searches in the pathology archives by using the term "inflammatory myofibroblastic tumor" and" bladder" in our hospital department of pathology from 2010 to 2021. Patient characteristics, clinical features, histopathological results, immunohistochemical staining results, and treatment outcomes were reviewed.

Results: Fourteen cases of IMTUB were retrieved. The mean age was 44.7 ± 18.9 years (range 12–74). Nine (64.3%) of the patients presented with hematuria, followed by seven (50%) with odynuria, five (35.7%) with urgent urination, and one (7.1%) with dysuria. Ten (71.4%) of the patients were treated with partial cystectomy (PC), three (21.4%) with transurethral resection of bladder tumor (TURBT), and one (7.1%) with radical cystectomy (RC). Histopathologically, eight (57.1%) had a compact spindle cell pattern. Anaplastic lymphoma kinase (ALK) staining was positive in six (75%) of 8 cases. During a mean follow-up period of 43.9 ± 38 months (range 3–117), a patient had recurrence within half a month. Then, the patient was treated with further TURBT surgery and had no recurrence within 6 months. Thirteen of the patients had no local recurrence or distant metastasis.

Conclusion: Inflammatory myofibroblastic tumor of the urinary bladder (IMTUB) is clinically rare and has a good prognosis. The disease is mainly treated with surgery to remove the tumor completely. It can easily be misdiagnosed as bladder urothelial carcinoma, leiomyosarcoma, or rhabdomyosarcoma, which may result in overtreatment and poor quality of life of patients.

Keywords: inflammatory myofibroblastic tumor (IMT), bladder, retrospective study, treatment, diagnosis

INTRODUCTION

An inflammatory myofibroblastic tumor (IMT) is a rare tumor made up of spindle cells with an associated inflammatory cell infiltrate (1). The pathogenesis and malignancy potential of the disease remain unclear (1, 2). The disease can occur anywhere in the body but is most commonly seen in the lungs, mesentery, and omentum (3, 4). In the genitourinary system, IMT is more likely to be found in the bladder. In previous literature, this disease has been reported in <1% of bladder tumors (5). Because of the low recurrence rate (only 4%), bladder-sparing treatment modalities, such as TURBT or partial cystectomy, are recommended (5, 6). Fourteen cases of IMTUB in our region were reviewed by retrospective analysis.

METHODS

A total of 14 patients diagnosed with IMTUB were recruited at Second Xiangya Hospital of Central South University in China from 2010 to 2021. Only IMTUB cases were included, and postoperative spindle cell nodule cases were excluded from our study. Each patient was treated primarily with surgery to remove the tumor and diagnosed by histopathological analysis. Immunohistochemical staining of anaplastic lymphoma kinase (ALK), S-100, desmin, smooth muscle actin (SMA), vimentin, cytokeratin (CK), CD34, CD68, CD117, Ki-67, and HMB-45 was performed to distinguish IMTUB from other tumors.

Clinical information included patient characteristics and tumor parameters. Patient characteristics, such as sex, age, presenting symptoms (including hematuria, odynuria, urgent urination, and dysuria), routine blood examination, routine urinalysis, preoperative urine culture, cystoscopy, abdominal computed tomography (CT), tumor parameter (tumor size in maximal dimension and tumor location in the urinary bladder), treatment and follow-up outcome, and histopathology and immunohistochemistry results were reviewed.

Histopathologically, IMTs can be categorized into three histopathological subtypes based on pathological morphology: the mucous/vascular type, the compact spindle cell type, and the hypocellular fibrous type (5, 7, 8). The mucous/vascular type features fasciitis, edema, or loose arrangement of plump cells in a mucinous stroma with prominent vessels. Inflammatory cells usually consist of more neutrophils and eosinophils and fewer plasma cells. The compact spindle cell type is mainly composed of proliferating spindle cells with bundles or layers. Large numbers of plasma cells and lymphocytes are typically mixed with spindle cells. The hypocellular fibrous type is similar to the fibromatosis type, but with vimineous rather than full spindle cells on a background of dense collagenous stroma, including sporadic plasma cells, eosinophils, and lymphocytes. Histopathologically, tumors can present with one type or a combination of two or three types (7, 8). In addition to the three histopathological types, other histopathological characteristics (such as the presence of necrosis, atypia, pleomorphism, abnormal mitosis, and mitotic figures) and a large number of inflammatory cells (such as lymphocytes, plasma cells, neutrophils, and eosinophils) were recorded. Depth of tumor invasion and all immunohistochemical results were recorded.

Because of the small number of patients, no statistical methods could be used. Informed consent was obtained from all the patients in our study, and this study was approved by the ethics committee of the Second Xiangya Hospital of Central South University.

Abbreviations: IMTUB, inflammatory myofibroblastic tumor of the urinary bladder; TURBT, transurethral resection of bladder tumor; PC, partial cystectomy; RC, radical cystectomy; ALK, anaplastic lymphoma kinase; IMT, inflammatory myofibroblastic tumor; SMA, smooth muscle actin; CK, cytokeratin; CT, computed tomography; NEUT%, neutrophil ratio; PCT, procalcitonin; CRP, C-reactive protein; ESR, erythrocyte sedimentation rate; EBV, Epstein–Barr virus.

RESULTS

Clinical Features

A total of 14 patients, nine women and five men, were included, with a mean age of 44.7 ± 18.9 years (range 12–74). Nine (64.2%) of the patients complained of hematuria, six (42.9%) complained of odynuria, five (35.7%) complained of urgent urination, and one (7.1%) complained of dysuria. Abdominal CT examinations indicated space-occupying changes in the bladder. No hydronephrosis or urinary calculus was found, but ureter invasion by the tumor was suspected in 1 case on imaging examination. Five (35.7%) of the patients were admitted with anemia, with a mean hemoglobin level of 97.6 ± 13.7 g/dl (range 80–113). All the patients had normal serum creatinine levels at presentation. Interestingly, in case 3 and case 9, preoperative urine culture indicated *Enterobacter cloacae* infection, which has never been reported in previous literature, and the perioperative anti-infection effect was remarkable. This may be a predisposing factor for IMT because of chronic inflammation in the bladder. The other patients had no significant predisposing factors such as pregnancy, infection, and surgery. In addition, one 14-year-old boy presented with severe bladder irritation with systemic inflammation. Routine white blood cell count was $18.2*10^9$/L, NEUT% was 92.7%, PCT was 6.57 ng/ml, CRP was 366 mg/l, and ESR was 59 mm/h. Mean tumor size in maximal dimension was 33.9 ± 14.8 mm (range 13–70). Regarding tumor location in the urinary bladder, five of the patients (35.7%) had tumors on the right lateral wall, four (28.6%) had tumors on the anterior wall, three (21.4%) had tumors in the dome, one (7.1%) had a tumor on the left lateral wall, and one (7.1%) had a tumor on the anterosuperior wall. The important clinical features are summarized in **Table 1**.

Treatment and Follow-Up

All the patients underwent minimally invasive surgery. Eleven (78.6%) of them were treated with partial cystectomy, three (21.4%) patients were treated with TURBT, and one (7.1%) patient was treated with radical cystectomy (RC). Of the 3 patients who initially underwent TURBT, 1 subsequently underwent TURBT again. The mean follow-up was 43.9 ± 38 months (range 3–117). A female patient experienced recurrence within half a month and then underwent further TURBT and had no recurrence within 6 months. The symptoms of the other patients were significantly relieved after surgery, without local

TABLE 1 | Clinical features, treatment and follow-up outcome of the 14 cases of IMTUB.

Case (*N*)	Age (years)	Gender (M/F)	Symptoms	Location	Size (mm)	Treatment	Follow-up (months)	Recurrence or distant metastases
1	41	M	Hematuria and urgent urination	Left lateral wall	27	PC	48	No
2	22	M	Urgent urination and odynuria	Anterior wall	70	PC	117	No
3	73	M	Urgent urination and odynuria	Right lateral wall	30	PC	96	No
4	62	F	Urgent urination	Right lateral wall	13	PC	100	No
5	54	F	Hematuria	Anterosuperior wall	36	PC	47	No
6	62	F	Hematuria	Right lateral wall	45	RC	48	No
7	40	M	Hematuria	Dome	35	PC	54	No
8	52	M	Hematuria	Right lateral wall	20	TURBT	24	No
9	14	M	Hematuria and odynuria	Anterior wall	45	PC	12	No
10	16	M	Hematuria and odynuria	Anterior wall	43	PC	48	No
11	70	F	Dysuria	Dome	20	PC	3	No
12	32	M	Urgent urination and odynuria	Dome	30	TURBT	6	No
13	43	F	Hematuria and odynuria	Anterior wall	43	PC	6	No
14	45	M	Hematuria and odynuria	Right lateral wall	30	TURBT	6	No

PC, partial cysectomy; RC, radical cysectomy; TURBT, transurethral resection of bladder tumor.

recurrence or distant metastasis. The patients had neither local recurrence nor distant metastasis by cystoscopy or CT scan. The treatment and follow-up outcomes are presented in **Table 1**.

Histopathological Features

Regarding the histopathological type, three (21.4%) tumors were myxoid/vascular type (**Figure 1A**), eight (57.1%) tumors were compact spindle-cell type (**Figure 1B**), one (7.1%) tumor was a hypocellular fibrous type (**Figure 1C**), one (7.1%) tumor was both myxoid/vascular and compact spindle cell type, and one (7.1%) tumor was both myxoid/vascular and hypocellular fibrous type (**Figure 1D**). Among eight cases with compact spindle cell types, all were characterized by spindle cells arranged in bundles or layers. Of the 14 patients, necrosis was found in six (42.9%), atypia was found in three (24.4%), mild atypia was found in one (7.1%), mild–moderate atypia was found in two (14.3%), and moderate–severe atypia was found in one (7.1%). Half of the patients (50%) did not have any atypia. Of the 14 patients, large amounts of lymphocytes, neutrophils, plasma cells, and eosinophils were found in 11 (78.6%), four (28.6%), two (14.3%), and one (7.1%), respectively. Only 1 case was noted to have two mitotic figures per 10 high-power fields. Of the 14 patients, tumor invasion to the muscularis propria was observed in 10 (71.4%), and invasion beyond the muscularis propria was observed in four (28.6%). The histopathological features are presented in **Table 2**.

Immunohistochemistry Features

Concerning immunohistochemistry outcomes, tissues from all the patients were stained differently. Anaplastic lymphoma kinase (ALK) staining was positive in six (75%) of eight patients (**Figure 2A**). Smooth muscle actin was positive in all the cases (11 focal, three diffuse) (**Figure 2B**). The mean Ki-67 level was 14 ± 8.2% (range 1–30%). S-100 was positive in four (28.6%) of the 14 cases. Vimentin (**Figure 2C**), cytokeratin (**Figure 2D**), desmin, CD117, CD68, CD34, and HMB-45 were positive in nine (100.0%) of nine, nine (64.3%) of 14, five (50%) of 10, one (14.3%) of seven, eight (100%) of, eight (66.7%) of the, and one (25.0%) of four cases, respectively. The immunohistochemical staining outcomes are presented in **Table 3**.

DISCUSSION

In 1939, IMT was first reported by Brunn as "myoma of the lung" (7, 9). In 1980, IMTUB, defined as a proliferative lesion of the submucosal stroma, was first proposed by Roth and showed low or uncertain malignant potential (9). In recent years, there have been different terminologies, such as inflammatory pseudotumor, pseudosarcomatous fibromyxoid tumor, pseudomalignant spindle-cell proliferation, and nodular fasciitis (6, 8). In 1994, IMT was defined as a neoplasm consisting of spindle cells characterized by myofibroblasts and a large number of associated inflammatory cells (3). An IMT can occur in the genitourinary system, but it is most common in the bladder and accounts for <1% of all bladder tumors (5, 7, 8). At present, the specific pathogenesis and etiology of IMT remain uncertain and might be connected with the following factors (4, 7, 10, 11): chronic inflammatory stimulation resulting from bacterial and viral microorganisms (mycobacteria, hepatitis B virus, Corynebacterium, Epstein–Barr virus, EBV, and human papillomavirus), history of bladder trauma or long-term use of hormone therapy, and rearrangements of the anaplastic lymphoma kinase (*ALK*) gene located on chromosome *2p23* (which occur in ∼50% of IMTs). This prevalence of *ALK* rearrangements not only makes *ALK* a promising marker to diagnose and distinguish IMT from other tumors but also suggests that IMT may be neoplastic rather than postoperative spindle-cell nodule (PSCN). It represents a benign reactive myofibroblastic proliferation of the genitourinary tract within 3 months after instrumentation (8, 9). The inflammatory

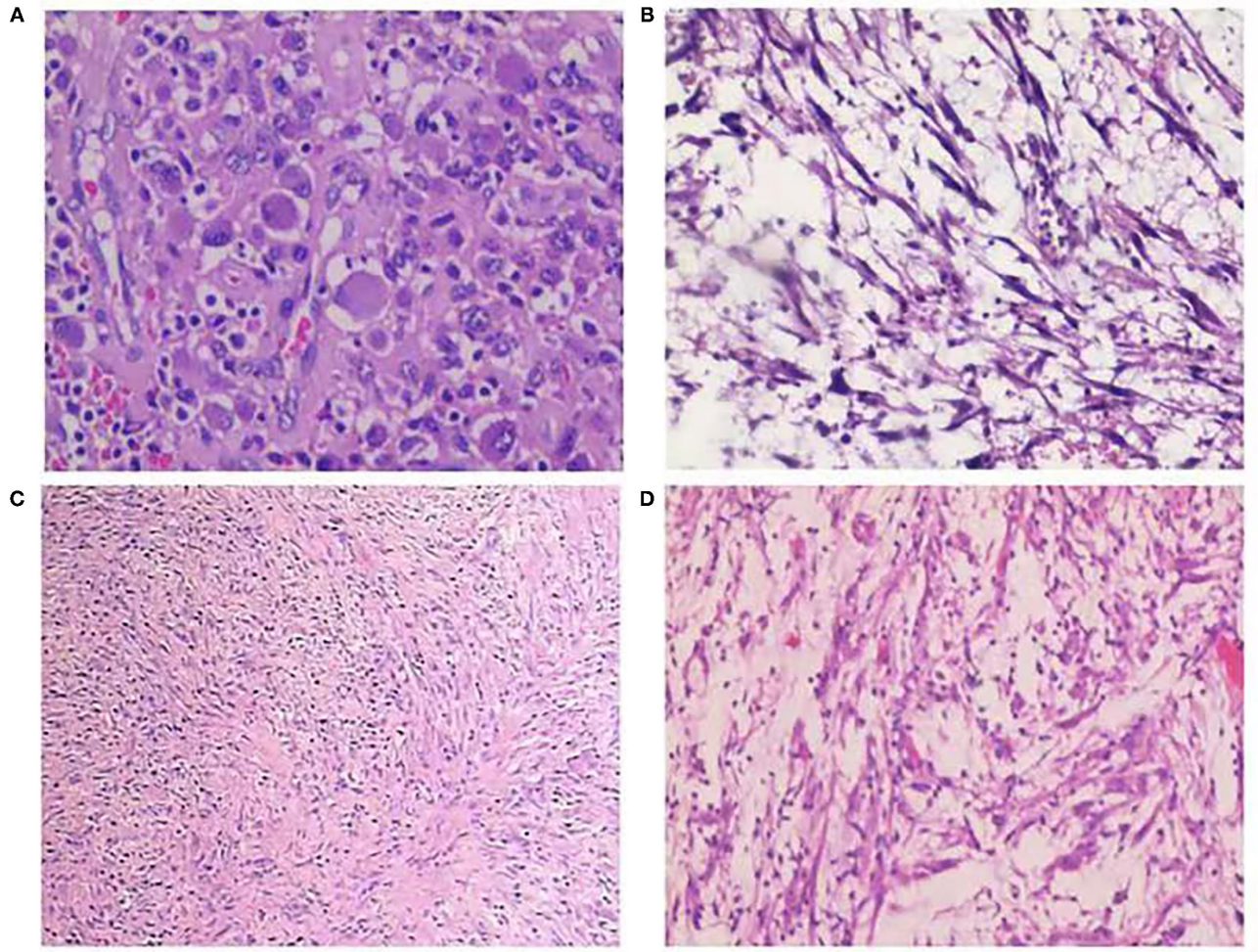

FIGURE 1 | (A) Myxoid/vascular type [hematoxylin and eosin (H&E) stain, ×200]. **(B)** Compact spindle cell type (H&E stain, ×100). **(C)** Hypocellular fibrous type (H&E stain, ×100); **(D)** Myxoid/vascular pattern and hypocellular fibrous type (H&E stain, ×100).

myofibroblastic tumor is a neoplasm of fibroblastic and myofibroblastic origin according to the 4th WHO classification. It is challenging to differentiate IMT from PSCN because of the overlap of morphology and immunohistochemistry; hence, clinical history can be helpful. Concerning genes, IMT may be more related to the clonal chromosomal rearrangement of *ALK* than PSCN. Leiomyosarcomas and sarcomatoid carcinomas usually lack *ALK* expression, especially when necrosis is present (2, 12, 13). A meta-analysis indicated that *ALK* played an important role in diagnosing and distinguishing IMTUB (14). The specificity and sensitivity were 0.99 (95% CI 0.67–1) and 0.86 (95% CI 0.58–0.96), respectively (14). The *Enterobacter cloacae*, a gram-negative bacillus that causes long-term chronic inflammatory stimulation of the bladder, was identified in urine cultures of two patients in this study. This bacterium has never been reported in previous literature.

Genomic rearrangements involving the *ALK* gene fusion with different partners, such as *TPM3, TPM4, CLTC, CARS, ATIC, SEC31L1, PPFIBP, DCTN1, EML4, PRKAR1A, LMNA, TFG, FN1,* and *HNRNPA1*, in IMTUB, have been described (8, 15–17). In recent years, novel *FN1-ALK* and *HNRNPA1-ALK* gene fusions have been discovered, which may suggest new targeted therapies in the future (15–18). However, Acosta, A.M et al. (16) reported that *FN1-ALK* gene fusion was characteristic of pseudosarcomatous myofibroblastic proliferation, which is a novel terminology for a tumor with significant clinicopathologic differences from IMT. Pseudosarcomatous myofibroblastic proliferation, with recurrence of 10–25% and without risk of metastasis, has a better prognosis than IMT. To further clarify the diagnosis, a FISH examination with the *ALK1* break-apart probe was carried out on cases 9 and 14. It confirmed no rearrangements of chromosome *2p23* (**Figure 3**). We advised the other patients to return to the hospital for the FISH test, but none of them complied.

The most common initial presentation of IMTUB is painless gross hematuria, but frequent urination, dysuria, abdominal/pelvic pain, and obstruction symptoms also exist (5, 8, 10, 11). Severe anemia can also develop. In a recent review

TABLE 2 | Histopathological features of the 14 cases of IMTUB.

Case (*N*)	Histology pattern	Appearance of necrosis	Appearance of atypia	Appearance of pleomorphism
1	Compact spindle cell type	−	Mild-moderate	−
2	Compact spindle cell type	+	Moderate-severe	−
3	Hypocellular fibrous type	−	+	−
4	Compact spindle cell type	−	−	−
5	Myxoid/vascular pattern and hypocellular fibrous type	+	Mild	−
6	Compact spindle cell type	−	Mild-moderate	−
7	Compact spindle cell type	−	−	−
8	Compact spindle cell and myxoid/vascular type	+	+	−
9	Myxoid/vascular type	−	−	−
10	Myxoid/vascular type	+	−	−
11	Compact spindle cell type	+	−	−
12	Compact spindle cell type	−	−	−
13	Compact spindle cell type	+	−	−
14	Myxoid/vascular type	−	+	−

Case (*N*)	Appearance of abnormal mitosis	Mitotic figure/10 HPFs	Tumor invasion into MP	Tumor invasion beyond MP	Inflammatory cell type
1	−	−	+	+	Lymphocytes, eosinophils
2	−	−	+	+	Lymphocyte
3	−	−	−	−	Lymphocyte
4	−	−	+	−	NA
5	−	2	+	+	Lymphocyte, neutrophil
6	−	−	+	−	Lymphocyte
7	−	−	−	−	NA
8	−	−	+	−	NA
9	−	−	−	−	Lymphocyte, neutrophil
10	−	−	+	+	Lymphocyte, neutrophil
11	−	−	+	−	Lymphocyte
12	−	−	+	−	Lymphocyte
13	−	−	+	−	Lymphocyte and plasma cells
14	−	−	−	−	Lymphocyte, neutrophil and plasma cells

MP, muscularis propria; HPFs, high power fields; NA, not available; +, positive; –, negative.

of children with IMTUB from 42 studies around the world, the mean age was 7.5 years (range 2–15) (13). Forty-one of the children underwent surgery to remove the tumor, and one was treated with a 2-week course of anti-inflammatory therapy (13). Local recurrence was suspected in only one asymptomatic patient who was found to have a residual mass in the trigone during follow-up (13). Li et al. reported data from eight children (11). The mean age was also 7.5 years (range 2.7–11.5) (11). Three of the patients had mean hemoglobin of 77 g/l due to severe hematuria (11). A systematic review (9) of 182 patients showed a mean age of 38.9 ± 16.6 years, and the majority of the patients were females. According to this review, the most common symptom was hematuria (71.9%), followed by dysuria (19.8%), increased urinary frequency (18.8%), lower abdominal pain (13.5%), and loin pain (2.1%) (9). A multicenter retrospective study presented nine patients with IMTUB with a mean age of 45.4 ± 22.8 years (range 11–78), and 55.6% of them were females (19). Eight (88.9%) of the patients presented with hematuria, four (44.4%) presented with dysuria, four (44.4%) presented with urinary frequency, and two (22.2%) presented with loin pain (19). Five (55.6%) of them showed anemia at presentation, with a mean hemoglobin level of 68 ± 13 g/l (range 48–80) (19). The ALK-positive IMTUB occurred more frequently in younger female patients than in patients in ALK-negative IMTUB, but there was no significant difference in prognosis between ALK-positive and ALK-negative IMTUB (9), which may be because IMTUB more commonly occurs in females than in males.

Radiographic examination usually indicates a space-occupying lesion with a lack of specificity in the bladder; therefore, it is difficult to differentiate IMTUB from bladder malignancy before surgery. However, Liang et al. (5, 6, 20) found that a primary finding of a lesion on the anterior wall of the bladder, with ring enhancement by contrast-enhanced

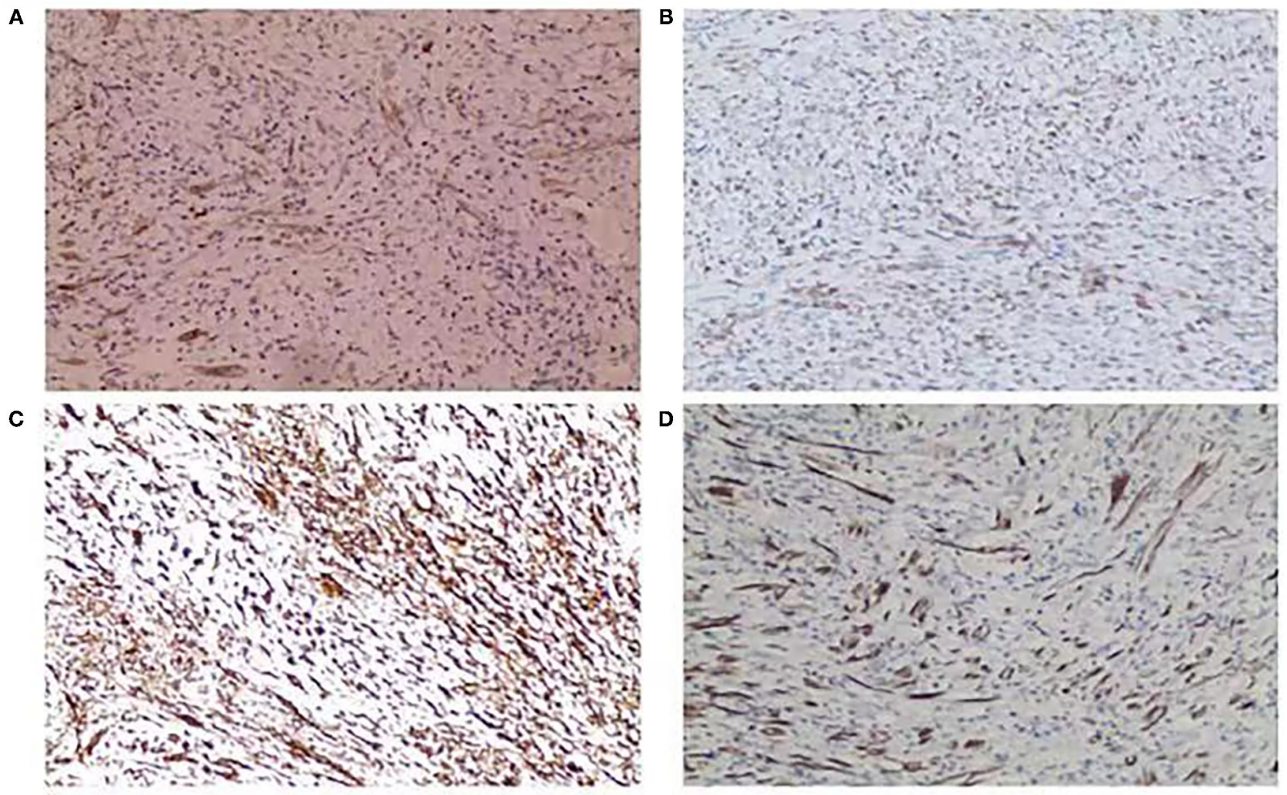

FIGURE 2 | (A) Positive anaplastic lymphoma kinase (ALK) staining (ALK stain, ×100). **(B)** Positive smooth muscle actin (SMA) staining (SMA stain, ×100). **(C)** Positive vimentin staining (vimentin stain, ×100). **(D)** Positive cytokeratin (CK) staining (CK stain, ×100).

TABLE 3 | Immunohistochemical characteristics of the 14 cases of IMTUB.

Case (*N*)	ALK	SMA	Ki-67	S100	Vimentin	CK	Desmin	CD117	CD68	CD34	HMB-45
1	NT	+	30%	−	NT	+	−	NT	+	NT	−
2	NT	++	10%	−	+	−	−	−	+	−	−
3	NT	+	1%	−	NT	+	NT	−	NT	NT	NT
4	+	+	5%	−	+	−	−	−	+	+	NT
5	++	+	10%	+	++	+	−	+	+	+	NT
6	−	++	25%	−	++	+	+	−	+	+	+
7	NT	++	10%	−	NT	−	NT	NT	NT	−	NT
8	NT	+	25%	−	+	+	NT	NT	+	+	NT
9	−	+	15%	−	NT	+	+	NT	+	−	NT
10	+	+	15%	+	+++	−	−	−	NT	+	−
11	NT	+	10%	+	+	+	NT	−	NT	+	NT
12	+	+	10%	+	NT	+	+	NT	NT	+	NT
13	+	+	20%	−	+	−	+	NT	+	+	NT
14	+	+	10%	−	+	+	+	NT	NT	−	NT

NT, not tested; –, negative; +, positve focally; ++, positive diffusely; +++, positive strongly.

CT, may be indicative of IMTUB. In our study, ring enhancement was observed on the anterior wall of the bladder in four (28.6%) out of the 14 cases and on the anterosuperior wall of the bladder in one (7.1%) on contrast-enhanced CT. The CT imaging features are described in **Figure 4**. Cystoscopy suggested a cauliflower-like mass in the bladder (**Figure 5**).

An IMT has a good prognosis and low risk of local recurrence and distant metastasis (6). The IMTUB shows a local recurrence rate of only 4% and a distant metastasis rate of lower than

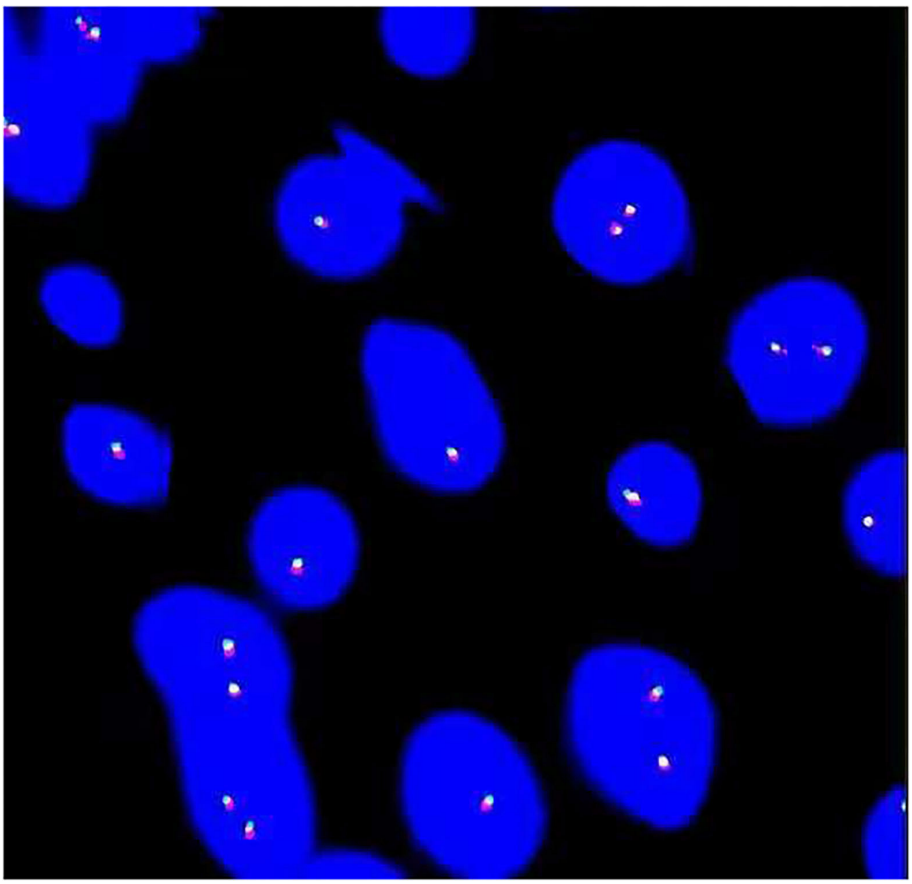

FIGURE 3 | Fluorescence *in situ* hybridization (FISH) analysis revealed no arrangement of *ALK* in chromosome *2p23*.

5% after surgery (6, 11, 18). The preferred treatment choices for IMTUB mainly include TURBT, partial cystectomy, and/or radical cystectomy (5). Concerning the benign characteristics of IMTUB, bladder-sparing treatment modalities, such as TURBT and partial cystectomy, were better and did not increase the risk of recurrence, and resulted in fewer complications than radical cystectomy in one study (5). Partial cystectomy may be a better option, especially for patients with tumors invading the muscularis propria or the ureter. A recent systematic review of (9, 18) that included 182 cases of IMTUB showed that 60.8% of patients were treated with TURBT, 29.2% were treated with partial cystectomy, and 9.2% were treated with radical cystectomy. Some patients who were first treated by TURBT underwent a second TURBT (5.5%), partial cystectomy (17.8%), and radical cystectomy (1.4%) (9). The IMTUB was successfully treated with a selective cyclooxygenase-2 (COX-2) inhibitor, prednisolone, and combined with minimally invasive surgery in three teenagers (21, 22). Therefore, a good adjuvant strategy is to reduce tumor size and help preserve bladder function for large tumors with a selective COX-2 inhibitor combined with hormones. Wang et al. (23) reported that a 14-year-old patient diagnosed with IMTUB and distant metastasis was successfully cured with 5 months of preoperative adjuvant chemotherapy combined with radical cystectomy. Reinhart et al. also reported that neoadjuvant treatment with an ALK inhibitor helped enable complete tumor resection by partial cystectomy for large tumors with a size of 70 mm (18). Libby et al. (24) first reported that IMTUB caused local tumor recurrence and distant metastasis to the peritoneum and large intestines in a 61-year-old male who underwent radical cystectomy. Unfortunately, this patient died 3 weeks after this operation. The IMTUB invaded the peritoneum, ileocecal junction, greater omentum, appendix, and other tissues in two reported cases (12, 23). Encouragingly, there was no local recurrence or distant metastasis in either adolescent after 6–12 months (12, 23). The tumor may be characterized by aggressive growth if it extends to tissues outside the bladder, such as the peritoneum, greater omentum, and ileocecal region.

CONCLUSION

An inflammatory myofibroblastic tumor of the urinary bladder (IMTUB) is a clinically rare tumor and has a good prognosis. The disease is mainly treated with TURBT and partial cystectomy to completely remove the tumor. It may be characterized by malignancy with aggressiveness if the tumor invades a distant site. Therefore, close follow-up is warranted. Based on this

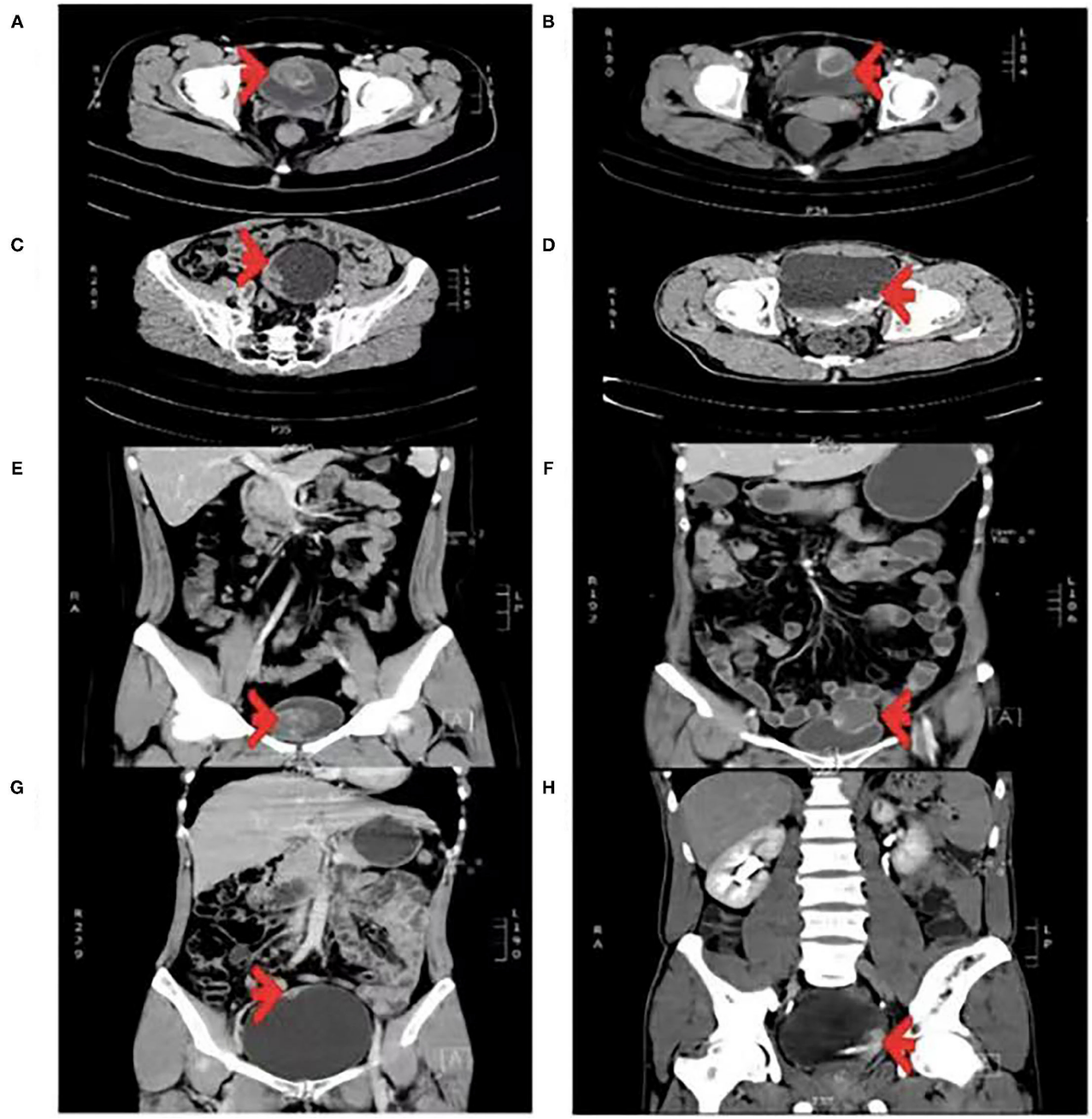

FIGURE 4 | (A–D) Transverse enhanced CT scan. **(E–H)** Coronal enhanced CT scan. **(A,E)** Tumor with a size of 43 × 40 mm was located on the anterior wall of the bladder, papillary protrusion into the cavity with ring enhancement was present, and the CT value was 53 HU. **(B,F)** Tumor with a size of 36 × 33 mm was located on the anterior-superior wall of the bladder, exophytic growth with ring enhancement was present, and the CT value was 54 HU. **(C,G)** Tumor with a size of 48 × 12 mm was located on the right lateral wall of the bladder, papillary protrusion into the cavity was present, and the CT value was 59 HU. **(D,H)** Tumor with a size of 27 × 21 mm was located on the left lateral wall of the bladder, papillary protrusion into the cavity and suspected invasion to the left ureter were present, and the CT value was 59 HU.

clinical retrospective study, more attention should be paid to IMTUB according to the features of CT and the pathology of IMTUB. It is really important to maintain patients' quality of life by preserving bladder function extensively, especially in young patients. Preoperative urine culture of *Enterobacter cloacae* in patients with IMTUB was an important discovery in our study. However, this finding may be incidental because of the limited number of cases. Therefore, further studies are needed to determine whether *Enterobacter cloacae* plays a role in IMTUB.

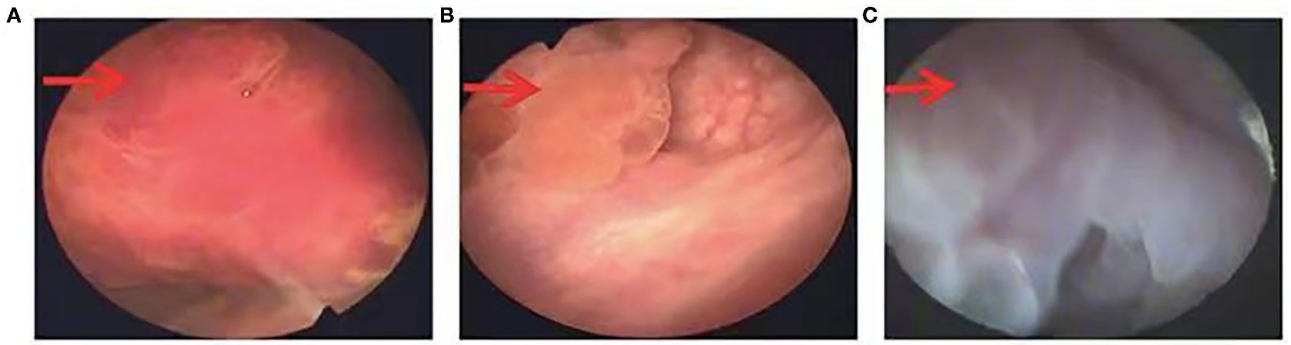

FIGURE 5 | (A–C) Cystoscopy revealed cauliflower-like masses on the anterior wall, left lateral wall, and anterior wall of the bladder.

DATA AVAILABILITY STATEMENT

The original contributions presented in the study are included in the article/supplementary material, further inquiries can be directed to the corresponding author/s.

ETHICS STATEMENT

The studies involving human participants were reviewed and approved by the Ethics Committee of the Second Xiangya Hospital of Central South University. Written informed consent to participate in this study was provided by the participants' legal guardian/next of kin. Written informed consent was obtained from the individual(s), and minor(s)' legal guardian/next of kin, for the publication of any potentially identifiable images or data included in this article.

AUTHOR CONTRIBUTIONS

RX and CC: conception and design. RX: administrative support. CC, MH, HH, SW, ML, JH, and HZ: provision of study materials or patients. CC, MH, HH, ML, and JH: collection and assembly of data. CC, MH, and HH: data analysis and interpretation. All authors: manuscript writing and final approval of the manuscript.

FUNDING

This study was supported by the grant from Science and Technology Agency of Hunan Province (no. 2020JJ4820).

REFERENCES

1. Lecuona AT, Van Wyk AC, Smit SG, Zarrabi AD, Heyns CF. Inflammatory myofibroblastic tumor of the bladder in a 3-year-old boy. *Urology.* (2012) 79:215–8. doi: 10.1016/j.urology.2011.04.052
2. Süer E, Gülpinar Ö, Mermerkaya M, Burgu B, Celepli P, Sertçelik A, et al. Inflammatory myofibroblastic tumor of the bladder in a 10-year-old girl. *Urology.* (2012) 80:1138–40. doi: 10.1016/j.urology.2012.07.023
3. Zhang HH, Qi F, Zu XB, Xu L, Liu LF, Qi L. Recurrence of inflammatory myofibroblastic tumor in bladder secondary to prostate treated with laparoscopic radical cystectomy. *Med SciMonit.* (2012) 18:CS63–6. doi: 10.12659/MSM.883255
4. Lu CH, Huang HY, Chen HK, Chuang JH, Ng SH, Ko SF. Huge pelvi-abdominal malignant inflammatory myofibroblastic tumor with rapid recurrence in a 14-year-old boy. *World J Gastroenterol.* (2010) 16:2698–701. doi: 10.3748/wjg.v16.i21.2698
5. Xu H, He B, Tu X, Bao Y, Yang L, Zhuo H, et al. Minimally invasive surgery for inflammatory myofibroblastic tumor of the urinary bladder: three case reports. *Medicine.* (2018) 97:e13474. doi: 10.1097/MD.0000000000013474
6. Song D, Jiao W, Gao Z, Liu N, Zhang S, Zong Y, et al. Inflammatory myofibroblastic tumor of urinary bladder with severe hematuria: a case report and literature review. *Medicine.* (2019) 98:e13987. doi: 10.1097/MD.0000000000013987
7. Wang K, Zhou H, Lu Y, Lu Q, Zhang C, Zhou X, et al. ALK-negative urachal inflammatory myofibroblastic tumor in an elderly female: a case report. *Medicine.* (2018) 97:e13619. doi: 10.1097/MD.0000000000013619
8. Alderman M, Kunju LP. Inflammatory myofibroblastic tumor of the bladder. *Arch Pathol Lab Med.* (2014) 138:1272–7. doi: 10.5858/arpa.2014-0274-CC
9. Teoh JY, Chan NH, Cheung HY, Hou SS, Ng CF. Inflammatory myofibroblastic tumors of the urinary bladder: a systematic review. *Urology.* (2014) 84:503–8. doi: 10.1016/j.urology.2014.05.039
10. Wang W, Zhang M,Lu JR, LiQY. Inflammatory myofibroblastic tumor of urinary bladder. *Chin Med J.* (2018) 131:2259–61. doi: 10.4103/0366-6999.240816
11. Li YP, Han WW, Yang Y, He LJ, Zhang WP. Inflammatory myofibroblastic tumor of the urinary bladder and ureter in children: experience of a tertiary referral center. *Urology.* (2020) 145:229–35. doi: 10.1016/j.urology.2020.07.050
12. Yi XL, Lu HY, Wu YX, Li WH, Meng QG, Cheng JW, et al. Inflammatory myofibroblastic tumor with extensive involvement of the bladder in an adolescent: a case report. *World J SurgOncol.* (2013) 11:206. doi: 10.1186/1477-7819-11-206
13. Collin M, Charles A, Barker A, Khosa J, Samnakay N. Inflammatory myofibroblastictumour of the bladder in children: a review. *J Pediatr Urol.* (2015) 11:239–45. doi: 10.1016/j.jpurol.2015.03.009
14. Wu S, Xu R, Wan Q, Zhu X, Zhang L, Jiang H, et al. Assessment of the potential diagnostic role of anaplastic lymphoma kinase for inflammatory myofibroblastictumours: a meta-analysis. *PLoS ONE.* (2015) 10:87. doi: 10.1371/journal.pone.0125087
15. Ouchi K, Miyachi M, Tsuma Y, Tsuchiya K, Iehara T, Konishi E, et al. FN1: a novel fusion partner of ALK in an inflammatory myofibroblastic tumor. *Pediatr Blood Cancer.* (2015) 62:909–11. doi: 10.1002/pbc.25424

16. Acosta AM, Demicco EG, Dal Cin P, Hirsch MS, Fletcher CDM, Jo VY. Pseudosarcomatousmyofibroblastic proliferations of the urinary bladder are neoplasms characterized by recurrent FN1-ALK fusions. *Mod Pathol.* (2021) 34:469–77. doi: 10.1038/s41379-020-00670-0
17. Inamura K, Kobayashi M, Nagano H, Sugiura Y, Ogawa M, Masuda H, et al. A novel fusion of HNRNPA1-ALK in inflammatory myofibroblastic tumor of urinary bladder. *Hum Pathol.* (2017) 69:96–100. doi: 10.1016/j.humpath.2017.04.022
18. Reinhart S, Trachsel Y, Fritz C, Wagner U, Bode-Lesniewska B, John H, et al. Inflammatory myofibroblastic tumor of the bladder with FN1-ALK gene fusion: different response to ALK inhibition. *Urology.* (2020) 146:32–5. doi: 10.1016/j.urology.2020.09.026
19. Teoh JY, Chan NH, Mak SM, Lo AW, Leung CY, Hui Y, et al. Inflammatory myofibroblastictumours of the urinary bladder: multi-centre 18-year experience. *Urol Int.* (2015) 94:31–6. doi: 10.1159/000358732
20. Liang W, Zhou X, Xu S, Lin S. CT manifestations of inflammatory myofibroblastic tumors (inflammatory pseudotumors) of the urinary system. *Am J Roentgenol.* (2016) 206:1149–55. doi: 10.2214/AJR.15.14494
21. Tsuma Y, Miyachi M, Ouchi K, Tsuchiya K, Iehara T, Naitoh Y, et al. Neoadjuvant treatment with cyclooxygenase-2 inhibitor and prednisolone allows conservative surgery for inflammatory myofibroblastic tumor of the bladder. *J PediatrHematolOncol.* (2016) 38:e283–5. doi: 10.1097/MPH.0000000000000604
22. Raja NS, Lee T, Kaffenberger S, Kraft K, Udager A, Ivancic V. Localized inflammatory myofibroblastic tumor involving the genitourinary system: adolescent case series and review. *Urology.* (2018) 122:162–4. doi: 10.1016/j.urology.2018.07.002
23. Wang X, Xu S, Tang D, Gu W, Shu Q. Malignant inflammatory myofibroblastic tumor of the urinary bladder in a 14-year-old boy. *J Pediatr Hematol Oncol.* (2015) 37:e402–4. doi: 10.1097/MPH.0000000000000398
24. Libby EK, Ellis LT, Weinstein S, Hammer RD, Murray KS. Metastatic inflammatory myofibroblastic tumor of the bladder. *Urol Case Rep.* (2019) 23:10–2. doi: 10.1016/j.eucr.2018.11.007

Conflict of Interest: The authors declare that the research was conducted in the absence of any commercial or financial relationships that could be construed as a potential conflict of interest.

Publisher's Note: All claims expressed in this article are solely those of the authors and do not necessarily represent those of their affiliated organizations, or those of the publisher, the editors and the reviewers. Any product that may be evaluated in this article, or claim that may be made by its manufacturer, is not guaranteed or endorsed by the publisher.

frontiers | Frontiers in Medicine

ORIGINAL RESEARCH
published: 12 April 2022
doi: 10.3389/fmed.2022.823065

Exploration of KCNJ5 Somatic Mutation and CYP11B1/CYP11B2 Staining in Multiple Nodules in Primary Aldosteronism

Jing Xie[1,2†], Cui Zhang[3†], Xuefeng Wang[4], Yiran Jiang[3], Luming Wu[3], Lei Ye[3], Xuan Wang[5], Wen Xie[6], Haimin Xu[2] and Weiqing Wang[3]*

[1] Department of Pathology, Shanghai Jiao Tong University School of Medicine, Shanghai, China, [2] Department of Pathology, Ruijin Hospital, Shanghai Jiao Tong University School of Medicine, Shanghai, China, [3] Department of Endocrine and Metabolic Diseases, Ruijin Hospital, Shanghai Institute of Endocrine and Metabolic Diseases, Shanghai Jiao Tong University School of Medicine, Shanghai, China, [4] Department of Clinical Laboratory, Ruijin Hospital, Shanghai Jiao Tong University School of Medicine, Shanghai, China, [5] Department of Pathology, Shanghai Pulmonary Hospital, Tongji University School of Medicine, Shanghai, China, [6] Department of Pathology, Zhongnan Hospital of Wuhan University, Wuhan, China

OPEN ACCESS

Edited by:
Luigi Tornillo,
University of Basel, Switzerland

Reviewed by:
Zhiyan Liu,
Shanghai Jiao Tong University, China
Sylvia L. Asa,
Case Western Reserve University, United States

***Correspondence:**
Weiqing Wang
wqingw61@163.com

[†]*These authors have contributed equally to this work*

Specialty section:
This article was submitted to Pathology, a section of the journal Frontiers in Medicine

Received: *26 November 2021*
Accepted: *28 February 2022*
Published: *12 April 2022*

Citation:
Xie J, Zhang C, Wang X, Jiang Y, Wu L, Ye L, Wang X, Xie W, Xu H and Wang W (2022) Exploration of KCNJ5 Somatic Mutation and CYP11B1/CYP11B2 Staining in Multiple Nodules in Primary Aldosteronism. Front. Med. 9:823065. doi: 10.3389/fmed.2022.823065

Objective: Unilateral primary aldosteronism (PA) includes aldosterone-producing adenoma (APA), unilateral adrenal hyperplasia, and unilateral multiple nodules. The correlation of multiple nodules, especially genotypic and pathological characteristics, remains unknown. KCNJ5 mutation accounts for 60–80% of unilateral PA, so we aimed to explore the correlation of KCNJ5 somatic mutation and CYP11B1/CYP11B2 staining in multiple nodules in unilateral PA.

Design and Methods: A total of 56 microdissected nodules from 24 patients with unilateral PA were included. We assessed somatic KCNJ5 mutations, immunohistochemistry for aldosterone synthase (CYP11B2)/cortisol synthase (CYP11B1), and histological cellular composition of nodules together with adjacent adrenal cortical statements.

Results: KCNJ5 mutations were identified in 17 (17/56, 30.4%) nodules from 11 adrenals (11/24, 45.8%). All KCNJ5-mutant nodules were positive for CYP11B2 staining, 6 cases (6/11) had only one KCNJ5-mutant nodular, and the other 5 cases (5/11) had more than one KCNJ5-mutant nodules. Three cases (3/11) had different KCNJ5 mutations in individual nodules. Compared with KCNJ5-positive adrenals, the cortices adjacent to the nodules in KCNJ5-negative adrenals showed significant proliferation (p = 0.004). CYP11B2/CYP11B1 expression patterns revealed great heterogeneity in intensity and range both in KCNJ5-mutant nodules and KCNJ5-WT ones.

Conclusion: There is great heterogeneity among nodules from patients with unilateral PA. Countable nodules could be considered as multiple APAs, featuring somatic KCNJ5 mutation, positive CYP11B2 staining, and lack of adjacent cortical proliferation in unilateral multiple nodules.

Keywords: KCNJ5, CYP11B2, CYP11B1, primary aldosteronism, unilateral multiple nodules

INTRODUCTION

Primary aldosteronism (PA) is characterized by hypertension, hypokalemia, increased plasma aldosterone, and suppressed renin levels and is the most potentially curable form of secondary hypertension, occurs in 6–10% of hypertensive patients (1–3). PA is divided into the unilateral and bilateral diseases by adrenal vein sampling (AVS). Unilateral PA is best treated by adrenalectomy, whereas bilateral PA requires treatment with mineralocorticoid receptor antagonists (4). In past years, most unilateral PAs are aldosterone-producing adenomas (APAs), and unilateral adrenal hyperplasia (UAH) is considered to be rare. However, an increasing number of studies have focused on UAH; in our center, we previously reported that UAH accounted for 19% of PA cases (5). Immunohistochemical analysis of CYP11B1 (cortisol synthase) and CYP11B2 (aldosterone synthase) provides important functional information and can aid in the histopathological diagnosis of unilateral nodules (6–9). Especially, an international group of pathologists and adrenal experts has published the histopathology of PA and reached a consensus in standardizing the histopathologic features of adrenals from patients with PA (10), UAH on histopathology is divided into multiple adrenocortical micronodules (MN) and diffuse hyperplasia of zona glomerulosa (DH) (11). However, many nodules in MN do not exhibit aldosterone-producing zona glomerulosa (ZG)-like cells (small, with a high nuclear–cytoplasmic ratio and a smaller lipid content), as would be expected, but zona fasciculata (ZF)-like cells (large clear cells with lipid-laden cytoplasm and small nuclei) normally produce cortisol (12–14). Small extra nodular cell clusters are observed with strong CYP11B2 expression and no CYP11B1 expression in the surrounding cortical tissue (7). Therefore, the pathogenesis of unilateral MN remains unknown.

In addition to histopathology and immunohistochemistry, molecular analysis is also important for pathogenesis. KCNJ5, first described in a case of familial hypertension III by Choi et al. (15), induces the activation of aldosterone synthesis and has been implicated in promoting the growth of aldosterone-secreting cells into APAs (8). Other mutations include CACNA1D, ATP1A1, and ATP2B3 (15, 16). In China, KCNJ5 mutations occur in up to 70.7% of APAs (17) and account for most unilateral adrenal diseases. APAs appear as a single well-circumscribed nodule with various degrees of adrenal cortex remodeling, i.e., atrophic, with a diffuse hyperplasia or nodular hyperplasia (18, 19).

Heterogeneity in PA has long been a focus of research and is a lasting topic of interest in this field. It was reported that different somatic gene mutations occurred at different CYP11B2-positive areas within the same tumor (20). There were few studies that focused on KCNJ5 mutation in the unilateral multinodular lesions. Especially whether KCNJ5 mutation occurred in different nodules within one adrenal gland remains unclear. In this study, we assessed the phenotypic and genotypic characteristics of 24 patients with unilateral multiple nodules in this topic.

MATERIALS AND METHODS

Subjects

We enrolled 24 patients with unilateral PA who underwent unilateral adrenalectomy and were diagnosed as multiple nodules by hematoxylin and eosin (HE) staining in Ruijin Hospital affiliated with Shanghai Jiao Tong University School of Medicine from 2016 to 2019. Informed consent was obtained from all participants in this study. Patients were diagnosed with PA by saline infusion test according to Endocrine Society Clinical Practice Guidelines 2016 (4). All patients underwent adrenal computed tomography (CT) scans. A unilateral CT performance was defined as a unilateral adenoma (>10 mm), with a smooth appearance observed for the contralateral glands. Bilateral CT was used to detect bilateral adrenal hyperplasia or nodules on CT. Adrenal venous sampling (AVS) was performed by an experienced radiologist. Cannulation was considered successful if the cortisol adrenal vein:cortisol peripheral vein ratio was greater than 3 without adrenal corticotropic hormone (ACTH) stimulation (17). Twenty-one patients underwent AVS with unilateral lateralization, and 3 patients were diagnosed with unilateral PA by CT scan. All the adrenals from these patients were identified to multiple nodules under microscopy.

Pathological Analysis

Histological examination of the removed adrenals was performed by two experienced pathologists. All adrenal gland examinations included gross observation and microscopic assessment.

Specimen were well prepared for all adrenal glands, embedded in paraffin, cut into 3 μm thick slices, stained with H&E, and then were analyzed to obtain a diagnosis of the multinodular lesion. The cellular composition was determined by examining known features: ZF, i.e., large and lipid-laden clear cells; ZG, i.e., small and clear cells; and zona reticularis (ZR), i.e., large and acidophilic lipid-deleted compact cells or in combination. The details of the adjacent cortex were determined as follows: atrophy or normal (0), slight or focal hyperplasia (1+), medium hyperplasia (2+), and remarkable/diffuse hyperplasia (3+) (**Supplementary Figure 1**). Aldosterone-producing cell clusters (APCCs) were defined as "CYP11B2-positive lesion (<10 mm diameter) composed of ZG cells located beneath adrenal capsule that do not differ in morphology from adjacent adrenocortical cells by H&E staining" according to the consensus in 2020 (10).

Immunohistochemical Analysis

We performed immunohistochemistry of CYP11B1 and CYP11B2 in all the nodules selected by microscopy to assess the cortisol- and aldosterone-secreting function of the adrenals, respectively. Immunohistochemistry was performed according to previously described protocols (7). The antibodies for CYP11B1 (monoclonal mouse anti-human CYP11B1, clone H-11, 1:100, SANTA CRUZ) and CYP11B2 (monoclonal mouse anti-human CYP11B2, clone 41-17B, 1:100, EMD Millipore) were used for immunohistochemistry on formalin-fixed paraffin-embedded sections using Chem Mate ENVISION kits (Dako).

Semiquantitative immunoreactivity scoring was used to investigate the functional significance of CYP11B1 and CYP11B2, which was assessed by the McCarty H-score (ranging from 0 to 300) with all tumors examined under a 20 × objective. In each field, the percentage of immunopositive cells was assessed and then multiplied by a factor from 0 to 3 according to the intensity of immunopositivity (21). The relative immunointensity of specific immunoreactivity was characterized as not present (0), weak but detectable above the control (1+), distinct (2+), or very strong (3+) (**Supplementary Figures 2, 3**).

Genotyping

All visible nodules were demarcated on the H&E-stained slides by a pathologist using a marker pen. Six 10-μm sections were manually microdissected for each nodule. Genomic DNA was prepared from all separate nodules and normal adrenals by overnight digestion with proteinase K and analyzed separately. KCNJ5 somatic mutations were performed by Sanger sequencing. DNA fragments were sequenced for PCR amplification using previously reported primers: 5'-TTGGCGACCAAGAGTGGATTCCTT-3' and 5'-CACCATGAAGGCATTGACGATGGA-3.

Statistical Analysis

Statistical Analysis System (SAS) 9.4 was used for the statistical analyses. Continuous variables are presented as the means ± standard deviation (SD) if they were normally distributed and P25 – P75 if they were not normally distributed. Categorical variables are presented as numbers (%). Continuous and categorical variables were compared using Student's *t*-test and Fisher's exact test, respectively. Statistical significance was defined as an α-level less than 0.05 on two-sided tests.

RESULTS

The 24 adrenal glands that were analyzed contained 56 nodules in total (2–4 nodules for each gland), which were all examined separately. There were no significant differences in sex, age, blood pressure (BP), and potassium level between patients with KCNJ5 mutations and those without any KCNJ5 mutations. However, the age in the KCNJ5 mutation group was younger than that of the KCNJ5-wild type (KCNJ5-WT) group. Serum cortisol, plasma aldosterone, and renin activity were similar between the two groups; however, plasma ACTH was lower in KCNJ5-mutant patients (**Table 1**).

All KCNJ5 mutations were present in CYP11B2-positive cells in 11 cases (11/24, 45.8%) comprising 17 nodules (17/56, 30.4%). The average size of KCNJ5-mutant nodules was 1.12 cm, which was larger than that of KCNJ5-WT (0.83 cm). However, no significant differences in the cell components were found between nodules in the KCNJ5-mutation and KCNJ5-WT groups, the KCNJ5 mutations were occurred in ZF-dominant nodules (9/17 in ZF-cells, 7/17 in ZF + ZR cells). The KCNJ5-WT nodules exhibited adjacent cortex hyperplasia (32/39) when compared to the KCNJ5-mutant nodules (7/17) ($p = 0.004$). Interestingly, the decrease in CYP11B1 expression was more remarkable than the increase in CYP11B2 ($p = 0.009$; **Table 2**).

In 5 cases (cases 5, 8, 11, 19, and 24), multiple KCNJ5 mutations were found in each adrenal nodular, 2 cases (cases 11 and 24) had the same mutations in different nodules within one gland, and 3 cases (cases 5, 8, and 19) had different mutations in separate nodules (**Table 3**). The hotspot mutations of KCNJ5 included 503 (168) T > G, 451 (151) G > A, and 451 (151) G > C. The nodules in one gland carrying the same mutations showed varied expressions of CYP11B2 but negative expressions of CYP11B1. While the nodules harbored different mutations in cases 5, 8, and 19, the situation is seemed different. In these cases, KCNJ5-mutated nodules showed uniform expression of CYP11B2 but a varied expression of CYP11B1.

In 5 cases (2, 7, 10, 12, and 14), every gland contained 2 nodules and only one of them had a KCNJ5 mutation (**Table 3**). The mutation site involved 503 (168) T > G and 451 (151) G > A. Compared to KCNJ5-WT nodules, KCNJ5-mutant nodules were prone to be larger ones (4/5 cases, cases 2, 10, 12, and 14). KCNJ5 mutations unlikely occurred in nodules that were CYP11B1-positive (intense > 2+ and range > 50%), even if CYP11B2 was partly positive (intense ≥ 2+, any range) (2/3 cases, cases 2, 12, and 14). Moreover, KCNJ5 mutations occurred

TABLE 1 | Clinical features of 24 patients with primary aldosteronism (PA).

Variables	KCNJ5-wild type (*n* = 13)	KCNJ5-mutant (*n* = 11)	*P*
Age (years)	52.4 ± 12.0	43.7 ± 11.8	0.09
Female (*n*, %)	4 (30.8)	5 (45.5)	0.46
Systolic BP (mmHg)	166.5 ± 19.7	169.0 ± 32.2	0.82
Diastolic BP (mmHg)	97.3 ± 9.3	100.7 ± 14.9	0.50
Serum potassium (mmol/L)	2.60 ± 0.70	2.77 ± 0.58	0.53
Aldosterone (ng/dL)	537.2 ± 350.8	462.5 ± 185.6	0.54
PRA (ng/mL/h)	0.40 ± 0.23	0.23 ± 0.23	0.15
Serum cortisol (8 a.m.)	11.5 ± 2.7	10.3 ± 3.0	0.32
ACTH (pg/mL)	38.5 ± 9.9	29.1 ± 9.7	0.04

Values are arithmetic (± SD) or the number of subjects (%).

TABLE 2 | Characteristics of 56 nodules with and without KCNJ5 mutations in 24 patients with primary aldosteronism (PA).

Characteristic	KCNJ5-Wild type (*n* = 39)	KCNJ5 mutant (*n* = 17)	*P*
Size (cm)	0.83 ± 0.51	1.12 ± 0.61	0.07
CYP11B1	123.0 ± 82.7	47.5 ± 44.3	0.009
CYP11B2	225.1 ± 108.8	258.5 ± 41.0	0.18
Cell components of nodules			
ZG + ZR	0 (0)	1 (5.9)	0.30
ZG + ZF	1 (2.6)	0 (0)	0.70
ZF	16 (41.0)	9 (52.9)	0.56
ZF + ZR	18 (46.2)	7 (41.2)	0.78
ZR + ZF	4 (10.3)	0 (0)	0.30
Hyperplasia in adjacent cortex	32 (82.1)	7 (41.2)	0.004

Values are arithmetic (± SD) or the number of subjects (%).

TABLE 3 | Characteristics of 56 nodules.

Case	Size (cm)	Spots of KCNJ5 mutation	Expression of B1	Expression of B2	Cell components of nodules	Status of adjacent cortex
1	N1 0.6	Neg	0	100% 3 +	ZG + ZF	2
	N2 0.5	Neg	70% 2+	2% +	ZF + ZR	2
2	N1 1.2	451 (151)G > A	50% 1 + 40% 2 +	60% 2 +	ZF	0
	N2 0.8	Neg	80% 2 +	20% 2 +	ZF + ZR	0
3	N1 1.0	Neg	5% 2 +	100% 3 +	ZF + ZR	2
	N2 0.6	Neg	80% 3 +	20% 1 +	ZF + ZR	2
4	N1 0.4	Neg	50% 2 +	0	ZR + ZF	2
	N2 0.5	Neg	50% 2 +	5% 2 +	ZF + ZR	2
	N3 0.6	Neg	80% 3 +	0	ZF + ZR	2
	N4 0.3	503 (168) T > G	100% 1 +	90% 3 +	ZF + ZR	2
5	N1 0.6	503 (168)T > G	30% 1 +	100% 3 +	ZF + ZR	0
	N2 1.5	451 (151)G > A	30% 1 +	100% 3 +	ZG + ZF	0
6	N1 0.8	Neg	0	0	ZF	1
	N2 1.7	Neg	20% 1 +	0	ZF	1
	N3 0.5	Neg	40% 2 +	0	ZF	1
	N4 0.8	Neg	40% 2 +	60% 3 +	ZF + ZR	1
7	N1 2.2	Neg	20% 1 +	80% 3 +	ZF	0
	N2 0.8	451 (151)G > A	0	80% 3 + 20% 2 +	ZF	0
8	N1 0.7	451 (151)G > A	10% 1 +	70% 3 +	ZF	0
	N2 1.5	503 (168)T > G	70% 1 +	80% 3 + 20% 2 +	ZF + ZR	0
9	N1 0.8	Neg	100% 1 +	0	ZF	2
	N2 0.6	Neg	100% 1 +	0	ZF + ZR	2
	N3 1.7	Neg	80% 1 +	100% 3 +	ZF	2
10	N1 0.5	503 (168)T > G	5% 2 +	100% 3 +	ZF	2
	N2 0.3	Neg	10% 3 +	100% 3 +	ZF	2
11	N1 2.0	503 (168)T > G	0	80% 3 + 10% 2 +	ZF + ZR	0
	N2 1.5	503 (168)T > G	0	90% 3 + 10% 2 +	ZF + ZR	0
	N3 0.6	503 (168)T > G	0	50% 3 + 50% 2 +	ZF + ZR	0
12	N1 1.0	451 (151)G > A	10% 1 +	90% 3 + 10% 2 +	ZF	0
	N2 0.6	Neg	60% 3 + 20% 2 +	0	ZF	0
13	N1 0.3	Neg	100% 1 +	0	ZR + ZF	0
	N2 0.4	Neg	100% 1 +	0	ZR + ZF	0
14	N1 2.0	503 (168)T > G	0	90% 3 + 10% 2 +	ZF + ZR	1
	N2 0.8	Neg	100% 3 +	0	ZF + ZR	1
15	N1 0.6	Neg	0	100% 3 +	ZF + ZR	2
	N2 0.4	Neg	20% 1 +	0	ZF + ZR	2
	N3 0.4	Neg	50% 3 + 40% 2 +	0	ZF + ZR	2
16	N1 1.5	Neg	60% 2 +	80% 3 + 10% 2 +	ZF + ZR	1
	N2 1.0	Neg	70% 1 + 10% 2 +	60% 3 + 20% 2 +	ZF + ZR	1
17	N1 0.8	Neg	80% 3 +	70% 1 +	ZR + ZR	3
	N2 0.7	Neg	70% 2 + 30% 1 +	30% 3 +	ZF + ZR	3
18	N1 1.0	Neg	10% 3 + 90% 2 +	10% 3 + (on the periphery)	ZF	2
	N2 1.5	Neg	10% 1 +	90% 3 + 10% 2 +	ZF + ZR	2
19	N1 0.8	Neg	30% 2 +	90% 3 + 10% 2 +	ZF	3
	N2 0.7	451 (151)G > A	30% 1 +	80% 3 + 10% 1 +	ZF	3
	N3 0.4	451 (151)G > C	30% 1 +	80% 3 + 10% 1 +	ZF	3
20	N1 1.0	Neg	0	100% 3 +	ZF + ZR	2
	N2 0.7	Neg	20% 1 +	0	ZF + ZR	2
21	N1 0.5	Neg	0	100% 3 +	ZF	3
	APCC (0.2)	Neg	0	100% 3 +	ZF	3
22	N1 0.5	Neg	0	80% 3 +	ZF	0
	N2 2.5	Neg	0	70% 3 +	ZF	0
23	N1 1.0	Neg	100% 1 +	100% 3 +	ZF	3
	N2 0.8	Neg	100% 1 +	100% 3 +	ZF	3
24	N1 2.2	503 (168)T > G	0	50% 3 + 40% 2 +	ZF	1
	N2 1.5	503 (168)T > G	0	70% 2 + 10% 3 +	ZF	1

in CYP11B1-negative nodules, nevertheless, the expression of CYP11B2 varied (cases 10 and 14).

In case 4, gross examination showed intensive hyperplasia of the gland with 3 well-demarcated nodules that were 0.4, 0.5, and 0.6 cm in diameter independently. Microscopically, countless micronodules were observed, and three nodules could be defined correspondingly (**Figure 1A**). Immunohistochemical staining indicated moderate to strong CYP11B1 expressions and negative CYP11B2 expressions (**Figures 1C,D**). Surprisingly, an irregular zone of 3 mm × 3 mm with weak CYP11B1 and strong CYP11B2 expressions was found (**Figures 1C,D**). This APCC-like pattern carried the KCNJ5 mutation of 503 (168) T > G (**Figure 1B**).

In the remaining cases, no KCNJ5 mutation was detected. CYP11B2/CYP11B1 expression patterns also revealed great heterogeneity in intensity and range (**Table 3**). CYP11B2 was strongly expressed in double-nodular glands in 4 cases (16, 21, 22, and 23). Among them, CYP11B1 expression varied in case 16, while in the other 3 cases (21, 22, and 23), CYP11B1 staining was almost negative. The 5 cases (1, 3, 9, 15, and 20) possessed one CYP11B2-positive nodule with completely negative or sporadically CYP11B2-positive signals in the other nodules, CYP11B1 expression varied in these CYP11B2-negative nodules.

In case 13, two well-demarcated nodules that are composed of acidophilic cells and clear cells (**Figures 2A,B**) showed completely negative staining for CYP11B2 and weak expression of CYP11B1 (**Figures 2C,D**). Several APCCs beneath the adrenal capsule were detected (**Figure 2D**). Though these CYP11B2-positive/CYP11B1-negative cell clusters might be markedly exhibited by CYP11B2 staining, they could hardly be detected by H&E staining.

There were 3 rare CYP11B2/CYP11B1 expression patterns that deserve further description. In case 17, the adrenal had 2 nodules with a mixture of acidophilic cells and clear cells by 0.7 and 0.8 cm in diameter, respectively (**Figure 3A**). The CYP11B2-positive/CYP11B1-weak positive area was occupied by approximately one-third of the clear cell dominant nodule; the rest of the nodule was CYP11B2-negative/CYP11B1-moderate positive (**Figures 3B,C**). A similar situation was observed in case 6 (**Figure 3D**); CYP11B2-positive expression was focused on an area of 4 mm × 3 mm in size on nodule 4 (0.8 cm), and this nodular displayed moderate CYP11B1 expression in the "CYP11B2-negative" zone (**Figures 3E,F**). The situation was more interesting in case 18. In addition to the nodule 2 of CYP11B2-positive, CYP11B2 staining was only demonstrated in

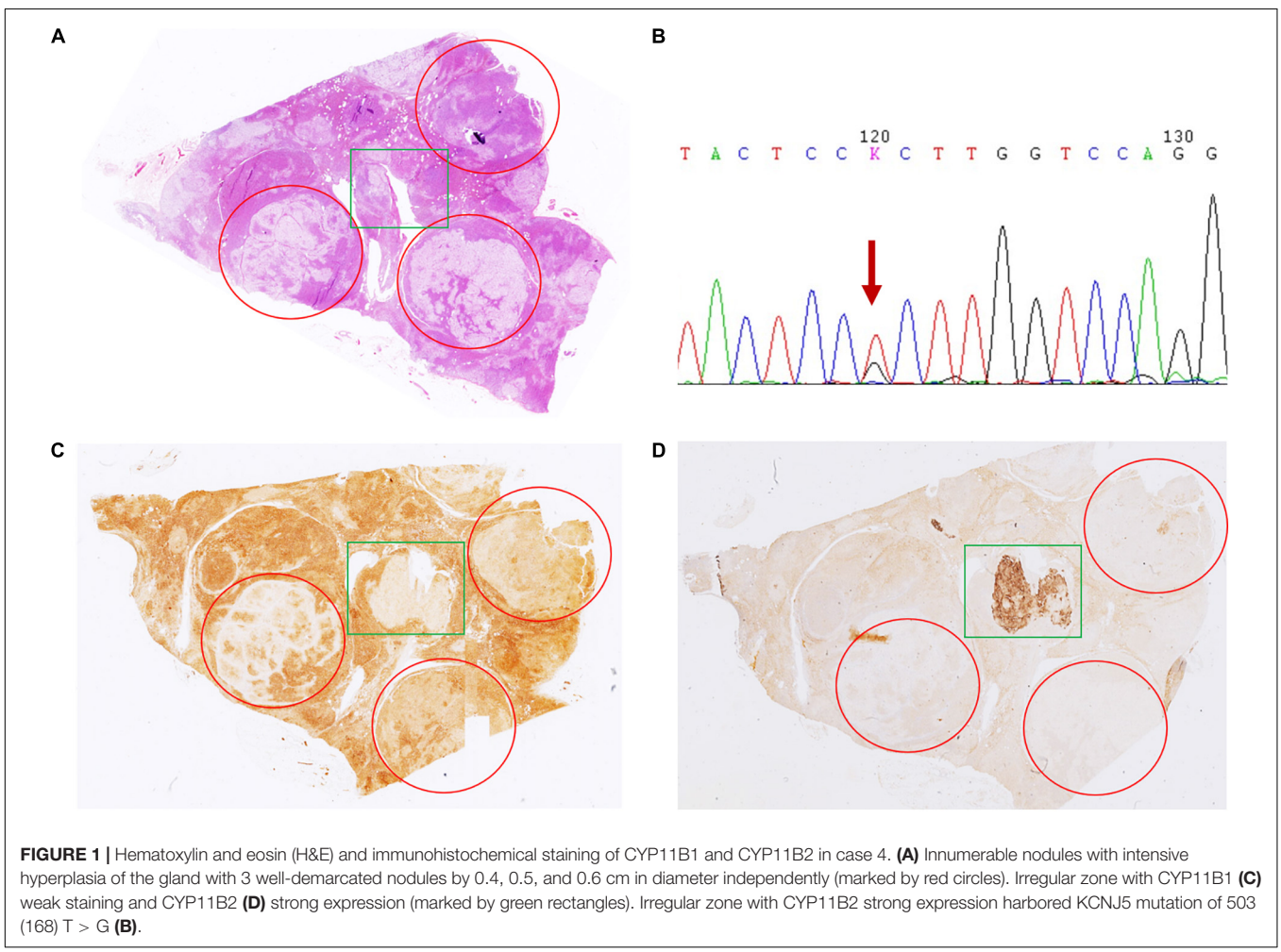

FIGURE 1 | Hematoxylin and eosin (H&E) and immunohistochemical staining of CYP11B1 and CYP11B2 in case 4. **(A)** Innumerable nodules with intensive hyperplasia of the gland with 3 well-demarcated nodules by 0.4, 0.5, and 0.6 cm in diameter independently (marked by red circles). Irregular zone with CYP11B1 **(C)** weak staining and CYP11B2 **(D)** strong expression (marked by green rectangles). Irregular zone with CYP11B2 strong expression harbored KCNJ5 mutation of 503 (168) T > G **(B)**.

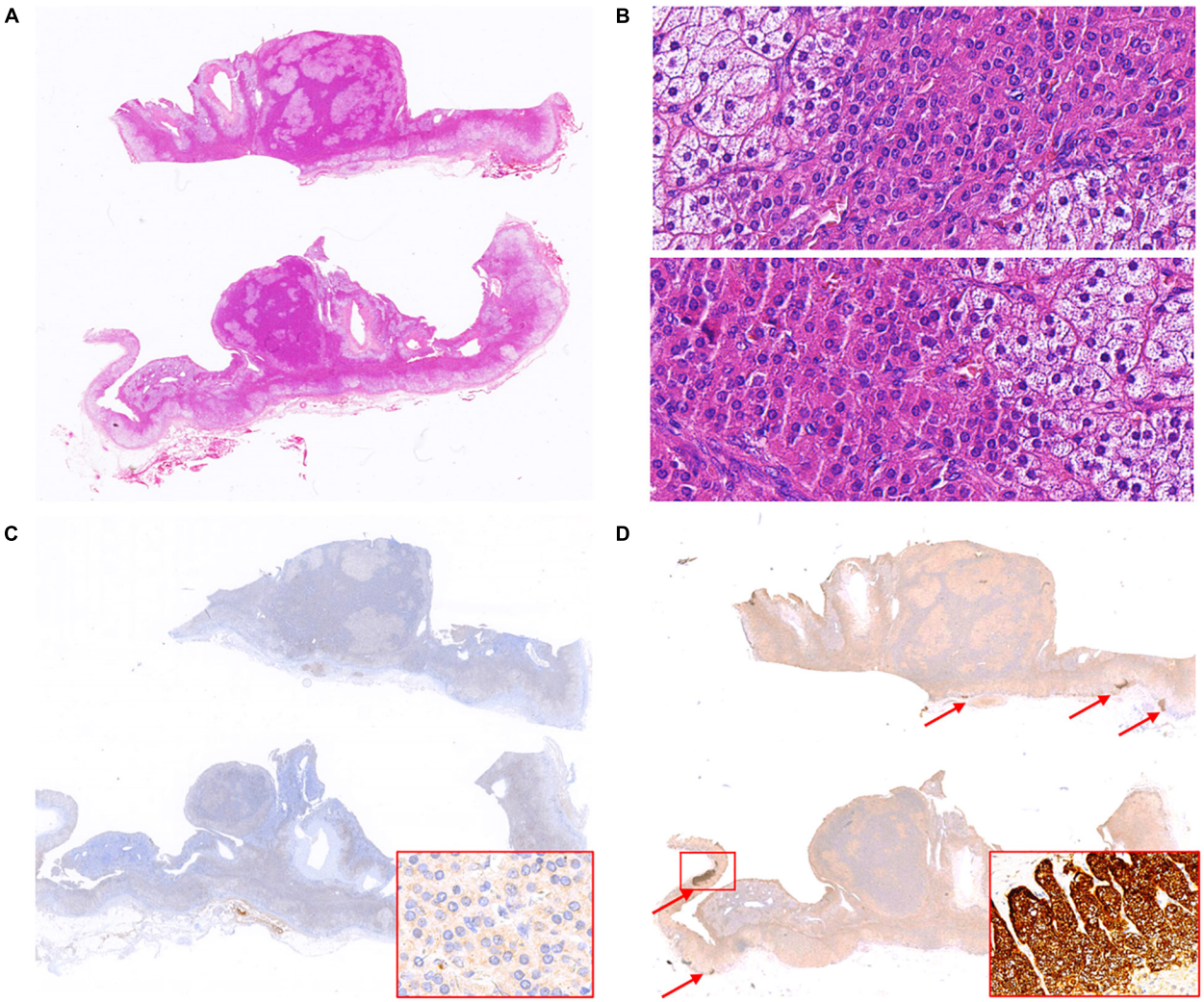

FIGURE 2 | Hematoxylin and eosin (H&E) and immunohistochemical staining of CYP11B1 and CYP11B2 in case 13. Two well-demarcated nodules in adrenal (**A**, up and down); two nodules both composed of acidophilic cells and clear cells (**B**, 400× magnification for nodules respectively, up and down). Weak expression of CYP11B1 (**C**, 400× magnification for insert), completely negative staining of CYP11B2 in both nodules, several APCCs detected in the adrenal cortex (**D**, indicated by red arrows, 200× magnification for insert).

the annular area on the periphery of nodule 1, and the expression of CYP11B1 was moderate (**Figures 3G–I**).

DISCUSSION

Unilateral multiple nodule is considered a rare subtypes of PA that is clinically characterized by unilateral adrenal hypersecretion of aldosterone and morphologically characterized by multiple adrenal nodules (22). The pathogenesis and correlation of different nodules were interesting and meaningful. In this study, we describe additional characteristics of multinodular adrenals that include KCNJ5 mutation and CYP11B1/CYP11B2 expression. Based on the microscopic morphological manifestations, immunohistochemistry, and molecular characteristics, some of the multiple nodules are consistent with a diagnosis of "adenoma." Therefore, we proposed "double adenomas" or "multiadenomas" as follows: multiple well-demarcated nodules; lack of adjacent cortical proliferation; KCNJ5 mutant; positive expression of CYP11B2; and negative/weak expression of CYP11B1. Our research has proved that multiple nodules in one adrenal could harbor different KCNJ5 mutation sites. This finding demonstrated that the nodules were originated from different clones and further suggested the possibility of multiple adenomas. The expressions of CYP11B2 were different among multiple KCNJ5-mutant nodules. This finding indicated that different nodules might contribute jointly to abnormal aldosterone synthesis and secretion. In addition, it has been reported that aldosterone adenoma occurred simultaneously (or successively) in the same or opposite adrenal glands (23, 24). Therefore, such multinodular lesions are obviously different from traditional

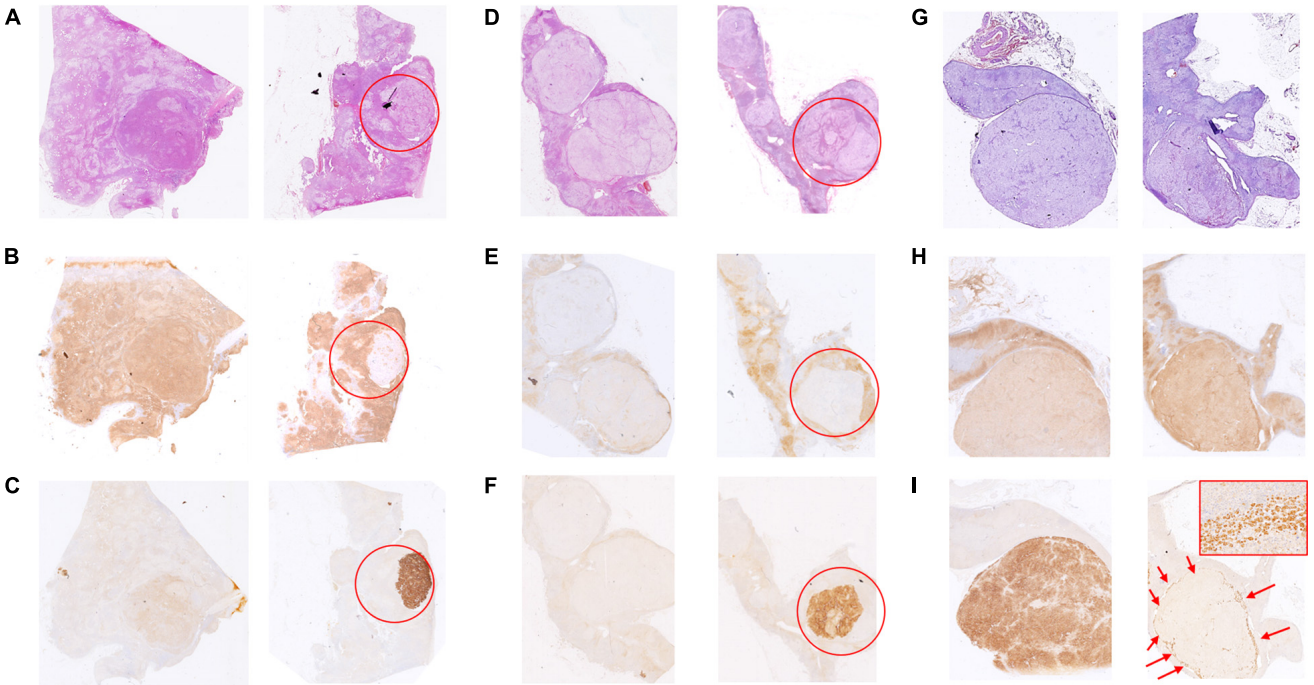

FIGURE 3 | Hematoxylin and eosin (H&E) and immunohistochemical staining of CYP11B1 and CYP11B2 in cases 17, 6, and 18. In case 17, one obscure nodular mainly with acidophilic cells (**A**, left), the other one with a mixture of acidophilic cells and clear cells (**A**, right, marked by the red circle). One-third of the nodules are positive for CYP11B2 (**C**, marked by the red circle) and weak positive for CYP11B1, moderate expression for CYP11B1 in the rest zone of the nodule (**B**, marked by red circle). In case 6, one of 4 clear cell nodules (0.8 cm in diameter) (**D**, marked by the red circle), focal CYP11B2-positive and CYP11B1-negative area by 4 mm × 3 mm **(E,F)**, moderate expression of CYP11B1 in the rest of nodule **(E)**. In case 18, 2 clear cell-dominant nodules (**G**, left and right), the rare annular-pattern of CYP11B2 expression on the periphery of the smaller nodule (**I**, indicated by red arrows, 200 × magnification for insert), moderate expression of CYP11B1 (**H**, right), strong expression of CYP11B2 (**I**, left), and slight expression of CYP11B1 (**H**, left) in the bigger one.

"nodular hyperplasia," and they should be distinguished from the subtype of multiple nodules (formally known as nodular hyperplasia).

KCNJ5 mutations were present in 35–60% of the glands (50% in APAs), and ATP2B3, ATP1A1, and CACNA1D mutations were found in cases of both solitary adenoma and nodular hyperplasia (20, 25–28). In our study, KCNJ5 mutations were found to exist in 45.8% of our 24 unilateral adrenalectomy samples, which is lower than our previous report in unilateral PA (17). All KCNJ5 mutations occurred in CYP11B2-positive nodules mostly composed of ZF-like cells, which was consistent with previous reports (25, 29). The KCNJ5 mutations in our study were found more often in younger patients without sex differences. KCNJ5 mutations were mostly detected in the larger nodular of unilateral multinodular adrenal specimens in five cases. This result is consistent with previous reports (30). In addition, our results showed that nodules without surrounding adrenocortical hyperplasia or with mild hyperplasia were more likely to have KCNJ5 mutations than nodules with obvious hyperplasia, which could be observed by pathological examination or CT scanning. This result suggests that we may need to carefully evaluate the adrenal nodules and the adjacent cortex preoperatively to predict the KCNJ5 mutation status in patients with PA.

Compared to KCNJ5-WT nodules, we found that the expression of CYP11B2 was increased and the expression of CYP11B1 was decreased in KCNJ5-mutant nodules. This indicates that the KCNJ5 mutation increases the expression of CYP11B2, while the expression of CYP11B1 is significantly suppressed. We also found the level of ACTH was lower in KCNJ5-mutant patients, which may need further study on melanocortin 2 receptor (MC2R) in KCNJ5-mutated nodules. Therefore, abnormal aldosterone synthesis and secretion should be caused by not only the expression of CYP11B2 but also the imbalanced expression of CYP11B1 and CYP11B2, the mechanism of which needs to be further clarified.

According to the expression of CYP11B2, it is convenient for pathologists to distinguish the APA/nodule in a resected specimen of PA. However, what about the rest of the nodules with CYP11B2-negative/CYP11B1-positive, even those double negative CYP11B2/CYP11B1. More research studies are needed to determine whether CYP11B2-negative nodules are hyperplastic nodules, non-functional adenomas, or potential/silent aldosteronoma inhibited by other CYP11B2-positive nodules.

The diversity and complexity of CYP11B2 expression attract many researchers. The heterogeneous expression of CYP11B2 has been described in some studies, and some have shown that KCNJ5 mutations are only present in CYP11B2-positive cells, although the nodules consist of CYP11B2-positive cells and CYP11B2-negative cells (6, 20, 25). In our study, in nodular 2 of

case 18, CYP11B2 expression was demonstrated in a rare circular pattern on the periphery of the nodule, in nodule 4 of case 6 and nodule 1 of case 17, CYP11B2 showed a partial positive area. Though these nodules are negative for KCNJ5 mutation, further investigation should be continued.

Aldosterone-producing cell clusters are described as cell nests with defined boundaries isolated from neighboring areas exhibiting remarkable CYP11B2 expression (31). In case 13, two nodules with clear borders that were similar to adenomas neither expressed CYP11B2 nor harbored KCNJ5 mutations. Several APCCs were detected in the neighboring adrenal cortex. The mechanism of this type of PA remains unclear. Some researchers assume that the cause of aldosterone hyperplasia is attributed to the multiple APCCs around CYP11B2-negative nodules. However, multiple APCCs can be found in PA and Cushing syndrome, even in normal adrenals. However, a recent report declared that KCNJ5 mutations could be detected in APCCs (32). Some researchers ascribe the negative findings to the pathologist, who failed to obtain the lesion during the specimen collection process, especially for some micronodules. In our study, all the adrenals were prepared for observation, so overlooking micronodules cannot fully explain this phenomenon. Therefore, there are likely some unknown mechanisms. Interestingly, in case 4, KCNJ5 mutation was detected in the irregular APCC-like zone instead of the 3 well-demarcated nodules. Whether those APCC-like cells are precursors to aldosterone adenoma remains to be further investigated.

There were some limitations in this study. We did not screen other mutations in the KCNJ5-WT nodules, such as ATP2B3, ATP1A1, and CACNA1D. We focus on KCNJ5 mutant and WT nodules because KCNJ5 mutation is the most common one. We can easily conclude the pathogenesis feathers of PA and we propose KCNJ5 is an important factor to make pathological diagnosis in PA. Various levels of CPY11B1 and CPY11B2 expressions illustrate the diversity and complexity in PA, the pathological diagnosis of PA is still full of challenges. In the future, we will study others mutations to improve pathological diagnoses. In conclusion, the term "multiple nodules" in PA should be reconsidered. Some nodules contained KCNJ5 mutations, positive CYP11B2 staining, and lack of adjacent cortical proliferation, which suggested the possibility of "double or multiple aldosteronomas" in PA.

DATA AVAILABILITY STATEMENT

The datasets presented in this study can be found in online repositories. The names of the repository/repositories and accession number(s) can be found in the article/ **Supplementary Material**.

ETHICS STATEMENT

The studies involving human participants were reviewed and approved by the Ruijin Hospital. The patients/participants provided their written informed consent to participate in this study.

AUTHOR CONTRIBUTIONS

JX: full access to all of the data in the study and takes responsibility for the integrity of the data and the accuracy of the data analysis. JX, CZ, and WW: concept and design, drafting of the manuscript, and statistical analysis. JX, CZ, YJ, LW, and LY: data collection. JX, CZ, XFW, XuW, WX, and HX: analysis and interpretation of data. All authors contributed to the article and approved the submitted version.

FUNDING

This study was supported by the National Natural Science Foundation of China (82170797), the Shanghai Hospital Development Center (SHDC2020CR2002A and SHDC2020CR6015), and the National Ministry of Science and Technology Project (2021YFC2501600).

ACKNOWLEDGMENTS

We are grateful to all the staff at the department of Endocrine and Metabolism Disease and the departments of Pathology that contributed to the work-up, the management, the collection of the patients' data, and made this work possible. Especially we thank Prof. Guang Ning, MD, for his critical revision and study design.

SUPPLEMENTARY MATERIAL

The Supplementary Material for this article can be found online at: https://www.frontiersin.org/articles/10.3389/fmed.2022.823065/full#supplementary-material

Supplementary Figure 1 | Microscopical assessment of adjacent cortex. **(A)** Atrophy or normal (0); **(B)** slight or focal hyperplasia (1+); **(C)** medium hyperplasia (2+); and **(D)** remarkable/diffuse hyperplasia (3+).

Supplementary Figure 2 | The assessment of CPY11B1 expression by immunohistochemistry. **(A)** Not present (0); **(B)** weak but detectable above control (1+); **(C)** distinct (2+); and **(D)** very strong (3+).

Supplementary Figure 3 | The assessment of CPY11B2 expression by immunohistochemistry. **(A)** Not present (0); **(B)** weak but detectable above control (1+); **(C)** distinct (2+); and **(D)** very strong (3+).

REFERENCES

1. Rossi GP, Bernini G, Caliumi C, Desideri G, Fabris B, Ferri C, et al. A prospective study of the prevalence of primary aldosteronism in 1,125 hypertensive patients. *J Am Coll Cardiol.* (2006) 48:2293–300. doi: 10.1016/j.jacc.2006.07.059
2. Young WF. Primary aldosteronism: renaissance of a syndrome. *Clin Endocrinol (Oxf).* (2007) 66:607–18. doi: 10.1111/j.1365-2265.2007.02775.x

3. Sang X, Jiang Y, Wang W, Yan L, Zhao J, Peng Y, et al. Prevalence of and risk factors for primary aldosteronism among patients with resistant hypertension in China. *J Hypertens.* (2013) 31:1465–71; discussion 71-2. doi: 10.1097/HJH.0b013e328360ddf6
4. Funder JW, Carey RM, Mantero F, Murad MH, Reincke M, Shibata H, et al. The management of primary aldosteronism: case detection, diagnosis, and treatment: an endocrine society clinical practice guideline. *J Clin Endocrinol Metab.* (2016) 101:1889–916. doi: 10.1210/jc.2015-4061
5. Jiang Y, Zhang C, Wang W, Su T, Zhou W, Jiang L, et al. Diagnostic value of ACTH stimulation test in determining the subtypes of primary aldosteronism. *J Clin Endocrinol Metab.* (2015) 100:1837–44. doi: 10.1210/jc.2014-3551
6. Nanba K, Tsuiki M, Sawai K, Mukai K, Nishimoto K, Usui T, et al. Histopathological diagnosis of primary aldosteronism using CYP11B2 immunohistochemistry. *J Clin Endocrinol Metab.* (2013) 98:1567–74. doi: 10.1210/jc.2012-3726
7. Nishimoto K, Nakagawa K, Li D, Kosaka T, Oya M, Mikami S, et al. Adrenocortical zonation in humans under normal and pathological conditions. *J Clin Endocrinol Metab.* (2010) 95:2296–305. doi: 10.1210/jc.2009-2010
8. Shigematsu K, Yamaguchi N, Nakagaki T, Sakai H. A case of unilateral adrenal hyperplasia being difficult to distinguish from aldosterone-producing adenoma. *Exp Clin Endocrinol Diabetes.* (2009) 117:124–8. doi: 10.1055/s-2008-1078737
9. Fallo F, Pezzi V, Barzon L, Mulatero P, Veglio F, Sonino N, et al. Quantitative assessment of CYP11B1 and CYP11B2 expression in aldosterone-producing adenomas. *Eur J Endocrinol.* (2002) 147:795–802. doi: 10.1530/eje.0.1470795
10. Williams TA, Gomez-Sanchez CE, Rainey WE, Giordano TJ, Lam AK, Marker A, et al. International histopathology consensus for unilateral primary aldosteronism. *J Clin Endocrinol Metab.* (2021) 106:42–54. doi: 10.1210/clinem/dgaa484
11. Yamazaki Y, Nakamura Y, Omata K, Ise K, Tezuka Y, Ono Y, et al. Histopathological classification of cross-sectional image-negative hyperaldosteronism. *J Clin Endocrinol Metab.* (2017) 102:1182–92. doi: 10.1210/jc.2016-2986
12. Enberg U, Volpe C, Hoog A, Wedell A, Farnebo LO, Thoren M, et al. Postoperative differentiation between unilateral adrenal adenoma and bilateral adrenal hyperplasia in primary aldosteronism by mRNA expression of the gene CYP11B2. *Eur J Endocrinol.* (2004) 151:73–85. doi: 10.1530/eje.0.1510073
13. Ganguly A. Cellular origin of aldosteronomas. *Clin Investig.* (1992) 70:392–5. doi: 10.1007/BF00235519
14. Neville AM, O'Hare MJ. Histopathology of the human adrenal cortex. *Clin Endocrinol Metab.* (1985) 14:791–820. doi: 10.1016/s0300-595x(85)80078-5
15. Choi M, Scholl UI, Yue P, Bjorklund P, Zhao B, Nelson-Williams C, et al. K+ channel mutations in adrenal aldosterone-producing adenomas and hereditary hypertension. *Science.* (2011) 331:768–72. doi: 10.1126/science.1198785
16. Beuschlein F, Boulkroun S, Osswald A, Wieland T, Nielsen HN, Lichtenauer UD, et al. Somatic mutations in ATP1A1 and ATP2B3 lead to aldosterone-producing adenomas and secondary hypertension. *Nat Genet.* (2013) 45:440–4; 4e1-2. doi: 10.1038/ng.2550
17. Zhang C, Wu L, Jiang L, Su T, Zhou W, Zhong X, et al. KCNJ5 mutation contributes to complete clinical success in aldosterone-producing adenoma: a study from a single center. *Endocr Pract.* (2021) 27:736–42. doi: 10.1016/j.eprac.2021.01.007
18. Boulkroun S, Beuschlein F, Rossi GP, Golib-Dzib JF, Fischer E, Amar L, et al. Prevalence, clinical, and molecular correlates of KCNJ5 mutations in primary aldosteronism. *Hypertension.* (2012) 59:592–8. doi: 10.1161/HYPERTENSIONAHA.111.186478
19. Boulkroun S, Samson-Couterie B, Dzib JF, Lefebvre H, Louiset E, Amar L, et al. Adrenal cortex remodeling and functional zona glomerulosa hyperplasia in primary aldosteronism. *Hypertension.* (2010) 56:885–92. doi: 10.1161/HYPERTENSIONAHA.110.158543
20. Nanba K, Chen AX, Omata K, Vinco M, Giordano TJ, Else T, et al. Molecular heterogeneity in aldosterone-producing adenomas. *J Clin Endocrinol Metab.* (2016) 101:999–1007. doi: 10.1210/jc.2015-3239
21. Fallo F, Castellano I, Gomez-Sanchez CE, Rhayem Y, Pilon C, Vicennati V, et al. Histopathological and genetic characterization of aldosterone-producing adenomas with concurrent subclinical cortisol hypersecretion: a case series. *Endocrine.* (2017) 58:503–12. doi: 10.1007/s12020-017-1295-4
22. Omura M, Sasano H, Fujiwara T, Yamaguchi K, Nishikawa T. Unique cases of unilateral hyperaldosteronemia due to multiple adrenocortical micronodules, which can only be detected by selective adrenal venous sampling. *Metabolism.* (2002) 51:350–5. doi: 10.1053/meta.2002.30498
23. Rizek P, Gorecki P, Lindenmayer A, Moktan S. Laparoscopic adrenalectomy for bilateral metachronous aldosteronomas. *JSLS.* (2011) 15:100–4. doi: 10.4293/108680811X13071180407230
24. Calvo-Romero JM, Ramos-Salado JL. Recurrence of adrenal aldosterone-producing adenoma. *Postgrad Med J.* (2000) 76:160–1. doi: 10.1136/pmj.76.893.160
25. Dekkers T, ter Meer M, Lenders JW, Hermus AR, Schultze Kool L, Langenhuijsen JF, et al. Adrenal nodularity and somatic mutations in primary aldosteronism: one node is the culprit? *J Clin Endocrinol Metab.* (2014) 99:E1341–51. doi: 10.1210/jc.2013-4255
26. Scholl UI, Nelson-Williams C, Yue P, Grekin R, Wyatt RJ, Dillon MJ, et al. Hypertension with or without adrenal hyperplasia due to different inherited mutations in the potassium channel KCNJ5. *Proc Natl Acad Sci U S A.* (2012) 109:2533–8. doi: 10.1073/pnas.1121407109
27. Azizan EA, Murthy M, Stowasser M, Gordon R, Kowalski B, Xu S, et al. Somatic mutations affecting the selectivity filter of KCNJ5 are frequent in 2 large unselected collections of adrenal aldosteronomas. *Hypertension.* (2012) 59:587–91. doi: 10.1161/HYPERTENSIONAHA.111.186239
28. Taguchi R, Yamada M, Nakajima Y, Satoh T, Hashimoto K, Shibusawa N, et al. Expression and mutations of KCNJ5 mRNA in Japanese patients with aldosterone-producing adenomas. *J Clin Endocrinol Metab.* (2012) 97:1311–9. doi: 10.1210/jc.2011-2885
29. Monticone S, Castellano I, Versace K, Lucatello B, Veglio F, Gomez-Sanchez CE, et al. Immunohistochemical, genetic and clinical characterization of sporadic aldosterone-producing adenomas. *Mol Cell Endocrinol.* (2015) 411:146–54. doi: 10.1016/j.mce.2015.04.022
30. Mulatero P, Stowasser M, Loh KC, Fardella CE, Gordon RD, Mosso L, et al. Increased diagnosis of primary aldosteronism, including surgically correctable forms, in centers from five continents. *J Clin Endocrinol Metab.* (2004) 89:1045–50. doi: 10.1210/jc.2003-031337
31. Weisbrod AB, Webb RC, Mathur A, Barak S, Abraham SB, Nilubol N, et al. Adrenal histologic findings show no difference in clinical presentation and outcome in primary hyperaldosteronism. *Ann Surg Oncol.* (2013) 20:753–8. doi: 10.1245/s10434-012-2670-2
32. De Sousa K, Boulkroun S, Baron S, Nanba K, Wack M, Rainey WE, et al. Genetic, cellular, and molecular heterogeneity in adrenals with aldosterone-producing adenoma. *Hypertension.* (2020) 75:1034–44. doi: 10.1161/HYPERTENSIONAHA.119.14177

Conflict of Interest: The authors declare that the research was conducted in the absence of any commercial or financial relationships that could be construed as a potential conflict of interest.

frontiers | Frontiers in Medicine

CASE REPORT
published: 18 April 2022
doi: 10.3389/fmed.2022.836012

Case Report: Hemangioblastoma-Like Clear Cell Stromal Tumor of the Left Lower Lung

Xiaowei Zhang[1], Bifei Huang[1], Hongquan Jiang[2] and Hangping Wei[3]**

[1] Department of Pathology, Affiliated Dongyang Hospital of Wenzhou Medical University, Dongyang, China, [2] Department of Thoracic Surgery, Affiliated Dongyang Hospital of Wenzhou Medical University, Dongyang, China, [3] Department of Medical Oncology, Affiliated Dongyang Hospital of Wenzhou Medical University, Dongyang, China

Background: Hemangioblastoma-like clear cell stromal tumor (HLCCST) is a recently reported neoplasm of the lung. Only 13 cases have been reported in four recent studies. Because HLCCST is very rare, it has not been included in the 2021 WHO classification of lung tumors.

Case Presentation: We report a case of HLCCST of the left lower lung in a 40-year-old female who was admitted to our hospital after pulmonary nodules were discovered. A plain chest CT scan showed a nodular high-density shadow measuring approximately 8 mm in diameter in the left lower lung. The lesion had clear borders, uneven internal density, and a low-density central vacuolar area. The left lower lung was partially resected by video-assisted thoracic surgery. Post-operative histopathologic diagnosis "hemangioblastoma-like clear cell stromal tumor" of the left lower lung.

Conclusion: The HLCCST is an extremely rare tumor and needs long-term follow-up after operation. Clinically, it may be easily confused with other benign and malignant tumors of the lung, and diagnosis is solely determined by histopathologic examination. This case suggests that immunohistochemical CD34 can be a strong positive marker.

Keywords: *Yap1*, TFE3, haemangioblastoma-like clear cell stromal tumour, pulmonary, pathology

OPEN ACCESS

Edited by:
Renato Franco, University of Campania Luigi Vanvitelli, Italy

Reviewed by:
Andrea Ronchi, University of Campania Luigi Vanvitelli, Italy
Zhiyan Liu, Shanghai Jiao Tong University, China

***Correspondence:**
Bifei Huang
hbfx711023@163.com
Hangping Wei
applewhp@163.com

Specialty section:
This article was submitted to Pathology, a section of the journal Frontiers in Medicine

Received: *15 December 2021*
Accepted: *03 March 2022*
Published: *18 April 2022*

Citation:
Zhang X, Huang B, Jiang H and Wei H (2022) Case Report: Hemangioblastoma- Like Clear Cell Stromal Tumor of the Left Lower Lung. Front. Med. 9:836012. doi: 10.3389/fmed.2022.836012

INTRODUCTION

Hemangioblastoma is a tumor that typically occurs in the central nervous system, particularly in the cerebellum, and is largely related to Von Hippel-Lindau (VHL) syndrome (1). Previously, it was uncommon to find Hemangioblastoma outside the central nervous system, although it has been reported in the liver, kidney, pancreas, and other parenchymal organs (2). Primary pulmonary neoplasms are mostly epithelial in origin, with adenocarcinoma being the most common; primary

Abbreviations: *YAP1*, Yes-associated protein 1; TFE3, Transcription factor E3; CT, Computed tomography; VATS, Video-assisted thoracic surgery; HLCCST, Hemangioblastoma-like clear cell stromal tumor; VHL, Von Hippel-Lindau; FISH, fluorescence *in situ* hybridization; IHC, Immunohistochemistry; WWTR1, WW domain containing transcription regulator 1; CAMTA1, Calmodulin binding transcription activator 1; PEComa, Perivascular epithelioid cell tumor.

mesenchymal tumors of the lung are considered unusual (3). Therefore, it is extremely rare to find a hemangioblastoma-like clear cell stromal tumor in the lung. To date, there are only 13 known cases reported in the literature. Herein, we report a case confirmed by post-operative histopathology and review the relevant literature to improve the understanding of surgeons and pathologists, to reduce misdiagnosis and incorrect treatment.

CASE DESCRIPTION

Case Presentation

The patient was a 40-year-old female who was admitted to our hospital after pulmonary nodules were detected incidentally, a year before presentation, in a chest CT. No cough, expectoration, chest tightness, shortness of breath, nausea, vomiting, low-grade fever, or night sweats were reported. On physical examination, her trachea was midline, and no deformities were noted in the thorax. Her breathing was stable and breath sounds were clear with no dry or wet rales; the activity of both the lungs was normal, and there was no obvious pleural friction. A plain chest CT scan showed a nodular high-density shadow, measuring approximately 8 mm in diameter, in the left lower lung. The lesion had clear borders, uneven internal density, and a low-density central vacuolar area (**Figure 1**). The left lower lung was partially resected by video-assisted thoracic surgery (VATS) was performed, and intra-operative frozen section pathological examination reported: "mesenchymal tumor of the left lower lung, the final result needs immunohistochemistry." Post-operative histopathological diagnosis was a hemangioblastoma-like clear cell stromal tumor of the left lower lung. The patient was followed up regularly for 3 months after the surgery, with no recurrence or development of distant metastasis.

Histopathology

The specimen submitted was from a wedge resection of the left lower lung lobe. The report of the gross specimen examination described the tumor as follows: postoperative gross specimen, left lower lung; wedge resection specimen: 7.9 × 6.3 × 4.1 cm, located 3.8 cm from the fault edge, with a peripheral gray-brown area of 0.9 × 0.8 cm seen in the lung tissue. The section was described as gray-white to gray-brown, with holes and unclear borders.

Microscopic analysis showed that the tumor was composed of solid, slightly lobulated flake cells with consistent morphology, and scattered dilated vacuolar components within the cells. Tumor cells were noted to be of medium size, with unclear borders, and a bright cytoplasm. The nucleus was deeply stained, oval to spindle-shaped. The nucleolus was not visible, and no necrosis or mitosis was noted (**Figure 2**). Immunohistochemistry (IHC) staining results revealed the expression of vimentin, Transcription factor E3 (TFE3) (weak), CD34 (strong), and Ki-67 (only 2% expression). The specimen was negative for HMB45, melan-A, S-100, Syn, CgA, CD56, napsin A, TTF-1, CK (AE1/AE3), PAX8, GFAP, desmin, MSA, inhibin-α, CD31, F8, DOG1, STAT6, ERG, ER, CAIX, and CD10 (**Figure 2**). Periodic acid-Schiff (PAS) staining was also negative. Fluorescent *in situ* hybridization (FISH) showed none Yes-associated protein 1 (*YAP1*)-*TFE3* gene fusions.

DISCUSSION

Hemangioblastoma are vascular neoplasms that typically occur in the central nervous system. However, they may be rarely found in the retroperitoneum, pelvic cavity, presacral region, kidney, maxillary sinus, and adrenal gland (4). In 2013, Falconieri et al. (5) reported the first two cases of pulmonary clear cell stromal tumors with previously unreported histological features similar to hemangioblastoma, which they named "hemangioblastoma-like clear cell stromal tumor of the lung". The HLCCST is very uncommon, to the best of the authors' knowledge, only 13 cases have been reported in four articles. Due to its rarity, it has not been included in the 2021 WHO classification of pulmonary mediastinal tumors. We reported a case of histopathologically confirmed HLCCST; compared to the previous literature, our case had distinctive IHC expression.

In the 13 cases discussed, the age range of patients was 29–77 years old. Among these, nine were women and four were men. The VHL syndrome, which is characterized by the presence of neoplasms affecting the central nervous system, kidneys, adrenal glands, pancreas, and reproductive organs (6), was not reported in any of the 13 patients. The clinical manifestations were non-specific: cough, dyspnea, fever, and hemoptysis with or without chest pain. Similarly, we report a 40-year-old female patient who was asymptomatic.

The gross examination of the specimen reported in the 13 cases revealed that the tumors were all non-encapsulated, but were clearly defined masses, with gray-yellow sections, focal bleeding, and with a maximum diameter of approximately 2–9.5 cm. Most tumors were found in the lung parenchyma, with a single case occurring in the bronchial lumen of the patient. Microscopically, the tumor was composed of solid flake cells with consistent morphology, slightly lobulated, with scattered dilated vacuolar components observed in the tumor cells. Tumor cells are of medium size, with unclear boundaries, and bright cytoplasm. The nucleus was deeply stained, oval to spindle-shaped, and the nucleolus was not visible. Vitreous degeneration was seen in the focal area, without necrosis and mitosis. Adipocytes could be seen in some cases.

The IHC staining in the previous reports showed that tumor cells expressed vimentin, and were positive for TFE3, but were negative for CK, EMA, TTF-1, P40, CGA, SYN, CD56, CD34, CD31, STAT6, desmin, calponin, SMA, GATA3, SOX-10, Bcl-2, S-100, HMB-45, etc. (7). The PAS staining was also negative. *YAP1-TFE3* gene fusions have recently been reported in 5 cases (8). The *YAP1-TFE3* fusion has only been described in a rare subset of epithelioid hemangioendothelioma (EHE), which was lacked the classic WW domain containing transcription regulator 1-Calmodulin binding transcription activator 1 (*WWTR1-CAMTA1*) fusion (9). In our case, IHC staining showed that tumor cells were positive for vimentin, strong expression of CD34, and weakly positive for TFE3; and FISH showed none

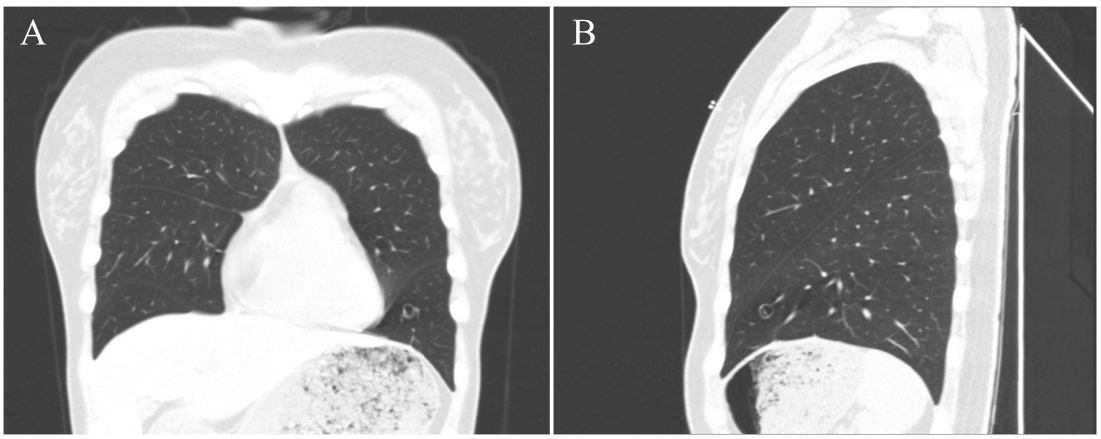

FIGURE 1 | CT images of this case. CT images [**(A)**, coronal position] [**(B)**, sagittal position] show the tumor nodular high-density shadow in the lower lobe of the left lung, with a clear boundary, uneven internal density, and low-density vacuolar area in the center of the lesion.

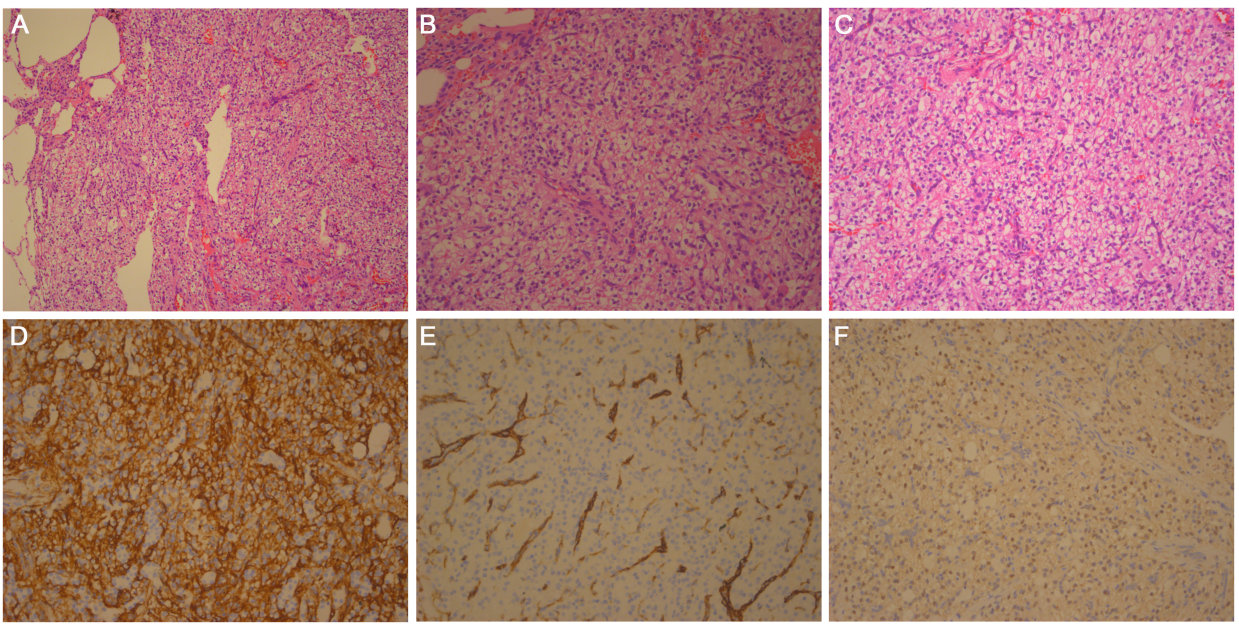

FIGURE 2 | Histologic findings: hematoxylin and eosin-stained section of **(A)** × 100, **(B)** × 200, and **(C)** × 400 magnifications show that the tumor boundary is clear, composed of solid, slightly lobulated flake cells with consistent morphology. Scattered dilated vacuolar components can be seen in the tumor cells. **(D)** Tumor cells are positive for CD34. IHC × 200. **(E)** Tumor cells are negative for F8, and vessel positive. IHC × 200. **(F)** Tumor cells are weakly positive for TFE3. IHC × 200.

YAP1-TFE3 gene fusions. Expression of *TFE3* was not consistent with *YAP1-TFE3* gene fusions in HLCCST. Similar to most of the previously reported cases, in this case, the tumor expressed vimentin and TFE3. However, it also strongly expressed CD34, which only 1 of the 13 cases previously reported focally expressed CD34. The FISH results were also different compared to the previous reports.

Differential diagnosis based on histopathology includes carcinoid tumor, paraganglioma, perivascular epithelioid cell tumor (PEComa) (clear cell "sugar" tumor), and intrapulmonary solitary fibrous tumor. Because HLCCST is a diagnosis of exclusion, a wide panel of IHC stains is particularly important. Carcinoid tumors may express neuroendocrine markers (i.e., SYN, CGA, and CD56) and epithelial markers (i.e., CK). Paraganglioma can also express neuroendocrine markers (i.e., SYN, CGA, and CD56), and S-100 is expressed in the sustentacular cells. The PEComa may express myocyte-derived and melanocyte-derived markers, such as actin, desmin, HMB45, and melan-A. Intrapulmonary solitary fibrous tumors can express CD34 and STAT6. This case was positive for CD34, but negative for STAT6, therefore, a solitary fibrous tumor was excluded.

Finally, it is also important to distinguish the tumor from hemangioblastoma, which can specifically express S-100 and inhibin-α. In FISH analysis, *YAP1-TFE3* gene fusion can increase confidence in the diagnosis, but it is not a prerequisite (10).

At present, the HLCCST is considered to have a benign biological behavior. To our knowledge, none of the patients had recurrence or distant metastasis after complete resection. We believe that the first choice of treatment for HLCCST should be partial pneumonectomy *via* VATS and that regular postoperative follow-up is crucial.

CONCLUSION

In summary, the HLCCST is an extremely rare tumor and needs long-term follow-up after operation. Clinically, it may be easily confused with other benign and malignant tumors of the lung, and diagnosis depends on histopathologic examination.

DATA AVAILABILITY STATEMENT

The original contributions presented in the study are included in the article/supplementary material, further inquiries can be directed to the corresponding author.

AUTHOR CONTRIBUTIONS

XZ and HW acquired the data. BH analyzed the histological images. XZ, HW, BH, and HJ prepared the manuscript. All authors contributed to the article and approved the submitted version.

ACKNOWLEDGMENTS

We thank the patient who kindly agreed to provide the data used in this case.

REFERENCES

1. Klingler JH, Gläsker S, Bausch B, Urbach H, Krauss T, Jilg CA, et al. Hemangioblastoma and von Hippel-Lindau disease: genetic background, spectrum of disease, and neurosurgical treatment. *Childs Nerv Syst.* (2020) 36:2537–52. doi: 10.1007/s00381-020-04712-5
2. Muscarella LA, Bisceglia M, Galliani CA, Zidar N, Ben-Dor DJ, Pasquinelli G, et al. Extraneuraxial hemangioblastoma: a clinicopathologic study of 10 cases with molecular analysis of the VHL gene. *Pathol Res Pract.* (2018) 214:1156–65. doi: 10.1016/j.prp.2018.05.007
3. Hashimoto H, Tsugeno Y, Sugita K, Inamura K. Mesenchymal tumors of the lung: diagnostic pathology, molecular pathogenesis, and identified biomarkers. *J Thorac Dis.* (2019) 11:S9–24. doi: 10.21037/jtd.2018.12.04
4. Bisceglia M, Muscarella LA, Galliani CA, Zidar N, Ben-Dor D, Pasquinelli G, et al. Extraneuraxial hemangioblastoma: clinicopathologic features and review of the literature. *Adv Anat Pathol.* (2018) 25:197–215. doi: 10.1097/PAP.0000000000000176
5. Falconieri G, Mirra M, Michal M, Suster S. Hemangioblastoma-like clear cell stromal tumor of the lung. *Adv Anat Pathol.* (2013) 20:130–5. doi: 10.1097/PAP.0b013e318286245d
6. Varshney N, Kebede AA, Owusu-Dapaah H, Lather J, Kaushik M, Bhullar JS. A review of Von Hippel-Lindau syndrome. *J Kidney Cancer VHL.* (2017) 4:20–9. doi: 10.15586/jkcvhl.2017.88
7. Lindholm KE, Moran CA. Hemangioblastoma-like clear cell stromal tumor of the lung: a clinicopathologic and immunohistochemical study of 5 cases. *Am J Surg Pathol.* (2020) 44:771–5. doi: 10.1097/PAS.0000000000001429
8. Dermawan JK, Azzato EM, McKenney JK, Liegl-Atzwanger B, Rubin BP. YAP1-TFE3 gene fusion variant in clear cell stromal tumour of lung:report of two cases in support of a distinct entity. *Histopathology.* (2021) 79:940–6. doi: 10.1111/his.14437
9. Antonescu CR, Le Loarer F, Mosquera JM, Sboner A, Zhang L, Chen CL, et al. Novel YAP1-TFE3 fusion defines a distinct subset of epithelioid hemangioendothelioma. *Genes Chromosomes Cancer.* (2013) 52:775–84. doi: 10.1002/gcc.22073
10. Agaimy A, Stoehr R, Michal M, Christopoulos P, Winter H, Zhang L, et al. Recurrent YAP1-TFE3 gene fusions in clear cell stromal tumor of the lung. *Am J Surg Pathol.* (2021) 45:1541–9. doi: 10.1097/PAS.0000000000001719

Conflict of Interest: The authors declare that the research was conducted in the absence of any commercial or financial relationships that could be construed as a potential conflict of interest.

frontiers | Frontiers in Medicine

ORIGINAL RESEARCH
published: 03 May 2022
doi: 10.3389/fmed.2022.874213

Immunotherapy in Penile Squamous Cell Carcinoma: Present or Future? Multi-Target Analysis of Programmed Cell Death Ligand 1 Expression and Microsatellite Instability

Marco Montella[1], Rosalaura Sabetta[1], Andrea Ronchi[1], Marco De Sio[2], Davide Arcaniolo[2], Ferdinando De Vita[3], Giuseppe Tirino[3], Alessandro Caputo[4], Antonio D'Antonio[5], Francesco Fiorentino[6], Gaetano Facchini[7], Giovanni Di Lauro[8], Sisto Perdonà[9], Jole Ventriglia[9], Gabriella Aquino[10], Florinda Feroce[10], Rodolfo Borges Dos Reis[11], Luciano Neder[12], Matteo Brunelli[13], Renato Franco[1] and Federica Zito Marino[1]*

[1] Pathology Unit, Department of Mental Health, Physic and Preventive Medicine University of Campania "Luigi Vanvitelli", Naples, Italy, [2] Urology Unit, Department of Woman Child and of General and Specialist Surgery, University of Campania "Luigi Vanvitelli", Naples, Italy, [3] Oncology Unit, Department of Precision Medicine, University of Campania "Luigi Vanvitelli", Naples, Italy, [4] Department of Medicine and Surgery, University Hospital "San Giovanni di Dio e Ruggi D'Aragona", University of Salerno, Salerno, Italy, [5] Department of Pathology, University Hospital "San Giovanni di Dio e Ruggi D'Aragona", Salerno, Italy, [6] Pathology Unit, S.M. delle Grazie Hospital, Pozzuoli, Italy, [7] Medical Oncology Unit, S.M. delle Grazie Hospital, Pozzuoli, Italy, [8] Urology Unit, S.M. delle Grazie Hospital, Pozzuoli, Italy, [9] Department of Urogynecology, National Cancer Institute, Pascale Foundation (Scientific Institute for Research and Healthcare), Naples, Italy, [10] Pathology Unit, Istituto Nazionale Tumori Fondazione G. Pascale IRCCS, Naples, Italy, [11] Urology Division, Department of Surgery and Anatomy, Ribeirão Preto School Medicine, University of São Paulo, Ribeirão Preto, Brazil, [12] Department of Pathology and Forensic Medicine, Ribeirão Preto Medical School, University of São Paulo, Ribeirão Preto, Brazil, [13] Department of Pathology, University of Verona, Verona, Italy*

OPEN ACCESS

Edited by:
Alessandro Morabito, G. Pascale National Cancer Institute Foundation (IRCCS), Italy

Reviewed by:
Luigi M. Terracciano, University of Basel, Switzerland
Francesco Merolla, University of Molise, Italy
Antonio Giordano, Temple University, United States

***Correspondence:**
Renato Franco
renato.franco@unicampania.it

Specialty section:
This article was submitted to Pathology, a section of the journal Frontiers in Medicine

Received: *11 February 2022*
Accepted: *04 March 2022*
Published: *03 May 2022*

Citation:
Montella M, Sabetta R, Ronchi A, De Sio M, Arcaniolo D, De Vita F, Tirino G, Caputo A, D'Antonio A, Fiorentino F, Facchini G, Lauro GD, Perdonà S, Ventriglia J, Aquino G, Feroce F, Borges Dos Reis R, Neder L, Brunelli M, Franco R and Zito Marino F (2022) Immunotherapy in Penile Squamous Cell Carcinoma: Present or Future? Multi-Target Analysis of Programmed Cell Death Ligand 1 Expression and Microsatellite Instability. Front. Med. 9:874213. doi: 10.3389/fmed.2022.874213

Background: Penile cancer (PC) is an extremely rare malignancy, and the patients at advanced stages have currently limited treatment options with disappointing results. Immune checkpoint inhibitors anti-programmed cell death 1 (PD-1)/programmed cell death ligand 1 (PD-L1) are currently changing the treatment of several tumors. Furthermore, the microsatellite instability (MSI) and the deficient mismatch repair system (dMMR) proteins represent predictive biomarkers for response to immune checkpoint therapy. Until present, few data have been reported related to PD-L1 expression and MSI in PC. The main aim of our study was the evaluation of PD-L1 expression in tumor cells (TCs) and tumor-infiltrating lymphocytes (TILs) in immune cells and the analysis of dMMR/MSI status in a large series of PCs.

Methods: A series of 72 PC, including 65 usual squamous cell carcinoma (USCC), 1 verrucous, 4 basaloid, 1 warty, and 1 mixed (warty-basaloid), was collected. Immunohistochemistry (IHC) was performed to assess PD-L1 expression using two different anti-PD-L1 antibodies (clone SP263 and SP142 Ventana) and MMR proteins expression using anti-MLH1, anti-PMS2, anti-MSH2, and anti-MSH6 antibodies. PCR analysis was performed for the detection of MSI status.

Results: Of the 72 PC cases analyzed by IHC, 45 (62.5%) cases were TC positive and 57 (79%) cases were combined positive score (CPS) using PDL1 SP263. In our cohort,

TILs were present in 62 out of 72 cases (86.1%), 47 (75.8%) out of 62 cases showed positivity to PDL1 clone SP142. In our series, 59 cases (82%) had pMMR, 12 cases (16.7%) had lo-paMMR, and only 1 case (1.3%) had MMR. PCR results showed that only one case lo-paMMR was MSI-H, and the case dMMR by IHC not confirmed MSI status.

Conclusion: Our findings showed that PD-L1 expression and MSI status represent frequent biological events in this tumor suggesting a rationale for a new frontier in the treatment of patients with PC based on the immune checkpoint inhibitors.

Keywords: penile cancer, penile SCC, PD-L1, MSI, HPV, immunotherapy, squamous cell carcinoma

INTRODUCTION

Penile cancer (PC) is a disease with high morbidity and mortality. Its prevalence is relatively rare, occurring predominantly in elderly men; specifically, the mean age at diagnosis is 60 years with an age-related incidence rising constantly and reaching its highest level at 70 years. The worldwide variation of PC incidence is related to differences in socioeconomic and religious conditions: it constitutes up to 10% of malignant disease in men in some African, Asian, and South American countries, while in Western Europe and the United States, it represents about 0.6% of all malignancies. Poor penile hygiene, smegma retention, phimosis, and infection with human papillomavirus (HPV), mainly type 16, represent the major risk factors involved in PC pathogenesis (1).

The vast majority (almost 95%) of PCs include squamous cell carcinoma (SCC), being the usual keratinizing type the most common histotype. Other rare subtypes of SCC are basaloid (4%), warty (6%), mixed warty-basaloid (17%), verrucous (8%), papillary (7%), other SCC mixed (7%), and sarcomatoid carcinomas (1%) (2). Organ-preserving surgery with safety margins of not more than a few millimeters plus local radiotherapy is the current therapeutic standard for the early stages of the disease. Lymphogenic metastasis must be treated with radical lymphadenectomy and adjuvant chemotherapy, but, nevertheless, patients at advanced stages have currently limited treatment options with disappointing results (3).

Immunotherapy is gaining renewed interest as a treatment for cancer due to the promising clinical results observed with immune checkpoint inhibitors in several cancer types, such as non-small cell lung carcinoma (NSCLC) (4), melanoma (5), renal cell carcinoma, urothelial bladder cancer (6), head and neck SCC (7), and Hodgkin's disease (8).

Programmed cell death 1 and ligand (PD-1/PD-L1) pathway represents one of the major immune checkpoint targets clinically investigated over the past few years. Currently, several clinical studies evaluating PD-1/PD-L1 inhibitors have been conducted in several different tumor types including breast, colorectal, anal, gastric, renal cell carcinoma, head, and neck, pancreatic, and hepatocellular cancer. The employment of immune checkpoint inhibitors has reported promising results consisting of increased survival and delayed tumor growth. Furthermore, to rationally design an ideal combination of cancer therapies based on tumor immunology, PD-L1 expression in TILs must also be evaluated (9).

Until present, few data have been reported related to PD-L1 expression in PC. The first report in 2016 revealed frequent PD-L1 expression in primary penile SCC unrelated to HPV status but associated with lymph node metastasis and shorter cancer-specific survival (10). More recently, some studies have found conflicting results about the prognostic value of PD-L1 expression in tumor cells (TCs) and/or TILs (11).

Another predictive biomarker for response to immune checkpoint therapy is MSI. The DNA mismatch repair (MMR) complex is a prominent cellular mechanism that protects cells from the accumulation of mutations occurring during DNA replication. The MMR system includes mainly four proteins (MLH1, PMS2, MSH2, and MSH6) that cooperatively detect and cut base-pair mismatches, leading to the consequent synthesis of the correct DNA strand.

Microsatellites are DNA sequences consisting of 1–6 repeated base pairs; their repetitive nature makes them prone to replication errors that are generally corrected by the MMR system (12). A deficient MMR system (dMMR) leads to MSI, a well-known sporadic event in tumors (10–15% of colorectal, gastric, and endometrial carcinomas), and the major background of hereditary non-polyposis colorectal cancer (HNPCC) syndrome. Recently, it has been shown that a dMMR system predicts a clinical benefit in response to immune checkpoint blockade therapy. The food and drug administration (FDA) approved the immune checkpoint inhibitors for the treatment of any solid cancer with a dMMR system and/or an MSI-high (MSI-H) genotype.

Until present, few data on the frequency of MSI and altered MMR protein expression are available for PC (13). In this context, we investigated the PD-L1 expression and the dMMR/MSI-H status in a large cohort of PCs could provide a rationale for a new frontier in the treatment of PC patients based on the immune checkpoint inhibitors.

MATERIALS AND METHODS

Specimen

A series of 72 PC were included in our study. All cases were collected in our records at the University of Campania "L. Vanvitelli" Hospital, Fondazione G. Pascale, the University Ribeirão Preto Hospital of São Paulo, the Istituto Nazionale Tumori, the "Azienda Ospedaliera Universitaria Integrata

Verona," Verona (Italy), the S.M. delle Grazie Hospital, and the "AOU San Giovanni di Dio e Ruggi d'Aragona," Salerno (Italy). The series included surgical samples and wide biopsies, as well as formalin-fixed paraffin-embedded (FFPE) samples. Sections of 4-μm thickness from each block (with a mean of 3 blocks per tumor) were stained with hematoxylin-eosin. All cases were reviewed according to the WHO histopathological classification (14).

Immunohistochemistry Analysis of Programmed Cell Death Ligand 1 Expression

Immunohistochemistry (IHC) for PD-L1 was performed on 4-μm thick whole sections for each case on an automated Benchmark ULTRA staining platform (Ventana Medical Systems, Tucson, AZ, United States). The antibody clones used were SP263 and SP142 (Spring Biosciences, Pleasanton, CA, United States). Two independent observers (M.M. and R.F.) carried out IHC analysis; both observers were blinded.

Tumor cells or TILs with specific membranous and cytoplasmic staining were considered positive. Positive TCs and positive TILs were scored as the percentage of viable TCs (tumor proportion score) and the percentage of available TILs (TILs score).

To compare the clinical diagnostic performance of the assays, scores were dichotomized into positive or negative according to the clinically relevant cut-off values defined for the corresponding assay by the package inserts, FDA safety and effectiveness of datasheets, and the associated clinical trials of lung cancers for SP263 and breast cancers for SP142:

- SP263: $< 1\%$ of TCs positivity, between 1 and 50% of TCs positivity and $> 50\%$ of TCs positivity (15).
- SP142: $> 1\%$ of the tumor area occupied by PD-L1 positive lymphocytes and/or $> 1\%$ of TCs (16).

Moreover, SP263 PD-L1 expression in the tumor-associated mononuclear lymphocytes was scored using a combined positive score (CPS). The CPS was defined as the total number of TCs and TILs stained with PD-L1 divided by the number of all viable TCs, then multiplied by 100 (17), as applied for oral SCC. Each core contained at least 100 viable TCs.

Immunohistochemistry Analysis of Mismatch Repair Protein Expression

Immunohistochemistry for four MMR proteins (MLH1, PMS2, MSH2, and MSH6) were performed on 4-μm thick whole sections for each case on an automated Benchmark ULTRA staining platform (Ventana Medical Systems, Tucson, AZ, United States). The antibody clones used were MLH1 (clone ES05, Agilent Technologies Canada Inc.), MSH2 (clone G219-1129, Becton Dickinson Biosciences, Canada), MSH6 (clone EPR3945, Abcam, Canada), and PMS2 (clone A16-4, BD Biosciences).

Adjacent normal tissue from each sample served as positive controls. MMR protein loss was defined by the absence of IHC staining in the nucleus of TCs while normal cells remained stained, ensuring the technical validity of the experiment. Immunohistochemical staining results were evaluated according to the scoring system reported in the literature: (i) proficient MMR (pMMR): cases with all four MMR staining positive; (ii) dMMR: cases with a loss of one of two heterodimers, including MLH1/PMS2 or MSH2/MSH6; we further considered another subset: (iii) cases with one MMR loss and/or the patchy expression of one or more MMR (lo-paMMR).

This heterogeneous patchy staining was defined according to the criteria established by Joost et al. as tumors show intra-tumor heterogeneity (strongly immunoreactive cells admixed with negative cells) and/or zonal loss (confluent areas of staining loss) (18).

In all cases labeled as showing MMR heterogeneity according to the patterns described above, there was a distinct loss of nuclear staining in tumor cells, while normal stroma and lymphocytes showed strong nuclear staining in the same areas, thus excluding artifact and/or staining failure. An arbitrary cut-off value of approximately 10% of the tumor showing either retention or loss of MMR proteins was used. All cases that showed a patchy expression and/or loss of MMR, they further analyzed by both IHC MMR and PCR on one or more tumor inclusions, if available. Two independent observers carried out the IHC analysis, both observers were blinded.

PCR Detection for Microsatellite Status

Serial sections of 6-μm thickness from formalin-fixed paraffin-embedded matched normal and tumor tissues were routinely stained, and representative normal and tumor regions were identified by microscopic examination. Genomic DNA was isolated from the paraffin-embedded tissues using the QIAamp DNA mini kit (Qiagen, Valencia, CA) following the separation of tumor and normal tissue by manual microdissection. MSI was determined on tumor DNA using the EasyPGX® ready MSI including the following mononucleotide repeats: BAT25, BAT26, NR21, NR22, NR24, NR27, CAT25, and MONO27; all data are summarized in **Supplementary Table 1**.

The test was performed according to the manufacturer's instructions. PCR results were evaluated as follows: (i) microsatellite stable (MSS): cases with none of the markers unstable; (ii) MSI-H: tumor with 2 or more unstable markers; and (iii) MSI-L: cases with only one marker unstable; in these cases, new testing was carried out on non-tumor tissue, if available, to define a germinal mutation.

Immunohistochemistry Analysis of p16 Expression

p16 IHC was carried out with a proprietary kit (CINtec Histology; MTM laboratories AG) using the clone E6H4 on a Ventana BenchMark automatic stainer (Ventana Medical Systems, Tucson, AZ, United States) for the detection of p16INK4a antigen. A PC with a high p16 expression was used as a positive control.

TABLE 1 | Clinical and pathological features.

Features	TOTAL*n*. (%)	PD-L1 SP263 TPS		PD-L1 SP263 CPS		PD-L1 SP142			IHC MMRPs		
		Positive	Negative	Positive	Negative	TILs +	TILs -	NA	pMMR	lo-pa MMR	dMMR
Mean age (years)											
< 60	27(37.5%)	20(27.8%)	7(9.7%)	22(30.6%)	5(7%)	19(26.4%)	8(11.1%)	/	19(26.4%)	7(9.7%)	1(1.4%)
≥ 60	45(62.5%)	25(34.7%)	20(27.8%)	35(48.6%)	10(13.9%)	28(38.9%)	7(9.7%)	10(13.9%)	40(55.6%)	5(7%)	/
Anatomical location											
Glans	68(94.4%)	41(56.9%)	27(37.5%)	53(73.6%)	15(20.8%)	43(59.7%)	15(20.8%)	10(13.9%)	55(76.4%)	12(16.7%)	1(1.4%)
Foreskin	4(5.6%)	4(5.6%)	/	4(5.6%)	/	4(5.6%)	/	/	4(5.6%)	/	/
T-STAGE											
T1	24(33.3%)	17(23.6%)	7(9.7%)	20(27.8%)	4(5.6%)	17(23.6%)	5(7%)	2(2.8%)	23(31.9%)	1(1.4%)	/
T2	25(34.7%)	14(19.4%)	11(15.3%)	19(26.4%)	6(8.3%)	14(19.4%)	7(9.7%)	4(5.6%)	17(23.6%)	7(9.7%)	1(1.4%)
T3	17(23.6%)	10(13.9%)	7(9.7%)	13(18%)	4(5.6%)	12(16.7%)	2(2.8%)	3(4.2%)	14(19.4%)	3(4.2%)	/
T4	5(7%)	3(4.2%)	2(2.8%)	4(5.6%)	1(1.4%)	4(5.6%)	/	1(1.4%)	4(5.6%)	1(1.4%)	/
In situ	1(1.4%)	1(1.4%)	/	1(1.4%)	/	/	1(1.4%)	/	1(1.4%)	/	/
Hystological classification											
USCC	65(90.3%)	40(55.6%)	25(34.7%)	53(73.6%)	12(16.7%)	44(61.1%)	12(16.7%)	9(12.5%)	52(72.2%)	12(16.7%)	1(1.4%)
Verrucous	1(1.4%)	1(1.4%)	/	1(1.4%)	/	1(1.4%)	/	/	1(1.4%)	/	/
Basaloid	4(5.6%)	4(5.6%)	/	3(4.2%)	1(1.4%)	2(2.8%)	2(2.8%)	/	4(5.6%)	/	/
Warty	1(1.4%)	/	1(1.4%)	/	1(1.4%)	/	/	1(1.4%)	1(1.4%)	/	/
Mixed(Warty-Basaloid)	1(1.4%)	/	1(1.4%)	/	1(1.4%)	/	1(1.4%)	/	1(1.4%)	/	/
Hystological grade											
G1	18(25%)	9(12.5%)	9(12.5%)	14(19.4%)	4(5.6%)	10(13.9%)	5(7%)	3(4.2%)	14(19.4%)	4(5.6%)	/
G2	39(54.2%)	26(36.1%)	13(18%)	33(45.8%)	6(8.3%)	28(38.9%)	6(8.3%)	5(7%)	34(47.2%)	4(5.6%)	1(1.4%)
G3	15(20.8%)	10(13.9%)	5(7%)	10(13.9%)	5(7%)	9(12.5%)	4(5.6%)	2(2.8%)	11(15.3%)	4(5.6%)	/
P16 IHC											
Positive	25(34.7%)	17(23.6%)	8(11.1%)	19(26.4%)	6(8.3%)	14(19.4%)	7(9.7%)	4(5.6%)	21(29.2%)	4(5.6%)	/
Negative	47(65.3%)	28(38.9%)	19(26.4%)	38(52.8%)	9(12.5%)	33(45.8%)	8(11.1%)	6(8.3%)	38(52.8%)	8(11.1%)	1(1.4%)
HPV ISH											
Positive	13(18%)	7(9.7%)	6(8.3%)	8(11.1%)	5(7%)	9(12.5%)	1(1.4%)	3(4.2%)	10(13.9%)	3(4.2%)	/
Negative	59(82%)	38(52.8%)	21(29.2%)	49(68%)	10(13.9%)	38(52.8%)	14(19.4%)	7(9.7%)	49(68%)	9(12.5%)	1(1.4%)
TOTAL	**72 (100%)**	45(62.5%)	27(37.5%)	57(79.2%)	15(20.8%)	47(65.3%)	15(20.8%)	10(13.9%)	59(82%)	12(16.7%)	1(1.4%)

TPS, tumor proportion score; CPS, combined proportion score; IHC, immunohistochemistry; MMRPs, mismatch-repair proteins; pMMRPs, proficient mismatch-repair proteins; dMMRPs, deficient mismatch-repair proteins; lo-pa MMRPs, loss/patchy mismatch-repair proteins; TILs+, tumor-infiltrating lymphocytes present; TILs-, tumor-infiltrating lymphocytes absent; NA, Not Available; USCC, usual squamous cell carcinoma.

The primary antibody was omitted from negative controls. In our analysis, we identified the subgroups with different p16 IHC staining as follows:

1. p16 high expression: tumors with staining ≥ 70% nuclear and cytoplasmic staining;
2. p16 moderate expression: tumors with staining 30–70% nuclear and cytoplasmic staining;
3. p16 low expression: tumors with staining 10–30% nuclear and cytoplasmic staining;
4. p16 negative: tumors with staining 1–10% nuclear and cytoplasmic staining.

In addition, the intensity was also evaluated. The slides were independently evaluated by two separate observers.

Automated Human Papillomavirus RNA *in situ* Hybridization

A section of 4-μm thickness from each case was used to perform the HPV RNA ISH test. Detection of high-risk HPV E6/E7 mRNA was performed using ready-to-use reagents from RNA scope 2.5 LS Reagent Kit-BROWN and the HPV-HR18 probe cocktail (Advanced Cell Diagnostics) that were loaded onto the Leica Biosystems' BOND RX Research Advanced Staining System according to the user manual (Doc. No. 322,100-USM). The slides were independently evaluated by two separate observers.

Ubiquitin C and dapB were used as positive and negative controls, respectively. A positive HPV ISH test result was defined as positive if any of the malignant cells showed brown punctate dot-like nuclear and/or cytoplasmic positivity (19).

Statistical Analysis

The Pearson χ^2-test was used to determine the association of clinical characteristics with the status of protein expression. The Spearman rank test was used to assess the correlation between protein phenotypes. Statistical significance was set at the value of $p = 0.05$. Data analysis and summarization were carried out using SPSS 20.0 for Mac (SPSS Inc., Chicago, IL).

TABLE 2 | Results of the PD-L1 IHC evaluation.

	PD-L1 evaluation		
	NEGATIVE N.cases (%)	**POSITIVE N.cases (%)**	
CPS score	<1 15 (21%)	1–≤ 20 18 (25%)	> 20 39 (54%)
TPS percentage	<1%27 (37%)	1–≤ 50%15 (21%)	> 50%30 (42%)
TILs positivity	15 (24%)	47 (76%)	

CPS, combined proportion score, TPS, tumor proportion score, TILs, tumor infiltrating lymphocytes.

RESULTS

Clinical and Pathological Features

In our series, patients older than 60 years were 45; the tumor site was the glans in 68 cases and the foreskin in 4. Usual squamous cell carcinoma (USCC) was observed in 65; a special histotype was diagnosed in 7 cases, particularly verrucous in 1 case, basaloid in 4 cases, warty in 1 case, and mixed warty-basaloid in 1 case. In the USCC histotype, the low grade (G1) was recorded in 18 cases, the moderate grade (G2) in 39 cases, and the high grade (G3) in 15 cases. Finally, the tumors were staged T1 in 24 cases, T2 in 25, T3 in 17, and T4 in 5, 1 case was *in situ* carcinoma.

p16 overexpression was recorded in 25 (34.7%) out of 72 cases, particularly 19 in USCC and 6 in special histotypes. p16 low-intensity expression was observed in 5 cases (7%), moderate-intensity expression in 6 cases (8%), and high-intensity expression in 13 cases (18%). HPV positive by ISH was observed in 13 (18%) out of 72 cases, particularly 9 in USCC and 4 in special histotypes. All data obtained are summarized in **Table 1**.

Immunohistochemistry Analysis of Programmed Cell Death Ligand 1 Expression

The penile SCCs showed variable positivity rates of PDL1 expression based on different clones and score applied, these data are summarized in **Table 2**. Of the 72 PC analyzed by PDL1 SP263 IHC, 45 (62.5%) cases showed positivity in TCs with different scores, particularly 27 cases (37%) showed TCs positivity < 1%, 15 cases (21%) showed TCs positivity between 1 and 50%, and 30 cases (42%) showed TCs positivity > 50% (**Figure 1**). PDL1 SP263 CPS evaluation showed 15 (21%) negative and 57 (79%) positive cases. Among these positive cases, 18 cases (25%) had a CPS between 1 and < 20, and 39 cases (54%) had a CPS > 20 (**Figure 2**).

In our cohort, TILs were present in 62/72 (86.1%), 47 (75.8%) out of 62 cases showed positivity to PDL1 clone SP142 (**Figure 3**). Instead, as expected, only 7 (9.7%) out of 62 cases showed positivity to PDL1 clone SP142 also in TCs.

Immunohistochemistry Analysis of Mismatch Repair Protein Expression

Of the 72 PC analyzed by IHC, there were 59 cases (82%) of pMMR, 12 cases (16.7%) of lo-paMMR (**Figure 4**), and only

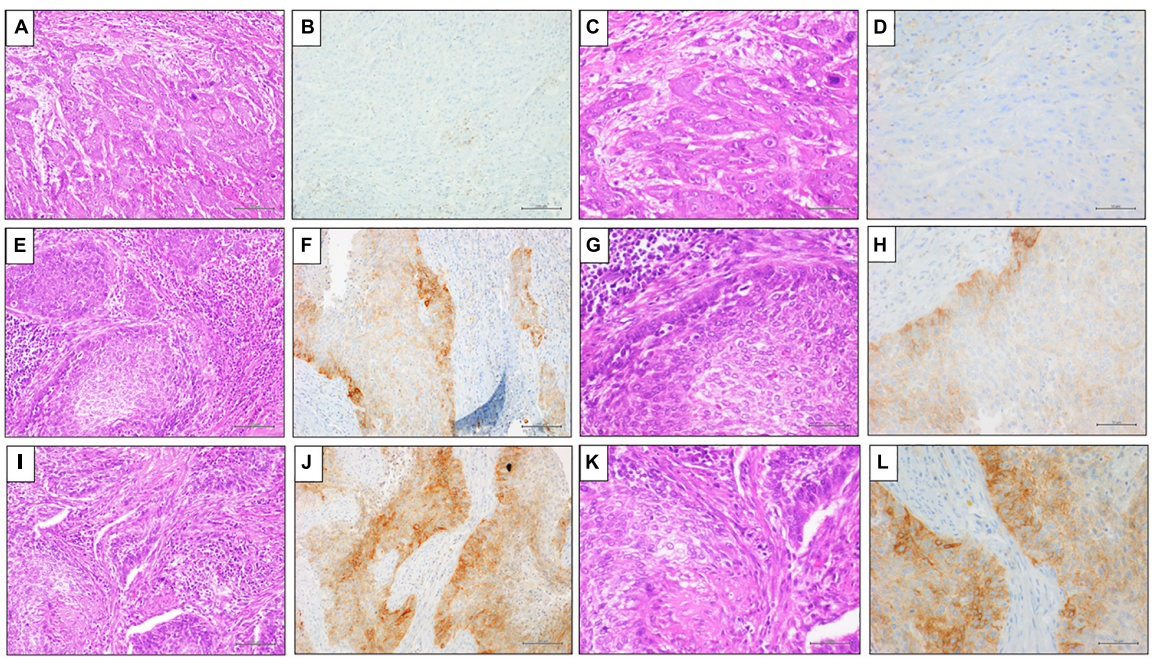

FIGURE 1 | Representative results of PD-L1 (clone SP263) IHC expression by TPS in penile SCC. **(A,E,I)** Hematoxylin and Eosin (H&E) staining (20x magnification, scale bar 100 μm); **(C,G,M)** Hematoxylin and Eosin (H&E) staining (40x magnification, scale bar = 200 μm); **(B,D)** PD-L1 (clone SP263) IHC expression < 1%, DAB staining (40x magnification, scale bar = 200 μm); **(F,H)** PD-L1 (clone SP263) IHC expression 1% ≤ score < 50%, DAB staining (40x magnification, scale bar = 200μm); **(L,N)** PD-L1 (clone SP263) IHC expression ≥ 50%, DAB staining (40x magnification, scale bar = 200 μm).

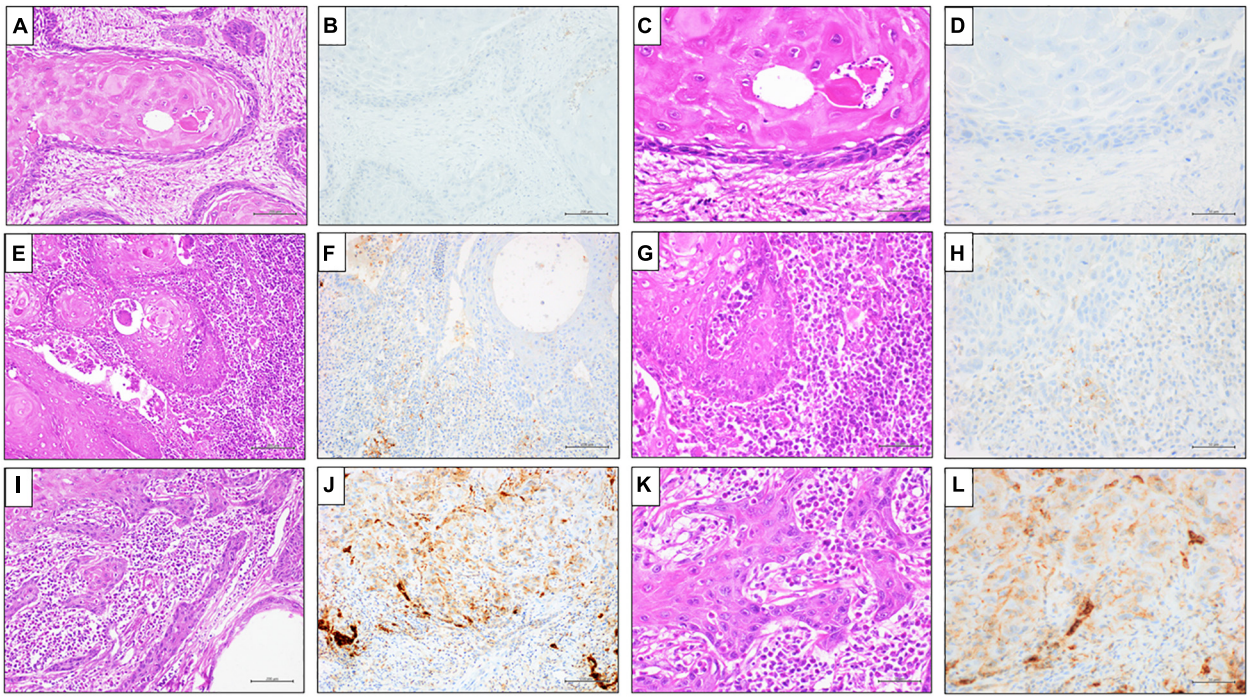

FIGURE 2 | Representative results of PD-L1 (clone SP263) IHC expression by CPS in penile SCC. **(A,E,I)** Hematoxylin and Eosin (H&E) staining (20x magnification, scale bar = 100 μm); **(C,G,M)** Hematoxylin and Eosin (H&E) staining (40x magnification, scale bar = 200 μm); **(B,D)** PD-L1 (clone SP263) IHC expression score ≤ 1%, DAB staining (40x magnification, scale bar = 200 μm); **(F,H)** PD-L1 (clone SP263) IHC expression 1% < score < 20%, DAB staining (40x magnification, scale bar = 200 μm); **(L,N)** PD-L1 (clone SP263) IHC expression ≥ 20%, DAB staining (40x magnification, scale bar = 200 μm).

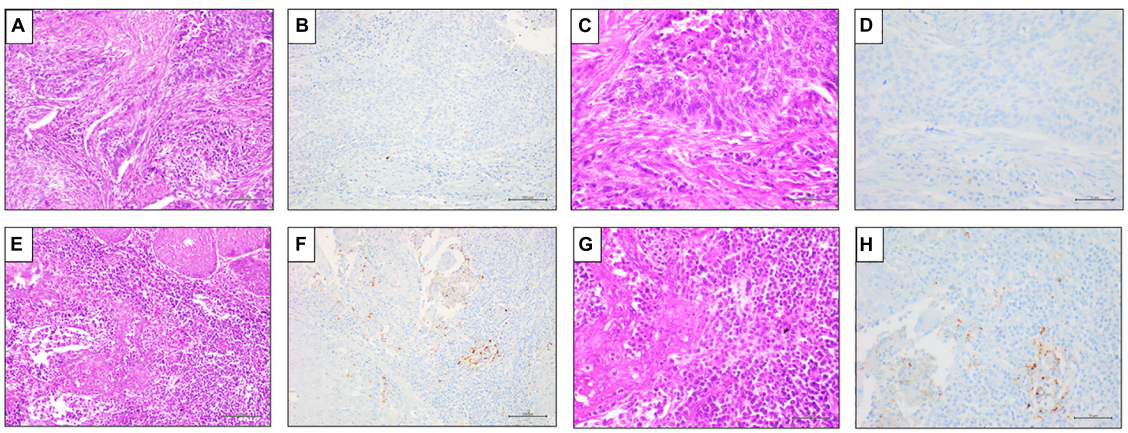

FIGURE 3 | Representative results of PD-L1 SP142 IHC expression in TILs in penile SCC. **(A,E)** Hematoxylin and Eosin (H&E) staining (20x magnification, scale bar = 100 μm); **(C,G)** Hematoxylin and Eosin (H&E) staining (40x magnification, scale bar = 200 μm); **(B,F)** negative PD-L1 (clone SP142) IHC expression in TILs, DAB staining (40x magnification, scale bar = 200 μm); **(D,H)** positive PD-L1 (clone SP142) IHC expression in TILs, DAB staining (40x magnification, scale bar = 200 μm).

1 case (1.3%) of dMMR (**Figure 5**). In detail, the dMMR case was negative for MLH1-PMS2. Among 12 cases of lo-paMMR, 7 cases showed the patchy expression of PMS2, 3 cases showed the patchy expression of two MMR, and 2 cases showed the patchy expression of MSH2 and loss of PMS2. These data are summarized in **Table 3**.

PCR Detection for Microsatellite Status

Of the 72 PC analyzed by IHC, all 13 cases harboring dMMR or lo-paMMR were analyzed by PCR. Among 13 cases, 11 cases were MSS, 1 case was MSI-H, and 1 case was MSI-L. In detail, MSI-H case showed the instability of BAT26, NR27, and MONO27 loci, while MSI-L showed the

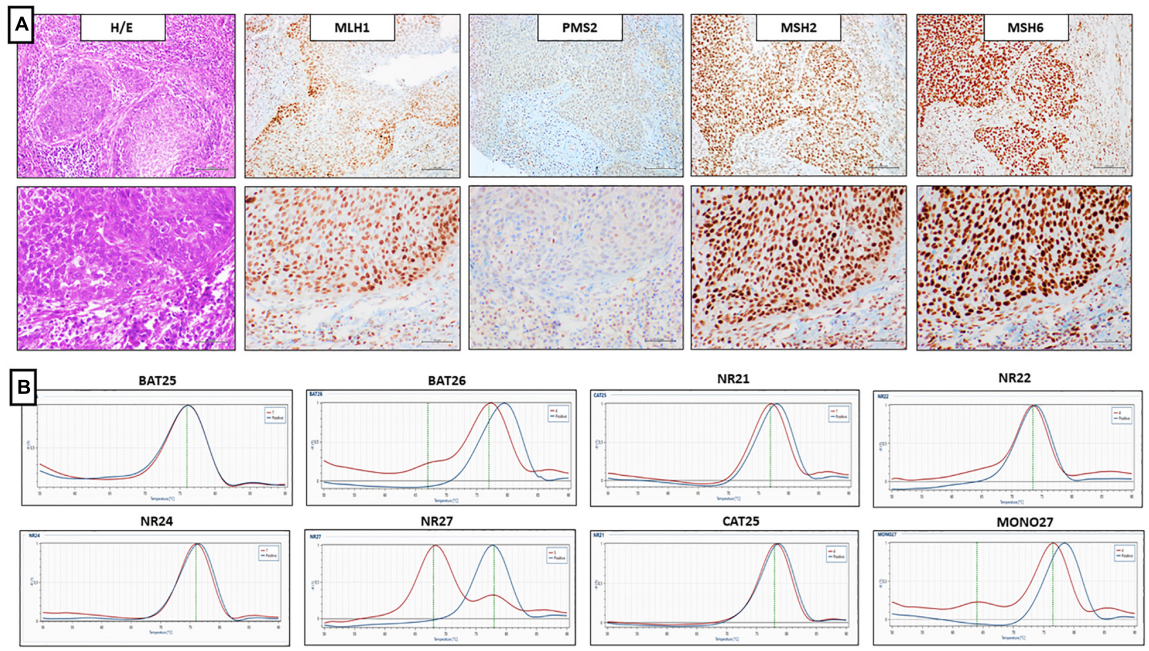

FIGURE 4 | Representative results of penile SCC case showing lo-paMMR IHC and MSI-H by PCR. **(A)** Upper line (from left to right) MMR-IHC results: Hematoxilin and Eosin penile SCC, intact exspression of MLH1, MSH2 and MSH6, loss-patchy expression of PMS2 (20x magnification, scale bar = 100 μm); lower line (from left to right) MMR-IHC results: Hematoxilin and Eosin penile SCC, intact exspression of MLH1, MSH2 and MSH6, loss-patchy expression of PMS2 (40x magnification, scale bar = 200 μm). **(B)** MSI-PCR results: stability of BAT25, NR21, NR22, NR24 and CAT25, instability of BAT26, NR27, and MONO27 (red lines indicate samples while blue lines indicate MSS controls).

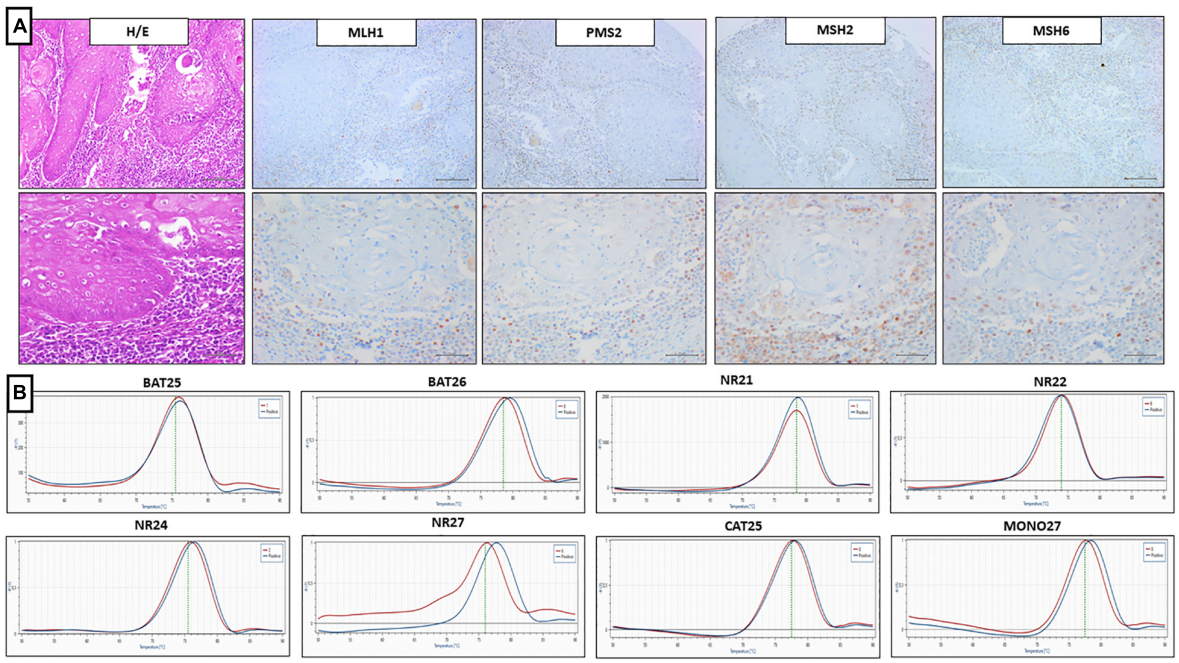

FIGURE 5 | Representative results of penile SCC case showing dMMR IHC and MSI-L by PCR. **(A)** Upper line (from left to right) MMR-IHC results: Hematoxilin and Eosin penile SCC, loss expression of MLH1 and PMS2, while loss-patchy expression of MSH2 and MSH6 (20x magnification, scale bar = 100 μm); lower line (from left to right) MMR-IHC results: Hematoxilin and Eosin penile SCC, loss expression of MLH1 and PMS2, while loss-patchy expression of MSH2 and MSH6 (40x magnification, scale bar = 200 μm). **(B)** MSI-PCR results: stability of BAT25, BAT26, NR21, NR22, NR24, CAT25, and MONO27, instability of NR27 (red lines indicate samples while blue lines indicate MSS controls).

TABLE 3 | Comparison of the results of MMR-IHC analysis and MSI-PCR analysis.

MMR-IHC		MSI-PCR		
		MSI-H	MSI-L	MSS
n.1 dMMR				
MLH1-PMS2	1		1	
n.12 lo-paMMR				
n.3 patchy heterodimer				
MLH1-PMS2	1			1
PMS2-MSH2	1			1
PMS2-MSH6	1			1
n.7 patchy one MMR				
PMS2	7	1		6
n.2 loss one MMR-patchy				
PMS2 lo and MSH2 P	2			2

instability of NR27 only. Unfortunately, the testing on non-tumor tissue was not performed as normal tissue was not available. Furthermore, a series of 40 control cases that were determined as pMMR by IHC was analyzed using PCR, and all cases confirmed MSS status.

Comparison of Mismatch Repair-Immunohistochemistry and Microsatellite Instability-PCR

Discordant results between IHC and PCR were obtained in penile SCC cases harboring dMMR or lo-paMMR. The case of dMMR by IHC resulted in MSI-L by PCR analysis. Among 12 cases of lo-paMMR, one case resulted in MSI-H and the remaining 11 cases resulted in MSS. These data are summarized in **Table 3**.

Comparison of Programmed Cell Death Ligand 1 Immunohistochemistry and Microsatellite Instability Status

Comparing PD-L1 expression with the MMR IHC, different results were observed related to the different clones used in our analysis. In particular, using SP263 PD-L1 antibody, among 12 lo-paMMR cases, 7 cases were positive with both scores [tumor proportion score (TPS) and CPS] and 5 cases were negative. Using SP142 PD-L1 antibody, 6 cases were positive and 6 were negative. The case of dMMR was PD-L1 positive with both clones, particularly SP263 TPS was 40%, SP263 CPS was 60%, and SP142 was 20%.

The correlation between SP263 PD-L1 TCs expression $> 1\%$ and the dMMR/lo-paMMR by IHC was statistically significant ($p < 0.005$).

DISCUSSION

Squamous cell carcinoma of the penis is a rare and biologically aggressive malignancy, characterized by limited treatment options, not always curative, but just palliative in the advanced stage (20). Thus, new and efficient therapeutic strategies are needed to improve patient survival rates.

In recent years, immunotherapy has led to substantial changes in the cancer therapeutic paradigm. Nonetheless, the treatment with immune checkpoints showed relatively poor efficacy and low response rates in some tumors (21, 22). Therefore, adequate eligibility for immunotherapy requires the identification of biomarkers to distinguish the really sensitive patients and to predict response. To date, PD-L1 expression and dMMR/MSI-H represent the pivotal biomarkers to select the patients for immune checkpoint blockade therapies in the clinical practice of several tumors.

PD-L1 expression has been described in primary SCCs in different districts, including head and neck, lung and cervix (23, 24). Until present, PD1/PDL1 inhibitors were approved for the treatment of advanced SCCs, particularly two anti-PD-1 monoclonal antibodies, namely, Cemiplimab for advanced cutaneous SCC and nivolumab for metastatic or recurrent SCC of the head and neck (25, 26). Based on the histological and etiological similarities between SCCs regardless of the district, PDL1 could also play a role in penile SCC (10). Although several studies have investigated the PD-1/PD-L1 pathway in other urological malignancies, up to date, few data have been reported about PDL1 expression in penile SCC (10, 11, 27–29). In previous studies, several different clones, such as E1L3N, ZR3, 5H1, Dako 28.8, and SP142, were used to analyze PDL-1 positivity in penile SCC (10, 11, 20, 27–30). Davidsson et al. observed different percentages of PDL1-positive TCs according to the different clones used, particularly 32% of positive cases using clone 28.8 while 7.3% using clone SP142 (11). According to previous results, our data showed the PDL1 positivity in TCs in 44 cases (61%) using SP263 clone while in only 7 cases (9.7%) using SP142 clone.

The difference in PDL-1 expression in neoplastic cells when using different clones could be attributable to the specificity of the antibodies. Indeed, the SP263 clone is more specific for neoplastic cells, while the SP142 clone appears more specific for inflammatory cells (31). Particularly, SP263 was approved as the companion diagnostic for pembrolizumab in lung cancer patients, while SP142 was used for a clinical trial with atezolizumab in several cancer patients (32–34).

The FDA approved the treatment of triple-negative breast cancer (TNBC) with atezolizumab, basing the selection of patients on the SP142PDL1 expression in TILs of any intensity covering $\geq 1\%$ of the tumor area (35).

In this context, the PDL1 expression in TILs must also be investigated in penile SCC to clarify its potential role as a predictive biomarker for the treatment with immune checkpoint inhibitors. Previous data reported the PDL1 immunohistochemical positivity in penile SCC in both TCs and TILs ranging between 32–62% and 64–80%, respectively (10, 11, 30).

In this study, the PD-L1 expression was evaluated on both TCs and TILs, using two different antibody clones, such as SP263 and SP142. In our series, approximately 75.8% of cases carrying TILs were PDL1 positive by IHC SP142. Our findings showed a

higher rate of PDL1 positivity in TILs compared with previous reports, probably attributable to different methods for detection, including the choice of scoring method, the anti-PD-L1 antibody and/or cut-off value (11).

Different scoring systems have been currently proposed for PDL1 positivity in cancer cells based on the specific tumor (36). The scoring system applied in our study considers three tiers: positivity in cancer cells > 1%, positivity between 1 and 50%, and positivity > 50%. To date, this scoring system is used in clinical practice to select lung cancer patients for the treatment with pembrolizumab. Indeed, the patient is excluded from the treatment with pembrolizumab, when PDL-1 positivity is lower than 1%, the treatment in II line is considered if the PDL-1 positivity range is between 1 and 50% and finally the treatment in I line is successfully used when PDL-1 positivity is higher than 50% (37).

In penile SCC, there is no consensus about the PD-L1 IHC scoring system in previous reports. Thus, in some reports, only positive and negative are identified (27); in contrast, in some studies, 1 or 5% were considered the threshold values of positivity (10, 11, 20, 28, 30).

A CPS is an alternative method to TPS for scoring PD-L1 expression defined by the ratio of total positive tumor and immune to the total number of viable TCs. It is used in the characterization of several tumors, such as head and neck squamous cell carcinomas (HNSCC), to address patients to the immune checkpoint inhibitor pembrolizumab (38). In addition, the eligibility of the treatment with pembrolizumab is based on the usage of the CPS with different cut-off values according to the tumor type/site, such as gastric or gastroesophageal junction adenocarcinoma (CPS $\geq$ 1), locally advanced or metastatic urothelial carcinoma (CPS $\geq$ 10), recurrent or metastatic cervical cancer (CPS $\geq$ 1), recurrent locally advanced or metastatic SCC of the esophagus (CPS $\geq$ 10) (39), and recurrent or metastatic SCC of the head and neck (CPS $\geq$ 20) (17).

Muller et al. analyzed the expression of PDL1 (clone ZR3) in a series of 60 penile SCC HPV + (29). They found that 13% of cases showed TPS 0%, 47% TPS between 0 and 10%, and 40 TPS > 10%; about 3% had CPS score of 0, 33% had CPS score between 0 and 10, and 63% had CPS score of > 10.

In our study, we adopted the guidelines proposed in the HNSCC. Thus, CPS is > 1 in 79% (57/72) of cases, and a CPS is < 1 in 21% (15/72) of cases. Although CPS $\geq$ 50 seems to be an equivalent predictor to TPS $\geq$ 50% for selection of HNSCC patients potentially sensible to immune checkpoint inhibitor, based on our results, the CPS would allow to enrolling a greater number of patients than the TPS (21% CPS < 1 vs. 37% TPS < 1%). According to the previous data, CPS seems to be more reliable than TPS at lower cut-off values (CPS $\geq$ 1) in relation to the successful treatment, supporting the significance of PD-L1–positive immune cells as a sensitive biomarker (38).

To date, different cut-off values and scoring systems for PD-L1 evaluation have been validated in various tumor types. In this context, the definition of the PD-L1 IHC scoring system also in penile SCC represents an important turning point for an adequate selection of treatable patients. In particular, using CPS score could increase the percentage of PC patients potentially eligible for immunotherapy approximately by 16% compared with TPS score, since SCC is frequently characterized by PDL1 positivity of TILs.

Furthermore, no statistically significant data were reported in our series regarding the possible correlation of PD L1 expression with other clinical and pathological features. Previously, De Bacco et al. described, in a cohort of 40 penile SCC, a statistically significant association between p16 positivity and PD-L1 expression (clone ZR3) in tumors with worse clinical outcomes. On the contrary, in our PC series, no correlation between p16 expression and positive HPV ISH with PD-L1 expression was observed (28).

Besides PDL-1 expression, the defective DNA mismatch repair (MMR) system also predicted a clinical benefit in response to immunotherapy (28, 40). Usually, a proficient MMR system corrects the eventual presence of accumulated mutations, while a defective MMR system leads to global instability of repetitive sequences and coding regions. This phenomenon, called MSI, is already well known as a sporadic event in cancerogenesis, non-tumor specific (10–15% of colorectal, gastric, and endometrial carcinomas) (41). MSI can be molecularly categorized into two distinct phenotypes, namely, MSI-H and MSI-L (42).

Thus, the FDA approved the immunotherapy of any solid cancer with a defective MMR system and/or an MSI-H genotype (35). This approval led to a comprehensive investigation of MSI status across 39 cancer types, including bladder carcinoma, breast carcinoma, cervical SCC, diffuse large B-cell lymphoma, head and neck SCC, kidney renal clear cell carcinoma, lung adenocarcinoma, and more (43).

So far, in addition to this study, only a report of data of the MSI status in penile SCC has been published (13). Stoehr et al. analyzed the MSI status of 105 FFPE penile SCCs through PCR and the immunohistochemical expression of the MMR proteins. They found that 96 out of 105 cases provided interpretable results, but none of them showed MSI or loss of expression of the MMR proteins (13). Contrary to these results, in our series, we observed 1 case (1.3%) of dMMR and 12 cases (16.7%) of lo-paMMR. These discordant results could be due to technical limits, mainly linked to pre-analytical factors, especially tissue fixation. Moreover, Stoehr et al. have performed the study on TMA, unlike our study carried out on whole sections that have overcome the possible heterogeneity immunohistochemical expression of MMR proteins. Interestingly, the RT-PCR analysis showed MSI-H status of one case lo-paMMR suggesting that MSI-H could play a driver role in the development of penile SCC. Although MMR IHC represents a valid screening method, our data suggest that molecular tests could be performed in cases with doubtful IHC to avoid false-negative results. Moreover, both the PD-L1 and MMR expression could be affected by the intra-tumor heterogeneity that can lead to critical implications in the correct stratification of the patients to enroll for immunotherapy. In this view, technical and interpretative precautions must be used in the evaluation of these biomarkers.

Furthermore, our study showed that dMMR and lo-paMMR were statistically significantly associated with PD-L1 expression. Particularly, the case dMMR was PD-L1 positive with both clones

regardless of the different scores used. Previous studies reported that PD-L1 + expression was closely related to dMMR/MSI-H status in other cancer types, particularly in colon-rectal cancers (4, 44, 45). Biologically, MSI-H tumors harbor a higher number of mutations in DNA coding sequences leading to increased production of the neoantigens and triggering immune activation (4, 46). For that reason, the association between the MSI-H status and PD-L1 expression could lead to increased sensitivity to immune checkpoint inhibitors due to an increased mutational burden of these tumors.

CONCLUSION

Immunotherapies have led to a revolutionary change in the treatment of several cancer types; immune checkpoint blockade therapy would also be desirable in patients with penile SCC. However, the definitions of specific predictive biomarkers are needed to distinguish responders from non-responders patients. PDL1 expression and MSI status could represent the potential biomarkers in predicting immunotherapy efficacy in penile SCC. Further clinical trials using immune checkpoint blockade regimes in patients with PDL1 expression and MSI-H status may clarify the efficacy of immunotherapy and its possible clinical application in penile SCC.

DATA AVAILABILITY STATEMENT

The original contributions presented in the study are included in the article/**Supplementary Material**, further inquiries can be directed to the corresponding author/s.

ETHICS STATEMENT

The studies involving human participants were reviewed and approved by the Università degli Studi della Campania L.Vanvitelli. The patients/participants provided their written informed consent to participate in this study.

AUTHOR CONTRIBUTIONS

All authors listed have made a substantial, direct, and intellectual contribution to the work, and approved it for publication.

SUPPLEMENTARY MATERIAL

The Supplementary Material for this article can be found online at: https://www.frontiersin.org/articles/10.3389/fmed.2022.874213/full#supplementary-material

REFERENCES

1. Stratton KL, Culkin DJA. Contemporary review of HPV and penile cancer. *Oncology (Williston Park).* (2016) 3:245–9.
2. Bleeker MC, Heideman DA, Snijders PJ, Horenblas S, Dillner J, Meijer CJ. Penile cancer: epidemiology, pathogenesis and prevention. *World J Urol.* (2009) 2:141–50. doi: 10.1007/s00345-008-0302-z
3. Hakenberg OW, Dräger DL, Erbersdobler A, Naumann CM, Jünemann KP, Protzel C. The diagnosis and treatment of penile cancer. *Dtsch Arztebl Int.* (2018) 115:646–52. doi: 10.3238/arztebl.2018.0646
4. Rizvi NA, Hellmann MD, Snyder A, Kvistborg P, Makarov V, Havel JJ, et al. Cancer immunology. Mutational landscape determines sensitivity to PD-1 blockade in non-small cell lung cancer. *Science.* (2015) 348:124–8. doi: 10.1126/science.aaa1348
5. Kvistborg P, Philips D, Kelderman S, Hageman L, Ottensmeier C, Joseph-Pietras D, et al. Anti-CTLA-4 therapy broadens the melanoma-reactive CD8+ T cell response. *Sci Transl Med.* (2014) 6:254ra128. doi: 10.1126/scitranslmed.3008918
6. Powles T, Eder JP, Fine GD, Braiteh FS, Loriot Y, Cruz C, et al. MPDL3280A (anti-PD-L1) treatment leads to clinical activity in metastatic bladder cancer. *Nature.* (2014) 7528:558–62. doi: 10.1038/nature13904
7. Chow LQM, Haddad R, Gupta S, Mahipal A, Mehra R, Tahara M, et al. Antitumor activity of pembrolizumab in biomarker-unselected patients with recurrent and/or metastatic head and neck squamous cell carcinoma: results from the phase Ib KEYNOTE-012 expansion cohort. *J Clin Oncol.* (2016) 32:3838–45. doi: 10.1200/JCO.2016.68.1478
8. Ansell SM, Lesokhin AM, Borrello I, Halwani A, Scott EC, Gutierrez M, et al. PD-1 blockade with nivolumab in relapsed or refractory Hodgkin's lymphoma. *N Engl J Med.* (2014) 372:311–9. doi: 10.1056/NEJMoa1411087
9. Zito Marino F, Ascierto PA, Rossi G, Staibano S, Montella M, Russo D, et al. Are tumor-infiltrating lymphocytes protagonists or background actors in patient selection for cancer immunotherapy? *Expert Opin Biol Ther.* (2017) 6:735–46. doi: 10.1080/14712598.2017.1309387
10. Udager AM, Liu TY, Skala SL, Magers MJ, McDaniel AS, Spratt DE, et al. Frequent PD-L1 expression in primary and metastatic penile squamous cell carcinoma: potential opportunities for immunotherapeutic approaches. *Ann Oncol.* (2016) 27:1706–12. doi: 10.1093/annonc/mdw216
11. Davidsson S, Carlsson J, Giunchi F, Harlow A, Kirrander P, Rider J, et al. PD-L1 expression in men with penile cancer and its association with clinical outcomes. *Eur Urol Oncol.* (2019) 2:214–21. doi: 10.1016/j.euo.2018.07.010
12. Gelsomino F, Barbolini M, Spallanzani A, Pugliese G, Cascinu S. The evolving role of microsatellite instability in colorectal cancer: a review. *Cancer Treat Rev.* (2016) 51:19–26. doi: 10.1016/j.ctrv.2016.10.005
13. Stoehr R, Wendler O, Giedl J, Gaisa NT, Richter G, Campean V, et al. No evidence of microsatellite instability and loss of mismatch-repair-protein expression in squamous cell carcinoma of the penis. *Pathobiology.* (2019) 86:145–51. doi: 10.1159/000495251
14. Moch H, Cubilla AL, Humphrey PA, Reuter VE, Ulbright TM. The 2016 WHO classification of tumours of the urinary system and male genital organs-part A: renal, penile, and testicular tumours. *Eur Urol.* (2016) 70:93–105. doi: 10.1016/j.eururo.2016.02.029
15. Antonia S, Goldberg SB, Balmanoukian A, Chaft JE, Sanborn RE, Gupta A, et al. Safety and antitumour activity of durvalumab plus tremelimumab in non-small cell lung cancer: a multicentre, phase 1b study. *Lancet Oncol.* (2016) 17:299–308. doi: 10.1016/S1470-2045(15)00544-6
16. Reddy SM, Carroll E, Nanda R. Atezolizumab for the treatment of breast cancer. *Expert Rev Anticancer Ther.* (2020) 20:151–8. doi: 10.1080/14737140.2020.1732211
17. Burtness B, Harrington KJ, Greil R, Soulières D, Tahara M, de Castro G Jr., et al. KEYNOTE- 048 Investigators. Pembrolizumab alone or with chemotherapy versus cetuximab with chemotherapy for recurrent or metastatic squamous cell carcinoma of the head and neck (KEYNOTE-048): a randomised, open-label, phase 3 study. Lancet. 2019 Nov 23;394(10212):1915-1928. Epub 2019 Nov 1. Erratum in: lancet. 2020 Jan 25;395(10220):272. Erratum in: lancet. 2020 Feb 22;395(10224):564. *Erratum Lancet.* (2021) 397:2252. doi: 10.1016/S0140-6736(19)32591-7

18. Joost P, Veurink N, Holck S, Klarskov L, Bojesen A, Harbo M, et al. Heterogenous mismatch−repair status in colorectal cancer. *Diagn Pathol.* (2014) 9:126. doi: 10.1186/1746-1596-9-126
19. Zito Marino F, Sabetta R, Pagliuca F, Brunelli M, Aquino G, Perdonà S, et al. Discrepancy of p16 immunohistochemical expression and HPV RNA in penile cancer. A multiplex in situ hybridization/immunohistochemistry approach study. *Infect Agent Cancer.* (2021) 1:22. doi: 10.1186/s13027-021-00361-8
20. Ottenhof SR, Djajadiningrat RS, de Jong J, Thygesen HH, Horenblas S, Jordanova ES. Expression of programmed death ligand 1 in penile cancer is of prognostic value and associated with HPV status. *J Urol.* (2017) 3 (Pt 1):690–7. doi: 10.1016/j.juro.2016.09.088
21. Brahmer J, Reckamp KL, Baas P, Crinò L, Eberhardt WE, Poddubskaya E, et al. Nivolumab versus docetaxel in advanced squamous-cell non-small-cell lung cancer. *N Engl J Med.* (2015) 373:123–35. doi: 10.1056/NEJMoa1504627
22. Robert C, Thomas L, Bondarenko I, O'Day S, Weber J, Garbe C, et al. Ipilimumab plus 630 dacarbazine for previously untreated metastatic melanoma. *N Engl J Med.* (2011) 364:2517–26.
23. Badoual C, Hans S, Merillon N, Van Ryswick C, Ravel P, Benhamouda N, et al. PD-1-expressing tumor-infiltrating T cells are a favorable prognostic biomarker in HPV-associated head and neck cancer. *Cancer Res.* (2013) 1:128–38. doi: 10.1158/0008-5472.CAN-12-2606
24. Mezache L, Paniccia B, Nyinawabera A, Nuovo GJ. Enhanced expression of PD L1 in cervical intraepithelial neoplasia and cervical cancers. *Mod Pathol.* (2015) 28:1594–602. doi: 10.1038/modpathol.2015.108
25. Migden MR, Rischin D, Schmults CD, Guminski A, Hauschild A, Lewis KD, et al. PD-1 blockade with cemiplimab in advanced cutaneous squamous-cell carcinoma. *N Engl J Med* (2018) 4:341–51. doi: 10.1056/NEJMoa1805131
26. Harrington KJ, Ferris RL, Blumenschein G, Colevas AD, Fayette J, Licitra L, et al. Nivolumab versus standard, single-agent therapy of investigator's choice in recurrent or metastatic squamous cell carcinoma of the head and neck (CheckMate 141): health-related quality-of-life results from a randomised, phase 3 trial. *Lancet Oncol.* (2017) 18:1104–15. doi: 10.1016/S1470-2045(17)30421-7
27. Cocks M, Taheri D, Ball MW, Bezerra SM, Del Carmen Rodriguez M, Ricardo BFP, et al. Immune-checkpoint status in penile squamous cell carcinoma: a North American cohort. *Hum Pathol.* (2017) 59:55–61. doi: 10.1016/j.humpath.2016.09.003
28. De Bacco MW, Carvalhal GF, MacGregor B, Marçal JMB, Wagner MB, Sonpavde GP, et al. PD- L1 and p16 expression in penile squamous cell carcinoma from an endemic region. *Clin Genitourin Cancer.* (2020) 18:e254–9. doi: 10.1016/j.clgc.2019.10.014
29. Müller T, Demes M, Lehn A, Köllermann J, Vallo S, Wild PJ, et al. The peri- and intratumoral immune cell infiltrate and PD-L1 status in invasive squamous cell carcinomas of the penis. *Clin Transl Oncol.* (2022) 2:331–41. doi: 10.1007/s12094-021-02694-7
30. Deng C, Li Z, Guo S, Chen P, Chen X, Zhou Q, et al. Tumor PD-L1 expression is correlated with increased TILs and poor prognosis in penile squamous cell carcinoma. *Oncoimmunology.* (2016) 6:e1269047. doi: 10.1080/2162402X.2016.1269047
31. Huang TH, Cheng W, Wang YH. Interpretation according to clone-specific PD-L1 cutoffs reveals better concordance in muscle-invasive urothelial carcinoma. *Diagnostics (Basel).* (2021) 3:448. doi: 10.3390/diagnostics11030448
32. Herbst RS, Giaccone G, de Marinis F, Reinmuth N, Vergnenegre A, Barrios CH, et al. Atezolizumab for first-line treatment of PD-L1-selected patients with NSCLC. *N Engl J Med.* (2020) 383:1328–39. doi: 10.1056/NEJMoa1917346
33. Cyprian FS, Akhtar S, Gatalica Z, Vranic S. Targeted immunotherapy with a checkpoint inhibitor in combination with chemotherapy: a new clinical paradigm in the treatment of triple-negative breast cancer. *Bosn J Basic Med Sci.* (2019) 19:227–33. doi: 10.17305/bjbms.2019.4204
34. McDermott DF, Sosman JA, Sznol M, Massard C, Gordon MS, Hamid O, et al. Atezolizumab, an anti-programmed death-ligand 1 antibody, in metastatic renal cell carcinoma: long-term safety, clinical activity, and immune correlates from a phase Ia study. *J Clin Oncol.* (2016) 34:833–42. doi: 10.1200/JCO.2015.63.7421
35. FDA. *FDA Approves First Cancer Treatment for Any Solid Tumor With a Specific Genetic Feature.* (2017). Available online at: https://www.fda.gov/ (accessed May 23, 2017).
36. Udall M, Rizzo M, Kenny J, Doherty J, Dahm S, Robbins P, et al. PD-L1 diagnostic tests: a systematic literature review of scoring algorithms and test-validation metrics. *Diagn Pathol.* (2018) 13:12. doi: 10.1186/s13000-018-0689-9
37. Paz-Ares L, Luft A, Vicente D, Tafreshi A, Gümüş M, Mazières J, et al. Pembrolizumab plus chemotherapy for squamous non-small-cell lung cancer. *N Engl J Med.* (2018) 379:2040–51.
38. Emancipator K, Huang L, Aurora-Garg D, Bal T, Cohen EEW, Harrington K, et al. Comparing programmed death ligand 1 scores for predicting pembrolizumab efficacy in head and neck cancer. *Mod Pathol.* (2021) 3:532–41. doi: 10.1038/s41379-020-00710-9
39. KEYTRUDA. *KEYTRUDA §(Pembrolizumab) for Injection, for Intravenous Use*. Whitehouse Station, NJ: Merck Sharp & Dohme Corp (2020).
40. Sahin IH, Akce M, Alese O, Shaib W, Lesinski GB, El-Rayes B, et al. Immune checkpoint inhibitors for the treatment of MSI-H/MMR-D colorectal cancer and a perspective on resistance mechanisms. *Br J Cancer.* (2019) 121:809–18. doi: 10.1038/s41416-019-0599-y
41. Zhang J, Shih DJH, Lin SY. Role of DNA repair defects in predicting immunotherapy response. *Biomark Res.* (2020) 8:23. doi: 10.1186/s40364-020-00202-7
42. Akagi K, Oki E, Taniguchi H, Nakatani K, Aoki D, Kuwata T, et al. Real-world data on microsatellite instability status in various unresectable or metastatic solid tumors. *Cancer Sci.* (2021) 3:1105–13. doi: 10.1111/cas.14798
43. Pawlik TM, Raut CP, Rodriguez-Bigas MA. Colorectal carcinogenesis: MSI-H versus MSI-L. *Dis Markers.* (2004) 20:199–206. doi: 10.1155/2004/368680
44. Bonneville R, Krook MA, Kautto EA, Miya J, Wing MR, Chen HZ, et al. Landscape of microsatellite instability across 39 cancer types. *JCO Precis Oncol.* (2017) 2017:10.1200/O.17.00073. doi: 10.1200/PO.17.00073
45. Zhao P, Li L, Jiang X, Li Q. Mismatch repair deficiency/microsatellite instability-high as a predictor for anti-PD-1/PD-L1 immunotherapy efficacy. *J Hematol Oncol.* (2019) 12:54. doi: 10.1186/s13045-019-0738-1
46. Gatalica Z, Snyder C, Maney T, Ghazalpour A, Holterman DA, Xiao N, et al. Programmed cell 698 death 1 (PD-1) and its ligand (PD-L1) in common cancers and their correlation with molecular cancer type. *Cancer Epidemiol Biomarkers Prev.* (2014) 23:2965–70. doi: 10.1158/1055-9965.EPI-14-0654
47. Le DT, Uram JN, Wang H, Bartlett BR, Kemberling H, Eyring AD, et al. PD-1 blockade in tumors with mismatch-repair deficiency. *N Engl J Med.* (2015) 372:2509–20.

Conflict of Interest: The authors declare that the research was conducted in the absence of any commercial or financial relationships that could be construed as a potential conflict of interest.

The handling editor AM declared a shared affiliation with the authors FFe, GA at the time of review.

Publisher's Note: All claims expressed in this article are solely those of the authors and do not necessarily represent those of their affiliated organizations, or those of the publisher, the editors and the reviewers. Any product that may be evaluated in this article, or claim that may be made by its manufacturer, is not guaranteed or endorsed by the publisher.

frontiers | Frontiers in Medicine

ORIGINAL RESEARCH
published: 31 May 2022
doi: 10.3389/fmed.2022.816012

Sex Cord-Stromal Tumors of Testis: A Clinicopathologic and Follow-Up Study of 15 Cases in a High-Volume Institute of China

Yin Huang[1,2†], Bo Chen[1†], Dehong Cao[1†], Zeyu Chen[1], Jin Li[1], Jianbing Guo[1], Qiang Dong[1], Qiang Wei[1] and Liangren Liu[1*]*

[1] Department of Urology, West China Hospital, Institute of Urology, Sichuan University, Chengdu, China, [2] West China School of Medicine, Sichuan University, Chengdu, China

OPEN ACCESS

Edited by:
Luigi Tornillo,
University of Basel, Switzerland

Reviewed by:
Yunxiang Li,
North Sichuan Medical College, China
José Manuel Lopes,
University of Porto, Portugal
Kris Ann Schultz,
Children's Hospitals and Clinics of Minnesota, United States

***Correspondence:**
Qiang Wei
weiqiang339@126.com
Liangren Liu
liangren_liu517@126.com

† These authors have contributed equally to this work

Specialty section:
This article was submitted to Pathology, a section of the journal Frontiers in Medicine

Received: 16 November 2021
Accepted: 21 April 2022
Published: 31 May 2022

Citation:
Huang Y, Chen B, Cao D, Chen Z, Li J, Guo J, Dong Q, Wei Q and Liu L (2022) Sex Cord-Stromal Tumors of Testis: A Clinicopathologic and Follow-Up Study of 15 Cases in a High-Volume Institute of China. Front. Med. 9:816012. doi: 10.3389/fmed.2022.816012

Objectives: To report the first series of testicular sex cord-stromal tumors (TSCSTs) with detailed clinicopathologic findings and long-term follow-up in the Chinese population.

Patients and Methods: From 2008 to 2018, 15 patients with TSCST were included in our study. The tumors were analyzed for epidemiological parameters, clinical characteristics, tumor markers, therapy, and follow-up data.

Results: The median age of the patients was 28 years (range, 13–80 years). Para-aortic lymph node metastases were detected in 2 patients after radiological evaluation. Orchiectomy was performed in all patients, and the median diameter of the tumor was 1.5 cm (range, 0.5–5.0 cm). Nine Leydig cell tumors (LCTs), 5 Sertoli cell tumors (SCTs), and 1 unclassified type were confirmed after pathologic evaluation. Thirteen patients (86.7%) were categorized as stage I, and 2 patients (13.3%) were categorized as stage II. The median clinical follow-up was 39.0 months (range, 5–97 months), which showed 10 alive patients, such as 1 patient with progression at 40 months after orchiectomy. The 3- and 5-year progression-free survivals were 100 and 90.0%, respectively.

Conclusion: Testicular sex cord-stromal tumor at stages I and II is a rare subtype with benign behavior and a favorable prognosis in the Chinese population. However, lymph node metastases may be the dominant risk factor for patients with TSCST.

Keywords: testis, testicular neoplasms, sex cord-stromal tumors, follow-up, orchiectomy

INTRODUCTION

Testicular sex cord-stromal tumor (TSCST) is a rare primary testicular neoplasm, accounting for approximately 4% of testicular tumors, while the remaining tumor is of germ cell origin. The most common subtype is Leydig cell tumor (LCT), accounting for 75% of TSCSTs, followed by Sertoli cell tumor (SCT), granulosa cell tumor (GCT), unclassified tumors, and mixed cell types (1, 2).

To date, TSCSTs have been poorly studied, and only a few case reports and small sample clinicopathologic studies have been published (3–13). Although there is a relatively large cross-sectional study of prognosis and cancer incidence based on the national cancer registry, the annual report from the National Central Cancer Registry of China unfortunately has limited information

about testicular cancer (14). In this study, we aimed to present the clinicopathologic characteristics and survival of TSCSTs in the Chinese population.

In our study, we presented a series of 15 patients with TSCSTs from 2008 to 2018. All patients were registered in the Department of Urology, West China Hospital, Sichuan University. We reported the clinical and pathological findings, treatment, and prognostic outcomes observed in patients with TSCSTs, with the purpose of evaluating the efficacy of our clinical approach and contributing to the literature data.

MATERIALS AND METHODS

Setting and Study Design

From January 2008 to December 2018, patients diagnosed with TSCST after surgical procedures at the Department of Urology, West China Hospital were included in our retrospective observational study. All clinical features (symptoms, physical signs, past medical history, and comorbidities), auxiliary examination results (hemogram, blood biochemistry, hormone assay, tumor markers [α-fetoprotein (AFP), β-human chorionic gonadotropin (β-HCG), and lactate dehydrogenase (LDH)], ultrasonography and radiology [computed tomography (CT) scan and magnetic resonance imaging (MRI)]), treatment (surgery and adjuvant therapy), and histopathological findings were retrieved from medical records if available. All diagnoses of TSCSTs were confirmed through postoperative pathological examination.

Treatment and Follow-Up

Orchiectomy was the first-choice treatment for all patients enrolled in our study. For patients with a retroperitoneal disease on preoperative radiological evaluation, we recommended retroperitoneal lymph node dissection (RPLND) after orchiectomy. Tumors were staged according to the National Comprehensive Cancer Network staging system for testicular tumors (15). The classification of testicular tumors was confirmed through the WHO classification of testicular tumors (1).

Based on the studies of Silberstein et al. (4) and Kim et al. (9), patients were stratified into 2 groups by 6 high-risk features, such as (1) tumor greater than 5 cm, (2) necrosis, (3) moderate or severe nuclear atypia, (4) angiolymphatic invasion, (5) infiltrating margins, and (6) more than 5 mitotic features per 10 high-power fields. Patients with 0 or 1 high-risk features and no evidence of retroperitoneal disease on radiological evaluation were classified as the low-risk group, and patients with 2 or more high-risk features or retroperitoneal disease on radiological evaluation were classified as the high-risk group.

After completion of the therapy, patients were followed up regularly for symptoms, physical examination, scrotal ultrasound, and radiology. Total follow-up was calculated as the time from orchiectomy to the last follow-up. Progression was noted as an event and defined as emerging or recurrent disease-related symptoms or any change in tumors on radiology after diagnosis.

Statistical Analysis

Progression-free survival (PFS) was calculated from the date of diagnosis to the date of progression and was estimated according to the Kaplan-Meier method. Categorical data were compared through the chi-square test, while numerical data were compared through the Kruskal-Wallis H test. All analyses were performed with SPSS® 19.0.

RESULTS

Clinical Characteristics

According to the records of West China Hospital, 15 eligible patients were included in our study from 2008 to 2018. The clinical features and the treatment are summarized in **Table 1**. The median body mass index and the age of 15 patients were 21.3 kg/m^2 (range, 17.7–30.1 kg/m^2) and 28 years (range, 13–80 years), respectively. The median age of patients with LCTs was 28 years (range, 13–80 years) while that of patients with SCTs was 27 years (range, 18–50 years). One patient with an unclassified TSCST was diagnosed at 40 years. In our series, we did not find significant differences between age and histopathological differentiation (p = 0.901, Kruskal-Wallis H). The left testis was involved in 5 (33.3%) patients, while the right testis was involved in 10 (66.7%) patients. With regard to the clinical presentation, a testis mass was the main symptom in all cases and was accompanied by pain in 2, varicocele in 2, urinary incontinence in 1, testicular hydrocele in 1, gynecomastia in 1, and cryptorchidism in 1. The median diameter of the mass was 1.5 cm (range 0.5–5.0 cm).

Tumor markers, such as AFP, β-HCG, and LDH, were normal in all patients before surgery except 2 patients with increased LDH levels. Hormone assays were performed preoperatively in 2 patients, and both showed high preoperative testosterone and estradiol levels. However, the sex hormone levels of patients with gynecomastia were unavailable. All patients received radiological evaluation before the surgical approach, which found suspicious para-aortic lymph node metastases in cases 1 and 10.

Treatment and Histopathological Findings

Orchiectomy was performed in all patients, and after that, no adjuvant treatment was performed. We recommended RPLND for the two patients (cases 1 and 10) with para-aortic lymph node metastases on radiological evaluation. However, both of them refused to receive RPLND. The pathologic evaluation was performed for all patients after surgery. LCTs were the leading histopathological entities (n = 9; 60%), followed by SCTs (n = 5; 33%). In one patient (7%), an unclassified TSCST with incomplete differentiation was described. Mitosis (5–8 mitoses per 10 high-power fields) and moderate nuclear atypia were observed in case 10. Tumor necrosis was identified in cases 10 and 15. None of the patients had angiolymphatic invasion or infiltrating margins. Of the 15 patients, 13 had no or 1 high-risk feature and no evidence of retroperitoneal disease on radiological evaluation, and they were classified

TABLE 1 | Clinical features and treatment in 15 patients with TSCSTs.

Case	Age (y)	BMI (kg/m^2)	Side	Clinical history	Treatment	Size (cm)	Stage	Histology	Group (No. high-risk features)	Follow-up
1	40	29.0	Right	Testis mass	Orchiectomy	4.0	II	Unclassified	High-risk group (0)	LTF
2	46	24.9	Right	Testis mass Urinary incontinence Bilateral varicocele	Orchiectomy	3.3	I	LCT	Low-risk group (0)	Alive and NED at 97 mo
3	25	Not available	Left	Testis mass Serum testosterone and estradiol levels were abnormal	Orchiectomy	4.1	I	LCT	Low-risk group (0)	LTF
4	18	21.3	Left	Testis mass and pain Serum LDH level was abnormal	Orchiectomy	3.0	I	SCT	Low-risk group (0)	Alive and NED at 88 mo
5	25	17.7	Right	Testis mass	Orchiectomy	1.0	I	SCT	Low-risk group (0)	LTF
6	26	Not available	Left	Testis mass	Orchiectomy	0.5	I	LCT	Low-risk group (0)	LTF
7	80	18.0	Right	Testis mass and pain Serum LDH level was abnormal	Orchiectomy	1.0	I	LCT	Low-risk group (0)	Alive and NED at 80mo
8	69	Not available	Right	Testis mass Left testicular hydrocele	Orchiectomy	3.7	I	LCT	Low-risk group (0)	LTF
9	50	Not available	Right	Testis mass Left varicocele	Orchiectomy	0.5	I	SCT	Low-risk group (0)	Alive and NED at 46 mo
10	50	21.3	Right	Testis mass	Orchiectomy	1.3	II	SCT	High-risk group (3)	Progress at 40 mo
11	65	30.1	Left	Testis mass Gynecomastia	Orchiectomy	1.7	I	LCT	Low-risk group (0)	Alive and NED at 38 mo
12	13	19.1	Left	Testis mass Serum testosterone and estradiol levels were abnormal	Orchiectomy	5.0	I	LCT	Low-risk group (0)	Alive and NED at 37 mo
13	27	20.4	Right	Testis mass	Orchiectomy	1.5	I	SCT	Low-risk group (0)	Alive at 24 mo
14	28	22.0	Right	Testis mass Left cryptorchidism	Orchiectomy	1.0	I	LCT	Low-risk group (0)	Alive at 5 mo
15	19	22.6	Right	Testis mass	Orchiectomy	0.8	I	LCT	Low-risk group (1)	Alive at 13mo

LDH, lactate dehydrogenase; LCT, Leydig cell tumor; SCT, Sertoli cell tumor; LTF, lost to follow-up; NED, no evidence of disease.

as the low-risk group. Two patients (cases 1 and 10) were classified into the high-risk group due to 2 or more high-risk features (case 10) or retroperitoneal disease on radiological evaluation (case 1) (**Table 1**). In all patients, sufficient clinical and pathological data were available for staging according to the National Comprehensive Cancer Network staging system. Thirteen patients (86.7%) were categorized as stage I, and 2 patients (13.3%) with para-aortic lymph node metastases were categorized as stage II.

Prognosis

Follow-up information was available for 10 patients with a median follow-up of 39.0 months (range, 5–97 months), which showed 10 alive patients. In the low-risk group (n = 13), all patients were alive, and no evidence of disease was observed during follow-up, except for 4 patients who were lost to follow-up. In the high-risk group (n = 2), one patient (case 10) had a novel inguinal mass with pain at 40 months after orchiectomy and was identified as having progression (inguinal lymph node metastases) through radiological evaluation. Comparing the preoperative and postoperative CT scans at 40 months in this patient (case 10), we found that the enlarged para-aortic lymph nodes detected before orchiectomy had diminished (**Figure 1**). Another patient (case 1) was alive without clinical or radiographic evidence of progression until a loss to follow-up at 108 months. The 3-r and 5-year PFSs were 100 and 90.0%, respectively (**Figure 2**). No additional surgery or adjuvant therapy was performed for any patients during follow-up except the one with progression. All patients without follow-up information were due to loss of contact with patients and their families. **Table 2** summarizes several studies of TSCSTs published previously.

DISCUSSION

Testicular sex cord-stromal tumors (TSCSTs) comprise approximately 4% of all testicular tumors, while the frequency increases to 8% in children (1). From 2008 to 2018, a total of 877 patients were diagnosed with testicular tumors at West China Hospital, and only 15 of them (1.7%) had TSCST, slightly lower than the overall proportion. A review of 9 studies published previously that included 313 cases of TSCSTs was performed with attention to the clinical features, treatment, and prognostic outcomes (3, 4, 7–13). In general, there is a wide age range for

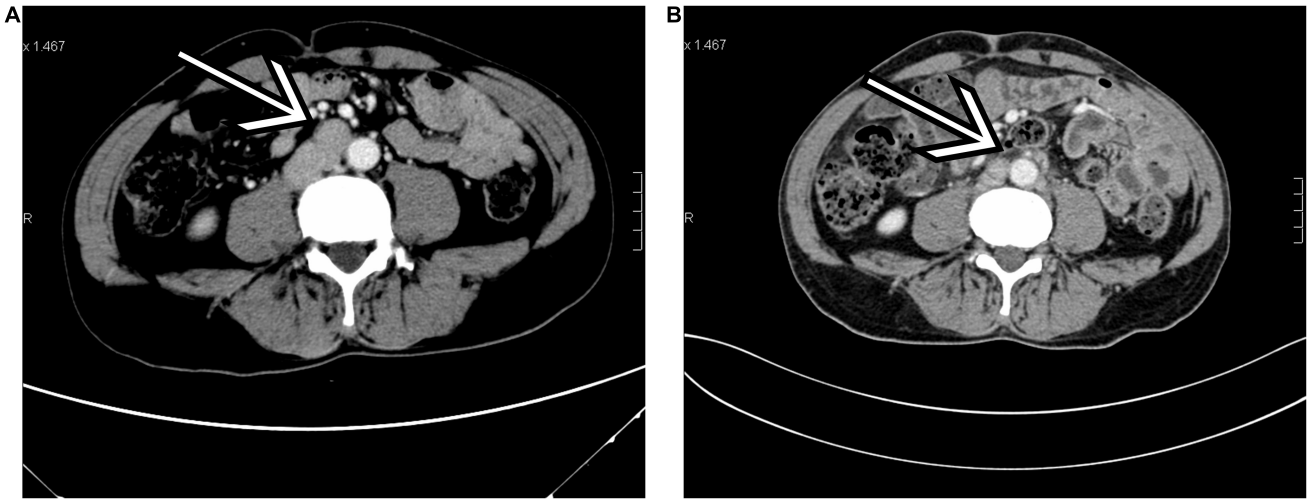

FIGURE 1 | A 50-year-old man with Sertoli cell tumors (SCT; case 10). **(A)** Transverse contrast-enhanced CT (arterial phase) performed before orchiectomy showed enlarged para-aortic lymph nodes (arrow). **(B)** The same level of contrast-enhanced CT (arterial phase) performed 40 months after orchiectomy found that the enlarged para-aortic lymph nodes had diminished (arrow). $^{**}p < 0.01$, $^{***}p < 0.001$.

TSCSTs, with ages in two contemporary series ranging between 14 and 87 years (7, 13). LCTs constitute approximately 3% of testicular neoplasms and occur in both adults and children. SCTs account for less than 1% of testicular tumors, and they occur both in children and in middle-aged adults and could be malignant in both (9, 16, 17). In our study, the median ages of patients with LCTs and SCTs were 28 and 27 years, respectively. However, we did not find significant differences between these two groups in age.

The pathogenesis of TSCSTs is poorly understood. Recently, a single recurrent somatic mutation in the *FOXL2* gene was identified in almost all morphologically adult granulosa cell tumors of the ovary (18, 19). *FOXL2* is a forkhead transcription factor that contains a fork-head DNA-binding domain, plays a role in ovarian development and function, and is essential for granulosa cell differentiation (18). Nevertheless, little is known about the biological activity of *FOXL2* in TSCSTs. Kalfa et al. (20) described aberrant and nuclear *FOXL2* expression in three testicular juvenile granulosa cell tumors. In their study, however, whether *FOXL2* alone had the capacity to induce the transformation of testis cells into malignant granulosa cells remained unclear. Moreover, Boyer et al. (21) reported that *Ctnnb1* mutant mice with the loss of *phosphatase and tensin homolog* (*Pten*) expression in their Sertoli cells had developed testicular GCTs. Richards et al. (22) confirmed that except for *Pten* loss, *Kras* activation in Sertoli cells of *Ctnnb1* mutant mice could also induce GCTs. However, despite these genetic findings, the pathogenesis of TSCSTs remains unclear.

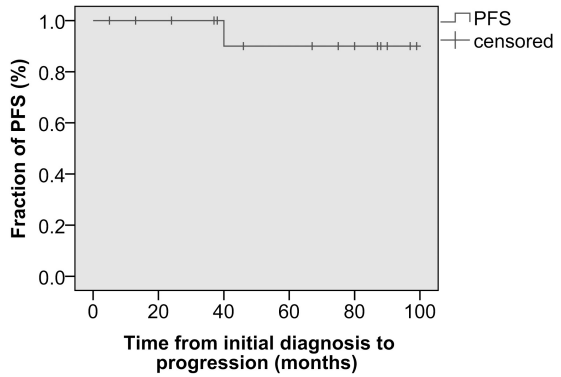

FIGURE 2 | Progression-free survival curve—the time from the initial diagnosis to progression.

Testicular sex cord-stromal tumors generally do not have aggressive behavior. LCTs are less aggressive in children than adults, and approximately 10% of LCTs present with malignant characteristics (23). Kim et al. (9) reported a clinicopathologic analysis of 40 patients with LCTs and found that 5 of them died of metastasis. Additionally, SCTs are considered well-differentiated tumors. However, 4 cases with metastasis were described in two series of patients with SCTs (7, 10). Some authors found that malignant tumors were larger, often had an infiltrative margin and spread beyond the testis, frequently exhibited blood vessel or lymphatic invasion, had a greater degree of cellular atypia and necrosis, and a higher mitotic rate than benign tumors (9, 10, 24). The wide morphological range of TSCSTs makes their diagnosis difficult, and the challenge remains in characterizing patients with benign or malignant tumors.

In most TSCSTs, the clinical presentation is similar to testicular germ cell tumors, of which a mass of testis was the most common symptom (16). Children with LCTs generally present with endocrinologic symptoms (virilization and gynecomastia) due to excessive secretion of sex steroids, while testicular mass and gynecomastia are more common in adult men (9, 11). In view of these findings, preoperative hormone assays may be

TABLE 2 | Summary of TSCSTs previously reported in the literature.

References	Country	No. Cases	Histology	Age (y)	Size (cm)	Treatment	Follow-up (mo)	Disease Status
Harms et al. 1997 (3)	Germany	29	SCTs (*n* = 18) GCTs (*n* = 11)	SCTs: mean, 4.2 (range, 0-14) GCTs: mean, 0.4 (range, 0-3)	SCTs: mean, 1.9 (range, 0.7-4.0) GCTs: mean, 2.0 (range, 1.0-2.2)	Orchiectomy (*n* = 23) Orchiectomy+ RPLND (*n* = 1) Orchiectomy+ RPLND+Ch (*n* = 1) Enucleation (*n* = 2)	SCTs: mean, 39.3 (range, 9-96) GCTs: mean, 46.1 (range, 7-117)	Alive and NED (*n* = 24)
Silberstein et al. 2014 (4)	United States	48	Unclassified (*n* = 5) LCTs (*n* = 28) SCTs (*n* = 13) GCTs (*n* = 2)	Low risk (median, 37) High risk (median, 48)	Low risk (median, 1.5) High risk (median, 5.0)	Orchiectomy (*n* = 37) Orchiectomy+ RPLND (*n* = 11)	Low risk (median, 15) High risk (median, 67)	Alive and NED (*n* = 43) Recurrence (*n* = 2) DOD (*n* = 3)
Kao et al. 2014 (7)	United States	20	SCTs	Mean, 37.0; median, 39 (range, 0.01-12)	Mean,1.7; (range, 0.5-6.0)	Orchiectomy (*n* = 14) Excisional biopsy (*n* = 3) Wedge biopsy (*n* = 2) Orchiectomy+ RPLND (*n* = 1)	Mean, 73.0 (range, 3-192)	Alive and NED (*n* = 9) Alive (*n* = 5) DOD (*n* = 1)
Nason et al. 2017 (8)	Ireland	22	LCTs	Median, 45.0	Not available	Testis-sparing surgery (*n* = 21) Testis-sparing surgery+orchiectomy (*n* = 1)	Median, 102.0 (range, 1-237)	Alive and NED (*n* = 17) Recurrence (*n* = 1) Died with NED (*n* = 4)
Kim et al. 1985 (9)	United States	40	LCTs	Mean, 46.5 (range, 2-90)	Mean, 3.0 (range, 0.5-10.0)	Not available	Mean, 48.0 (range, 2-264)	Alive and NED (*n* = 25)
Young et al. 1998 (10)	United States	60	SCTs	Mean, 45 (range, 15-80)	Mean, 3.6 (range, 0.3-15)	Not available	Mean, 100.8	DOD (*n* = 5) Alive and NED (*n* = 9) Alive (*n* = 4) DOD (*n* = 3)
Carmignani et al. 2006 (11)	Italy	24	LCTs	Mean, 37.8 (range, 22-61)	Mean, 1.5 (range, 0.5-4.5)	Orchiectomy (*n* = 24)	Mean, 117 (range, 11-241)	Alive and NED (*n* = 24)
Featherstone et al. 2009 (12)	United Kingdom	38	LCTs (*n* = 31) SCTs (*n* = 6) LCCSCT (*n* = 1)	Mean, 43 (range, 18-79)	Mean, 1.7 (range, 0.5-8.0)	Orchiectomy (*n* = 36) Surgical enucleation (*n* = 2)	Median, 76.6 (range, 16.8-300)	Alive (*n* = 36)
Cornejo et al. 2014 (13)	United States	32	GCTs	Mean, 40.0 (range, 14-87)	Mean, 2.8 (range, 0.5-6.0)	Orchiectomy (*n* = 30) Wedge excision (*n* = 2)	Mean, 51.0 (range, 1-169)	Alive and NED (*n* = 18) Metastasis (*n* = 1)

LCTs, Leydig cell tumors; SCTs, Sertoli cell tumors; GCTs, granulosa cell tumors; LCCSCT, large cell calcifying Sertoli cell tumor; RPLND, retroperitoneal lymph nodes dissection; Ch, chemotherapy; NED, no evidence of disease; DOD, died of disease.

helpful in the diagnosis of TSCSTs, especially LCTs. However, in our series, only 2 patients received hormone assays, and both showed increased serum estradiol and testosterone levels without any presentation of endocrinologic symptoms. It is unfortunate that the hormone levels of the patient with gynecomastia were unavailable. Moreover, patients with SCTs usually present with a testicular mass and gynecomastia induced by estrogen secretion of the tumor, which were not found in our patients. In men, large-cell calcifying SCTs can be found in patients with Peutz-Jeghers syndrome or the Carney complex (25, 26). However, no clinical data indicated that Peutz-Jeghers syndrome or the Carney complex existed in our patients. Radiological evaluation is helpful in the early diagnosis of TSCSTs. However, there are no pathognomonic radiological features that can accurately determine the presence of a TSCST and differentiate the benign and malignant forms of TSCSTs (8, 27).

The treatment for TSCSTs is still controversial around the world. In principle, orchiectomy constitutes the main therapy for TSCSTs (15). However, Cecchetto et al. (17) suggested that a testis-sparing surgery should be taken into consideration when preoperative normal levels of AFP can rule out a malignant germ cell tumor and ultrasound shows a small and encapsulated

mass. Furthermore, Nason et al. (8) found only one local recurrence after the organ-preserving procedure in 22 patients with LCTs, and no progressive disease was reported. Another multicenter retrospective study that includes 204 cases also observed benign behavior and favorable prognosis of LCTs, in which testis-sparing surgery was performed for all patients (28). In addition, Grogg et al. (29) performed a systematic literature review and meta-analysis of outcomes in 435 patients with SCTs. They found that few local recurrences after testis-sparing surgery without adjuvant therapy could be regarded as a standard of care. Age, tumor size, necrosis, tumor extension to the spermatic cord, angiolymphatic invasion, and mitotic index are predictive of metastatic disease. The American Urological Association guidelines have recommended that testis-sparing surgery combined with a frozen-section is an option for preservation of hormonal function and fertility in patients with solitary testis or bilateral synchronous malignancy, especially for patients with masses < 2.0 cm, equivocal ultrasound/physical examination findings and negative tumor markers (β-HCG and AFP) (Grade C) (30). Nevertheless, it is worth noting that this strategy has not been validated prospectively, and few data have demonstrated its long-term oncologic and functional superiorities for TSCST (31). Moreover, the value of RPLND for patients with TSCSTs is uncertain. Silberstein et al. (4) found that patients with one or no high-risk feature can be safely observed without RPLND. Early RPLND may be beneficial in those with two or more high-risk features. However, in another series of 52 patients with LCTs, no retroperitoneal disease was observed after pathologic evaluation in 5 patients who received RPLND (i.e., 2 patients with a retroperitoneal disease on preoperative radiology) (32). In our study, all patients were treated with orchiectomy without any adjuvant therapy after surgery. No patient developed novel metastatic disease or disease-related death during follow-up, except that 1 patient in the high-risk group had inguinal lymph node metastases at 40 months. Interestingly, we found that enlarged para-aortic lymph node metastases had diminished when compared with the preoperative and postoperative CT scans at 40 months in this patient (case 10), although the patient refused to receive RPLND after orchiectomy. Therefore, in our opinion, the value of preoperative radiological evaluation in predicting the malignancy and prognosis of TSCSTs is limited. RPLND should be reserved for patients with stage II TSCC and those with 2 or more high-risk features.

In general, the majority of studies, such as our study, confirmed the benign biological behavior and favorable prognosis of TSCSTs. Kim et al. (9) found that the size, cellular atypia, necrosis, mitosis, and invasion of the tumor are related to the degree of malignancy of TSCSTs, which may predict the prognosis of the tumor. In addition, patients with LCTs or SCTs could present with hormonal manifestations as the endocrine function of tumors (9, 11). Therefore, hormone assays have potential clinical value in predicting the subtype of TSCSTs. However, it is unclear whether serum hormone levels are a prognostic factor. With regard to GCTs, after a systematic review of published case series data, Grogg et al. (33) reported that tumor size, presence of angiolymphatic invasion, or gynecomastia represent risk factors for metastatic disease. In our study, only one patient with preoperative lymph node metastases had progression during follow-up, indicating that lymph node metastases may be a dominant factor for the prognosis of TSCSTs.

We must acknowledge several limitations of our study. First, only 15 patients were included in our study, and prospective studies with larger samples are needed in the future. Second, some patient data, such as serum hormone levels, were not available because of the limitation of retrospective studies. Finally, some patients were lost to follow-up even if we tried to contact their relatives and families, which may reduce the accuracy of our findings.

CONCLUSION

Our study confirmed that TSCST at stages I and II is a rare subtype with benign behavior and a favorable prognosis in the Chinese population. However, lymph node metastases may be the dominant risk factor for patients with TSCSTs. Large-scale and multicenter prospective studies are needed to further evaluate the efficacy and safety of orchiectomy, testis-sparing surgery, and adjuvant therapy for TSCST.

DATA AVAILABILITY STATEMENT

The original contributions presented in the study are included in the article/supplementary material, further inquiries can be directed to the corresponding author/s.

ETHICS STATEMENT

The studies involving human participants were reviewed and approved by the Ethics Committee on Biomedical Research, West China Hospital of Sichuan University. Written informed consent to participate in this study was provided by the participants' legal guardian/next of kin. Written informed consent was obtained from the individual(s), and minor(s)' legal guardian/next of kin, for the publication of any potentially identifiable images or data included in this article.

AUTHOR CONTRIBUTIONS

YH, BC, and DC: conception and design, data analysis, interpretation, and provision of study materials or patients. QD, LL, and QW: administrative support. YH, BC, DC, ZC, JG, and JL: collection and assembly of data. YH, BC, DC, ZC, JL, JG, QD, LL, and QW: manuscript writing. All authors contributed to the article and approved the submitted version.

FUNDING

This study was funded by the National Natural Science Foundation of China (grant no. 82000721) and Programs from the Department of Science and Technology of Sichuan Province (grant no. 2020YJ0054).

REFERENCES

1. Idrees MT, Ulbright TM, Oliva E, Young RH, Montironi R, Egevad L, et al. The World Health Organization 2016 classification of testicular non−germ cell tumours: a review and update from the International Society of Urological Pathology Testis Consultation Panel. *Histopathology.* (2017) 70:513–21. doi: 10.1111/his.13115
2. Young RH. Sex cord-stromal tumors of the ovary and testis: their similarities and differences with consideration of selected problems. *Mod Pathol.* (2005) 18:S81. doi: 10.1038/modpathol.3800311
3. Harms D, Kock L. Testicular juvenile granulosa cell and Sertoli cell tumours: a clinicopathological study of 29 cases from the Kiel Paediatric Tumour Registry. *Virchows Arch.* (1997) 430:301–9. doi: 10.1007/BF01092753
4. Silberstein JL, Bazzi WM, Vertosick E, Carver BS, Bosl GJ, Feldman DR, et al. Clinical outcomes of local and metastatic testicular sex cord-stromal tumors. *J Urol.* (2014) 192:415–9. doi: 10.1016/j.juro.2014.01.104
5. Thomas JC, Ross JH, Kay R. Stromal testis tumors in children: a report from the prepubertal testis tumor registry. *J Urol.* (2001) 166:2338–40. doi: 10.1016/s0022-5347(05)65583-8
6. Rosenblum F, Koenig RG, Mikhail FM, Porterfield JR, Nix JW, Eltoum IEA. An adolescent with large cell calcifying sertoli cell tumor of the testis and undiagnosed Carney Complex: a case report. *Diagn Cytopathol.* (2017) 45:634–9. doi: 10.1002/dc.23700
7. Kao C-S, Kum JB, Idrees MT, Ulbright TM. Sclerosing Sertoli cell tumor of the testis: a clinicopathologic study of 20 cases. *Am J Surg Pathol.* (2014) 38:510–7. doi: 10.1097/pas.0000000000000132
8. Nason G, Redmond E, Considine S, Omer S, Power D, Sweeney P. The natural history of Leydig cell testicular tumours: an analysis of the National Cancer Registry. *Ir J Med Sci.* (2018) 187:323–6. doi: 10.1007/s11845-017-1662-4
9. Kim I, Young RH, Scully RE. Leydig cell tumors of the testis. A clinicopathological analysis of 40 cases and review of the literature. *Am J Surg Pathol.* (1985) 9:177–92. doi: 10.1097/00000478-198503000-00002
10. Young RH, Koelliker DD, Scully RE. Sertoli cell tumors of the testis, not otherwise specified: a clinicopathologic analysis of 60 cases. *Am J Surg Pathol.* (1998) 22:709–21. doi: 10.1097/00000478-199806000-00008
11. Carmignani L, Salvioni R, Gadda F, Colecchia M, Gazzano G, Torelli T, et al. Long-term followup and clinical characteristics of testicular Leydig cell tumor: experience with 24 cases. *J Urol.* (2006) 176:2040–3. doi: 10.1016/j.juro.2006.07.005
12. Featherstone JM, Fernando HS, Theaker JM, Simmonds PD, Hayes MC, Mead GM. Sex cord stromal testicular tumors: a clinical series–uniformly stage I disease. *J Urol.* (2009) 181:2090–6. doi: 10.1016/j.juro.2009.01.038
13. Cornejo KM, Young RH. Adult granulosa cell tumors of the testis: a report of 32 cases. *Am J Surg Pathol.* (2014) 38:1242–50. doi: 10.1097/PAS.0000000000000216
14. Chen W, Zheng R, Baade PD, Zhang S, Zeng H, Bray F, et al. Cancer statistics in China, 2015. *CA Cancer J Clin.* (2016) 66:115–32. doi: 10.3322/caac.21338
15. Motzer RJ, Jonasch E, Agarwal N, Beard C, Bhayani S, Bolger GB, et al. Testicular cancer, version 2.2015. *J Natl Compr Canc Netw.* (2015) 13:772–99. doi: 10.6004/jnccn.2015.0092
16. Albers P, Albrecht W, Algaba F, Bokemeyer C, Cohn-Cedermark G, Fizazi K, et al. Guidelines on testicular cancer: 2015 update. *Eur Urol.* (2015) 68:1054–68. doi: 10.1016/j.eururo.2015.07.044
17. Cecchetto G, Alaggio R, Bisogno G, Virgone C, Dall'Igna P, Terenziani M, et al. Sex cord-stromal tumors of the testis in children. A clinicopathologic report from the Italian TREP project. *J Pediatr Surg.* (2010) 45:1868–73. doi: 10.1016/j.jpedsurg.2010.02.120
18. Shah SP, Köbel M, Senz J, Morin RD, Clarke BA, Wiegand KC, et al. Mutation of FOXL2 in granulosa-cell tumors of the ovary. *N Engl J Med.* (2009) 360:2719–29.
19. Al-Agha OM, Huwait HF, Chow C, Yang W, Senz J, Kalloger SE, et al. FOXL2 is a sensitive and specific marker for sex cord-stromal tumors of the ovary. *Am J Surg Pathol.* (2011) 35:484–94. doi: 10.1097/PAS.0b013e31820a406c
20. Kalfa N, Fellous M, Boizet-Bonhoure B, Patte C, Duvillard P, Pienkowski C, et al. Aberrant expression of ovary determining gene FOXL2 in the testis and juvenile granulosa cell tumor in children. *J Urol.* (2008) 180:1810–3. doi: 10.1016/j.juro.2008.03.097
21. Boyer A, Paquet M, Laguë M-N, Hermo L, Boerboom D. Dysregulation of WNT/CTNNB1 and PI3K/AKT signaling in testicular stromal cells causes granulosa cell tumor of the testis. *Carcinogenesis.* (2009) 30:869–78. doi: 10.1093/carcin/bgp051
22. Richards J, Fan H-Y, Liu Z, Tsoi M, Laguë M-N, Boyer A, et al. Either Kras activation or Pten loss similarly enhance the dominant-stable CTNNB1-induced genetic program to promote granulosa cell tumor development in the ovary and testis. *Oncogene.* (2012) 31:1504. doi: 10.1038/onc.2011.341
23. Farkas LM, Székely JG, Pusztai C, Baki M. High frequency of metastatic Leydig cell testicular tumours. *Oncology.* (2000) 59:118–21. doi: 10.1159/000012147
24. Cheville JC, Sebo TJ, Lager DJ, Bostwick DG, Farrow GM. Leydig cell tumor of the testis: a clinicopathologic, DNA content, and MIB-1 comparison of nonmetastasizing and metastasizing tumors. *Am J Surg Pathol.* (1998) 22:1361–7. doi: 10.1097/00000478-199811000-00006
25. Chang B, Borer JG, Tan PE, Diamond DA. Large-cell calcifying Sertoli cell tumor of the testis: case report and review of the literature. *Urology.* (1998) 52:520–2. doi: 10.1016/s0090-4295(98)00246-5
26. Brown B, Ram A, Clayton P, Humphrey G. Conservative management of bilateral Sertoli cell tumors of the testicle in association with the Carney complex: a case report. *J Pediatr Surg.* (2007) 42:e13–5. doi: 10.1016/j.jpedsurg.2007.06.008
27. Dogra VS, Gottlieb RH, Rubens DJ, Liao L. Benign intratesticular cystic lesions: US features. *Radiographics.* (2001) 21(Suppl_1):S273–81. doi: 10.1148/radiographics.21.suppl_1.g01oc15s273
28. Ruf CG, Sanatgar N, Isbarn H, Ruf B, Simon J, Fankhauser CD, et al. Leydig-cell tumour of the testis: retrospective analysis of clinical and therapeutic features in 204 cases. *World J Urol.* (2020) 38:2857–62. doi: 10.1007/s00345-020-03079-1
29. Grogg J, Schneider K, Bode PK, Kranzbühler B, Eberli D, Sulser T, et al. Sertoli cell tumors of the testes: systematic literature review and meta-analysis of outcomes in 435 patients. *Oncologist.* (2020) 25:585–90. doi: 10.1634/theoncologist.2019-0692
30. Stephenson A, Eggener SE, Bass EB, Chelnick DM, Daneshmand S, Feldman D, et al. Diagnosis and treatment of early stage testicular cancer: AUA guideline. *J Urol.* (2019) 202:272–81. doi: 10.1097/ju.0000000000000318
31. Nicolai N, Necchi A, Raggi D, Biasoni D, Catanzaro M, Piva L, et al. Clinical outcome in testicular sex cord stromal tumors: testis sparing vs radical orchiectomy and management of advanced disease. *Urology.* (2015) 85:402–6. doi: 10.1016/j.urology.2014.10.021
32. Di Tonno F, Tavolini IM, Belmonte P, Bertoldin R, Cossaro E, Curti P, et al. Lessons from 52 patients with leydig cell tumor of the testis: the GUONE (North-Eastern Uro-Oncological Group, Italy) experience. *Urol Int.* (2009) 82:152–7. doi: 10.1159/000200790
33. Grogg JB, Schneider K, Bode PK, Kranzbühler B, Eberli D, Sulser T, et al. Risk factors and treatment outcomes of 239 patients with testicular granulosa cell tumors: a systematic review of published case series data. *J Cancer Res Clin Oncol.* (2020) 146:2829–41. doi: 10.1007/s00432-020-03326-3

Conflict of Interest: The authors declare that the research was conducted in the absence of any commercial or financial relationships that could be construed as a potential conflict of interest.

Advantages of publishing in Frontiers

OPEN ACCESS
Articles are free to read for greatest visibility and readership

FAST PUBLICATION
Around 90 days from submission to decision

HIGH QUALITY PEER-REVIEW
Rigorous, collaborative, and constructive peer-review

TRANSPARENT PEER-REVIEW
Editors and reviewers acknowledged by name on published articles

Frontiers
Avenue du Tribunal-Fédéral 34
1005 Lausanne | Switzerland

Visit us: www.frontiersin.org
Contact us: frontiersin.org/about/contact

REPRODUCIBILITY OF RESEARCH
Support open data and methods to enhance research reproducibility

DIGITAL PUBLISHING
Articles designed for optimal readership across devices

FOLLOW US
@frontiersin

IMPACT METRICS
Advanced article metrics track visibility across digital media

EXTENSIVE PROMOTION
Marketing and promotion of impactful research

LOOP RESEARCH NETWORK
Our network increases your article's readership